Characterisation of Cellular Responses to Pandemic Influenza in Naturally Infected Individuals

Shaima Begom

Imperial College London

National Heart and Lung Institute

Submitted for the degree of PhD

February 2015

DECLARATION OF ORIGINALITY

I certify that this thesis, and the research to which it refers, are the product of my own work, conducted during the years 2010 and 2014 of the PhD in the Section of Respiratory Medicine at Imperial College London. Any ideas or quotations from the work of other people published or otherwise, or from my own previous work are fully acknowledged in accordance with the standard referencing practices of the discipline.

Furthermore, I would like to acknowledge Professor Ajit Lalvani and Dr Saranya Sridhar who designed the ImmunoFlu study cohort. Dr Sridhar recruited subjects for the ImmunoFlu study, and I participated in collection and bio-banking of biological samples during the PhD period. Dr Sridhar and I equally contributed to the laboratory work presented in Results sections 3.2 and 3.3 of this thesis.

COPYRIGHT DECLARATION

ACKNOWLEDGEMENTS

Firstly, all praise is to Allah. A special thank you to my supervisors Prof Ajit Lalvani and Dr Saranya Sridhar, for giving me the opportunity and inspiration to undertake this project, for training me in various techniques and for support, advice and insightful discussions throughout. Thank you to all the volunteers who donated samples used in this study. Thanks to everyone in the department of Respiratory Medicine at St Mary's hospital for making the last 4 years an enjoyable experience. The 'Flubercoidosis Protocols' will serve as a constant reminder to me of the wonderful friends and colleagues I have worked with. Thank you to Robert Sampson for help and advice on the flow cytometry staining panel. Thank you to Dr Nazneen Siddiqui for your encouragement during the final phase of writing this thesis. This thesis is dedicated to my family; my parents, husband and siblings, your constant support and patience made this dream a reality.

AUTHORED PUBLICATIONS AND PRESENTATIONS

Published papers

Sridhar S, Begom S, Bermingham A, Ziegler T, Roberts KL, Barclay WS, Openshaw, P, Lalvani A. Predominance of heterosubtypic IFN-gamma-only-secreting effector memory T cells in pandemic H1N1 naive adults. *European Journal of Immunology.* 2012 Nov; 42(11):2913-24.

Sridhar S, Begom S, Bermingham A, Hoschler K, Adamson W., Carman W., Lalvani A. Higher incidence of natural infection during the third pandemic wave compared to the second pandemic wave. *Emerging Infectious Diseases*, 2013. 19: 1866-1869.

Sridhar S, Begom S, Bermingham A, Hoschler K, Adamson W., Carman W., Barclay WS, Lalvani A. Cellular Immune Correlates for protection against pandemic influenza. *Nature Medicine*, 2013 Oct, 19(10):1305-12.

Sridhar S, Begom S, Hoschler K, Bermingham A, Adamson W, Carman W, Riley S, Lalvani A. Longevity and Determinants of Protective Humoral Immunity Following Pandemic Influenza Infection. *AJRCCM*, 2014 Dec. [Epub ahead of print].

Manuscripts in preparation

Begom S, Sridhar S, *et al*., Evolution, longevity and immune determinants of protection-associated CD8+ effector T cells following natural pandemic influenza infection.

Begom S, Sridhar S, Siddiqui N, Kwok J and Lalvani A. IFN-γ/IL-2 fluorescence-immunospot: a reproducible assay for quantifying clinically relevant functional T cell subsets in human studies.

Conference presentations

6th - 10th Dec 2010. British Society for Immunology Congress, Liverpool, UK. **Poster presentation: Shaima Begom,** Saranya Sridhar, Alison Bermingham, Samuel Bremang, Lisa Grass, Murphy Magtoto, Lee Potiphar, Peter Openshaw, Ajit Lalvani. **'Cross-reactive T cells to pandemic influenza H1N1 are predominantly of an effector phenotype'.**

29th May – 1st June, 2013. Mechanisms of Antigen Specific Immune Responses (MASIR), Dubrovnik, Croatia. **Poster presentation: Shaima Begom,** Saranya Sridhar, Chi Kwok, Nazneen Siddiqui, Prof Ajit Lalvani. **'Assessing clinical performance parameters of a fluorescence-immunospot assay to quantify dual cytokine-secreting cells'**.

5th -10th September 2013. Options for the Control of Influenza VIII. Cape Town, South Africa. **Poster presentation: Saranya Sridhar, Shaima Begom,** Alison Bermingham, Katja Hoschler, Walt Adamson, William Carman, Thomas Bean, Wendy Barclay, Jonathan Deeks, Ajit Lalvani. **'CD8+ T cells correlate with protection against symptomatic illness following natural pandemic influenza infection in humans'**.

ABBREVIATIONS

AF700	Alexa Fluor 700
APC	Antigen presenting cell (or allophycocyanin antibody congugate)
APC-Cy7	Allophycocyanin conjugated to a Cyanine-7
ASC	Antibody secreting cell
BSA	Bovine serum albumin
BV570	Brilliant Violet 570
CD	Cluster of differentiation
CI	Confidence interval
CMV	Cytomegalovirus
CTL	Cytotoxic T lymphocyte
CV	Coefficient of variation
DC	Dendritic cell
DMSO	Dimethyl sulphoxide
EBV	Epstein bar virus
EDTA	Ethylenediaminetetraacetic acid
ELISpot	Enzyme-linked immunosorbent spot
ESAT-6	6kDa early secreted antigenic target from *Mycobacterium tuberculosis*
FACS	Fluorescence activated cell sorting
FBS	Fetal bovine serum
Fig.	Figure
FITC	Fluorescin Isothiocyanate
FMO	Fluorescence minus one
GALT	Gut-associated lymphoid tissue
$\gamma\delta$	Gamma-delta
HA	Haemagglutinin
HAI	Haemagglutination inhibition
HIV-1	Human immunodeficiency virus-1
HLA	Human leukocyte antigen
HSI	Heterosubtypic immunity
IAV	Influenza A virus
ICS	Intracellular cytokine staining
IFN	Interferon
IFN-γ	Interferon-gamma
IgG	Immunoglobulin G
IgA	Immunoglobulin A
IgM	Immunoglobulin M
IL-1	Interleukin-1
IL-2	Interleukin-2
IL-4	Interleukin-4
IL-5	Interleukin-5
IL-6	Interleukin-6
IL-10	Interleukin-10
IL-12	Interleukin-12
IL-13	Interleukin-13
IL-17	Interleukin-17
ILI	Influenza-like illness
ILC	Innate lymphoid cell
iNKT	Invariant Natural Killer T cell

IQR	Interquartile range
L/D	Live/Dead
LAIV	Live attenuated influenza vaccine
LCMV	Lymphocytic choriomeningitis virus
LM	*Listeria monocytogenes*
LRT	Lower respiratory tract
M1	Matrix protein 1
mAb	Monoclonal antibody
MACS	Magnetic activated cell sorting
MAIT	Mucosa-associated invariant T cell
MALT	Mucosa-associated lymphoid tissue
MHC	Major Histocompatibility Complex
MOI	Multiplicity of infection
NA	Neuraminidase
NALT	Nasopharynx-associated lymphoid tissue
NK	Natural Killer
NLR	Nod-like receptor
NP	Nucleoprotein
OR	Odds ratio
PB1	Polymerase basic protein 1
PBMC	Peripheral blood mononuclear cell
PBS	Phosphate buffered saline
PE	Phycoerythrin
PE-CF594	Phycoerithrin conjugated to Carmen Fluorochrome 594
PE-Cy5	Phycoerythrin conjugated to Cyanine-5
PE-Cy7	Phycoerythrin conjugated to Cyanine-7
PerCP-Cy5.5	Peridinin Chlorophyll Protein conjugated to Cyanine-5.5
pH1N1	2009 pandemic H1N1
PHE	Public Health England
PMA/I	Phorbol myristate acetate/Ionomycin
PPD	Purified protein derivative
QDot605	Quantum Dot 605
Qdot655	Quantum Dot 655
RT-PCR	Reverse transcriptase polymerase chain reaction
SA	Strepavidin
SD	Standard deviation
SEM	Standard error of mean
SFC	Spot-forming cell
Tcm	Central memory T cell
TCR	T cell receptor
Tem	Effector memory T cell
Temra	Late effector memory T cell
Th1	T helper 1
Th2	T helper 2
Th17	T helper 17
TIV	Trivalent inactivated vaccine
TLR	Toll-like receptor
TNF-α	Tumour necrosis factor alpha
Trm	Resident memory T cell
URT	Upper respiratory tract

V450	Violet 450
WHO	World Health Organisation

TABLE OF CONTENTS

LIST OF FIGURES AND TABLES

0 ABSTRACT

Understanding the relevance of T cells in limiting influenza illness severity will facilitate the rational design and evaluation of T cell-based universal influenza vaccines. The aim of this thesis was to characterise pre-existing T cell responses to influenza and follow the kinetics of these T cell responses to infection by exploiting the 2009 H1N1 pandemic (pH1N1). Peripheral blood mononuclear cells (PBMCs) were collected from healthy adults naïve to pH1N1 who were longitudinally followed over 2 influenza seasons from 2009 – 2011. *Ex vivo* pH1N1-specific memory CD4+ and CD8+ T cell responses were characterised by IFN-γ/IL-2 fluorescence-immunospot and 14-colour flow cytometry. In pH1N1 seronegative adults in a community setting, pre-existing influenza-specific T cells cross-reacting with pH1N1 were prevalent, pre-dominantly of a single-cytokine positive (IFN-γ+, IL-2+ or TNF-α+) and effector memory (CD45RA-CCR7-) or late effector (CD45RA+CCR7-) phenotype and expressed lung homing receptor (CCR5+) and cytotoxic degranulation marker (CD107ab+). Pre-existing CD8+IFN-γ+IL-2- Temra (CD45RA+CCR7-) cells limited disease severity following incident pH1N1 infection in the absence of protective strain-specific antibodies. Furthermore, we show that this protection-associated T cell subset is durably maintained in the absence of re-infection up to 1.5 years post-infection. The identification of a protection-associated immune correlate, the frequencies of which were increased and durably maintained by natural infection, is highly relevant for the development of a universal influenza vaccine inducing long-lasting, protective T cells.

1 INTRODUCTION

1.1 General introduction to the problem of influenza

1.1.1 Influenza virology and epidemiology

Influenza remains a huge health burden globally with an estimated 250,000 – 500,000 deaths and 3 – 5 million cases of severe influenza worldwide every year (WHO, 2014b). There are 3 types of influenza virus: A, B and C that vary according to their genome organisation, host range, and pathogenicity. Influenza types B and C are mainly isolated from humans whereas influenza A virus (IAV) infects a wide range of species including humans, birds, pigs and horses. Of the 3 types, IAV is the most virulent and prevalent in humans (Knipe *et al.*, 2006).

The virus was first isolated in 1933 and is an enveloped, single-stranded, negative-sense RNA virus belonging to the *Orthomyxoviridae* family (Knipe *et al.*, 2006). The eight-piece segmented genome encodes at least 11 viral proteins. There are two main surface glycoproteins that are involved in infection of host cells. Haemagglutinin (HA) is a trimeric lectin that attaches to sialic acid residues on the surface of target cells. Neuraminidase (NA) is an enzyme that cleaves sugar bonds to enable viral entry into the host cell and release of progeny virus particles from infected cells. Another surface protein expressed at a lower abundance in the virion than HA and NA, is matrix protein 2 (M2) that forms tetrameric ion-channels. The remaining eight proteins are: polymerase basic proteins 1, 1-F2 and 2 (PB1, PB1-F2 and PB2); polymerase acid (PA); matrix protein 1 (M1); non-structural proteins 1 and 2 (NS1 and NS2) and nucleoprotein (NP) (Knipe *et al.*, 2006).

Although each IAV strain displays only one subtype of HA and NA molecule, there are 18 different subtypes of HA and 11 different subtypes of NA characterised to date giving rise to a number of possible IAV subtype combinations (Knipe *et al.*, 2006, Kapoor & Dhama, 2014). The HA subtypes are further characterised into group 1 (H1, H2, H5, H6, H8, H9, H11, H12, H13, H16, H17 and H18) and group 2 (H3, H4, H7, H10, H14, and H15) phylogenetic groups (Kapoor & Dhama, 2014). Viral strain nomenclature is according to the virus type, place of initial isolation, strain number, and year of isolation. H3N2 and H1N1 are subtypes currently in circulation as 'seasonal' strains (sH3N2 and pH1N1 derivatives) in the human population. IAV has a high mutation rate, especially in the surface proteins HA and NA resulting in IAV antigenic 'drift' variants responsible for seasonal influenza epidemics. Larger changes and reassortment of genetic material between 2 or more different influenza strains infecting the same host cell can result in antigenic 'shift' variants, leading to the generation of new potentially 'pandemic' strains (Knipe *et al.*, 2006). In 1918, the 'Spanish Flu' pandemic was caused by H1N1 introduced into the human population. In 1957, H2N2 viruses replaced the H1N1 subtype and caused the 'Asian Flu' pandemic. In 1968, H3N2 viruses replacing the previously circulating H2N2 subtype caused the 'Hong Kong' pandemic. A swine-origin H1N1 IAV (pH1N1) emerged in April 2009 and caused the first pandemic of the 21st century declared on 11th June 2009 (WHO, 2010). This pH1N1 contained components from Classical Swine (HA, NP, NS), Eurasian swine (NA, M) and North American Swine (PA, PB1, PB2) lineage reassortants (Garten *et al.*, 2009).

Although the H1 subtype has previously been encountered through a human pandemic (1918 H1N1) and the derivatives that became sH1N1 viruses in circulation prior to 2009, pH1N1 was still able to cause a pandemic in 2009. There was significant divergence (20 – 24%) in the protein sequence of the HA of pH1N1 compared to the HA of seasonal H1 subtypes, whereas it was more closely related to North American swine influenza strains (only 1 – 9% divergence) (Gatherer, 2009). The majority of the world's population had little or no immunity to this antigenically shifted virus, hence potentiating pandemic spread of the virus.

1.1.2 Epidemiology of pH1N1

In the United Kingdom (UK) there were 3 waves of pH1N1 infection: the first wave occurred in April to August 2009, the second wave occurred in September 2009 – April 2010, and the third wave occurred in August 2010 – April 2011 (WHO, 2014a). The WHO announced the beginning of the post-pandemic phase on 10 August 2010. A systematic review of serological studies from various countries (Australia, Canada, England, Hong Kong, India, New Zealand, Norway and Singapore) estimating the cumulative incidence of pH1N1 infection prior to the initiation of pH1N1 vaccination calculated a population cumulative incidence of 11% – 21% (Kelly *et al.*, 2011). This study also revealed differences in susceptibility among different age groups, with the highest estimated cumulative incidence among children (16% – 28% in pre-school aged and 34% – 43% in school-aged) compared to 12% – 15% in young adults and the lowest incidence (2 – 3%) in adults over 60 years old (Kelly *et al.*, 2011).

A wide clinical spectrum of illness was observed during the pH1N1 pandemic, including self-limited illness presenting most commonly with fever, cough and sore throat, and sometimes diarrhea and vomiting. Infection outcome also included more severe disease with respiratory failure associated with viral or bacterial pneumonia and death (Novel Swine-Origin Influenza A (H1N1) Virus Investigation Team, 2009). Although the WHO had originally estimated that 18,500 laboratory confirmed pH1N1-related deaths had occurred worldwide, a later study suggested a much higher global mortality for pH1N1 (Dawood *et al.*, 2012).

1.1.3 Natural history of influenza infection

Influenza virus causes an acute respiratory tract infection and seasonal influenza virus infections are usually mild with self-limiting symptoms in otherwise healthy individuals. The annual attack rates are 5 – 10% in adults and 20 – 30% in children (WHO, 2014b) with individuals repeatedly infected during their lifetime. A cohort study of the prevalence of serum antibodies specific to seasonal influenza in children aged 1 month to 7 years old in the Netherlands found that the first influenza infections occur at least 6 months after birth and all children are seroconverted to at least one influenza strain by age 6 years (Bodewes *et al.*, 2011a). Asymptomatic infection can occur in up to a third of infected individuals (Carrat *et al.*, 2008). The wide clinical spectrum of influenza disease can be determined by virus intrinsic factors such as virulence of the strain, and/or host intrinsic factors such as host genetics (Everitt *et al.*, 2012) and co-morbidities. After an incubation period of about 2 days, infected individuals experience rapid onset of influenza-like-illness (ILI) symptoms including fever (≥38°C), cough, sore throat, headache and myalgia

(Monto *et al.*, 2000). The typical duration of systemic symptoms in humans is 3 – 5 days (Carrat *et al.*, 2008), but respiratory symptoms such as a cough may persist for 1 – 2 weeks. There are significant age-dependent differences in the immune response to influenza and in the severity of disease. An estimated 90% of the mortality associated with seasonal influenza in the United States occurs among the 65 years and older age group (Thompson et al., 2010); hence these high-risk groups are the primary target of annual influenza vaccination programmes.

1.1.4 Pathogenesis of influenza in humans

Influenza disease pathogenesis is determined by the interaction of virus intrinsic virulence factors, host intrinsic factors, as well as the host immune response to influenza infection (Kuiken *et al.*, 2012). Influenza virus enters the human respiratory tract via virus-containing respiratory droplets, and infection proceeds viral attachment (via influenza HA) to sialic acid receptors on ciliated epithelial cells in the upper respiratory tract (URT) (van Riel *et al.*, 2010). Following attachment to the host cell membrane, the influenza virus is endocytosed and acidification in late endocytic vesicles induces a conformational change in viral HA to generate a fusogenic protein that enables viral and endosomal membrane fusion. The viral M2 ion channel imports H+ ions into the virion from the acidified late endosome, disrupting the low pH-sensitive interaction between M1 and viral RNA. This releases viral RNA into the cell cytoplasm for import into the nucleus to be transcribed, followed by translation and synthesis of viral structural and envelope proteins. New virions capable of infecting neighbouring epithelial cells are released by budding from the apical

membrane of infected epithelial cells, via the cleavage action of viral NA (Knipe *et al.*, 2006) (Figure (Fig.) 1.1, middle panel).

Influenza viral tissue tropism is an important determinant of disease phenotype, with seasonal influenza viruses showing strong tropism for the human URT and lower respiratory tract (LRT) (van Riel *et al.*, 2007). Furthermore, influenza viral attachment is preferentially through sialic acid receptors of epithelial cells terminating in galactose α-(2,6)-linkages in humans (Rogers & Paulson, 1983). Viral infectivity is determined by the cleavage and activation of influenza HA by specific host proteases, hence replication permissive influenza infection appears mainly restricted to the epithelial cells of URT and LRT (Zambon, 2001). Local URT disease symptoms including rhinitis, sinusitis, pharyngitis, laryngitis and tracheobronchitis fit with this pattern of virus attachment and tissue restriction for replication (Kuiken *et al.*, 2012, Zambon, 2001). Systemic symptoms (including muscle aches, fatigue, headache and fever) with influenza infection and viral replication have been associated with levels of nasal wash IFN-α and IL-6 and IL-6 in the circulation in human volunteer challenge studies (Hayden *et al.*, 1998, Skoner *et al.*, 1999). This suggests that induction of such proinflammatory cytokines may explain the expression of systemic symptoms from a localised infection (Van Reeth, 2000). Importantly, a recent study identified mucosal inflammatory mediators including nasal lavage monocyte chemotactic protein-3, IFN-α2, as well as plasma IL-10 levels in an innate immune profile that predicted severe influenza disease outcome, independent of age and viral load (Oshansky *et al.*, 2014). This suggests that regulation of innate immune responses can have a significant impact on disease outcome.

1.1.5 Antiviral drugs against influenza

The two main classes of antivirals in use specifically target and inhibit the influenza proteins NA (oseltamivir, zanamivir, peramivir and laninamivir) and M2 (adamantanes including amantadine and rimantadine) (Cox *et al.*, 2004). These drugs may reduce severe complications and deaths associated with influenza, however they are most effective when administered early post infection (within 48 hours post onset of symptoms). Furthermore, the development of resistance can limit the effectiveness of antivirals, and as such the currently circulating influenza viruses are resistant to adamantanes (WHO, 2014b). While antivirals may be useful therapeutic adjuncts, influenza vaccination remains the main form of prophylaxis against influenza.

1.1.6 Licensed influenza vaccines

Currently available seasonal influenza vaccines are the trivalent inactivated virus (TIV), the live attenuated influenza virus (LAIV) vaccine, or the recently approved baculovirus-expressed recombinant HA protein subunit vaccine (Jin & Chen, 2014). All are trivalent composed of two seasonal IAV strains (variants of sH3N2 and sH1N1) and one influenza B virus strain (Nichol & Treanor, 2006), although a quadrivalent LAIV containing two IAVs and two B strains (Victoria-like and Yamagata-like) was first available in 2013 – 2014 influenza season in the US (Jin & Chen, 2014). TIV and recombinant HA subunit vaccines are administered intramuscularly whereas LAIV vaccines are administered intranasally (Jin & Chen, 2014).

Inactivated influenza vaccines are traditionally produced by reassortment in eggs, whereby embryonated eggs are co-infected with the circulating influenza strain and a well-characterised, high yield egg adapted influenza virus (commonly the A/Puerto Rico/8/1934 strain). The resulting combinations are then screened to select the reassortant strain containing the appropriate HA and NA genes along with the remaining genes from the egg adapted strain (Knipe *et al.*, 2006). LAIV vaccines can also be produced by reverse genetics whereby cultured cells are co-transfected with plasmids encoding the HA and NA gene segments of the circulating strain along with plasmids encoding the remaining 6 internal gene segments from donor viruses (commonly the A/Ann Arbor/6/1960 and B/Ann Arbor/1/1966 strains). The donor viruses contain genetic loci conferring cold adapted (efficiently replicate at 25°C, which is otherwise restrictive for replication of wild type strains), temperature-sensitive (replication restricted at 37°C or 39°C) and attenuated (reduced replication in the LRT) phenotypes (Jin & Chen, 2014). TIV is chemically inactivated whole virion, detergent mediated split virus, or subunit vaccine containing purified HA and NA and variable amounts of internal viral proteins (Co *et al.*, 2009). In contrast, LAIV vaccine comprises an attenuated, replication-competent virus and therefore all influenza viral proteins can be expressed.

The monovalent 2009 pandemic vaccine was available in the UK from 21 October 2009 as an inactivated split virus (Pandemrix®, GSK) containing A/California/07/09(H1N1)-virus like strain, or inactivated whole virus vaccine (Celvapan®, Baxter) containing wild-type A/California/07/09(H1N1) (Department of

Heath, 2009). Vaccines used in subsequent influenza seasons post pandemic 2009 in the Northern hemisphere have been trivalent vaccines containing a A/California/07/09(H1N1)-virus like strain, a H3N2 strain (A/Perth/16/2009 (H3N2)-like virus or A/Victoria/361/2011 (H3N2)-like virus) and a B strain (B/Brisbane/60/2008-like virus or B/Wisconsin/1/2010-like virus) (Public Health England, 2012). In the UK in the 2013 – 2014 influenza season, an LAIV (Fluenz, Astra Zeneca) was available for the first time, as was a quadrivalent vaccine containing B/Brisbane/3/2007 (Yamagata lineage strain) in addition to the trivalent strain recommendations (WHO, 2013).

Current influenza vaccines induce protective neutralising antibody responses to surface proteins HA and NA which is effective against infection with matched homologous influenza strains, but poor at protecting against infection with un-matched heterologous (different strains within a given subtype) or heterosubtypic (different subtype) influenza strains (Ellebedy & Webby, 2009). Constant virus mutation generates antibody-escape variants that evade host humoral immunity. This necessitates yearly reformulation, production and deployment of influenza vaccines with little preparation for the infrequent but unpredictable event of a novel strain of pandemic potential. A recent meta-analysis reported an average vaccine efficacy of 59% (95% confidence interval (CI), 51 – 67%) for inactivated influenza vaccines in adults aged 18 – 65 years, and 83% (95% CI, 69 – 91%) for LAIV in children aged 6 months – 7 years (Osterholm *et al.*, 2012). At best, vaccine efficacy of inactivated influenza vaccine against antigenically matched influenza strains was 65% (95% CI, 54% to 73%) while vaccine efficacy against un-matched strains was 52% reported in another meta-analysis (Tricco *et al.*, 2013).

During the recent 2009 H1N1 pandemic, the first wave of the pandemic had already occurred before a matched vaccine was available, further highlighting the need for better vaccine preparedness (Abelin *et al.*, 2011). A universal influenza vaccine capable of inducing durable protective immunity against infection or illness severity with all strains of IAV, including novel reassortant strains could alleviate the constant threat of a severe influenza pandemic.

1.1.7 Experimental universal influenza vaccine development

Much research effort has been directed toward the development of influenza vaccines affording broad protection, particularly against IAVs. The strategies employed target conserved influenza antigens including the HA stalk domain, the M2 protein ectodomain and internal viral proteins including M1, NP, PB1 and PB2. These antigenic targets are naturally weakly immunogenic, hence novel vaccine designs focus on vaccine delivery systems for optimal antigen presentation to improve immunogenicity (Zhang *et al.*, 2014, Lee *et al.*, 2014).

The amino terminal of the ectodomain of influenza M2 (M2e) is highly conserved among human IAVs, and several experimental influenza vaccines have been targeted to induce M2e-specific antibodies to this domain. Candidates completing phase I clinical trials include an adjuvanted intranasal virus-like particle (VLP) M2e conjugated to Hepatitis B core protein (M2e-HBc, ACAM-FLU-ATM) (De Filette *et al.*, 2006), and a fusion protein of M2e with *Salmonella typhimurium* flagellin (M2e-

flagellin, VAX102) given intramuscularly (Turley *et al.*, 2011). These have demonstrated safety and immunogenicity in humans, and reduced morbidity in animal models. Multiple mechanisms have been proposed that may be involved in M2e vaccine-mediated protection including antibody dependent cellular cytotoxicity (ADCC), antibody dependent NK cytotoxicity, complement-mediated lysis, and activation of M2e-specific CD4+ and CD8+ T cells (Zhang *et al.*, 2014, Lee *et al.*, 2014). However, virus neutralising protection is not provided by M2e-based vaccines and hence these may be useful adjuncts to other TIV or LAIV that induce neutralising antibodies (Zhang *et al.*, 2014).

The long α-helix domain of influenza HA stalk (HA2 subunit) is another highly conserved epitope region of IAVs (Wang *et al.*, 2010), and low levels of stalk-reactive antibodies are elicited during seasonal influenza infection (Pica *et al.*, 2012). Monoclonal antibodies targeting the HA stalk are broadly reactive against many IAV subtypes encompassing the 2 phylogenetic groups, group 1 (including H1 subtypes) and group 2 (including H3 subtypes). Passive transfer of such monoclonal stalk-reactive antibodies has demonstrated effective protection in animal models (Zhang *et al.*, 2014, Lee *et al.*, 2014). Furthermore, gene delivery using Adenovirus of a monoclonal stalk-reactive antibody (F16) provided broad protection in mice and ferrets (Limberis *et al.*, 2013). Several experimental approaches have been pursued to enhance the exposure of the stalk domain, including 'headless' stalk domain that require stabilisation (Bommakanti *et al.*, 2010); short stalk peptides fused with carrier proteins (Wang *et al.*, 2010); sequential vaccination with chimeric HA containing the same stalk but different head domains (Krammer *et al.*, 2013), and glycosylation modified head domains to redirect immunogenicity to the stalk domain (Eggink *et al.*,

2014). These approaches can induce neutralising and non-neutralising anti-stalk antibodies. Hence in addition to virus neutralisation, stalk reactive antibodies inhibit viral fusion and HA maturation, as well as mediating ADCC (Zhang *et al.*, 2014). Some stalk-reactive non-neutralising antibodies have demonstrated enhanced disease, highlighting the need for careful evaluation in the development of such stalk-reactive non-neutralising antibodies (Zhang *et al.*, 2014).

The highly conserved internal influenza proteins including NP, M1, PB1 and PB2 are targets of T cell-based universal influenza vaccines. One such candidate is Multimeric-001, containing conserved linear epitopes from the NP, and M1 and also HA proteins of IAVs and type B strains (Atsmon *et al.*, 2012). In phase I and II clinical trials in healthy elderly adults, intramuscular administration of Multimeric-001 has been shown to be safe and immunogenic, inducing Multimeric-001 protein-specific serum immunoglobulin G (IgG) and demonstrating sera-mediated lysis of target cells infected with H1N1, H3N2 and influenza B strains. Furthermore, in the presence of vaccine, PBMC proliferation and increase in cytokines IFN-γ and IL-2 were observed (Atsmon *et al.*, 2012). Another candidate currently in phase I clinical trials to assess safety and immunogenicity is modified vaccinia Ankara (MVA) viral vector encoding NP and M1 (ClinicalTrials.gov, 2014). In an earlier smaller Phase I study, MVA-NP+M1 vaccination (intradermal and intramuscular) induced significant NP- and M1-specific CD8+IFN-γ+ T cells post-vaccination (Berthoud *et al.*, 2011). In a phase IIa MVA-NP+M1 vaccination and intranasal challenge (H3N2, A/Wisconsin/67/2005) study, clinical efficacy was demonstrated with a moderate but statistically significant reduction in days of viral shedding post-challenge in vaccinees compared to controls (Lillie *et al.*, 2012). Although frequencies of M1 immunodominant epitope tetramer-

specific CD8+ T cells up to day 7 post challenge were similar between vaccinees and controls, there were differences in the quality of antigen-specific T cells, since T cells in vaccinees showed higher levels of expression of cytotoxicity markers including granzyme A and perforin (Powell *et al.*, 2013).

Considering the recent introduction of LAIV vaccination in the UK, it is important to highlight some LAIV based universal influenza vaccine candidates that are in pre-clinical research phases of development. A pseudotyped influenza virus made replication deficient through disruption of the HA open reading frame (S-FLU) has been produced (Powell *et al.*, 2012). The A/PR/8/34 (H1N1) strain on which S-FLU is based is otherwise highly virulent in mice, but S-FLU preparation completely lacked virulence and induced protection against homologous H1N1 and also heterologous H3N2 IAVs. Robust NP- and HA- specific CTL responses were induced in the lung and were associated with protection including reduced lung virus replication and prevention of weight loss following challenge (Powell *et al.*, 2012).

1.2 The immune response to influenza

1.2.1 The innate immune response to influenza

Influenza primarily infects ciliated mucosal epithelial cells in the human respiratory tract (Matrosovich *et al.*, 2004, Hers, 1966) and initiates innate and adaptive immune responses ultimately resulting in inhibition of viral replication (Kreijtz *et al.*, 2011) (summarised in Fig. 1.2.1). Before reaching these target cells, inhaled influenza virus

encounters a number of host defence mechanisms in the respiratory tract (Nicholls, 2013).

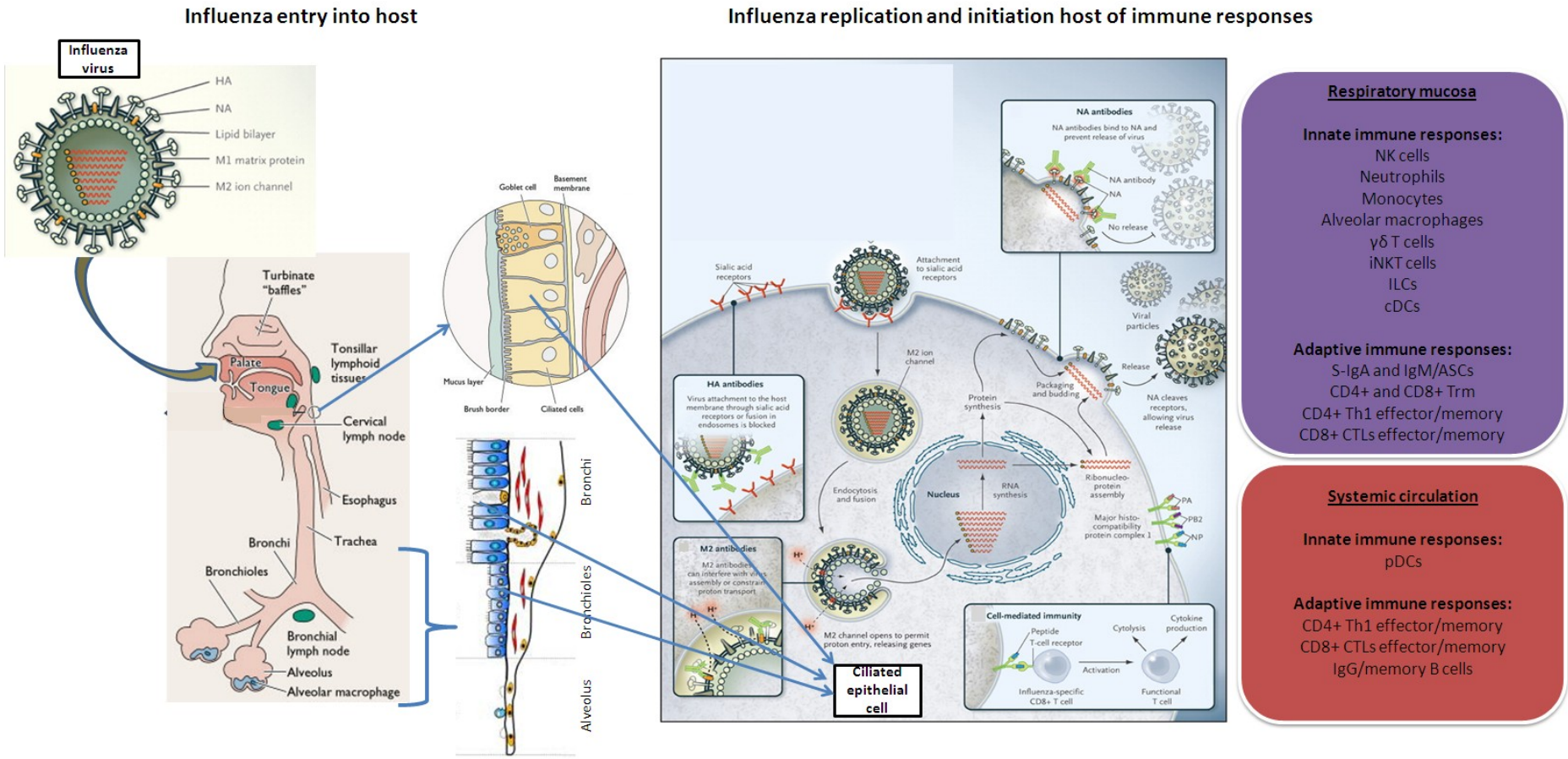

Figure 1.2.1 Immune responses to influenza infection and replication in the human respiratory tract.

Figure adapted from images in (Trifonov *et al.*, 2009, Racaniello, 2009, Behrens & Stoll, 2006, Lambert & Fauci, 2010).

Mucins are secreted or epithelial cell-associated glycoproteins that bind cells, cell debris and polypeptides constituting mucus in the airways. These glycoproteins are highly sialylated, hence mucins can bind influenza virus and the viscous gel-like nature of mucus also act as a physical barrier to infection (Nicholls, 2013, Cohen *et al.*, 2013). However, influenza NA activity enables the virus to cleave sialic acid residues in mucin and penetrate (Cohen *et al.*, 2013). Influenza viruses penetrating to the lung alveoli encounter lectins, proteins that bind carbohydrates and of which there are various types (Ng *et al.*, 2012). The C-type lectins surfactant protein A (SP-A) and surfactant protein D (SP-D) are produced by Type II pneumocytes of the alveoli and are the two main anti-influenza lectins in the lungs. SP-A contains sialic acid and acts as a decoy receptor to bind free influenza virus, and SP-D binds mannose type oligosaccharides on glycosylated HA and NA thereby aggregating virus particles (Nicholls, 2013) resulting in viral opsonisation.

Various cell populations in the respiratory mucosa and lungs are involved in the innate immune response to influenza. Neutrophils are not abundant cell types in the lungs, however, during influenza infection neutrophils can be recruited as an early responder population and a protective role in influenza infection has been demonstrated in mouse models (Tate *et al.*, 2011). These phagocytic cells can bind lectin opsonised influenza and eliminate virus through neutrophil respiratory burst responses (Hartshorn *et al.*, 1996). Other important phagocytic cells are resident alveolar macrophages that express mannose receptor and galactose-type lectin receptor to bind glycosylated influenza virus for phagocytosis. Resident alveolar

macrophages are also permissive to influenza viral infection and replication (Yu *et al.*, 2011).

Intracellularly, influenza RNA is recognised by pathogen recognition receptors Toll-like receptor 7 (TLR7), NOD-like receptor 3 (NLRP3) and retinoic acid inducible gene I (RIG-I). These are expressed in target cells and influenza infection activates signal transduction and initiates an immediate inflammatory response that includes expression of pro-inflammatory cytokines IL-12 and IL-6, and type I interferons (IFNs) (McGill *et al.*, 2009). Type I IFNs inhibit viral replication by inducing interferon stimulated genes and inhibiting protein synthesis in infected host cells (Hsu *et al.*, 2012). However, influenza viruses have evolved strategies to evade this antiviral immunity, for example through the IFN antagonising effect of the NS-1 protein (Hsu *et al.*, 2012). Hence other arms of the host immune system are induced.

The inflammatory milieu activates resident leukocytes and recruits other immune cells such as CCR2+ CD11b+ monocytes that can modulate inflammation and mediate killing of virally infected cells (Valkenburg *et al.*, 2011). *In vitro* infection of primary human alveolar macrophages induces pro-inflammatory cytokines including TNF-α and chemokines such as CXCL-10 (also known as Inteferon gamma-induced protein, IP-10) that activate and attract other immune cells to the site of infection (Yu *et al.*, 2011). Natural killer (NK) cells can be directly activated via type I IFN signaling following influenza virus infection to mount target cell lysis and cytokine production, including IFN-γ (Hwang *et al.*, 2012). Furthermore, NK cell-derived IFN-γ production has been shown to require IL-2 from influenza-specific T cells in human PBMC (He

et al., 2004), highlighting the interactions between the innate and adaptive immune response to influenza.

The involvement of other innate cell populations in the immune response to influenza has also been reported. The innate-like lymphocytes invariant natural killer T (iNKT) cells have been shown to be important in regulating the early innate immune response to influenza infection (Ho *et al.*, 2008, Kok *et al.*, 2012). iNKT cells also influenced the adaptive immune response by maintaining lung-homing dendritic cells (DCs) that enhance influenza-specific CD8+ T cell response in draining lymph nodes and lungs of mice (Paget *et al.*, 2011). Another innate-like lymphocyte population, gamma-delta T ($\gamma\delta$ T) cells have been proposed in the regulation and resolution of inflammation in the lungs of influenza-infected mice (Carding *et al.*, 1990). *Ex vivo* $\gamma\delta$ T cells from human PBMC infected with influenza virus were found to rapidly upregulate activation markers and secrete antiviral IFN-γ (Jameson *et al.*, 2010). The recently identified Group 2 innate lymphoid cells (ILC2s) or nuocytes producing type 2 cytokines such as IL-5, found as lung resident populations in mice and humans, were shown to be important in maintaining lung epithelial integrity in the resolution phase of influenza infection in mice (Monticelli *et al.*, 2011). The relevance and importance of these other innate cell populations in human influenza infection remains to be determined.

DCs are the main professional antigen presenting cells (APCs) of the immune system and include two main subsets: conventional DCs (cDCs) and plasmacytoid DCs (pDCs) (GeurtsvanKessel & Lambrecht, 2008). Lung DCs are pivotal in the

initiation of influenza-specific CD8+ T cell responses for rapid viral clearance in mice (McGill *et al.*, 2008). Two populations of resident lung DCs with distinct anatomical localisation can be distinguished based on the expression of the alpha-E and alpha-M integrins CD103 and CD11b respectively (Sung *et al.*, 2006). CD103+CD11b- migratory lung DCs that localise to the airway mucosa have been shown to transport influenza antigen from the lungs via the afferent lymphatics to mediastinal draining lymph nodes as soon as 20 hours post-infection, and process and present antigen via Major Histocompatibility Complex class I (MHC-I) to naive CD8+ T cells (Ho *et al.*, 2011). CD103-CD11b+ DCs that are localised to the submucosa and lung parenchyma, efficiently take up influenza antigen post-infection and produce pro-inflammatory cytokines such as TNF-α, but this subset migrates poorly (Ho *et al.*, 2011). pDCs that are recruited from the circulation have also been shown to activate influenza-specific CD4+ and CD8+ T cells, in addition to their antiviral role in producing type I IFN in response to influenza (Fonteneau *et al.*, 2003). However, pDCs were not required for influenza clearance from the lungs of infected mice (GeurtsvanKessel *et al.*, 2008).

1.2.2 The adaptive immune response to influenza

Naïve CD4+ and CD8+ T cells in the lung draining lymph nodes are presented with antigen by migratory cDCs. Naïve B cells in the mediastinal lymph nodes also encounter antigen transported by antigen-carrying DCs (Sealy *et al.*, 2003). In humans, both CD4+ and CD8+ T cells from PBMC induced by seasonal H3N2 and H1N1 IAVs through prior exposure are directed toward the relatively conserved core proteins M1 and NP, and also PB1, PB2 and PA (Lee *et al.*, 2008). However, only

CD4+ T cells recognised epitopes from the influenza surface glycoproteins HA and NA presented by Major Histocompatibility Complex class II (MHC-II), whereas CD8+ T cells recognised epitopes from the core antigens, particularly NP, M1 and PA presented by MHC-I (Lee *et al.*, 2008).

Intra- (helper T cell-dependent) and extra- follicular (helper T cell-independent) B cell responses are initiated following recognition of viral antigens (Sealy *et al.*, 2003), particularly directed to HA and NA antigens (Potter & Oxford, 1979). Cognate antigen recognition as well as co-stimulation signals and polarising cytokines from APCs results in clonal expansion of influenza-specific T cells and B cells (Kreijtz *et al.*, 2011, Valkenburg *et al.*, 2011).

Activated effector CD4+ T helper 2 (Th2) cells produce IL-4 and IL-13 and promote intra-follicular B cell responses, whereas IFN-γ and IL-2 producing CD4+ T helper 1 (Th1) cells promote cellular responses including induction of CD8+ cytotoxic T lymphocytes (CTL) (Kreijtz *et al.*, 2011). Activated effector CD8+ T cells traffic out of the mediastinal lymph node via the efferent lymphatics and are recruited to the site of infection where they carry out FAS/perforin- (Topham *et al.*, 1997) and TRAIL- (Brincks *et al.*, 2008) mediated lysis of infected cells. Influenza-specific CD8+ T cells also sequentially secrete IFN-γ, TNF-α and IL-2 upon recognition of antigen (La Gruta *et al.*, 2004). Other subsets of CD4+ T cells, including regulatory T cell (Tregs) and T helper 17 (Th17) cells are activated upon influenza infection in mice. Tregs regulate effector CD4+ and CD8+ T cells (Betts *et al.*, 2012), and have also been reported to regulate CD8+ T cell memory development (Brincks *et al.*, 2013) in

influenza infected mice. Th17 cells were shown to play an important role in protecting naïve mice against lethal influenza challenge infection (Hamada *et al.*, 2009). Interestingly, IL-10 from influenza-specific CD8+ T cells in the lungs of influenza infected mice has also been shown to limit immunopathology (Sun *et al.*, 2009).

Following LAIV (sH1N1 or sH3N2 strain) primary challenge infection in children aged 1.5 – 4.5 years old, anti-HA immunoglobulin classes G, (IgG), IgM, and the less prevalent IgA antibodies were all detectable in serum within 2 weeks of infection. IgM and IgA antibodies reached a peak and declined whereas IgG antibodies peaked at 4 – 7 weeks post LAIV infection (Murphy *et al.*, 1982) (Fig. 1.3.1). Waning of mean titres of serum anti-HA antibodies after infection or vaccination with IAV and B viruses occurred over the first 6 months post-peak response, and then levels were maintained for 2 – 3 years in the absence of further antigen re-exposure (Cate *et al.*, 1977, Couch & Kasel, 1983). Anti-HA IgG antibodies from the serum or secreted at the airway mucosal surfaces mainly bind to the trimeric globular head of the HA, thereby inhibiting virus attachment and entry into host cells and effectively neutralising the virus to give sterilising immunity (Potter & Oxford, 1979, Couch & Kasel, 1983). Anti-NA antibodies bind and inhibit the enzymatic activity of NA, thereby preventing the cleavage of sialic acid residues on the infected cell surface that facilitates the release and spread of progeny virions (Couch & Kasel, 1983, Gerhard, 2001). Antibodies against the less abundant viral membrane protein M2 have been reported in mice (Zebedee & Lamb, 1988), but are rare following natural infection in humans (Couch & Kasel, 1983). Anti-NP IgG antibodies have also been

reported to mediate viral clearance in mice (Lamere *et al.*, 2011) but anti-M2 or anti-NP antibodies cannot protect against infection in humans (Couch & Kasel, 1983).

Mouse studies suggest antigen is cleared within 10 to 14 days of primary influenza infection (Flynn *et al.*, 1999) although prolonged antigen presentation to CD4+ T cells for up to 3 to 4 weeks has been reported (Jelley-Gibbs *et al.*, 2005). A meta-analysis of human volunteer influenza challenge studies (with H1N1, H3N2 or Influenza B virus) found that influenza virus shedding increased during day 1 after intra-nasal inoculation, peaked on day 2 and lasted less than 5 days, with virus clearance by day 8 (Carrat *et al.*, 2008) (Fig. 1.3.1).

1.2.3 Mucosal immune responses to influenza

Influenza enters and initiates replication at the human respiratory mucosa hence mucosal immunity can provide a critical first line of defence. Mucosal immune effector mechanisms include mucosal antibodies (IgA, IgM and IgG isotypes) that neutralise viruses; evoke cytotoxic effects on infected cells via eosinophilic and neutralphilic granulocytes and NK cells; and opsonise pathogens for phagocytes to process and present antigens to activate mucosal effector T cells. The mucosa-associated lymphoid tissue (MALT) encompasses nasopharynx-associated lymphoid tissue (NALT) and gut-associated lymphoid tissue (GALT). In humans, NALT comprises of the nasopharyngeal adenoids, paired tubal tonsils, and the paired palatine and lingual tonsils (Rose *et al.*, 2012). Similar to the systemic lymphoid tissues, the MALT is anatomically and functionally organized, with activation sites at follicles where B and T cells are activated, clonally expand and differentiate into

effector cells. Effector cells migrate from the NALT via the cervical lymph nodes and thoracic duct into the general circulation, to reach effector sites in the lamina propria underneath the mucosal epithelium covering the internal surface of the whole body. Hence effector functions of CTLs and antibody secreting cell (ASC) -secreted mucosal IgA and IgM induced at one site can act across this common mucosal immune system (Rose *et al.*, 2012, Tamura & Kurata, 2004).

Secretory IgA (S-IgA) are dimeric IgA antibodies produced by ASCs and are the main antibody isotype found in mucosal secretions (Rose *et al.*, 2012). A high prevalence of influenza-specific ASCs were found in nasal mucosa of individuals with no reported influenza in the preceding year (Brokstad *et al.*, 2001). Furthermore, in the absence of serum antibodies, nasal wash S-IgA was a major determinant of resistance to infection and illness in volunteer challenge studies (Clements *et al.*, 1986). Hence mucosal S-IgA appears to play a significant role in anti-influenza immunity. However, mucosal protection mediated by S-IgA can be substituted, since mice deficient in IgA ($IgA^{-/-}$) have similar lung viral titres and morbidity as wild type mice ($IgA^{+/+}$) upon influenza infection (Mbawuike *et al.*, 1999).

Respiratory mucosal immunity against influenza can also be mediated by cellular components including mucosal NK cells, $\gamma\delta$T cells, ILCs (as discussed in the above section on the innate immune response to influenza) and mucosal T cells (as discussed below on memory T cell subsets and memory T cell response to influenza infection).

1.3 Immunological memory to influenza

1.3.1 Humoral memory response to influenza infection

Following natural pH1N1 infection in humans, there is a rise in neutralising serum anti-HA IgG antibody response that was shown to peak at 1 month post-infection followed by waning in the antibody response within 11 months post-infection (Liu *et al.*, 2012). However, in one pH1N1-infected individual followed longitudinally, strain-specific serum antibodies were detectable up to 700 days post-infection (Wagar *et al.*, 2011). Strain-specific serum antibodies to influenza have been detected in individuals surviving infection with 1918 H1N1 up to 90 years later (Yu *et al.*, 2008). Furthermore, epidemiological evidence suggests that protective immunity to H1N1 can last as long as 20 years (Couch & Kasel, 1983). In a mouse model of influenza infection, it has been suggested that the long-term maintenance of the humoral response and serum antibodies to influenza is from the continual conversion of influenza-specific splenic memory B cells to long-lived antibody-secreting plasma cells that reside in the bone marrow (Ng *et al.*, 2014).

pH1N1-specific neutralising antibody responses to pH1N1 inactivated vaccine in vaccinated individuals followed similar kinetics to natural pH1N1 infection (Liu *et al.*, 2012). Although the post-vaccination haemagglutination inhibition (HAI) titre was higher at 2 months post-vaccination compared to infected individuals, the antibody response was more durable over the 14 month study period in naturally infected

individuals compared to vaccinated individuals (Liu *et al.*, 2012). Whilst strain-specific serum antibodies may be long-lived against homologous virus, the antigenic targets (HA and NA) have high mutation rates due to host immune pressure. Hence humoral immunity is evaded by heterologous influenza strains, enabling multiple infections of the same individuals over their lifetime.

1.3.2 Memory T cell subsets

Human peripheral blood CD4+ and CD8+ T cells subdivided based on the expression of the lymph node homing receptor CCR7 in combination with the cell activation marker CD45RA (differentially expressed on human naïve and memory T cells) led to the identification of distinct subsets of circulating memory T cells and the coining of central memory (Tcm) and effector memory (Tem) T cells (Sallusto *et al.*, 1999). The two subsets therefore possess differential migratory capacity, with CCR7+ Tcm representing an antigen-experienced, clonally expanded circulating population that can enter lymphoid organs and mount secondary proliferative responses. CCR7- Tem showed enhanced responsiveness to activation, representing an antigen-experienced, peripherally circulating population that can enter inflammatory tissues and readily mediate inflammatory or cytotoxic effector functions. Both subsets were shown to proliferate in response to recall tetanus toxoid antigen in PBMC from individuals up to 10 years post-vaccination, demonstrating *in vivo* maintenance. Furthermore, progressive shortening of telomere length in CD4+ naïve compared to Tcm and Tem cells suggested progressively increasing number of cell divisions among the subsets. *In vitro* stimulation revealed a stepwise differentiation program of naïve to Tcm to Tem (Sallusto *et al.*, 1999). CD45RA is

also re-expressed on a population of CD8+ T cells termed terminal late effectors (Temra) (Hamann *et al.*, 1997, Champagne *et al.*, 2001).

Subsequently, studies in mice have identified these subsets, addressed the lineage relationships, and compared the persistence and protective capacities of Tem versus Tcm *in vivo*. The initial study had proposed division of labour among phenotypically and functionally distinct memory T cell subsets located in anatomically different sites (Sallusto *et al.*, 1999). In support of this, other studies in mice have found that memory CD8+ T cells in non-lymphoid organs had more robust cytotoxic activity than memory CD8+ T cells in lymphoid organs following systemic vesicular stomatitis virus or oral *Listeria monocytogenes* (LM) infection (Masopust *et al.*, 2001). Similarly, CD4+ T cells in non-lymphoid organs produced higher levels of IFN-γ relative to IL-2 compared to memory CD4+ T cells in lymphoid organs following vaccination with ovalubumin peptide and lipopolysaccharide (Reinhardt *et al.*, 2001).

Due to their enhanced proliferative capacity, adoptively transferred antigen-specific CD8+ Tcm cells were more effective than antigen-specific CD8+ Tem cells in controlling Lymphocytic choriomeningitis virus (LCMV) or vaccinia viral replication in models of infection, irrespective of the routes or sites of infection (Wherry *et al.*, 2003). Similarly, in a melanoma tumour mouse model, adoptive transfer of *in vitro* generated tumour-reactive CD8+ Tcm cells was more effective than Tem cells in tumour eradication (Klebanoff *et al.*, 2005). However, other studies have suggested the converse with respect to the memory subset correlating with protection. Antigen-specific CD8+ Tem cells were more efficient than Tcm cells in secondary recall

response to intranasal parainfluenza virus infection in mice (Roberts & Woodland, 2004). CD8+ Tem and effector T cells also mediated protection against peripheral vaccinia virus infection (Bachmann *et al.*, 2005, Olson *et al.*, 2013) and LM infection (Olson *et al.*, 2013), whereas protection against systemic LCMV infection was mediated by Tcm (Bachmann *et al.*, 2005) in mice.

In contrast to the results dissecting lineage relationships of Tem and Tcm from *in vitro* studies on human PBMC (Sallusto *et al.*, 1999), a linear differentiation of naïve to effector to Tem to Tcm cells was observed in mice *in vivo* (Wherry *et al.*, 2003). Further, the self-renewing Tcm cells exhibited long-term persistence *in vivo*, whereas Tem cells represented an intermediate state in the effector-to-memory transition (Wherry *et al.*, 2003).

The original seminal work (Sallusto *et al.*, 1999) provided a conceptual model for the organisation of various circulating memory T cell subsets. But subsequent contrasting results on the protective capacities of Tem and Tcm cautions at the simplicity of the model, although differences in the experimental conditions including the route of infection, pathogen dose, or pathogen tropism could account for this (Kaech, 2014). Distinct from circulating Tem and Tcm cells, tissue-resident memory T cells (Trm) have been identified at mucosal sites that provide defense at portals of pathogen entry (Schenkel *et al.*, 2013, Wu *et al.*, 2014). Therefore, optimal protection against pathogens may require diverse populations of memory T cells (Kaech, 2014).

1.3.3 Memory T cells to influenza infection

Influenza is an acute infection with rapid antigen clearance; with a shift from effector T cells to memory T cells following resolution of infection and antigen clearance (Pantaleo & Harari, 2006). In human peripheral blood, a decrease in influenza tetramer-specific CD8+ effector and Temra but an increase in Tcm following natural infection has been reported (Hillaire *et al.*, 2011b). Mouse studies have also highlighted the importance of long-lived, influenza-specific Trm cells in the lungs to provide rapid effector function and T cell dependent influenza immunity at the site of infection (Masopust & Picker, 2012, Hogan *et al.*, 2001).

There are limited reports on the kinetics (Fig. 1.3.1) of influenza-specific T cell responses following natural infection in humans. One study prospectively following a single infected individual showed robust pH1N1-specific CD4+IFN-γ+ and CD8+IFN-γ+ T cell responses in the peripheral blood that peaked at 3 weeks post-infection, and then declined reaching baseline levels by day 700 post-infection (Wagar *et al.*, 2011). Another study suggested that there is a rapid recall CD8+ T cell response peaking within a week post-infection with pH1N1 that contracted within 3 weeks post-infection at group level, but there were also inter-individual differences in the kinetics (Hillaire *et al.*, 2011b). H1N1-specific CTL activity measured at 2 weeks post-infection showed an increase compared to 2 weeks pre-infection in one individual infected with H1N1 in 1978 (McMichael *et al.*, 1983a). In the same study, during a 6-year period between 1977 and 1982, there was a decline in CTL responses in healthy individuals with an estimated CTL half-life of 2 – 3 years within

the cohort, coinciding with reduced influenza activity in the community during the same period (McMichael *et al.*, 1983a).

While some influenza-specific T cell responses are thought to be protective, they have also been implicated in influenza illness exacerbation. Frequencies of NP- and M1- specific CD4+IFN-γ+ T cells were higher in PBMC during the early phase of disease from hospitalised patients subsequently developing more severe pH1N1 illness, compared to mild infections and PBMC responses from healthy controls (Zhao *et al.*, 2012). In 2 individuals where paired lung and peripheral blood sampling was performed, a significantly higher number of tetramer-specific CD8+ T cells were observed in bronchoalveolar lavage samples compared to PBMC, implying homing of influenza-specific CD8+ T cells to the site of disease. In this study (Zhao *et al.*, 2012), sampling was within 48 hours of hospital admission without longitudinal follow-up of T cell responses, hence the kinetics of the pH1N1-specific CD4+ T cell response over the course of infection was not reported. Thus it is unclear how the influenza-specific CD4+ T cells, which are associated with severity of illness (demonstrated at an early time-point post-infection), develop with resolving infection.

Polyfunctional T cells are important in T cell memory and vaccine clinical trials (Seder *et al.*, 2008). These are defined as cells capable of producing 2 or more cytokines and with or without proliferation capability, and have been shown to be functionally superior to monofunctional (single cytokine producing) T cells in viral (Harari *et al.*, 2004, Betts *et al.*, 2006), bacterial (Wilkinson & Wilkinson, 2010) and

parasitic (Darrah *et al.*, 2007) infections. However, the prevalence and role of polyfunctional T cells in response to influenza infection in humans is not known.

1.3.4 Memory T cells to influenza vaccination

In humans the duration of inactivated vaccine-induced boost in CTL responses has been reported to last less than 12 months (McMichael *et al.*, 1981, Ennis *et al.*, 1981), whereas boosting following natural infection appears to last longer (McMichael *et al.*, 1983a). Many studies have demonstrated enhanced *ex vivo* IFN-γ production from human PBMC detected from 7 to 10 days (He *et al.*, 2006, He *et al.*, 2008); 4 weeks (Avetisyan *et al.*, 2005); 1 month (Tu *et al.*, 2010) and from 2 weeks to 1 month or 2 months (Co *et al.*, 2008, Terajima *et al.*, 2008) post-vaccination with TIV compared to pre-vaccination. Similarly, *ex vivo* IFN-γ production from human PBMC was enhanced following LAIV vaccination compared to pre-vaccination (He *et al.*, 2006, He *et al.*, 2008, Forrest *et al.*, 2008).

Enhanced influenza-specific T cell proliferation following TIV vaccination (Co *et al.*, 2008, Guthrie *et al.*, 2004, Murasko *et al.*, 2002) and recombinant HA vaccination (Powers *et al.*, 1997) has been observed, suggesting vaccine-induced clonal expansion of antigen-specific cells. *In vitro* CTL cytotoxicity following LAIV vaccination (Gorse & Belshe, 1990, McMichael *et al.*, 1983b) has also been reported. Together these studies demonstrate that influenza vaccination can enhance influenza-specific T cell responses in humans.

Importantly a few studies have also correlated influenza vaccine-induced T cell responses with protection against clinical influenza disease (Forrest *et al.*, 2008, Murasko *et al.*, 2002, McElhaney *et al.*, 2006). In a large placebo-controlled efficacy trial of LAIV in young children aged 3 – 36 months, vaccine-induced IFN-γ+ PBMC responses correlated with protection against community-acquired, culture confirmed influenza. The majority of individuals with vaccine-specific cells greater than 100 IFN-γ+ SFC per million PBMC (on 7 – 10 days post-vaccination) were protected, proposing a possible level of cellular response to target in influenza vaccine development and evaluation (Forrest *et al.*, 2008). In a prospective study of elderly (older than 60 years) individuals, *ex vivo* influenza virus-specific PBMC responses, including the mean IFN-γ:IL-10 ratio and granzyme B levels in PBMC lysate were significantly lower pre- and post- TIV vaccination in individuals subsequently developing laboratory diagnosed influenza illness compared to those who did not. In contrast however, pre- or post-vaccination serum antibody titres did not distinguish between these individuals (McElhaney *et al.*, 2006). In another study of the elderly who were vaccinated every year over the four years of the study period, the risk of developing influenza disease was the highest in individuals without vaccine-induced serum antibody or T cell proliferative responses. However, the risk of developing influenza disease subsequent to vaccination was the same in individuals with a cell-mediated response alone, an antibody response alone, or both cell-mediated and antibody responses (Murasko *et al.*, 2002). Thus the importance of cell-mediated immune responses in vaccine-induced protection from influenza disease has been demonstrated in at least a subset of the population, including the very young and the elderly.

Influenza vaccine adjuvants, the route of vaccination and the type of vaccine used (inactivated or LAIV), have all been shown to affect the quantity and/or the quality of human T cell responses. The frequency of proliferation marker Ki-67-expressing influenza-specific CD4+ T cells in PBMC that produce IFN-γ, IL-2 and/or TNF-α *in vitro* showed a sharp but transient rise at 4 - 6 days after vaccination with non-adjuvanted inactivated pH1N1 vaccine (Li *et al.*, 2012). The frequency of Ki-67+ CD4+ T cells then declined rapidly, and at 10 days after vaccination, both Ki-67+ and overall influenza-specific CD4+ T cell numbers returned to pre-vaccination levels (Li *et al.*, 2012). In healthy adults, single and multi-cytokine CD4+ T cells positive for combinations of IFN-γ, TNF-α and IL-2 were significantly increased at 7, 14 and 21 days post-vaccination with GSK Pandemrix monovalent split virus vaccine adjuvanted with oil-in-water adjuvant AS03, compared to pre-vaccination (Pathirana *et al.*, 2012). Using the same adjuvanted vaccine, a higher increase in frequency of activation marker (CD40L) or cytokine (IFN-γ, IL-2 or TNF-α) positive CD4+ T cell responses was observed over 42 days following vaccination with adjuvanted compared to non-adjuvanted inactivated pH1N1 vaccine in healthy adults (Roman *et al.*, 2011). Thus adjuvanted pH1N1 vaccine appears to induce a higher magnitude and longer duration of activated influenza-specific CD4+ T cell responses compared to non-adjuvanted vaccine.

Regarding the route of administration, intramuscular seasonal TIV vaccination of healthy adults induced only CD4+ T cell responses to influenza vaccine at 14 and 28 days post influenza vaccination, whereas transcutaneous TIV vaccination induced both CD4+IFN-γ+ and CD8+IFN-γ+ T cells to influenza vaccine (Vogt *et al.*, 2008).

Regarding the functional profile of natural influenza infection or inactivated vaccine – induced T cell responses, one study suggests a greater proportion of antigen-specific CD4+IFN-γ+IL-2+ dual cytokine positive cells following pH1N1 vaccination of healthy adults compared to a predominant CD4+IFN-γ+IL-2- T cell signature following natural pH1N1 infection (Schmidt *et al.*, 2012).

Currently available inactivated influenza vaccines are designed and selected to preferentially induce neutralising antibody responses, hence it is expected that some CD4+ helper T cell responses will be induced to provide B cell help for antibody production. Indeed, recent reports have correlated the circulating counterpart of follicular helper T (Tfh) cells induced post-vaccination (with inactivated vaccine) that predict neutralising antibody titre rise (Spensieri *et al.*, 2013). In children aged 6 – 35 months vaccinated with combinations of TIV vaccine and LAIV prime-boost, only regimens containing LAIV showed enhanced IFN-γ positive and proliferating CD4+ and CD8+ T cells and $\gamma\delta$ T cells at 1 month and 60 days post-vaccination (Hoft *et al.*, 2011). Enhanced frequencies of CD4+IFN-γ+ and CD8+IFN-γ+ T cell responses were reported following LAIV vaccination compared to TIV vaccination in 5 to 9 year old children, although this was not the same for healthy adults (He *et al.*, 2006). However, increased CTL activity measured 1 month post-vaccination in healthy adults was more frequent in inactivated whole virus vaccines (detected in 6/8 individuals) compared to inactivated subunit vaccines (detected in 3/9 individuals) (McMichael *et al.*, 1983b). Together these studies demonstrate that LAIV may be superior to TIV in inducing T cell (including CD8+ T cells) responses, especially in young children. Furthermore, different types of inactivated vaccines may differ in their ability to induce cell-mediated immunity in healthy adults.

The existing literature reports on memory T cells to influenza infection (section 1.3.3) or influenza vaccination demonstrate induction of antigen-experienced influenza-specific T cells following infection or vaccination, and notably, some have demonstrated a significant role of cell-mediated immunity in vaccine-induced protection against influenza disease. Outstanding knowledge gaps include the longevity of these influenza-specific responses, particularly in the context of natural influenza infection. This can be addressed through the careful, prospective study of T cell responses and a comprehensive assessment of their phenotype in healthy individuals naturally exposed to influenza.

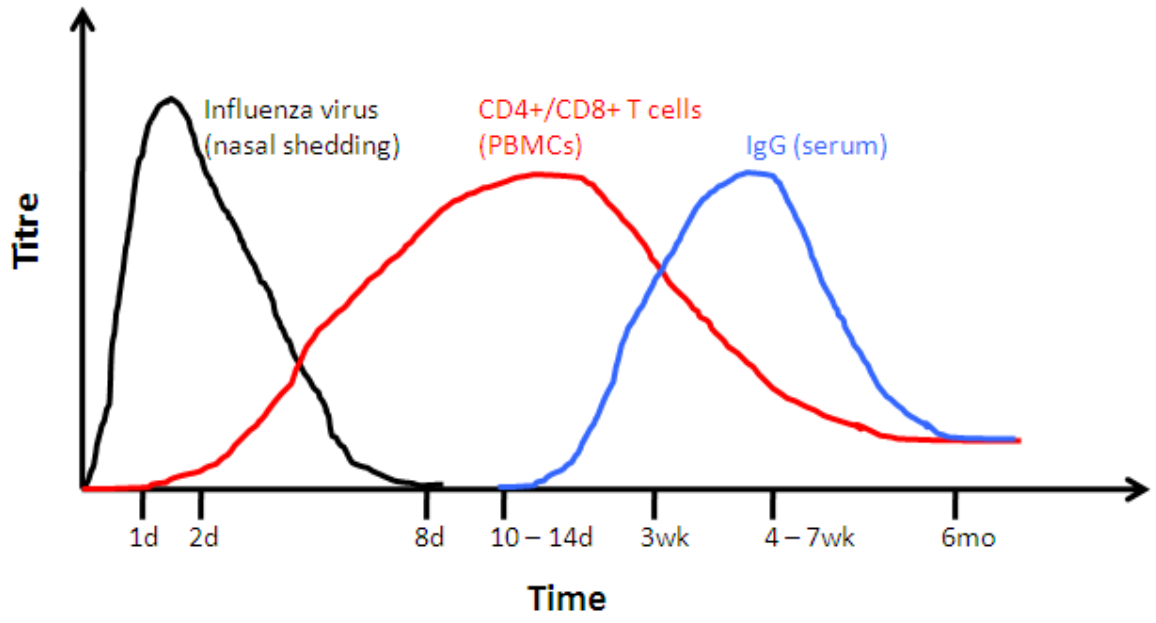

Figure 1.3.1 Course of viral shedding and adaptive immune responses to influenza measured in peripheral blood of humans naturally infected or following primary infection with LAIV.

Figure constructed with data from (Carrat *et al.*, 2008, Murphy *et al.*, 1982, Cate *et al.*, 1977, Wagar *et al.*, 2011, Hillaire *et al.*, 2011b).

1.4 Heterosubtypic immunity (HSI) to influenza

1.4.1 The immunological basis for HSI

Cross-reactive immune responses to conserved regions of one influenza subtype generated through prior exposure to a different influenza subtype may provide some protection against disease, and this HSI was first described in 1965 (Schulman & Kilbourne, 1965). Priming with an H1N1 virus 4 weeks prior to lethal challenge infection with a H2N2 virus resulted in reduced lung viral titres (as early as 24 – 28 hours post-challenge), less extensive lung lesions and decreased mortality in mice (Schulman & Kilbourne, 1965). Subsequently, many studies have corroborated and extended knowledge of HSI in different species including mice (Table 1.4.1), chickens (Table 1.4.1), ferrets (Table 1.4.1), nonhuman primates (Table 1.4.1), pigs (Table 1.4.1), cotton rats (Straight *et al.*, 2006), ducks (Fereidouni *et al.*, 2009) and guinea pigs (Steel *et al.*, 2010).

Both B cell and T cell components of the adaptive immune system can mediate HSI (Grebe *et al.*, 2008). Early work showed that a large proportion of CTLs induced after influenza infection in humans (McMichael *et al.*, 1983b, Gotch *et al.*, 1987, McMichael *et al.*, 1986) or mice (Yewdell *et al.*, 1985, Townsend & Skehel, 1984) were directed against the conserved NP and M1 proteins of influenza, and target cell lysis by mouse CTLs was cross-reactive between different influenza subtypes

(Zweerink *et al.*, 1977a, Zweerink *et al.*, 1977b). More recent immunoinformatic analysis of all the known influenza-specific B cell and T cell epitopes listed in the Immune Epitope Database (www.immuneepitope.org) has shown that conservation of T cell epitopes (51%) between recently circulating H1N1 strains and the novel pH1N1 is much greater than conservation of B cell epitopes (31%), reflecting the conservation or variability in respective antigens from which the epitopes are derived (Greenbaum *et al.*, 2009). Furthermore, CD8+ T cell epitopes had a higher level of sequence similarity (69%) compared to epitopes targeting CD4+ T cells (41%) (Greenbaum *et al.*, 2009). IFN-γ producing memory T cell PBMC responses cross-reactive between seasonal (sH3N2) and avian (H5N1) IAVs detected in healthy individuals showed the highest prevalence of responses directed to the conserved core proteins M1, NP and PB1 (Lee *et al.*, 2008). Cross-reactivity of circulating memory CD4+ (Ge *et al.*, 2010, Richards *et al.*, 2010) and CD8+ (Tu *et al.*, 2010, Gras *et al.*, 2010, Scheible *et al.*, 2011) T cells with pH1N1 in PBMC obtained from healthy individuals before the 2009 pandemic has also been reported. Targeting such conserved influenza proteins to induce immune responses that are therefore cross-reactive between influenza subtypes forms the basis of HSI to influenza.

1.4.2 B cell-mediated heterosubtypic anti-influenza immunity

Pre-existing, broadly cross-reactive virus neutralising antibodies directed towards conserved regions of H3, H5 and H7 subtypes have been detected at very low levels (0.001% of total IgG) in human serum (Sui *et al.*, 2011). IgM+ memory B cells recovered from recent seasonal influenza vaccinees enabled identification of H5N1 and H1N1 cross-reactive antibodies directed towards an epitope on the conserved stem region of HA (Throsby *et al.*, 2008). Furthermore, this monoclonal antibody

given prophylactically to mice enhanced survival against lethal challenge 24 hours later with H5N1 or H1N1 (Throsby *et al.*, 2008). Similarly, HA stem-reactive monoclonal antibodies were isolated from immortalised IgG+ B cells of individuals previously vaccinated with seasonal influenza vaccines (Corti *et al.*, 2010). These monoclonal antibodies could neutralise many influenza HA subtypes *in vitro* including the pH1N1 strain, and showed *in vivo* protection in mice (Corti *et al.*, 2010). Furthermore, broadly neutralising antibodies targeting the HA stem region have been detected in individuals naturally infected with pH1N1 (Wrammert *et al.*, 2011).

While the identification of influenza-specific, broadly neutralising antibodies has revealed conserved potential antibody target sites, experimental vaccine efforts to date have not yet been able to generate effective, fully cross-reactive neutralising antibody responses (Li *et al.*, 2013, Laursen & Wilson, 2013).

1.4.3 T cell-mediated heterosubtypic anti-influenza immunity in animal models

T cell-mediated heterosubtypic immunity against influenza is well documented in many animal models (Table 1.4.1). Using various adoptive transfer or depletion of T cell subset experiments, it has been shown that heterosubtypic immunity is primarily mediated by cross-reactive cytotoxic CD8+ T cells, and epitope mapping revealed specificity of protective cross-reactive T cells directed to NP, PB2 and PA influenza antigens (Table 1.4.1). Rather than preventing infection of a host, cross-reactive CTLs mediate protection from morbidity and mortality demonstrated by reduced viral replication, accelerated viral clearance, enhanced recovery from disease and enhanced survival following lethal challenge (Table 1.4.1). Thereby, cross-reactive T

cell responses reduce disease severity in animal models. Studies defining the induction of cross-reactive CTLs have demonstrated the importance of priming via the mucosal route that induces long-lived, protective mucosa-associated CTLs (Christensen *et al.*, 2000). Low dose priming was also able to induce protective HSI (Powell *et al.*, 2007). Although the exact mechanism of HSI has not been elucidated, most studies suggest it is via CTL activity and/or antiviral cytokines. HSI was directly related to the frequency of responding cross-reactive CD8+ T cells in a mouse model (Christensen *et al.*, 2000). Also in a mouse model, CTL mediated cross-protective immunity with reduced lung viral titre was demonstrable up to 1 year after an initial priming infection (Liang *et al.*, 1994). Interestingly, in a ferret model of HSI, a longer duration of protection of up to 18 months post-priming was observed (although this study did not identify the immune mediator of protection) (Yetter *et al.*, 1980). Whilst T cell-mediated HSI has been detected in many different animal models of influenza infection (Table 1.4.1), some studies have observed HSI independent of CD8+ CTLs under some circumstances (Epstein *et al.*, 1997, Nguyen *et al.*, 2001). Variable HSI observed between these studies highlights the effect of dissimilar experimental designs, but is also suggestive of the redundancy of the immune system, where more than one mechanism can mediate heterosubtypic immunity in animal models.

1.4.4 T cell heterosubtypic anti-influenza immunity in humans

There is paucity of data assessing the role of HSI in natural human influenza infection. Epidemiological studies provide some indirect evidence of T cell-mediated HSI in humans when a pandemic virus entered a naïve population previously exposed to a different virus subtype. Adults who experienced H1N1 infection 2 – 3

months (Slepushkin, 1959) or up to 4 – 6 years (Epstein, 2006) prior to 1957, were less likely to develop symptomatic illness with influenza infection during the 1957 H2N2 pandemic. Experimental challenge studies have also demonstrated T cell-mediated HSI in humans without detectable pre-challenge antibodies. Pre-challenge CTL responses were associated with decreased viral shedding following experimental challenge with a live H1N1 virus (McMichael *et al.*, 1983b). Pre-challenge CD4+ T cells have also been inversely associated with viral shedding and illness severity following challenge with live influenza vaccine strain sH3N2 and sH1N1 viruses (Wilkinson *et al.*, 2012). These few studies, together with the extensive data from animal models, support the importance of T cell-mediated immune responses in limiting influenza illness, and suggest that T cell-mediated HSI may lessen influenza disease severity during a pandemic.

Species	The immune mediator/correlate of protection (and anatomical location if applicable)	Experiment	Priming strain	Challenge strain	Protection measure(s)	Timing/ duration of protection if applicable	Comments (notable findings)	Reference
Mouse	MHC-I restricted (but not MHC-II restricted) CTLs	Adoptive transfer (H2-haplotype matched/mis-matched cells or anti-Ly1.1/anti-Ly2.1 serum treated cells)	H1N1	H1N1	Reduction of lung virus titre and prevented death from lethal dose challenge	Peak CTL activity and protection around 6 days post-infection	1st demonstration of specific T cell subset to have a protective effect in host with a respiratory viral infection	(Yap *et al.*, 1978, Yap & Ada, 1978)
Mouse (Nude)	CTLs	Adoptive transfer of radiolabelled spleen cells	H3N2	H3N2	More rapid clearance of virus from lungs	Lung viral titres reduced by day 7 post infection (compared to mice without adoptive transfer)		(Wells *et al.*, 1981)
Human	CTLs in peripheral blood (in the absence of antibodies)	Experimental challenge of subjects with LAIV	(Donors born pre- (prior H1N1 exposure) or post- (no prior H1N1) 1950)	H1N1	Decreased nasal viral shedding		1st evidence of CTL mediated HSI in humans	(McMichael *et al.*, 1983b)

Mouse	CTL clones	Adoptive transfer	H2N2	H1N1	Reduction of lung virus titre and prevented death from lethal dose challenge		Cross-reactive and subtype-specific CTLs reduced lung viral titres but only cross-reactive CTLs could promote recovery from lethal heterosubtypic infection	(Lukacher *et al.*, 1984)
Mouse	NP-specific CTL clones	Adoptive transfer	H3N2	H1N1, H3N2, H2N2	Reduction of lung virus titre and prevented death from lethal dose challenge		Protective effect of an antigenically mapped cross-reactive CTL clone	(Taylor & Askonas, 1986)
Mouse	Cross-reactive NP-specific CTLs	Purified NP protein priming	NP from H3N2	H1N1	Enhanced recovery from disease and protected against death from lethal dose challenge	Protective effect with lethal challenge infection at 1 month post priming		(Wraith *et al.*, 1987)
Mouse	Cross-reactive NP-specific CTLs and Th clones	Adoptive transfer	H3N2	H3N2	Reduction of lung virus titre		Cloned CTLs are more effective at clearing virus in lungs of challenged mice than cloned Th (protective effect of Th is more variable)	(Askonas *et al.*, 1988)

Mouse	CD4+ and CD8+ T cells in nose and CD8+ CTLs in lungs	Depletion of T cells	H1N1	H3N2	Reduction of virus titre in respiratory tract	Protective effect demonstrable with challenge infection up to 1 year post priming	Contribution of different T cell subsets to heterosubtypic immunity can differ between upper and lower respiratory tract	(Liang *et al.*, 1994)
Mouse	CTLs induced in MALT (mediastinal lymph nodes)	Mucosal versus systemic routes of priming	H3N2	H1N1	Enhanced recovery from disease and protected against death from lethal dose challenge	Protective effect with lethal challenge infection at 10 months post priming	Mucosal immunization (compared to systemic immunization) induces longer-lived CTL responses in mucosa-associated lymphoid organs that correlated with protective heterosubtypic immunity	(Nguyen *et al.*, 1999)
Mouse	Sequential double priming with heterosubtypic influenza strains to increase NP-specific cross-reactive CD8+ memory T cells	Depletion of CD8+ T cells	H1N1 followed by H3N2	H7N7	Reduction of lung (and brain) viral titres of lethal H7N7 challenge	Lung viral titres reduced by day 3 post challenge in doubly primed mice (compared to single primed or naïve mice)	Heterosubtypic protection directly related to the frequency of responding CD8+ T cells	(Christensen *et al.*, 2000)

Mouse KO for IFN-γ	CTLs induced in MALT (mediastinal lymph nodes)	Depletion of CD8+ T cells	H3N2	H1N1	Reduction of lung virus titres, enhanced recovery from disease and protected against death from lethal dose challenge		IFN-γ is not required for CTL mediated HSI	(Nguyen *et al.*, 2000)
Mouse KO for μMT	NP or PB2-specific CTLs	Prime-challenge	H9N2	H5N1	Enhanced recovery from disease and reduced mortality following lethal challenge		In B cell deficient mice, HSI correlated with CTL responses to NP or PB2	(O'Neill *et al.*, 2000)
Mouse KO for Ig, CD1 or γδ	CD4+ and CD8+ T cells	Depletion of CD4+ and CD8+ T cells	H1N1	H3N2, H2N2	Reduction of lung and upper respiratory tract virus titres and protected against death from lethal dose challenge		Ig, NKT cells or γδT cells are not required for HSI	(Benton *et al.*, 2001)
Pigs	CD8+ T cells	Prime-challenge	H1N1	H3N2	Reduced virus shedding and no fever associated with illness			(Heinen *et al.*, 2001)

Chickens	CD8+ CTLs	Adoptive transfer	H9N2	H5N1	Reduced mortality following lethal challenge	Protective effect with lethal challenge infection at 3 to 70 days post priming		(Seo & Webster, 2001)
Chickens	CD8+IFN-γ+ T cells in lungs	Depletion of T cells	H9N2	H5N1	Reduced mortality following lethal challenge	Declining protective immunity over time (20 – 100 days) lasting 100 days after priming correlated with declining CD8+IFN-γ+ T cells in the lungs	Vβ1 αβTCR+ T cells but not Vβ2 αβTCR+ or γδTCR+ T cell subset required for protection	(Seo *et al.*, 2002)
Mouse	CD8+VLA-1+ T cells in lungs	Blocking of VLA-1 (integrinα4β1) on T cells	H3N2	H1N1	Reduced mortality following lethal challenge		VLA-1 retains CD8+ T cells in the lungs that mediate HSI	(Ray *et al.*, 2004)
Mouse	$NP_{366–374}$-specific CTLs	Prime-challenge	H3N2	H1N1	Reduction of lung virus titres, enhanced recovery from disease and reduced mortality following lethal challenge			(Kreijtz *et al.*, 2007)

Mouse	NP –specific CTLs	T cell depletion	H3N2 cold-adapted virus	H1N1	Enhanced lung viral clearance, enhanced recovery fom disease and reduced mortality following lethal challenge	T cell-mediated HSI effective within 5-6 days post lethal challenge and persists for > 70 days	Low dose priming with cold-adapted virus can achieve T cell-mediated HSI against high dose lethal challenge	(Powell *et al.*, 2007)
Mouse	NP- and PA-specific CTLs	Prime-challenge	H3N2	H5N1	Reduction of lung virus titres, enhanced recovery from disease and reduced mortality following lethal challenge			(Kreijtz *et al.*, 2009)
Ferrets	CTLs	Prime-challenge	H3N2	H5N1	Reduction of lung virus titres, reduces virus associated histopathologic-al changes in the brain, enhanced recovery from disease and reduced mortality following lethal challenge		HSI in ferret model that more closely resembles human influenza HSI hampered by prior vaccination	(Bodewes *et al.*, 2011b)

Mouse	CD4+ and CD8+ T cells	Depletion of CD4+ and CD8+T cells	H3N2	pH1N1	Reduction of lung virus titres, enhanced recovery from disease and reduced mortality following lethal challenge		1st *in vivo* evidence of HSI against pH1N1	(Guo *et al.*, 2011)
Mouse	CD4+ and CD8+ T cells	Adoptive transfer of CD4+ and CD8+ T cells	H3N2	pH1N1	Enhanced lung viral clearance and enhanced recovery from disease			(Hillaire *et al.*, 2011a)
Nonhuman primate	CD4+ and CD8+ T cells	Prime-challenge	H1N1	pH1N1	Enhanced lower and upper respiratory tract viral clearance		More physiological and immunological relevant model of influenza in humans (compared to mice or ferrets)	(Weinfurter *et al.*, 2011)
Humans	NP- and M- specific CD4+ T cells (but not CD8+ T cells) in peripheral blood (in the absence of antibodies to challenge strains)	Experimental challenge of subjects with TIV	(Donors without antibodies to challenge strains)	H1N1, H3N2	Decreased nasal viral shedding, reduced severity of illness			(Wilkinson *et al.*, 2012)

Mouse (including KO for μMT)	Lung resident CD8+ T cells (and antibodies)	Adoptive transfer	H1N1	H3N2	Reduction of lung virus titres, enhanced recovery from disease and protected against death following lethal challenge	Lung Trm numbers decreased over time and correlated with reduced HSI by 7 months post-priming	Pulmonary priming required for optimal HSI, circulating T cells (including effector T cells) recruited to lungs during viral clearance not required for HSI Importance of lung Trm cells in HSI	(Wu *et al.*, 2014)

Table 1.4.1 Evidence of T cell-mediated HSI.

1.4.5 Heterosubtypic T cell responses to influenza vaccination

By definition, strain-specific neutralising antibodies induced by influenza vaccination would not be expected to provide sterilising immunity against heterosubtypic influenza infection. This is particularly the case for inactivated influenza vaccines, however LAIV may provide broader immunity (Cox *et al.*, 2004). Interestingly, following seasonal TIV vaccination in healthy adults, H5N1 cross-reactive CD4+ T cells producing IFN-γ and IL-2 were detectable from *in vitro* expanded PBMC obtained 30 days post-vaccination (Gioia *et al.*, 2008), suggesting that seasonal influenza vaccination may boost H5N1 cross-reactive cellular immune responses. LAIV induced a broader range of anti-influenza cytotoxicity against homosubtypic and heterosubtypic strains than TIV vaccination at 14 or 28 days post-vaccination in chronically ill older adults (Gorse & Belshe, 1990). In mice, LAIV induces heterosubtypic immunity that reduces lung virus titres, prevents weight loss and reduces inflammatory cytokines in the lungs following challenge infection 3 weeks later (Lanthier *et al.*, 2011). This LAIV-induced heterosubtypic immunity was associated with enhanced expression of chemokines involved in T cell recruitment to the lungs of mice. Furthermore, similar memory T cell response characterised by IFN-γ and chemokines involved in T cell and DC recruitment were induced in supernatants of LAIV-stimulated PBMC from healthy adults vaccinated with LAIV (Lanthier *et al.*, 2011).

A meta-analysis showed a moderate level of cross-protection (34 – 38%) of seasonal TIV vaccination against laboratory confirmed pH1N1 illness and hospitalization

across studies in all age groups, but mainly in healthy adults (Yin *et al.*, 2012). It has been postulated that the observed cross-protection may be due to heterosubtypic humoral and/or cellular immune responses activated by seasonal influenza vaccines (Johns *et al.*, 2010).

1.5 Immune correlates of protection against influenza

1.5.1 B cell-mediated immune correlates of protection against influenza

Seminal work in 1972 identified levels of HAI assay (described in Materials and methods section 2.13) titre required to provide 50% protection against influenza infection in adult challenge experiments (Hobson *et al.*, 1972). This evidence is the historical basis for the currently used surrogate of influenza vaccine-induced protection of HAI titre ≥ 1:40 (Katz *et al.*, 2009). Whilst this is a well-characterised and routinely used correlate of protection, compared to young adults, higher HAI titres are required to achieve the same or higher protection rates in children (Black *et al.*, 2011). Furthermore, this surrogate for sterilising humoral immunity cannot evaluate potential universal influenza vaccines that include components to reduce viral shedding and transmission or disease severity.

Anti-NA serum antibodies have been shown to be protective against influenza illness in humans (Couch *et al.*, 1974, Couch *et al.*, 2013). Other humoral responses (mucosal IgG, IgM and IgA anti-HA antibodies, HA stalk-reactive serum IgG antibodies, anti-M2 serum IgG antibodies) that may contribute to protection against

influenza require other assays lacking standardisation and the minimal requirements for protection are yet unknown (Kreijtz *et al.*, 2011).

1.5.2 T cell-mediated immune correlates against influenza

Cellular responses to influenza are becoming increasingly used measures in the evaluation of vaccine-induced immunity. In elderly individuals, cellular responses provide a better correlate of influenza TIV vaccine-induced protection than antibody responses (McElhaney *et al.*, 2006, McElhaney, 2008, Shahid *et al.*, 2010). Furthermore, serum antibodies have not been proven to be predictive of efficacy for LAIV (Forrest *et al.*, 2008), which induce immune responses that may differ from those induced by inactivated influenza vaccines (Hoft *et al.*, 2011). Thus there is a concensus among the literature that there is a need for incorporation of *ex vivo* measures of cell-mediated immunity into the evaluation of existing influenza vaccines. Influenza-specific serum antibody responses as the sole measure of vaccine efficacy may have limited value, particularly in the older adult population and also in young children vaccinated with LAIV. Furthermore, measures of cell-mediated immunity are required in the development of new influenza vaccines, especially for some T cell-based universal influenza vaccines.

The high conservation among different influenza subtypes in the antigenic targets of influenza specific CD4+ and CD8+ T cells makes them attractive candidates for universal influenza vaccine design (Atsmon *et al.*, 2012, Berthoud *et al.*, 2011). Since T cell responses significantly correlated with decreased viral shedding and illness severity to experimental challenge in humans (McMichael *et al.*, 1983b,

Wilkinson *et al.*, 2012), testing this in natural influenza infection in humans and defining the frequency and phenotype of such a protection-associated T cell correlate is a logical step towards establishing a relevant minimal requirement for protection.

1.5.3 Measuring antigen-specific T cells

Assessment of influenza-specific cross-reactive T cell responses is complicated given the low frequency of circulating antigen-specific memory T cells in humans. Quantification of the memory T cell response usually involves the measurement of IFN-γ producing cells using a sensitive T cell Enzyme-linked Immunosorbent Spot-forming (ELISpot) assay. Further analysis in strong responders uses multi-parameter flow cytometry and intracellular cytokine staining (ICS). ELISpot has higher sensitivity than flow-cytometry which is ideal for detecting low frequency influenza-specific memory T cell responses (Lee *et al.*, 2008). Memory T cells can be characterised based on expression of cell surface markers (Harari *et al.*, 2006). The phenotypic characterisation based on the expression of the lymph node homing receptor CCR7 in combination with the cell activation marker CD45RA also correlates with IFN-γ and IL-2 cytokine secretion patterns, allowing categorisation of functional subsets: IFN-γ-IL-2+ secreting Tcm, IFN-γ+IL-2+ dual secreting Tem, and IFN-γ+IL-2- secreting effector T cells (Teff) (Sallusto *et al.*, 1999). However, this correlation is not absolute and there is functional heterogeneity in memory T cell populations within CD4+ and CD8+ T cell subsets depending on the cell-surface phenotypic markers used (Harari *et al.*, 2006, Seder & Ahmed, 2003, Mahnke *et al.*, 2013).

The novel fluorescence-immunospot assay (Casey *et al.*, 2010) can be used to detect cytokine secretion patterns at the single-cell level with sensitivity equivalent to ELISpot (Gazagne *et al.*, 2003) and enables the assessment of antigen-specific single IFN-γ+ or IL-2+, and co-localised IFN-γ+IL-2+ dual cytokine secretion patterns as surrogates of the main memory T cell subsets. The utility of fluorescence-immunospot to identify clinically relevant immune responses and protective immune correlates in the context of infection, cancer and vaccination has been demonstrated by a few recent studies. Casey *et al.* used fluorescence-immunospot to identify T-cell cytokine signatures of pathogen burden in distinct clinical stages of tuberculosis infection (Casey *et al.*, 2010). Chemotherapy-induced immunosupression of multiple-cytokine-secreting T cell responses in patients with haematological malignancies has been determined using fluorescence-immunospot (Ohrmalm *et al.*, 2013). Chauvat *et al.* report that the combination of IL-2 and IFN-γ responses facilitated enumeration of more frequent influenza vaccine-specific responses than that determined by detection of either cytokine alone (Chauvat *et al.*, 2013). However, the experimental conditions required for reliability and reproducibility of the fluorescence-immunospot assay have not been extensively demonstrated in existing reports.

1.6 Hypotheses, aims and outline of thesis

Conclusively defining the role of T cell-mediated HSI in humans requires a natural experiment involving the spread of an antigenically shifted influenza virus through a population lacking protective antibodies. A novel IAV entering a human population naïve to this virus allows the assessment of the level of pre-existing cross-reactive T

cells in the population, and the degree of protection if any, afforded by such HSI from influenza cross-reactive T cell responses in the absence of strain-specific antibodies. The 2009 H1N1 pandemic was exactly such a natural experiment and was exploited to characterise pH1N1 cross-reactive T cells, assess their association with influenza infection outcomes, and longitudinally follow pH1N1-specific responses in infected individuals. Using the study population, this thesis postulated the following hypotheses:

1. Pre-existing pH1N1 cross-reactive T cells established following prior influenza infection or vaccination (experienced > 6 months previously) are prevalent in healthy individuals naïve to pH1N1, and are predominantly of an IL-2 secreting functional Tcm memory subset.
2. Pre-existing pH1N1 cross-reactive T cells protect against symptomatic influenza disease following natural pH1N1 influenza infection.
3. Natural pH1N1 infection increases the frequency of pH1N1-specific T cells. The frequency of pre-existing pH1N1 cross-reactive IL-2+ functional memory T cell response predicts the magnitude of the IFN-γ+ effector T cell response following natural pH1N1 infection.

To address the above hypotheses, the aims of this thesis are to:

1. Optimise experimental conditions of a sensitive assay to measure frequencies of antigen-specific functional T cells (**Results section 3.1**).
2. Characterise the pre-existing influenza-specific cross-reactive memory T cell responses (**Results sections 3.2 and 3.4**).

3. Identify a cellular correlate of protection against symptomatic influenza infection (**Results section 3.3**).
4. Characterise the kinetics and longitudinal development of influenza-specific cross-reactive, polyfunctional cellular memory responses in the context of natural influenza infection and vaccination (**Results section 3.5**).

2 MATERIALS AND METHODS

2.1 Blood samples and PBMC processing

Blood samples for Results section 3.1 (optimisation of fluorescence-immunospot conditions): peripheral blood was obtained from healthy volunteers within the Section of Respiratory Infections, National Heart and Lung Institute, St Mary's Hospital campus, Imperial College London.

Blood samples for Results sections 3.2 – 3.5: Healthy adult (>18 years) staff and students of Imperial College London were invited to participate in the 'ImmunoFlu' study. The study outline and samples selected for analysis in respective results sections is shown in Fig. 2.1.1. Individuals already vaccinated for influenza or likely to be offered pandemic vaccination (as per the UK government guidelines in September 2009) were ineligible. Written informed consent was obtained following study approval by the North West London Research Ethics Committee (REC reference: 09/H0724/27).

20 – 30 mL whole blood was collected into heparinised tubes from participants. PBMCs were isolated by Ficoll-Paque^{PLUS} (GE Healthcare, Amersham, UK) density centrifugation. Blood was diluted with RPMI 1640 (Sigma-Aldrich, UK) at 1:1, layered over Ficoll-Paque^{PLUS} without mixing and centrifuged at 2000 rounds per minute (rpm) without brake for 20 minutes at 23°C. PBMC were taken from the gradient/plasma interface and washed twice in RPMI 1640 supplemented with 10% heat-inactivated foetal bovine serum (FBS), (Invitrogen, UK), (R10) by centrifugation (1600 rpm with brake for 5 minutes at 23°C). PBMC pellet was re-suspended in R10

medium and 10 μL of cell suspension was removed and added to 0.4% trypan blue stain (Invitrogen, UK) at 1:1 to count viable cells using the Countess automated cell counter (Invitrogen, UK). PBMC were used immediately or cryopreserved in FBS supplemented with 10% dimethyl sufoxide (DMSO, Sigma-Aldrich, UK) for storage in liquid Nitrogen. Cryoperserved PBMC were rapidly thawed in 37°C water bath for 1 - 2 minutes, washed and re-suspended in warm R10, and rested (for up to 1 hour) at 37°C prior to use.

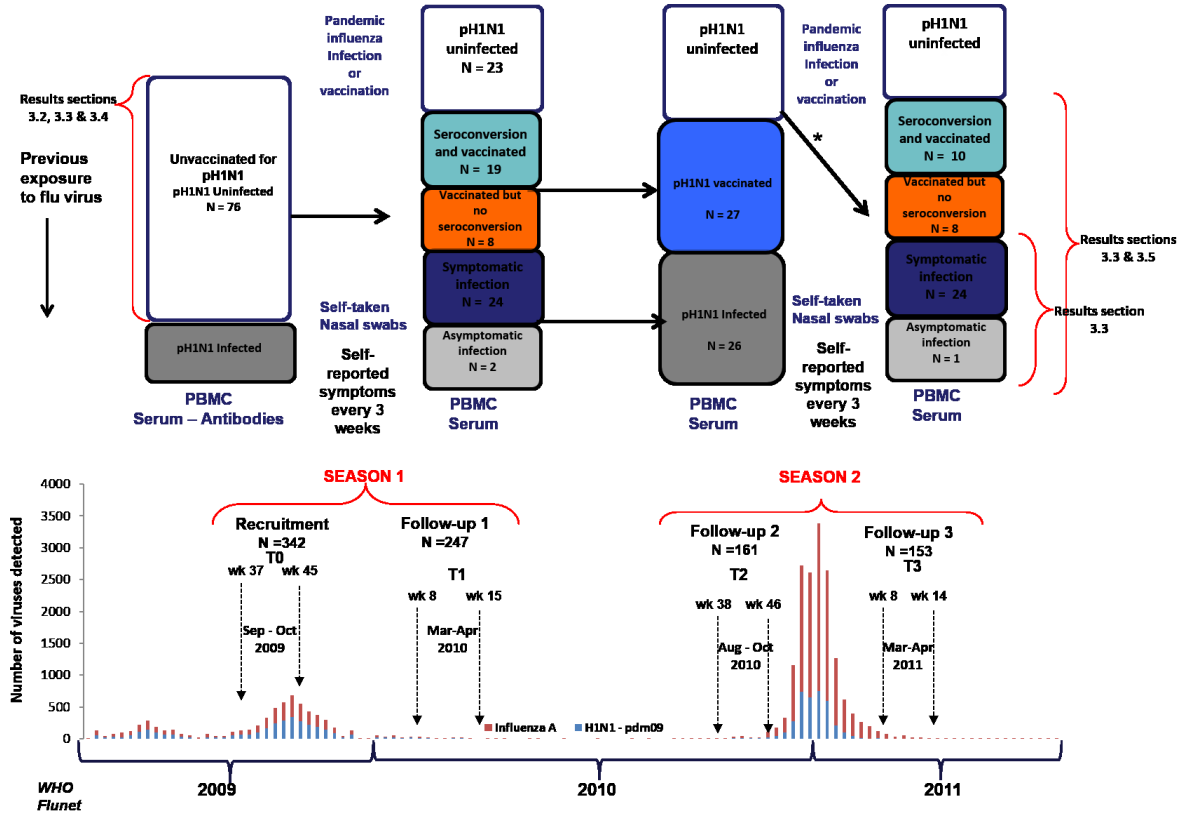

Figure 2.1.1 Study outline and samples selected for analysis.

Study outline and timeline of the 2009–2010 and 2010–2011 pandemic waves in the UK. Shown is the outline of the study (top) in the context of the timeline of the evolving pH1N1 pandemic (bottom). The bar chart shows UK influenza virological surveillance data from the World Health Organisation's FluNet (WHO, 2014a) highlighting the study recruitment and follow-up time points for seasons 1 and 2 in relation to influenza activity in the UK during

2009 – 2011. Red bars indicate influenza A, and blue bars indicate the number of cases of pH1N1 detected by virological national surveillance. Week number was measured from the start of each year. Healthy adults recruited just after the first wave of the pandemic had passed in the UK were followed over two influenza seasons (T0–T3), with PBMC and serum samples collected before and at the end of each winter influenza season. During each influenza season, symptom questionnaires were emailed to participants every 3 weeks with automated weekly reminders. Nasal swabs were collected by participants if they were symptomatic and were returned to the laboratory. Infection was defined by detection of pH1N1 virus in the returned nasal swabs or a four-fold rise in pH1N1 HAI titre in paired serum samples. Nasal swab reverse transcriptase polymerase chain reaction (RT-PCR) and serum HAI assay were performed by Public Health England (PHE), (formerly known as the Health Protection Agency (HPA)). Arrows between the boxes denote the longitudinal progression of individuals during the study; coloured boxes represent the various infection or vaccination outcomes of the samples used in respective results sections. *9/18 individuals were re-vaccinated in season 2.

2.2 Sample size estimation

The primary hypothesis was to identify whether individuals developing mild or asymptomatic illness had higher frequencies of pre-existing cross-reactive CD8+ T cells. 100 infected individuals with a prevalence of 60% asymptomatic infection (Monto *et al.*, 1985) would allow for the detection of a moderate effect size (odds ratio, OR of 4) between symptomatic and asymptomatic infection for each tenfold increase in cross-reactive T cell frequency (prevalence of 60%) (Lee *et al.*, 2008) with 80% power at p = 0.05 (two-tailed) significance. Based on 30% incidence of

infection during the first wave of the UK pandemic (Miller *et al.*, 2010), a sample size of 350 participants was estimated to attain 100 infected individuals (calculations and recruitment conducted by Dr Saranya Sridhar).

2.3 Culturing Madin Darby Canine Kidney cells

Madin Darby Canine Kidney (MDCK) cells (kindly gifted from Professor Wendy Barclay) were stored cryopreserved in liquid Nitrogen in 5% DMSO with DMEM essential media (DMEM medium with high glucose, L-Glutamine and Sodium pyruvate (Sigma-Aldrich, UK), supplemented with 10% FBS, 2% non-essential amino acid 100X solution (Sigma-Aldrich, UK), 100 U penicillin (Invitrogen, UK) and 100 µg/mL streptomycin (Invitrogen, UK)). Cryopreserved MDCKs were rapidly thawed in 37°C water bath for 1 – 2 minutes, washed and re-suspended in DMEM essential media prior to use. Thawed MDCK cells were seeded and cultured at 37°C, 5% CO_2 in T75 tissue culture flasks with DMEM essential media and checked daily microscopically (VWR optical microscope) for confluence. Confluent MDCK cell cultures (attained on day 2 - 3 post seeding) were washed once with sterile phosphate buffered saline (PBS) treated for 5 - 10 minutes at 37°C, 5% CO_2 with trypsin/ Ethylenediaminetetraacetic acid (EDTA) solution 1X (Sigma-Aldrich, UK) diluted 1 in 5 with PBS to dissociate adherence. Dissociated MDCK cell suspension was washed with DMEM essential media and cell pellet was either cryopreserved (in 5% DMSO and DMEM essential media) for storage in liquid Nitrogen, or MDCK cells were seeded for growing or quantifying influenza stocks (see below sections 2.4 – 2.6).

2.4 Titrating influenza trypsin

MDCK cells were plated in 12-well plates in 1 mL/well serum-free DMEM essential media and dilutions (range: 0.1 – 2 μL/mL) of TPCK treated influenza-trypsin (Worthington Biochemical Corporation, New Jersey, USA). Seeded plates were incubated for 2 - 3 days at 37°C, 5% CO_2 to achieve confluence (checked daily microscopically). The concentration of influenza-trypsin at which confluence occurred without significant MDCK cell detachment or cell death was used in growing recombinant influenza (1 μL/mL).

2.5 Growing recombinant influenza

Cryopreserved MDCKs were thawed, seeded and cultured (for 2 – 3 days) at 37°C, 5% CO_2 in T75 tissue culture flasks with DMEM essential media until 80 – 90% confluent (checked daily using microscope). Media was removed from confluent cells and cells were washed twice with 10 mL PBS. A recombinant A/England/195/09 strain virus (kindly gifted from Professor Wendy Barclay) was diluted in serum-free DMEM essential media to infect MDCKs at multiplicity of infection (MOI) = 0.0001. Infected cells were incubated for 1 hour at 37°C, 5% CO_2 with gentle rocking every 10 – 20 minutes. Virus inoculum was removed from MDCK monolayer and serum-free DMEM essential media with 1 μL/mL titrated influenza-trypsin was added to the MDCK monolayer for incubation at 37°C, 5% CO_2. Infected MDCKs were checked daily and virus was harvested when cell adherence was < 20% (around days 2 – 3 post-infection). Virus-containing media was removed into falcon tubes and centrifuged at 2000 rpm for 10 minutes at 4°C to separate dead cell pellet from virus-

containing supernatant. 1 mL virus aliquots were stored at -80°C and used each time without multiple freeze-thawing.

2.6 Influenza plaque assay

MDCKs were thawed (as described above), seeded in 12-well plates and incubated at 37°C, 5% CO_2 overnight to form a confluent monolayer. The following day MDCK cell monolayers were washed with PBS and infected in duplicate with 100 μL of 10-fold dilutions of influenza A/England/195/09 stock virus and incubated for 1 hour at 37°C, 5% CO_2. 2% agarose (Oxoid LTD, UK) added to overlay medium warmed to 37°C (distilled water with 10X MEM (Invitrogen, UK), 7.5% bovine serum albumin (BSA) fraction V (Invitrogen, UK), 200 mM L-Glutamine (Invitrogen, UK), 7.5% Sodium bicarbonate solution (Invitrogen, UK), 1 M HEPES (Invitrogen, UK), 1% dextran (Sigma-Aldrich, UK), 10,000 U/mL penicillin, 10,000 μg/mL streptomycin) with 1 μL/mL influenza trypsin (Worthington Biochemical Corporation, New Jersey, USA, TPCK treated Code: TRTPCK) was added to each well containing washed MDCK cell monolayer. Plates were incubated at 37°C for 3 days to enable plaques to form. After 3 days, visible plaques were marked on plates before removing agarose disks and plaques were stained for counting by adding 1 mL/well crystal violet stain (40 mL 1% crystal violet (Sigma-Aldrich, UK) in 80 mL methanol and 300 mL distilled water). Virus concentration was calculated in plaque-forming units (pfu) per mL using the following formula:

Virus titre (pfu/mL) = ((average number of plaques in well X dilution of virus in well)/ volume of virus in well (μL)) x 1000

2.7 Antigens and influenza vaccine strains used in fluorescence-immunospot

Live pH1N1 virus was obtained by growing a recombinant A/England/195/09 strain in MDCK cells as described above and used at MOI = 1 in IFN-γ and IL-2 fluorescence-immunospot assays and MOI = 5 in flow cytometry. Inactivated vaccine strain viruses used were reassortant pandemic H1N1 (A/California/07/09, NYMCX-179A, 5 µg /mL, National Institute for Biological Standards and Control (NIBSC), UK), seasonal H1N1 (A/Brisbane/59/2007, IVR-148, 5 µg/mL, NIBSC, UK) and seasonal H3N2 (A/Uruguay/716/2007, NYMC X-175C, 5 µg/mL, NIBSC, UK). Peptide pools used were 9-mer peptides representing highly conserved reported HLA class I restricted epitopes in influenza A virus from PB1, M1 and NP proteins (Appendix Table 6.1) (NR-2667, 5 µg/mL per peptide) (NIH Biodefense and Emerging Infections Research Resources Repository, NIAID, USA); and peptide pool of 15-mer peptides overlapping by 10-mer covering the entire sequence of influenza (A/California/07/09) M1, NP and PB1 proteins (5 µg /mL per peptide) (ThinkPeptide, UK) (Appendix Tables 6.2, 6.3, 6.4). Cell culture lysates from cells infected with Cytomegalovirus (CMV) and Epstein Bar Virus- (EBV) (East Coast Biologicals Inc., USA, 10 µg /mL), purified protein derivative (PPD, Statens Serum Institut, Denmark, 16.67 µg /mL) and 6kDa early secreted antigenic target from *Mycobacterium tuberculosis* (ESAT-6 antigen, Pepceuticals Limited, UK, 10 µg/mL) were also used. Phytohaemagglutinin (at 4 µg/mL unless otherwise stated in figure legends) (PHA, MP Biomedicals, UK) was used as positive control and R10 medium alone as negative control.

2.8 *Ex vivo* IFN-γ and IL-2 fluorescence-immunospot assays

Freshly isolated or cryopreserved and thawed PBMC were counted using the Countess automated cell counter (as described above in section 2.1). Viability index was calculated as the ratio of the average viability of frozen-thawed PBMC to the average viability of fresh PBMC (viability data obtained from countess cell count readings). Fluorescence-immunospot pre-coated low fluorescence polyvinylidene fluoride (PVDF) plates (coated with mAb 1D1K/IL2

0I/249, FluoroSpot, Mabtech, UK) were directly blocked with 10% FBS in PBS for 30 minutes at room temperature. PBMC pre-stimulated in most experiments (except where indicated) with 0.5 μg/mL (or indicated concentrations in anti-CD28 titration experiment) monoclonal anti-CD28 IgG antibody (Mabtech, UK) were plated at 2.5 x 10^5 cells/well (or otherwise indicated cell input numbers in cell titration experiment) with R10 or antigens and incubated for 18 hours at 37°C, 5% CO_2. After 18 hours incubation, supernatant was discarded and plates were washed with PBS and incubated with 2 μg/mL biotinylated anti-IL-2 (IL2-II-biotin, Mabtech, UK) and monoclonal FITC-conjugated anti-IFN-γ (7-B6-1-FS-FITC, Mabtech, UK) at 100 μL/well for 2 hours in the dark at room temperature (Mabtech, antibodies were diluted in PBS supplemented with 0.1% BSA). Plates were washed with PBS and incubated with 1 μg/mL secondary detection antibodies anti-FITC-PF 488P and streptavidin-PF555 (Mabtech, 100 μL/well) for 1 hour in the dark at room temperature. Plates were washed with PBS, incubated with 50 μL fluorescence enhancer (Mabtech, UK) for 15 minutes before discarding and drying plates in the dark. Spot forming cells (SFC) were counted using a fluorescence spot reader

(iSpot, AutoimmunDiagnostika GmbH, Germany) fitted with colour filters for FITC and Cy3 detecting PF488 and PF555 respectively. Threshold size and intensity settings for spot enumeration were optimised for fluorescence-immunospot methodology presented in results section 3.1 (Appendix Table 6.5) and ImmunoFlu study sample experiments presented in results sections 3.2 and 3.3 (Appendix Table 6.6).

2.9 Sorting cells by magnetic bead isolation for fluorescence-immunospot

PBMC were depleted of CD4+ or CD8+ T cells with magnetic activated cell sorting (MACS) by labelling with CD4 or CD8 microbead kits respectively and passing through LD columns (Miltenyi Biotec, Germany) according to manufacturer's protocol. Freshly isolated or cryopreserved and thawed PBMC were counted using the Countess automated cell counter (as described above in section 2.1). Undepleted PBMCs were stored at 37°C, 5% CO_2 incubator until required. Remaining PBMC were washed by centrifugation (at 4000 rpm, 10 mins, brake on) and the cell pellet was re-suspended in 80 μL MACS buffer (PBS with 0.5% BSA and 2 mM EDTA) and 20 μL CD8 or CD4 microbeads. Cell suspension and microbeads were mixed well and incubated at 4ºC for 22 minutes. LD column was pre-wet by placing on a magnetic column holder and washing with 2 mL MACS buffer. Cell suspension and microbeads were applied to the top of the column and effluent was collected as the negative fraction (CD8 or CD4 depleted). LD column was washed out 3 times with 0.5 mL MACS buffer. A 20 μL aliquot of effluent was taken into FACS tubes for staining (only for CD3, CD4 and CD8 antibody conjugates from Table 2.11.1). The purity of the depletion of CD4 or CD8 populations was assessed

by flow cytometry staining and was > 94% on all occasions (representative plots shown in Fig. 2.9.1). Collected MACS column effluent was washed by centrifugation (at 4000 rpm, 10 minutes, brake on) and cell pellet was re-suspended in R-10 and plated in fluorescence-immunospot plated at 2.5 x 10^5 cells per well. Undepleted PBMC were also plated at 2.5 x 10^5 cells per well for comparison.

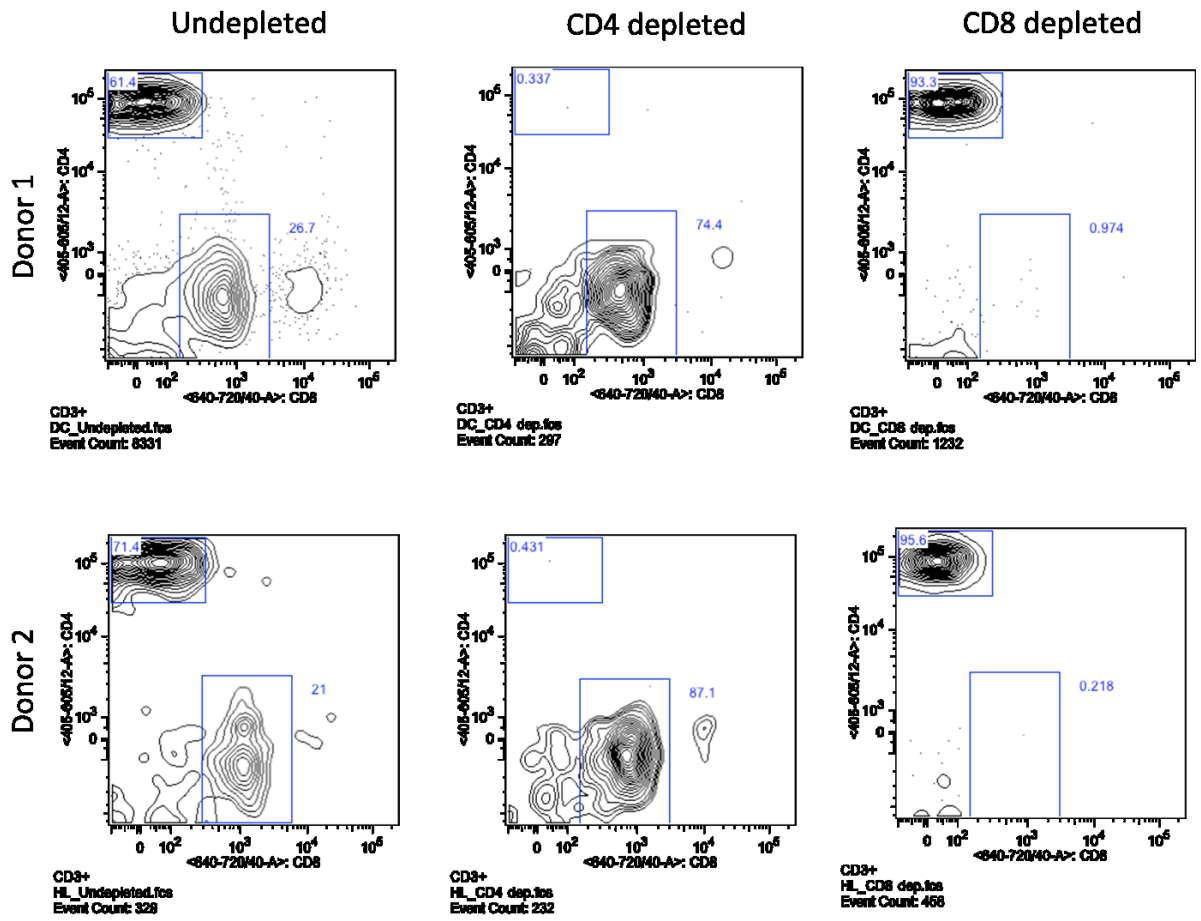

Figure 2.9.1 Representative flow cytometry staining and purity check for CD4+ and CD8+ T cell depletion by MACS.

Populations are gated on live single cells with low forward and side scatter for lymphocyte population.

2.10 Optimising 14-colour flow-cytometry staining panel

Antibody conjugates were selected based on availability of cell markers, fluorochrome conjugations and compatibility of fluorochrome combinations for the BD Fortessa using the BD spectrum viewer online tool (http://www.bdbiosciences.com/research/multicolor/spectrum_viewer/). Each antibody was titrated independently on PBMC to determine optimal staining (Appendix Fig. 6.1 and Appendix Tables 6.7 - 6.18). IL-2-PE and TNF-α-APC were used at concentrations previously optimised in the laboratory (for the same antibody clone). Antibodies were combined into one panel (Table 2.11.1) following ascertainment of optimal concentrations giving appropriate compensation values and staining of distinct populations was achieved. A time-course experiment was conducted to determine the time for stimulation to detect all cytokines using live influenza. MOI was also varied to determine the optimal MOI to detect all influenza-specific cytokines and degranulation marker. There was a trend in higher IFN-γ, IL-2 and TNF-α responses with increasing stimulation time and higher responses in influenza MOI = 5 compared to MOI = 1 (Fig. 2.10.1), although there were no statistically significant differences between time-points in each cytokine or marker measured for each stimulation, or any significant differences due to co-stimulation (0.1 μg/mL anti-CD28 and 0.1 μg/mL anti-CD49d, BD Biosciences, UK). For consistency between fluorescence-immunospot and flow cytometry assays, we selected 18 hours stimulation time. An MOI of 5 was selected to increase the sensitivity for detection of influenza-specific cytokine positive T cell responses by flow cytometry. Peptide pool-specific responses were undetectable or very low

frequency, even in the presence of co-stimulation, hence only live virus stimulation was used in flow cytometry staining experiments.

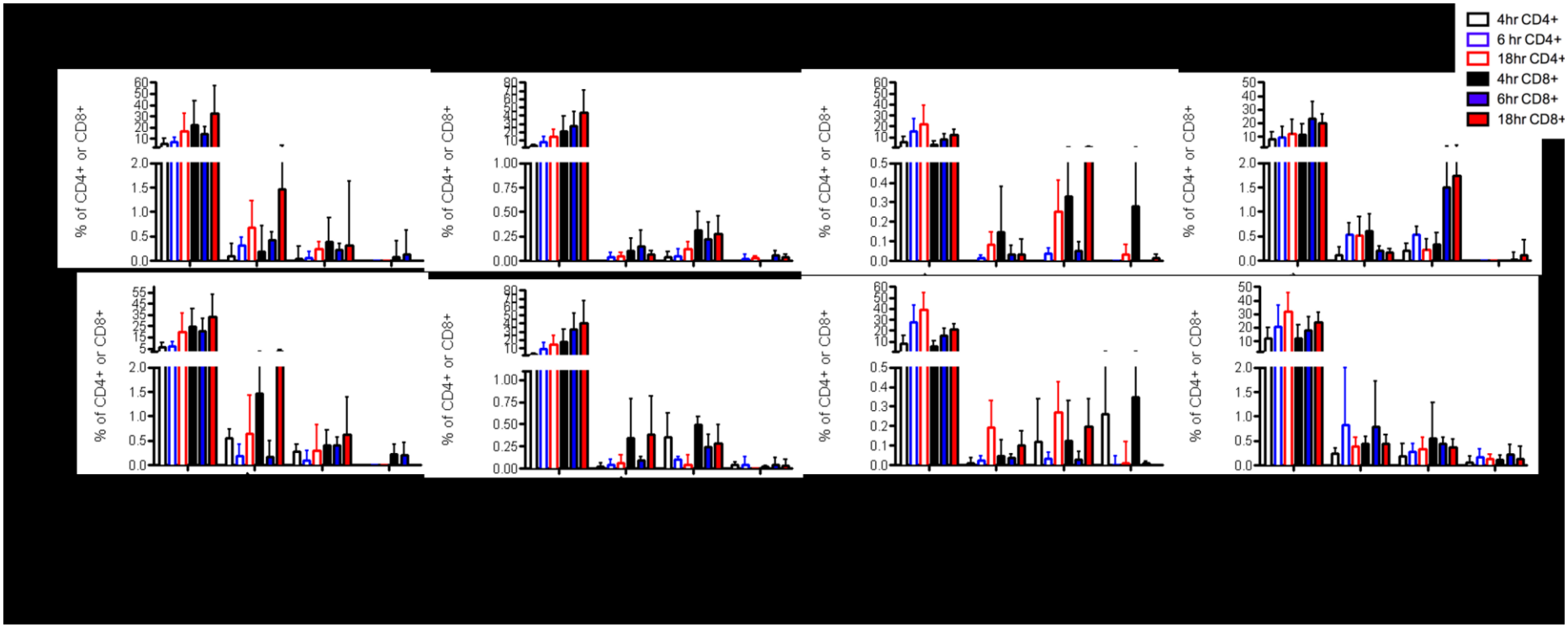

Figure 2.10.1 Time-course of stimulation and influenza multiplicity of infection for intracellular cytokine staining by flow cytometry.

Bars show mean and SD (n = 3 – 4). One-way ANOVA followed by Dunn's multiple comparison correction, not significant.

2.11 PBMC stimulation and staining for flow-cytometry

Staining of PBMC was undertaken following 18 hours stimulation of PBMC (3 x 10^6 per condition) in 24-well plates with R10 media (negative control), phorbol myristate acetate (PMA, 5 ng/mL) (Sigma-Aldrich, UK) and Ionomycin (500 ng/mL) (Sigma-Aldrich, UK) (PMA/I, positive control), live pH1N1 (A/England/09/195) virus (MOI = 5) or CMV lysate (10 μg/mL, antigen control). 2 mM Monesin A in sodium hydroxide (Sigma-Aldrich, UK) was added 2 hours after addition of stimulus. Staining with CD107a (clone H4A3, Becton Dickinson and company (BD) Biosciences, UK) and CD107b (clone H4B4, BD Biosciences, UK) was undertaken at the time of stimulation. Following overnight stimulation, PBMC were harvested into 4 mL polystyrene conical base tubes and washed in FACS buffer (PBS with 0.5% BSA) by centrifugation (1600 rpm with brake = 5 for 5 minutes at 4°C). Supernatant was discarded and cell pellet was re-suspended in 1 mL FACS buffer to stain with amine-reactive viability dye Live/dead Blue (Invitrogen, UK) as a live/dead marker (20 minutes in the dark at 4°C). Live/dead Blue stained cells were washed in FACS buffer by centrifugation (1600 rpm with brake = 5 for 5 minutes at 4°C), supernatant was discarded and cell pellet was blocked (20 minutes in the dark at 4°C) with 10 % human AB serum (Sigma-Aldrich, UK) to prevent non-specific antibody binding prior to staining with surface staining fluorochrome-labelled markers (Table 2.11.1). CD14-Biotin, CD19-Biotin and CD56-Biotin staining mix was prepared and added directly to the cell pellet in FC block (100 μL/tube). Following incubation for 20 minutes in the dark at 4°C, cells were washed in FACS buffer by centrifugation (1600 rpm with brake = 5 for 5 minutes at 4°C), supernatant

was discarded and cell pellet was stained with a master-mix containing the remaining surface staining fluorochrome-labeled markers (25 μL/tube, Table 2.11.1) for 20 minutes in the dark at 4°C. Intracellular cytokine staining (ICS) was performed with BD Cytofix/Cytoperm Plus kit (BD Biosciences, UK) according to the manufacturer's instructions. Surface stained cells were washed in FACS buffer by centrifugation (1600 rpm with brake = 5 for 5 minutes at 4°C), supernatant was discarded and cell pellet was fixed and permeabilised with 200 μL Cytofix/Cytoperm solution (BD Cytofix/Cytoperm Plus kit) for 15 minutes at 4°C. Fixed and permeablised cells were washed by centrifugation (1600 rpm with brake = 5 for 5 minutes at 4°C) in 10X Perm/Wash buffer (BD Cytofix/Cytoperm Plus kit) diluted 1 in 10 with distilled water. Supernatant was discarded and cell pellet was stained with IFN-γ (cloneB27, BD Biosciences), IL-2 (clone MQ1-17H12, BD Biosciences) and TNF-α (clone MAb11, BD Biosciences) antibodies (50 μL/tube, Table 2.11.1) for 30 minutes in the dark at 4°C. Fully stained cells were washed once in Perm/Wash buffer followed by another wash with FACS buffer by centrifugation (1600 rpm with brake = 5 for 5 minutes at 4°C), supernatant was discarded and cell pellet was re-suspended in FACS buffer for acquisition on BD LSR Fortessa (BD Biosciences, UK). Fluorescence minus one controls were PBMC stimulated with live pH1N1 virus that were used for identifying positive populations on all fluorochrome-labeled markers in the first experiment validating the panel, and then only on CCR7, CD107AB, CCR5 and CD45RA in all experiments (to minimise sample expenditure). Compensation controls for all fluorochrome-labeled antibodies were prepared using anti-mouse or anti-rat Ig κ Compbead kits (BD Biosciences, UK) as per manufacturer's instructions. In all samples, 500,000 –

1 million live events were collected and analysed. Antigen-specific cytokine responses were calculated only if the responses were > 0.001% of the parent population. Flow cytometric analyses were performed using a Fortessa (BD Biosciences, UK) and data were analyzed with Flow Jo, version 9.7.5 software (Tree Star, USA) and SPICE, version 5 software (NIH, USA).

Fluorochrome or biotin	Conjugate	Clone	Dilution (by volume)	LSR Fortessa Laser configurations	Bandpass filter
Live/Dead Blue	N/A	N/A	1:1000	355	450/50
PE-CF594	CD3	UCHT1	1:10	561	620/10
AF700	CD8	RPA-T8	1:5	640	720/40
QDot605	CD4	S3.5	1:80	405	605/12
Qdot655	CD45RA	MEM56	1:100	405	655/8
PE-Cy7	CCR7	3D12	1:10	561	780/60
PerCP-Cy5.5	CD69	FN50	1:10	488	710/50
APC-Cy7	CCR5	2D7/CCR5	1:10	640	780/60
BV570	CD57	HCD57	1:100	405	585/15
V450	IFN-γ	B27	1:20	405	450/50
PE	IL-2	MQ1-17H12	1:50	561	582/15
FITC	CD107A	H4A3	1:25	488	530/30
FITC	CD107B	H4B4	1:25		
APC	TNF-α	MAb11	1:10	640	670/14
Biotin	CD14	HCD14	1;250	N/A	N/A
Biotin	CD19	HIB19	1:4000		
Biotin	CD56	HCD56	1:4000		
PE-Cy5	Streptavidin	N/A	1:320	488	675/20

Table 2.11.1 Flow cytometry staining panel.

2.12 RT-PCR for pH1N1 virus

PHE laboratories performed this assay. The influenza A(H1)v specific assay of PHE contains primers and a dual-labelled TaqMan MGB probe (Applied

Biosystems, USA) targeting conserved sequences in the HA gene of A(H1N1) variant viruses, and the positive control swine A(H1N1) virus A/Aragon/3218/2009, in a 1-step TaqMan PCR assay as previously described in detail (Ellis *et al.*, 2009). Data was analysed by Dr Saranya Sridhar.

2.13 HAI assay

PHE laboratories performed this assay. Antibody responses to the virus strain A/England/195/2009, circulating in the UK during our study, were detected by use of HAI assay according to standard methods at the Centre for Infections, PHE (London, UK) (Miller *et al.*, 2010). Briefly, human sera were treated with receptor-destroying enzyme (RDE) II, (Denka Seiken, Japan) for 18 hours followed by heat inactivation for 1 hour at 56°C. Sera were screened in a limiting dilution range using the NIBRG122 virus (a reverse-genetic virus containing hemagglutinin and neuraminidase from the influenza A/England/195/2009 strain) and incubated with the HA antigen suspension for 1 hour followed by addition of 0.5% turkey red blood cell suspension. The reaction is left for 1 hour at room temperature before reading. Each sample is titrated in duplicate and individual titres reported did not differ by more than a two-fold serial dilution. The serum titre is equal to the highest reciprocal dilution, which induces a complete inhibition of haemagglutination. Suitable control serum samples were included in all analyses, with post-infection ferret serum samples raised against the pH1N1 virus strain as positive controls; human pooled serum samples from individuals with either high antibody titres to the circulating influenza H1, H3, and B strains or from individuals with no

antibody titres to these seasonal strains were used as negative controls. Data was analysed by Dr Saranya Sridhar.

2.14 Symptom score

A summed symptom score was designed by totaling the weight for each of the canonical influenza symptoms used in clinical studies (Monto *et al.*, 2000) and reported by returned symptom surveys, with a weight of 0 for none, 1 to mild symptoms and 4 for severe symptoms attributed to each symptom (Table 2.14.1). Mild symptoms were of a severity that did not interfere with normal daily activities while severe symptoms were those that affected normal daily activity or required medical attention. Symptom survey data was analysed by Dr Saranya Sridhar.

Symptom	Weight for no symptoms	Weight for mild symptoms	Weight for severe symptoms
Fever	0	1	4
Cough	0	1	4
Sore throat	0	1	4
Headache	0	1	4
Myalgia	0	1	4

Table 2.14.1 Symptom scores.

2.15 Statistical analysis

GraphPad Prism 5 software (California, USA) and SPSS version 21 (IBM, UK) were used to construct graphs and perform statistical analyses. P values were estimated by Mann-Whitney nonparametric test for un-paired comparisons and Wilcoxon-signed rank nonparametric test for paired data comparions. Spearman rank correlation coefficient was used to test association between variables and linear regression was used to assess linearity of data. Specific statistical tests and significance values are indicated in figures and figure legends.

Antigen-specific responses in fluorescence-immunospot were calculated only in samples with a positive control response (indicating viable cells). Responses per well were normalised to per million PBMC. The median background frequencies of the IFN-γ and IL-2 responses were 4 SFCs per million (range = 0 – 56) and 12 SFCs per million (range = 0 – 156) PBMC, respectively. A threshold for calculating antigen-specific responses was derived using background data such that responses were calculated if they were two standard deviations above mean background (IL-2 = 68 and IFN-γ = 25). The frequencies of antigen-specific cells (total IFN-γ+, total IL-2+ and IFN-γ+IL-2+ dual) were calculated by subtracting the average number of SFCs in negative control wells from the number of SFCs in antigen-containing test wells for each donor. IFN-γ+IL-2- and IFN-γ-IL-2+ responses were calculated by subtracting the dual from the total total IFN-γ+ or total IL-2+ response respectively. The frequency of total cytokine-secreting cells to peptide pool antigens was calculated by summing the frequencies of the three functional subset IFN-γ+IL-2−, IFN-γ−IL-2+ and IFN-γ+IL-2+ T cells.

To assess reproducibility of the fluorescence-immunospot assay (results section 3.1), experiments were repeated on two to three separate occasions using cryopreserved PBMC with 5 – 6 replicates for 2 – 4 different antigen stimulations. Coefficient of variation (CV) was calculated using the following fomula: CV = Standard deviation (SD) / Mean

3 RESULTS

3.1 Optimising IFN-γ/IL-2 fluorescence-immunospot assay

In clinical studies with serial sampling conducted over a long duration with bio-banked samples, assessing multiple-cytokine secreting T cell responses requires an assay suited to the inherent challenges of such settings. This includes quantifying functional antigen-specific T cells that are often rare populations in peripheral blood; where the quantity of biological samples may be limited; and samples from multiple longitudinal time-points may be cryopreserved and bio-banked to be processed in batch. Thus a comprehensive assessment of the basic parameters concerning the execution and performance of IFN-γ/IL-2 fluorescence-immunospot was performed.

3.1.1 Lower background IFN-γ responses compared to IL-2 responses in fluorescence-immunospot

Enumeration of antigen-specific responses requires the subtraction of non-specific background responses. Background cytokine secretion in total IFN-γ+ and total IL-2+ responses were measured in 323 independent PBMC samples and individual well responses were normalised to spot forming cells (SFC) per million PBMC. Background IL-2 responses were higher and showed greater inter-individual variation than background IFN-γ responses (median = 12 and 4, with range = 0 – 156 and 0 – 56 spot forming cells (SFC) per million PBMC respectively, $p < 0.0001$ Fig. 3.1.1). The greater variation in background IL-2 responses was also evident when compared to other fluorescence-

immunospot datasets using a similar assay protocol (two standard deviations (SD) above mean background IL-2 = 68 (n = 323) (present study), 48 (n = 90) (Casey *et al.*, 2010), and 28 (n = 62) (Sridhar *et al.*, 2012) SFC per million PBMC). Background IFN-γ responses were similar across different datasets (two SD above mean background IFN-γ = 25 (present study), 32 (Casey *et al.*, 2010) and 20 (Sridhar *et al.*, 2012) SFC per million PBMC).

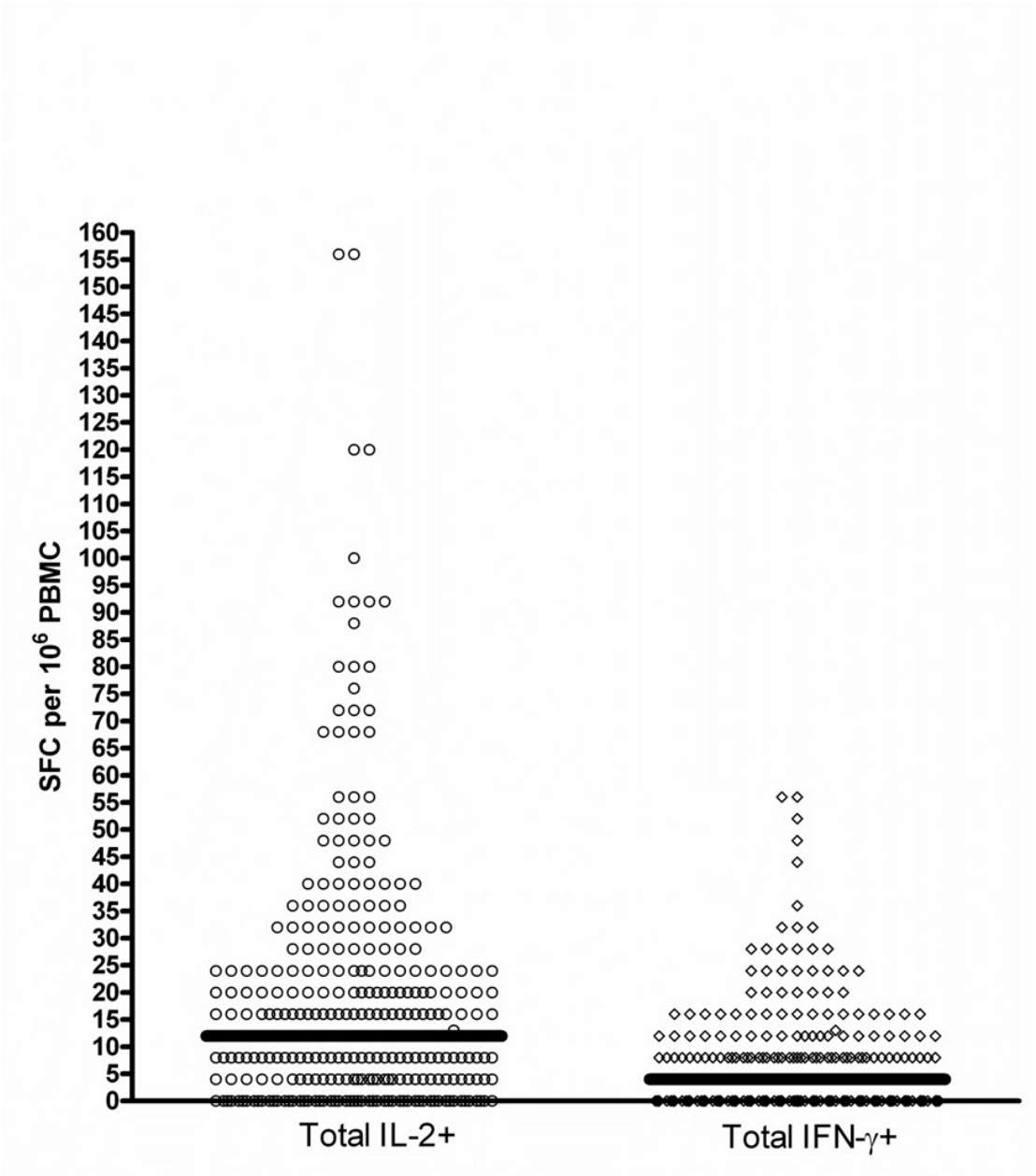

Figure 3.1.1 Background fluorescence-immunospot responses in negative control wells.

Cryopreserved PBMC (2.5 x 10^5 per well) were unstimulated and background cytokine secretion in pre-coated fluorescence-immunospot assays was quantified (n = 323). Dot plot shows individual responses with lines at median for total IFN-γ+ and total IL-2+ responses normalised to spot forming cells (SFC) per million PBMC. Wilcoxon signed-rank test for difference between means, $p < 0.0001$.

3.1.2 Effect of input PBMC quantity on fluorescence-immunospot responses

Biological samples, especially in human studies are often limited and sample expenditure can determine the choice of assay used. Boulet *et al.* report 200,000 input cells as optimal for detecting HIV-1 antigen-specific responses from HIV-1-infected patient samples using dual colour ELISpot and a range of input numbers from 150,000 to 300,000 cells per well (Boulet *et al.*, 2007). To determine whether a similar optimal exists for fluorescence-immunospot using PBMC from healthy individuals, input cell numbers were used in the range 100,000 – 400,000 per well. There were no significant changes in total IL-2+, total IFN-γ+ and IFN-γ+IL-2+ dual non-specific background responses over this input cell number range (Fig. 3.1.2). Linear regression shows lack of a significant non-zero slope in background responses (Fig. 3.1.2 A, B, C). Similarly, CMV lysate- specific total IFN-γ+ and IFN-γ+IL-2+ dual responses (Fig. 3.1.2 E and F) and EBV lysate-specific total IL-2+ and IFN-γ+IL-2+ dual responses (Fig. 3.1.2 G and I) enumerated did not vary significantly with increasing input cell number per well. However, due to well saturation with high frequency responses above 500 single-stained spots, increasing input cell number negatively affected quantification of EBV lysate-specific total IFN-

γ+ responses (r^2 = 0.17, p = 0.024, Fig. 3.1.2 H). Enumeration of CMV lysate-specific total IL-2+ response was also inversely affected by increased input cell number per well (r^2 = 0.90, p = 0.004, Fig. 3.1.2 D).

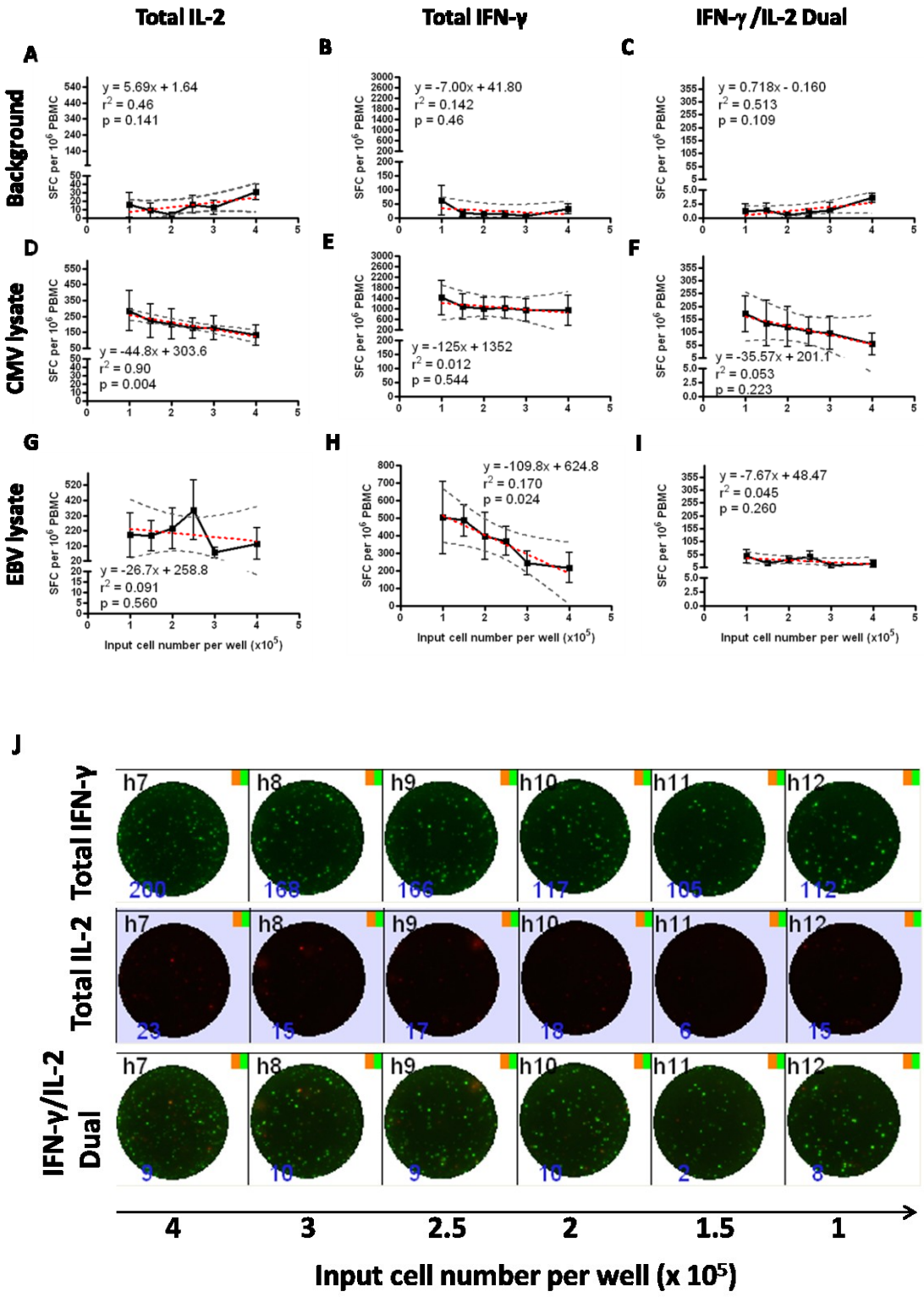

Figure 3.1.2 Input T cell number per well in fluorescence-immunospot.

Cryopreserved PBMC were plated in fluorescence-immunospot plates at input T cell numbers ranging 1 – 4 x 10^5 PBMC (n = 4 - 6) per well unstimulated (background) or stimulated in duplicate for each donor with Cytomegalovirus (CMV) lysate (10 µg/mL) or Epstein Bar virus (EBV) (10 µg/mL). The mean and standard error of mean for total IL-2+ (A, D, G), total IFN-γ+ (B, E, H) and IFN-γ+IL-2+ dual (C, F, I) normalised spot forming cells (SFC) per million PBMC are shown for input PBMC range. One-way ANOVA followed by Dunn's Multiple comparison post-test comparing responses at each input PBMC number to each other, $p > 0.05$ in all comparisons. Equation of linear regression and p-values indicated on graph with linear regression and 95% confidence intervals shown by dotted lines. A representative image of well responses from total IFN-γ+, total IL-2+ and IFN-γ+IL-2+ dual responses from PBMC stimulated with EBV-lysate with increasing input T cells (J).

3.1.3 Stronger correlation in IFN-γ responses than IL-2 responses between freshly isolated and frozen-thawed PBMC responses

Clinical trials often involve high-throughput sample collection from multiple time-points necessitating cryopreservation of PBMC samples for later batch processing. To assess whether cryopreserved samples can be used in fluorescence-immunospot, freshly isolated and frozen-thawed PBMC responses were compared. Viability of cells used fresh or frozen aliquots of PBMC from the same donors after cryopreservation for at least 2 weeks was always >85% and average viability index (viability of frozen/viability of fresh x 100) was 103%. Median frequencies of background or antigen-specific responses from frozen-thawed PBMC were not significantly different to

corresponding responses from freshly isolated PBMC in any of the three cytokine-secreting (IFN-γ+IL-2-, IFN-γ-IL-2+ and IFN-γ+IL-2+) populations (Fig. 3.1.3 A-C). Fresh and frozen-thawed total IFN-γ+ secreting cell responses were strongly correlated ($r = 0.791$, $p < 0.0001$, Fig. 3.1.3 E). Similarly, fresh and frozen-thawed IFN-γ+IL-2+ dual responses were strongly correlated ($r = 0.741$, $p < 0.0001$, Fig. 3.1.3 F). A moderate correlation was observed between fresh and frozen-thawed total IL-2+ responses ($r = 0.598$, $p = 0.0013$, Fig. 3.1.3 D). Importantly, the cytokine secretion profiles from frozen-thawed samples were similar to fresh PBMC responses in all antigens or individual antigens (Fig. 3.1.3 G).

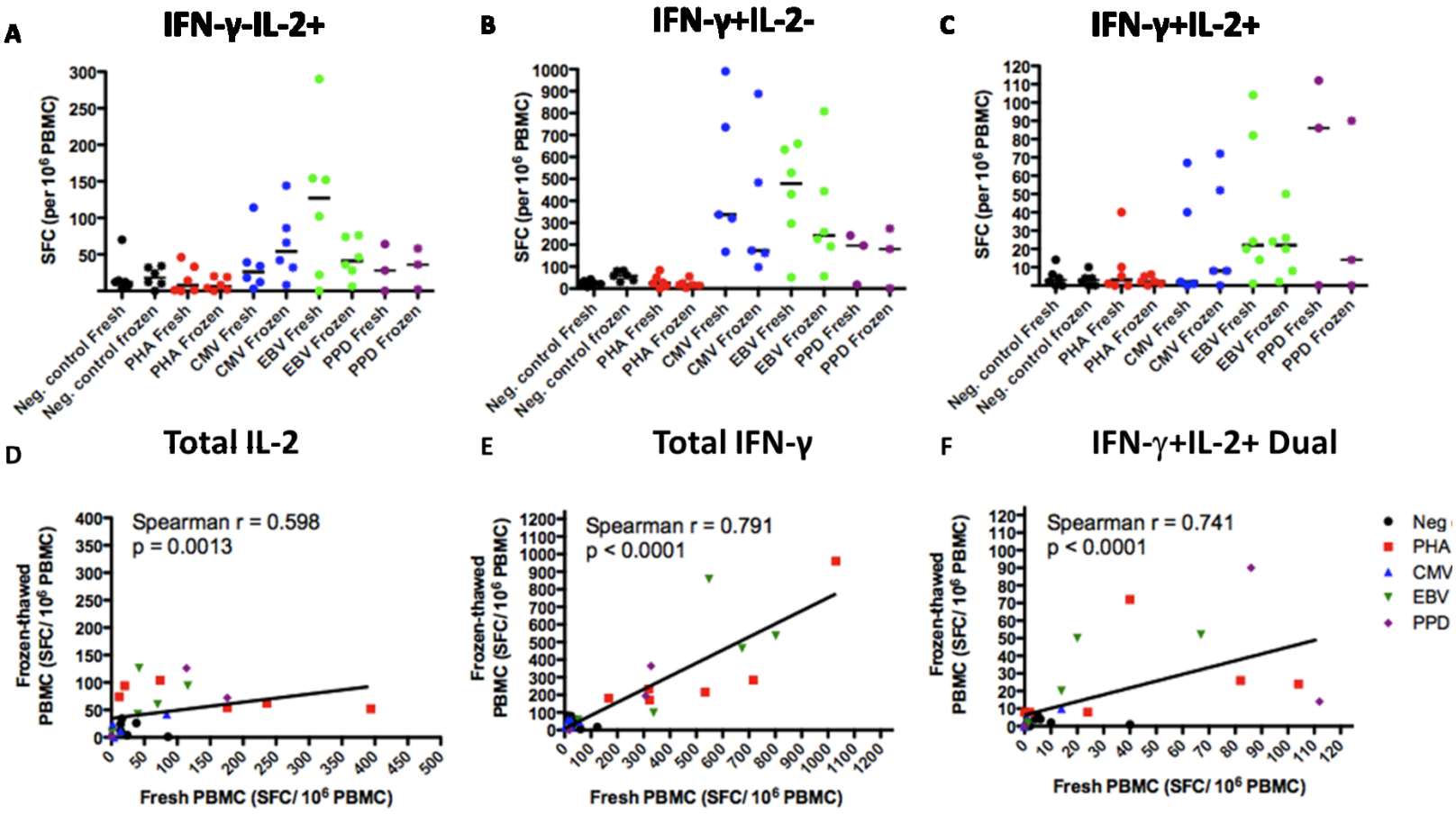
A
IFN-γ-IL-2+
SFC (per 10^6 PBMC)
Neg. control Fresh
Neg. control frozen
PHA Fresh
PHA Frozen
CMV Fresh
CMV Frozen
EBV Fresh
EBV Frozen
PPD Fresh
PPD Frozen
B
IFN-γ+IL-2-
C
IFN-γ+IL-2+
D
Total IL-2
Spearman r = 0.598
p = 0.0013
Frozen-thawed PBMC (SFC/ 10^6 PBMC)
Fresh PBMC (SFC/ 10^6 PBMC)
E
Total IFN-γ
Spearman r = 0.791
p < 0.0001
F
IFN-γ+IL-2+ Dual
Spearman r = 0.741
p < 0.0001
Neg
PHA
CMV
EBV
PPD

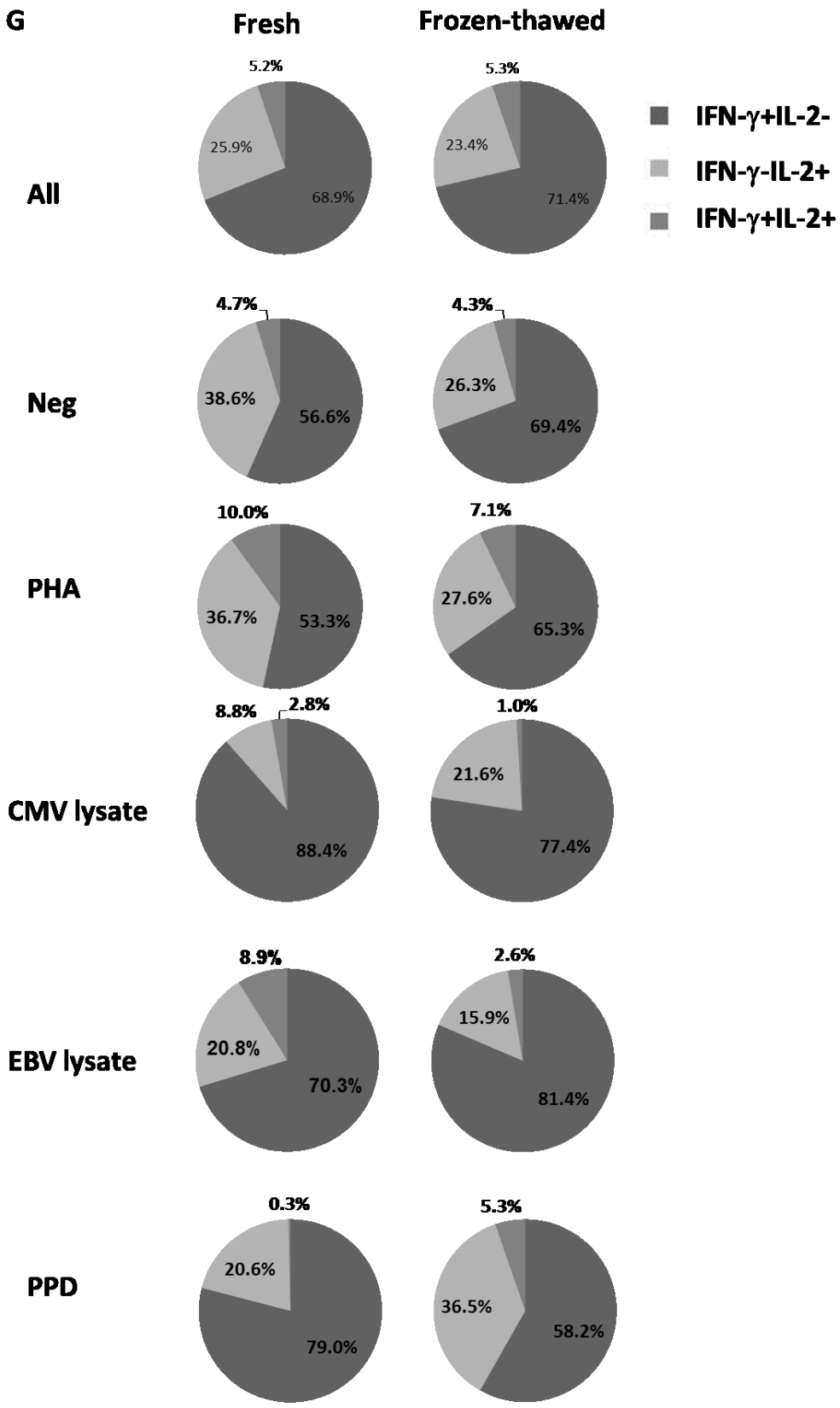

Figure 3.1.3 Comparison of fluorescence-immunospot responses in fresh PBMC versus frozen-thawed PBMC from same donor samples.

PBMC (n = 3 – 6) freshly isolated or a frozen aliquot (cryopreserved for 2 weeks prior to thawing) were unstimulated (black circles) or stimulated with antigens phytohaemagglutinin (PHA, 0.2 µg/mL, red squares), Cytomegalovirus (CMV) lysate (10 µg/mL, blue triangles), Epstein Bar virus (EBV) lysate (10 µg/mL, green inverted triangles) or purified protein derivative (PPD, 16 µg/mL, purple diamonds) in fluorescence-immunospot. Dot plots show individual responses from fresh or frozen-thawed PBMC with lines at median for IFN-γ-IL-2+ (A), IFN-γ+IL-2- (B) and IFN-γ+IL-2+ (C) responses normalised to spot forming cells (SFC) per million PBMC. Wilcoxon signed-rank test between fresh and frozen cytokine-secreting responses to each antigen, not significant. Graphs show Spearman rank correlation between fresh PBMC and frozen-thawed PBMC responses for total IL-2+ (D), total IFN-γ+ (E) and IFN-γ+IL-2+ dual SFC (F) per million PBMC. Pie charts show average proportion response from IFN-γ+IL-2-, IFN-γ-IL-2+ and IFN-γ+IL-2+ dual subsets for all or each stimulation in fresh or frozen-thawed responses (G).

3.1.4 Reproducibility of fluorescence-immunospot

Reproducibility of measurements within and between assays is important to assess when an assay is used to process samples in batch and results are compared between different batches. Fluorescence-immunospot assays were performed on 2 to 3 separate occasions (with 5 – 6 replicates per antigen) to determine intra- and inter- assay coefficient of variation. A non-linear relationship is observed when intra-assay coefficient of variation (CV) is plotted against the mean SFC for 18 replicates (6 replicates per antigen and 3 antigen stimulations per donor) in fluorescence-immunospot (Fig. 3.1.4). As the mean response approaches zero the intra-assay CV increases to 245% at 2 SFC per million PBMC in total IL-2+ (Fig. 3.1.4 A), 78.4% at 20 SFC per

million PBMC in total IFN-γ+ (Fig. 3.1.4 B) and 245% at 1 SFC per million PBMC IFN-γ+IL-2+ dual responses (Fig. 3.1.4 C). Median intra-assay CV for 6 replicates per antigen stimulation using three different antigens and 2 independent donor samples were 12.20% (IQR = 3.71% - 20.70%), 12.10% (IQR = 6.18% - 18.03%) and 13.90% (IQR = 4.27% - 23.54%) for total IL-2+, total IFN-γ+ and IFN-γ+IL-2+ dual responses respectively (Fig. 3.1.4 A, B, C).

To determine variability of fluorescence-immunospot responses from PBMC aliquots of the same sample in assays conducted on 2 to 3 separate occasions, inter-assay CV was determined. Median inter-assay CV was 22.64% (IQR = 9.13% - 36.15%), 23.85% (IQR = 11.31% - 36.39%) and 14.81% (IQR = 7.49% - 22.14%) for total IL-2+, total IFN-γ+ and IFN-γ+IL-2+ dual responses respectively (Fig. 1.4 D, E, F).

PPD responses in fluorescence-immunospot were measured in 5 different donors during the above CV experiments, hence the means and standard deviations of SFC for total IL-2+, total IFN-γ+ and IFN-γ+IL-2+ dual responses were plotted to determine inter-individual variation (Fig. 3.1.4 G). PPD-specific responses measured by fluorescence-immunospot showed large inter-individual differences as indicated by large standard deviations for total IL-2+, total IFN-γ+ and IFN-γ+IL-2+ dual responses (SD = 171.8, 218.6 and 105.3 respectively, Fig. 3.1.4 G). The CV values are compared to those reported in other published studies in Table 3.1.1.

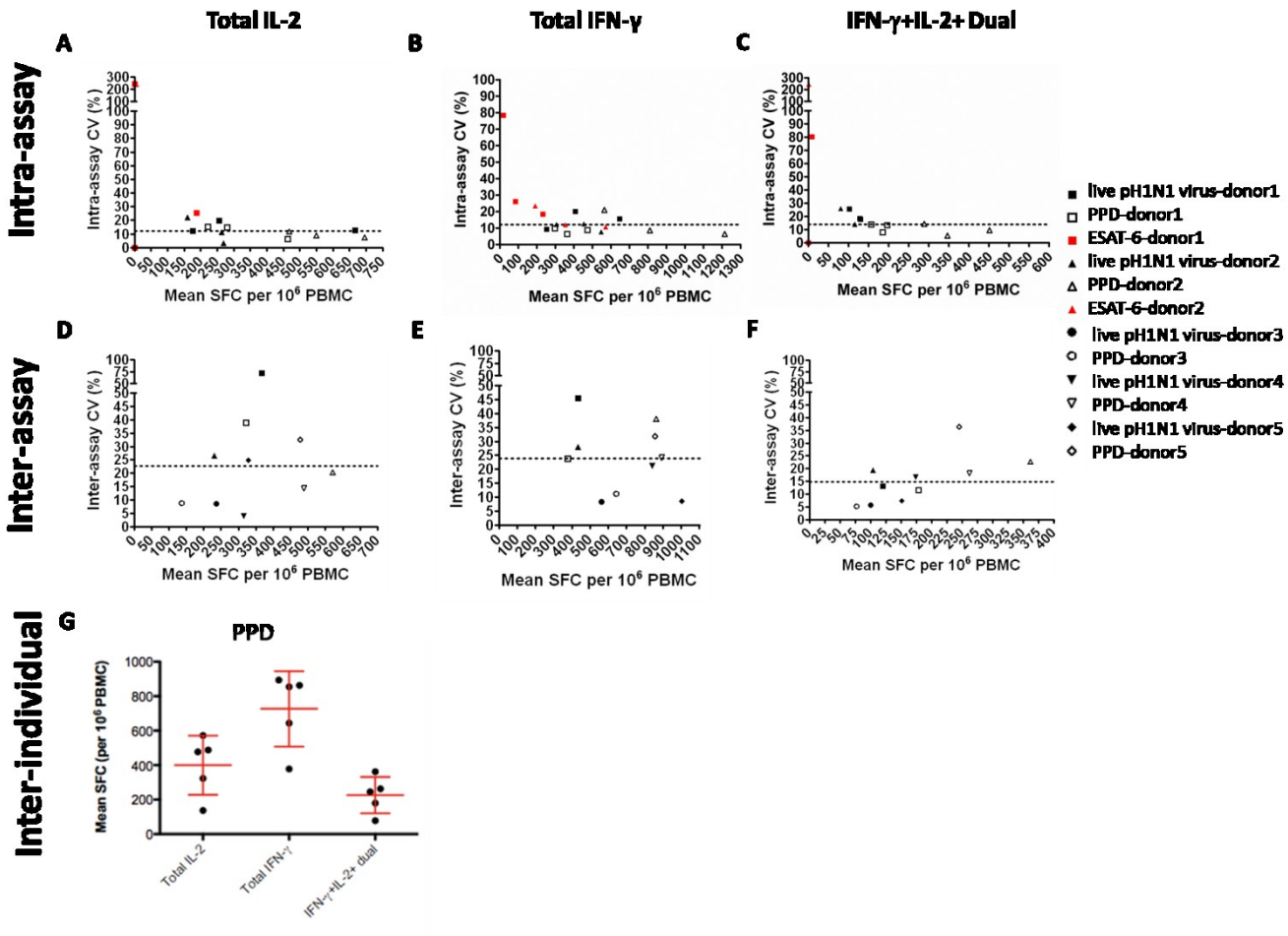

Figure 3.1.4 Intra-assay and inter-assay coefficient of variation and inter-individual variation in fluorescence-immunospot.

PBMC (2.5 x 10^5 per well) were stimulated with 5 µg/mL pH1N1 inactivated vaccine (A/California/07/09, NYMCX-179A), or sH1N1 inactivated vaccine (A/Brisbane/59/2007, IVR-148) (closed black symbols), 16 µg/mL purified protein derivative (PPD) (open symbols) and 10 µg/mL ESAT-6 (red symbols) in replicates of 5 – 6. Two – three independent experiments were conducted on separate occasions on the aliquots of cryopreserved PBMC samples from 5 different donors (different donors represented by different symbol shapes). Dot plot graphs show mean response in spot forming cells (SFC) per million PBMC against intra-assay coefficient of variation (CV) for total IL-2+ (A), total IFN-γ+ (B) and IFN-γ+IL-2+ dual (C) and inter-assay coefficient of variation across all experiments for total IL-2+ (D), total IFN-γ+ (E) and IFN-γ+IL-2+ dual (F) responses. All responses are shown after subtraction of background (unstimulated). Dotted horizontal lines show median intra-assay or inter-assay CVs for each cytokine response. Inter-individual variation in fluorescence-immunospot responses to PPD shown by dot plot with individual responses represented by black circles and red lines at mean with standard deviation (G).

Assay	Intra- or inter-assay CV	IFN-γ+IL-2- response	IFN-γ-IL-2+ response	IFN-γ+IL-2+ dual response	Reference
Dual colour IFN-γ/IL-2 ELISpot on human PBMC for HIV-1 antigen-specific responses	Intra-assay	10.8%	16.4%	17%	(Boulet *et al.*, 2007)
	Inter-assay	11.1%	13.9%	12.8%	
IFN-γ single colour ELISpot on human PBMC for HIV-1 antigen-specific responses	Intra-assay	17%	NA	NA	(Mwau *et al.*, 2002)
	Inter-assay	11%	N/A	N/A	
IFN-γ ICS on human PBMC for CMV pp65 peptide pool-specific responses on same samples performed by different laboratories	Intra-assay	Individual analysis: 28% -39% Central analysis: 18% – 23%	N/A	N/A	(Maecker *et al.*, 2005)
	Inter-assay	N/A	N/A	N/A	
Dual colour IFN-γ/IL-2 fluorescence-immunospot on human PBMC for pH1N1 or sH1N1 vaccine, PPD, ESAT-6 responses	Intra-assay	12.1%	12.2%	13.9%	Present study
	Inter-assay	23.9%	22.6%	14.8%	

Table 3.1.1 Intra- and inter- assay CV values of fluorescence-immunospot compared to CVs reported in other studies.

3.1.5 Co-stimulatory anti-CD28 enhances the proportion of IFN-γ-IL-2+ response

One of the technical challenges associated with the IFN- γ/IL-2 fluorescence-immunospot is the dependence of IFN-γ secretion on IL-2 as the IL-2 is captured by the fluorescence-immunospot membrane. The addition of anti-CD28 monoclonal antibody in the assay compensates for the effect of IL-2 sequestration on IFN-γ responses (Quast *et al.*, 2005). To determine the effect of anti-CD28 on the magnitude and phenotype of fluorescence-immunospot responses, PBMC were unstimulated or stimulated with antigens without or with 0.5 μg/mL anti-CD28 co-stimulation. A representative image of well responses from total IFN-γ+, total IL-2+ and IFN-γ+IL-2+ dual cytokine secreting responses is shown (Fig. 3.1.5 A). Anti-CD28 co-stimulation significantly increased IFN-γ+IL-2-, IFN-γ-IL-2+ and IFN-γ+IL-2+ dual EBV lysate-specific responses ($p = 0.001$, 0.0024 and 0.0005 respectively, Fig. 3.1.5 D) and CMV lysate-specific IFN-γ-IL-2+ and IFN-γ+IL-2+ dual responses ($p = 0.0005$ and 0.0098 respectively, Fig. 3.1.5 C). Anti-CD28 did not significantly alter CMV lysate-specific IFN-γ+IL-2- responses ($p = 0.339$, Fig. 3.1.5 C). The frequency of non-specific background IFN-γ-IL-2+ and IFN-γ+IL-2+ dual responses were significantly increased in the presence of anti-CD28 ($p = 0.002$ and 0.008 respectively, Fig. 3.1.5 B). Low frequency M1 peptide pool-specific IFN-γ-IL-2+, IFN-γ+IL-2- or IFN-γ+IL-2+ dual responses were not significantly enhanced in the presence of anti-CD28 (Fig. 3.1.5 E), even when a higher anti-CD28 concentration was used (Fig. 3.1.5 F). Furthermore, anti-CD28 co-stimulation increased the proportion IFN-γ-IL-2+ CMV lysate-specific and proportion IFN-γ-IL-2+ EBV-specific responses ($p = 0.0117$ and $p = 0.117$

respectively, Fig. 3.1.5 G), although increased background and M1- peptide pool-specific IFN-γ-IL-2+ proportion in the presence of anti-CD28 did not reach statistical significance. Importantly, this enhancement on proportion IFN-γ-IL-2+ responses with anti-CD28 was apparent whether the PBMC were fresh or frozen-thawed PBMC responses (Fig. 3.1.5 G). The relative contribution of CD4+ and CD8+ T cells to antigen-specific cytokine responses for the antigens used in fluorescence-immunospot was assessed by flow cytometry (Fig. 3.1.6). Negative control background IL-2 responses were mainly from CD4+ whereas IFN-γ responses were from CD8 (Fig. 3.1.6 B). EBV lysate-specific IL-2 and IFN-γ responses were mainly from CD4+ T cells (Fig. 3.1.6 B). M1 peptide pool-specific IL-2 and IFN-γ responses were from CD4+ and CD8+ T cell subsets Fig. 3.1.6 B). Similarly, CMV lysate-specific IL-2 responses were from both CD4+ and CD8+ T cells, whereas the majority of IFN-γ responses were from CD4+ T cells Fig. 3.1.6 C).

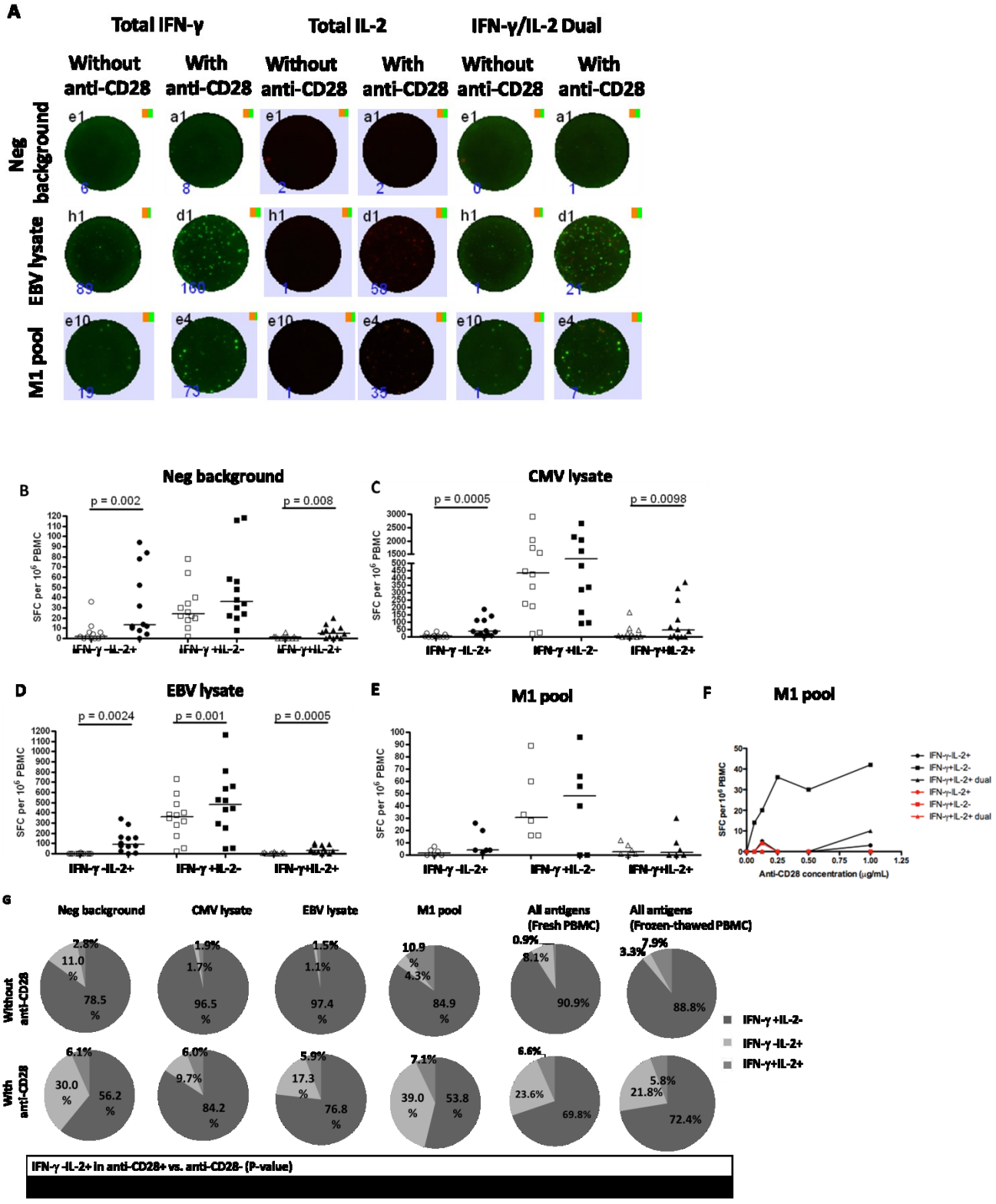

Figure 3.1.5 Anti-CD28 co-stimulation in fluorescence-immunospot preferentially enhances IL-2 responses.

A representative image of well responses from total IFN-γ+, total IL-2+ and IFN-γ+IL-2+ dual responses from PBMC unstimulated or stimulated with Epstein Bar virus (EBV) lysate, or M1 peptide pool without or with addition of anti-CD28 monoclonal antibody (A). Frequency of responses for unstimulated (Neg, B) or PBMC stimulated with CMV lysate (10 μg/mL) (C) EBV lysate (10 μg/mL) (D) or influenza M1 antigen peptide pool (5 μg/mL) (E) in duplicates for each donor without addition of anti-CD28 monoclonal antibody prior to plating PBMCs (open symbols) or with anti-CD28 (closed symbols). Dot plot graphs show individual donor responses with lines at median IFN-γ-IL-2+, IFN-γ+IL-2- and IFN-γ+IL-2+ responses in spot forming cells (SFC) per million PBMC. (F) Titration of anti-CD28 concentration in PBMC stimulated with influenza M1 antigen peptide pool (5 μg/mL) in 2 donors (red and black lines represent different donors). (G) Pie charts show average proportion response from IFN-γ+IL-2-, IFN-γ-IL-2+ and IFN-γ+IL-2+ dual subsets for all or each stimulation without or with anti-CD28 co-stimulation. P-values for Wilcoxon signed rank test between proportions of IFN-γ-IL-2+ in anti-CD28 co-stimulated or unstimulated conditions.

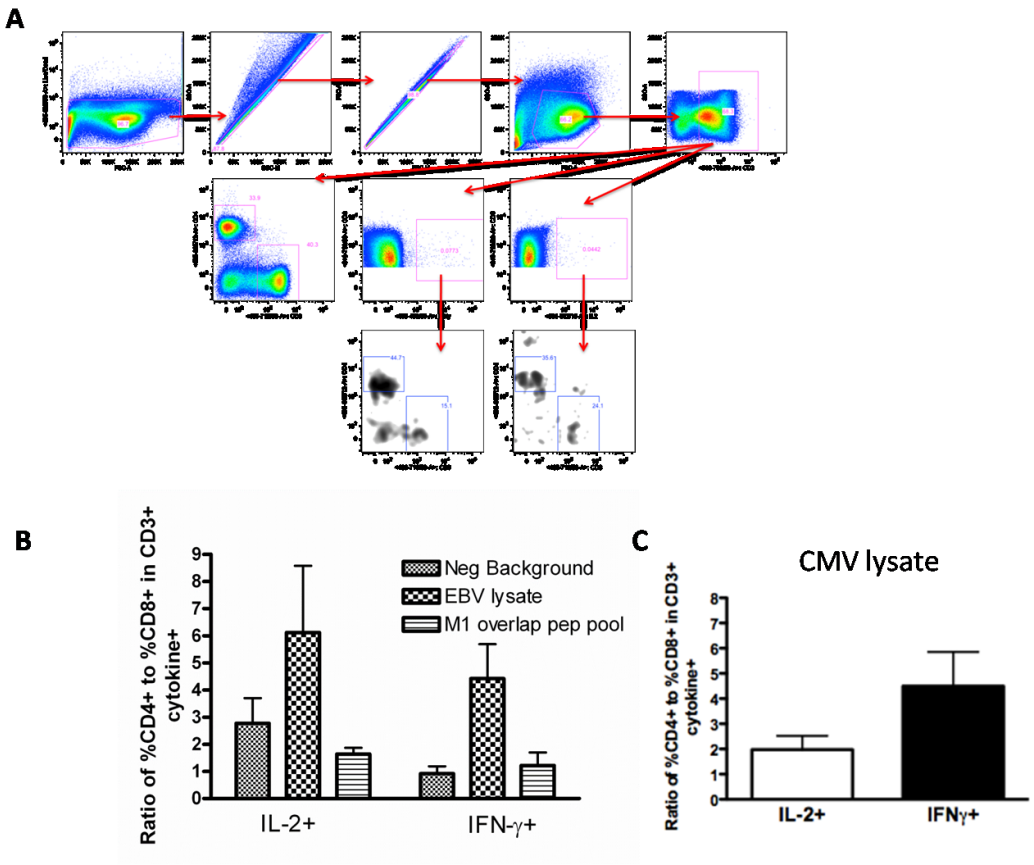

Figure 3.1.6 Relative contributions of CD4+ and CD8+ T cells to antigen-specific cytokine responses.

PBMCs unstimulated or stimulated for 18 hours with CMV lysate (10 μg/mL), EBV lysate (10 μg/mL) or influenza M1 antigen peptide pool (5 μg/mL) were stained for surface and intracellular markers and analysed by flow cytometry. (A) Gating strategy. PBMCs were gated on live, single cells, low forward and side scatter and CD3+ for lymphocytes positive for IFN-γ+ or IL-2+ followed by gating CD4+CD8- or CD4-CD8+ T cells within each cytokine positive population. Bar charts show mean and standard error of mean for the ratio of CD4+ to CD8+ cytokine positive T cell response to stimulation antigens, n = 4 (B), n = 54 or 60 (C).

3.2 pH1N1 cross-reactive cellular responses in pH1N1 naïve individuals

Using the sensitive and optimized fluorescence-immunospot assay, PBMC responses to pH1N1 core antigen peptide pools, recombinant antigens, inactivated vaccine strain viruses and live virus was assessed. Influenza is considered an acute infection with rapid antigen clearance (Pantaleo & Harari, 2006) and based on this model we hypothesized that pH1N1-naïve individuals unexposed to influenza for at least 6 months prior (last possible exposure in February 2009), would have memory T cells to core proteins (PB1, M1 and NP) of the pH1N1 virus with a cytokine signature predominantly IL-2 secreting, representing Tcm (Sallusto *et al.*, 1999).

3.2.1 Cohort characteristics

The 76 participants had a median age of 34 years with a range of 18 – 72 years. 43% (33 individuals) were male and 57% (43 individuals) were female. All participants were seronegative (HAI $\leq$ 1:8) by HAI assay to detect pH1N1-specific antibodies. None were vaccinated for pH1N1 at the time of recruitment and only 3 individuals gave a history of influenza-like illness in the 3 months preceding recruitment.

3.2.2 High prevalence of pH1N1 core-antigen-specific cross-reactive cellular responses in pH1N1 naïve individuals

PBMC responses to one or more of three core proteins of pH1N1 virus (PB1, M1, NP) were measured by fluorescence-immunospot and were found in 58% of individuals (44/76 individuals). All individuals with detectable responses had IFN-γ+IL-2- secreting pH1N1 cross-reactive cells to core proteins of pH1N1 (Fig. 3.2.1A), while 34/76 (45%) and 38/76 (50%) had detectable IFN-γ-IL-2+ (Fig. 3.2.1B) and IFN-γ+IL-2+ dual (Fig. 3.2.1C) secreting cells respectively.

The prevalence of cross-reactive cells was highest to PB1 (40/76 individuals, 53%) followed by NP (31/76 individuals, 41%) and M1 (24/76 individuals, 32%) proteins (Fig. 3.2.2A). However, 75% (57/76) of individuals had detectable cross-reactive cellular responses to live pH1N1 virus and a similarly high proportion of individuals had responses to pH1N1 inactivated vaccine (63%, 48/76 individuals), sH1N1 inactivated vaccine (76%, 58/76 individuals) and the sH3N2 inactivated vaccine (72%) (Fig. 3.2.2B).

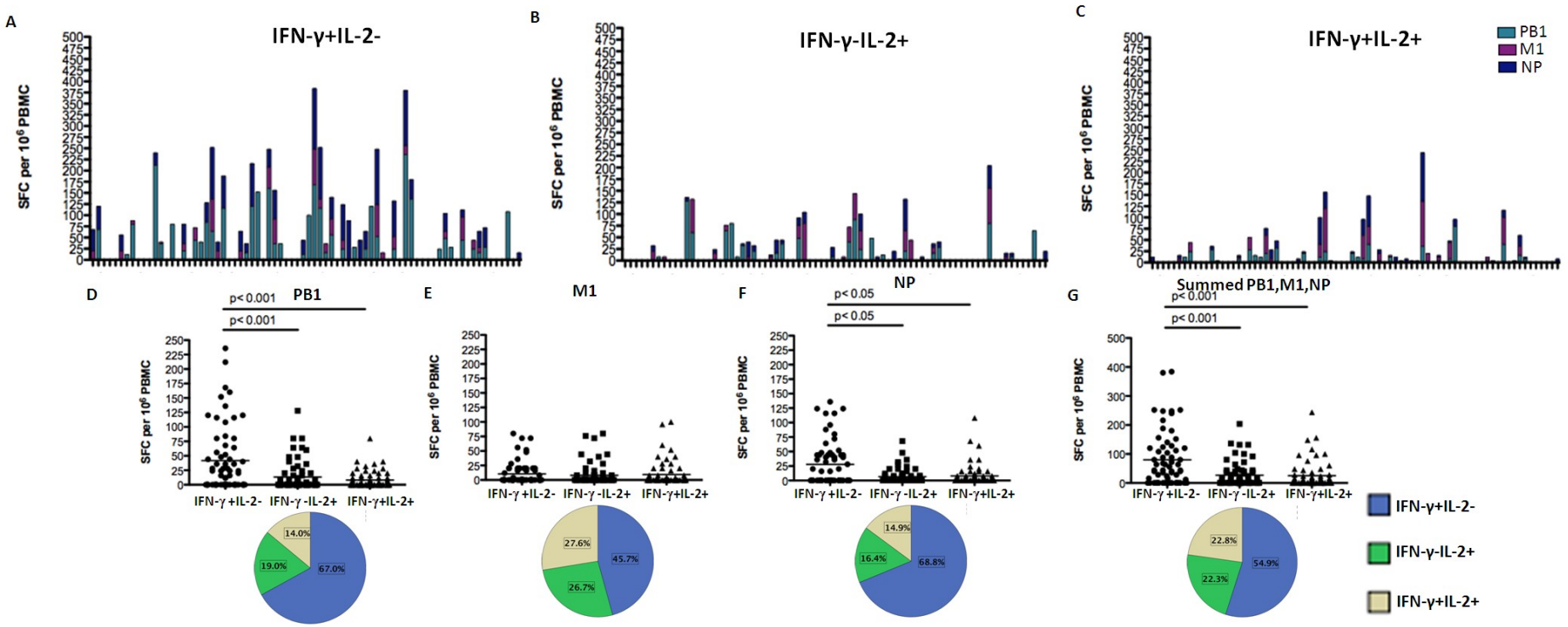

Figure 3.2.1 Pre-existing cross-reactive memory T cell responses to pH1N1 core proteins in pH1N1 sero-negative individuals.

Total magnitude of *ex vivo* PBMC responses from the (A) IFN-γ+IL-2-, (B) IFN-γ-IL-2+, and (C) IFN-γ+IL-2+ dual cytokine-secreting subsets to overlapping peptide pools of PB1, M1 and NP of pH1N1 (A/California/04/09) virus in each individual was measured by fluorescence-

immunospot. Individuals are shown in the same order in (A through C) (n = 76). PB1: polymerase basic protein 1, M1: matrix protein 1, NP: nucleoprotein, SFCs: spot forming cells, PBMCs: peripheral blood mononuclear cells. HAI assay was performed to confirm sero-negativity to H1 of A/England/195/09 and A/California/04/09. Magnitude of *ex vivo* PBMC responses from the IFN-γ+IL-2-, IFN-γ-IL-2+ and IFN-γ+IL-2+ dual-secreting subsets to overlapping peptide pools of PB1 (D), M1 (E), NP (F), and the summed response to PB1, M1 and NP of pH1N1 (A/California/04/09) virus (G). Each symbol represents a single individual and horizontal lines represent the mean response. Differences between subset responses were estimated by Friedman test. Pie charts represent mean proportions of cytokine-secreting responses. Non-responders to antigens excluded, PB1: n = 70, M1: n = 70, NP: n = 69, Summed antigens: n = 63.

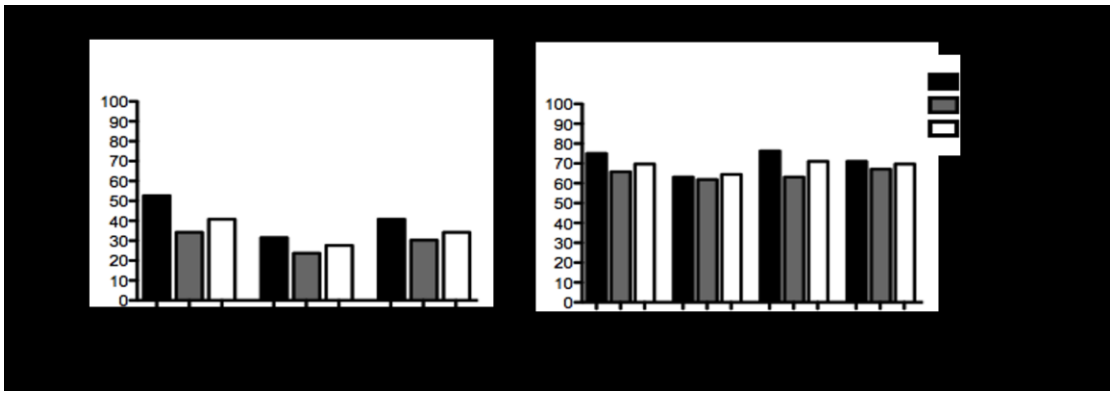

Figure 3.2.2 Prevalence of pH1N1 cross-reactive memory T cell responses.

The proportion of pH1N1 sero-negative individuals with *ex vivo* PBMC responses to overlapping peptide pools of (A) PB1, M1 and NP of pH1N1 (A/California/04/09) and (B) live pH1N1 virus, pH1N1 inactivated vaccine, sH1N1 inactivated vaccine and sH3N2 inactivated vaccine from IFN-γ+IL-2- (black bars), IFN-γ-IL-2+ (grey bars) and IFN-γ+IL-2+ dual (white bars) cytokine-secreting subsets (n = 76) was evaluated by fluorescence-immunospot. Each bar represents the average proportion.

3.2.3 Predominance of IFN-γ+IL-2- secreting pH1N1 cross-reactive cellular responses in pH1N1 naïve individuals

The frequency of the total cellular response summed to all three proteins PB1, M1 and NP was significantly higher ($p < 0.001$) in the IFN-γ+IL-2- secreting (mean 80 SFC/million PBMC, SEM 12) compared to the IFN-γ-IL-2+ (mean 27 SFC/million PBMC, SEM 5) and IFN-γ+IL-2+ dual (mean 25 SFC/million PBMC, SEM 6) secreting cells (Fig. 3.2.1G). Similarly, the frequency of IFN-γ+IL-2- secreting cells were significantly higher for the individual antigen responses PB1 (Fig. 3.2.1D) and NP (Fig. 3.2.1F) but not for M1 protein (Fig. 3.2.1E). However, the relative proportion of IFN-γ+IL-2- secreting subset was

significantly higher compared to the IFN-γ-IL-2+ and IFN-γ+IL-2+ dual secreting subsets for each of the three core proteins and the summed total response (pie charts in Fig. 3.2.1D-G).

We next assessed whether influenza-specific memory T cells that recognise synthetic peptides also recognise naturally processed peptides from APCs in PBMC infected with live virus and recombinant viral proteins. Despite absence of prior exposure to the pH1N1 virus or vaccine, 53/76 (70%) and 45/76 (59%) individuals had memory T cell responses recognising naturally processed peptides presented by APCs infected with live pH1N1 virus or the pH1N1 inactivated vaccine respectively (Fig. 3.2.2B). Similar to responses to pH1N1 core proteins, the frequency and proportion of antigen-specific T cells to pH1N1 virus was predominantly IFN-γ+IL-2- secreting cells (Fig. 3.2.3A). The frequency of IFN-γ+IL-2- secreting subset to live pH1N1 virus was significantly higher (mean 100 SFC/million PBMC, SEM 15) compared to the IFN-γ-IL-2+ (mean 31 SFC/million PBMC, SEM 5) and IFN-γ+IL-2+ dual (mean 28 SFC/million PBMC, SEM 5) secreting subsets. pH1N1 vaccine - specific responses were not significantly different between the three cytokine secreting subsets (Fig. 3.2.3B).

The predominance of IFN-γ+IL-2- secreting cells was not restricted to cross-reactive responses only since PBMC stimulated with inactivated sH1N1 and sH3N2 viruses, the strains circulating prior to the emergence of pH1N1, were also prevalent (Fig. 3.2.2 B) and predominantly IFN-γ+IL-2- secreting subset

(Fig. 3.2.3C). However, the frequency of IFN-γ+IL-2- secreting T cell response to sH1N1 inactivated vaccine was significantly higher than IFN-γ+IL-2- secreting responses to live pH1N1 virus ($p = 0.0421$, Fig. 3.2.3 C compared to A) and pH1N1 inactivated vaccine ($p < 0.0001$, Fig. 3.2.3 C compared to B). The relative proportion IFN-γ+IL-2- secreting T cell response to homosubtypic sH1N1 inactivated vaccine was also significantly higher than cross-reactive pH1N1 inactivated vaccine ($p < 0.0001$, Fig. 3.2.3 C compared to B, pie charts), although there was no difference in the proportion IFN-γ+IL-2- secreting subset between homosubtypic responses to sH1N1 inactivated vaccine and cross-reactive responses to live pH1N1 virus (Fig. 3.2.3 A compared to C, pie charts). Interestingly, the IFN-γ+IL-2- secreting response to sH3N2 inactivated vaccine, was significantly higher than the sH3N2-specific IFN-γ-IL-2+ response but not significantly different to the IFN-γ+IL-2+ dual response (Fig. 3.2.3 D). Furthermore, the frequency IFN-γ+IL-2- secreting T cell response to sH3N2 inactivated vaccine was significantly lower than IFN-γ+IL-2- secreting responses to live pH1N1 virus ($p <0.0001$, Fig. 3.2.3 D compared to A) but not different to pH1N1 inactivated vaccine ($p = 0.762$, Fig. 3.2.3 D compared to B).

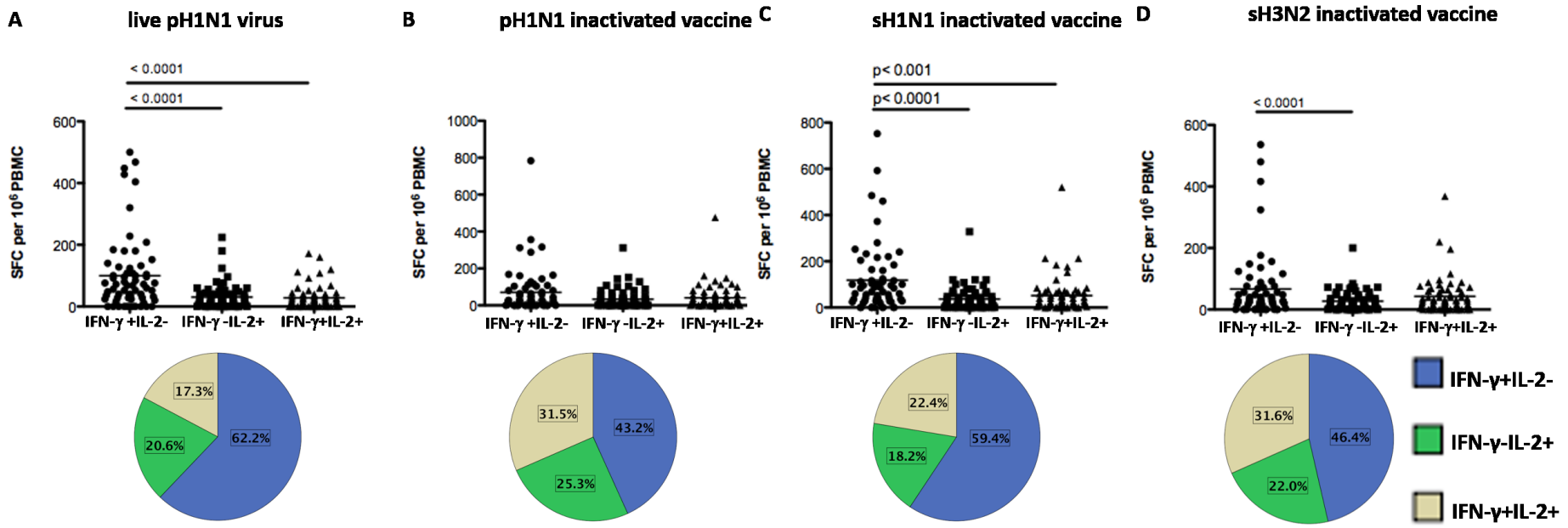

Figure 3.2.3 Cross-reactive memory T cell responses to naturally processed pH1N1 epitopes.

The magnitude of *ex vivo* PBMC responses from the IFN-γ+IL-2-, IFN-γ-IL-2+, and IFN-γ+IL-2+ dual cytokine-secreting subsets to (A) pH1N1 live virus (A/England/195/2009), (B) pH1N1 inactivated vaccine (A/California/07/09, NYMCX-179A), (C) sH1N1 inactivated vaccine (A/Brisbane/10/2007, IVR-148) and (D) sH3N2 inactivated vaccine (A/Uruguay/716/2007, NYMC X-175C) in pH1N1 sero-negative individuals was determined by fluorescence-immunospot. Each symbol represents a single individual and horizontal lines represent means. Pie charts

represent mean proportions of cytokine-secreting responses. Differences between subset responses were estimated by Kruskall-Wallis test. Non-responders to stimulation excluded, pH1N1 live virus (n = 70), pH1N1 vaccine (n = 67), sH1N1 vaccine (n = 68), sH3N2 vaccine (n = 62).

3.2.4 Effect of reported previous seasonal vaccination on pH1N1 cross-reactive responses

To investigate the effect of seasonal influenza vaccination on maintaining cross-reactive T cell responses, the magnitude and cytokine-secreting profile of T cell responses were compared between previous vaccine recipients and unvaccinated individuals. Of the 76 individuals, 6 individuals reported vaccination with the 2008 seasonal influenza vaccine. While this is a small proportion of individuals to enable statistically meaningful comparisons, there was no difference in the magnitude or the functional profile of cytokine secreting T cells to pH1N1 core antigens PB1, M1 or NP (Fig. 3.2.4A-C) between previously vaccinated and unvaccinated individuals. Similarly, there was no difference in the magnitude or the functional profile of cytokine secreting T cells to naturally processed epitopes of live pH1N1 virus or pH1N1 inactivated vaccine between previously vaccinated and unvaccinated individuals (Fig. 3.2.4D-E).

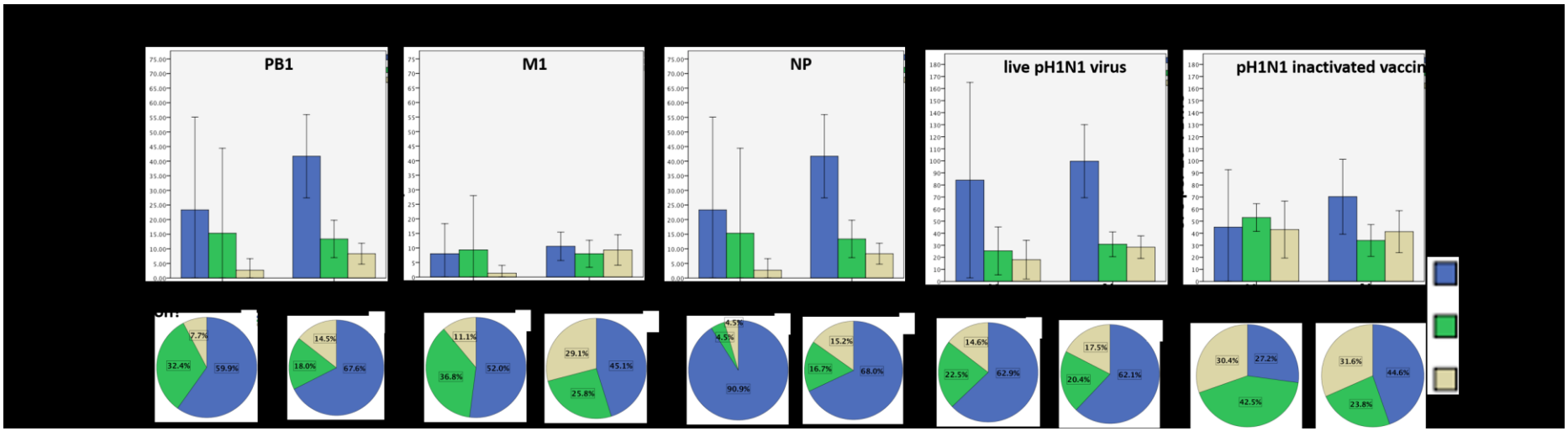

Figure 3.2.4 Previous influenza vaccination does not affect magnitude or cytokine-secreting profile of cross-reactive T cell memory responses to pH1N1.

(A–C) Magnitude of *ex vivo* PBMC responses from the IFN-γ+IL-2-, IFN-γ-IL-2+ and IFN-γ+IL-2+ dual-secreting subsets to overlapping peptide pools of (A) PB1, (B) M1, and (C) NP of pH1N1 (A/California/04/09) virus, (D) pH1N1 live virus or (E) pH1N1 inactivated vaccine in pH1N1 sero-negative individuals among those who reported having the 2008 seasonal influenza vaccine (n = 6) and those who did not have the vaccine (n = 64) as determined by fluorescence-immunospot. Bars show mean responses with two standard error of the mean. Pie charts represent mean proportions of cytokine-secreting responses.

3.3 Cellular correlate of protection against symptomatic influenza

The role of cross-reactive T cells in protection against influenza illness was addressed by correlating pre-existing cross-reactive cellular responses to pH1N1 virus and conserved CD8 T cell epitopes with favourable clinical outcomes of influenza infection in naturally infected individuals. The hypothesis was that pre-existing pH1N1 cross-reactive T cells would protect against symptomatic influenza disease following natural influenza infection.

3.3.1 Study samples

49 individuals were infected with pH1N1 influenza during the study period and had sufficient quantity stored PBMC for analysis. In 25 of these individuals, the date, symptoms and symptom score for the influenza infection episode could be reliably determined (analysis performed by Dr Saranya Sridhar). The median age of the 49 infected individuals was 33 years (IQR = 27 – 40 years) and 57% were female. 23 age- and gender- matched individuals that remained uninfected during the study were selected; they had a median age of 37 years (IQR = 18 – 53 years) and 65% were female. There were no significant differences in age or gender between infected and uninfected individuals.

3.3.2 Pre-existing pH1N1 cross-reactive T cells and illness severity

Firstly, the CD4 or CD8 dependency of cytokine secreting responses from PBMC in fluorescence-immunospot was checked by CD4+ or CD8+ T cell

depletion. Live pH1N1 virus-specific IFN-γ+IL-2- and IFN-γ+IL-2+ dual responses were from both CD4+ and CD8+ T cells since there was no abrogation of the responses on depletion on either T cell subset (Fig. 3.3.1 A). IFN-γ-IL-2+ responses were abrogated when CD4+ but not CD8+ T cells were depleted, confirming that the pH1N1 virus-specific IFN-γ-IL-2+ response is from the CD4+ T cells (Fig. 3.3.1 A). CD8+ depletion reduced IFN-γ+IL-2- response to CD8 conserved epitopes (but this did not reach statistical significance), suggesting that the response was mainly mediated by CD8+ T cells (Fig. 3.3.1 B).

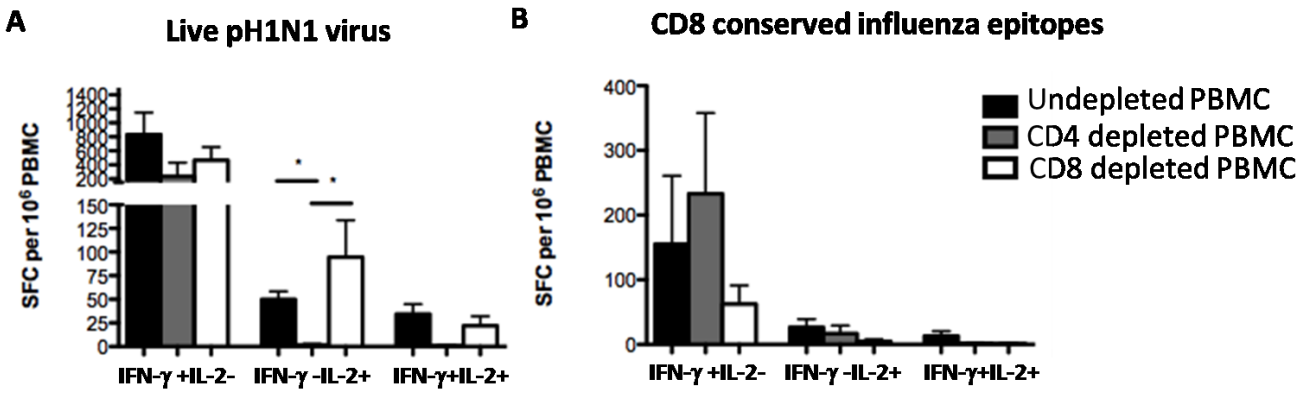

Figure 3.3.1 Contribution of CD4+ and CD8+ T cells to pH1N1 live virus and CD8 conserved epitope pool responses.

PBMCs undepleted or depleted of CD4+ or CD8+ T cells by labelling with CD4 or CD8 microbeads respectively and passing through LD columns, were stimulated overnight with pH1N1 live virus or CD8 conserved epitope pools. The purity of the depletion in each case was > 94% by flow cytometry staining (see Materials and methods section 2.9). Frequencies of cytokine secreting T cell subsets were

enumerated using fluorescence-immunospot (n = 9). Bars show mean and standard error of the mean.

There were no significant differences in frequencies of pre-existing pH1N1 cross-reactive total cytokine secreting or cytokine secreting subsets between individuals who subsequently became infected with pH1N1 and age- and gender- matched individuals who remained uninfected (Fig. 3.3.2). Higher frequencies of pre-existing cross-reactive total cytokine secreting T cell responses to live pH1N1 virus were detected in individuals who developed illness without fever and in individuals without fever and cough and sore throat, although this did not reach statistical significance (Fig. 3.3.3A). However, higher frequencies of total cytokine secreting T cells to conserved CD8 epitopes approached statistical significance ($p = 0.0639$) in individuals who developed illness without fever and cough and sore throat compared to individuals who developed illness with these ILI symptoms (Fig. 3.3.3D). Frequencies of total cytokine secreting T cells to control CMV lysate were not significantly different between the different symptomatic groups (Fig. 3.3.3G). Of the three functional subsets enumerated by fluorescence-immunospot, IFN-γ+IL-2- cytokine secreting cells were the predominant subset. Statistically non-significant higher frequencies of pre-existing cross-reactive total cytokine secreting T cell responses to live pH1N1 virus and conserved CD8 epitopes were detectable in individuals who developed illness without fever, and in individuals without fever and cough and sore throat compared to individuals who developed illness accompanied by fever or illness with fever and cough and sore throat (Fig. 3.3.3 B-C, E-F).

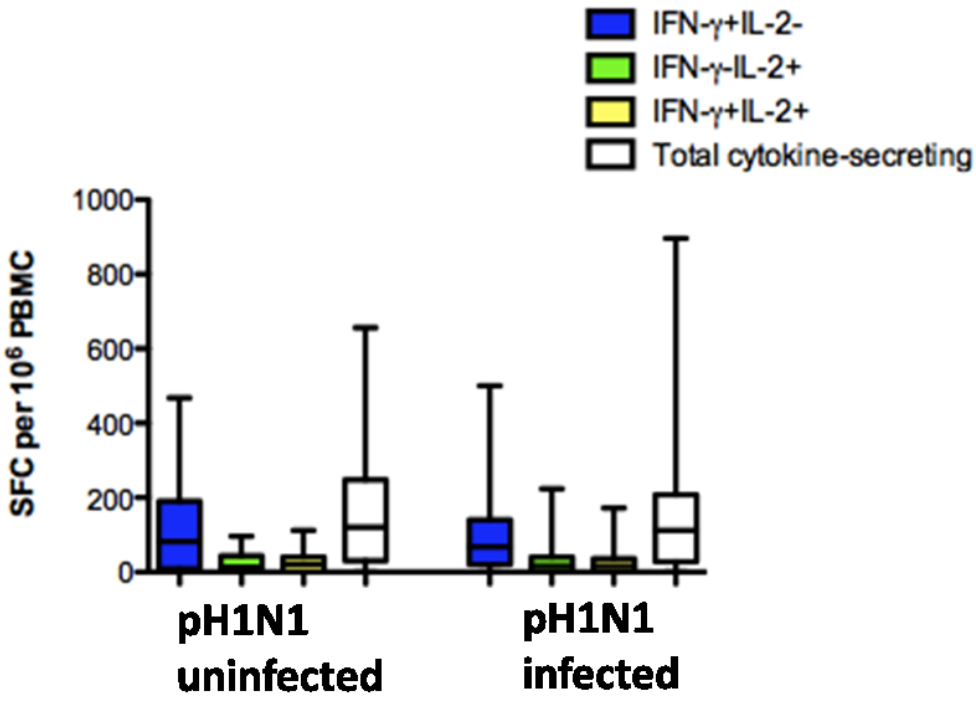

Figure 3.3.2 Pre-existing frequencies of influenza-specific cytokine-secreting T cells in individuals who develop infection versus uninfected individuals.

Comparison of the magnitude of baseline *ex vivo* PBMC responses from the IFN-γ+IL-2−, IFN-γ− IL-2+ and IFN-γ+IL-2+ dual subsets and the total cytokine secreting cells to pH1N1 live virus measured by fluorescence- immunospot between individuals who subsequently develop infection (n=49) and age and gender- matched individuals who remain uninfected (n=23). In the box plots, the box represents the third centile (75%) and first centile (25%), with the horizontal line representing the median (50%). The whiskers represent 1.5 times the IQR. SFC, spot-forming cells.

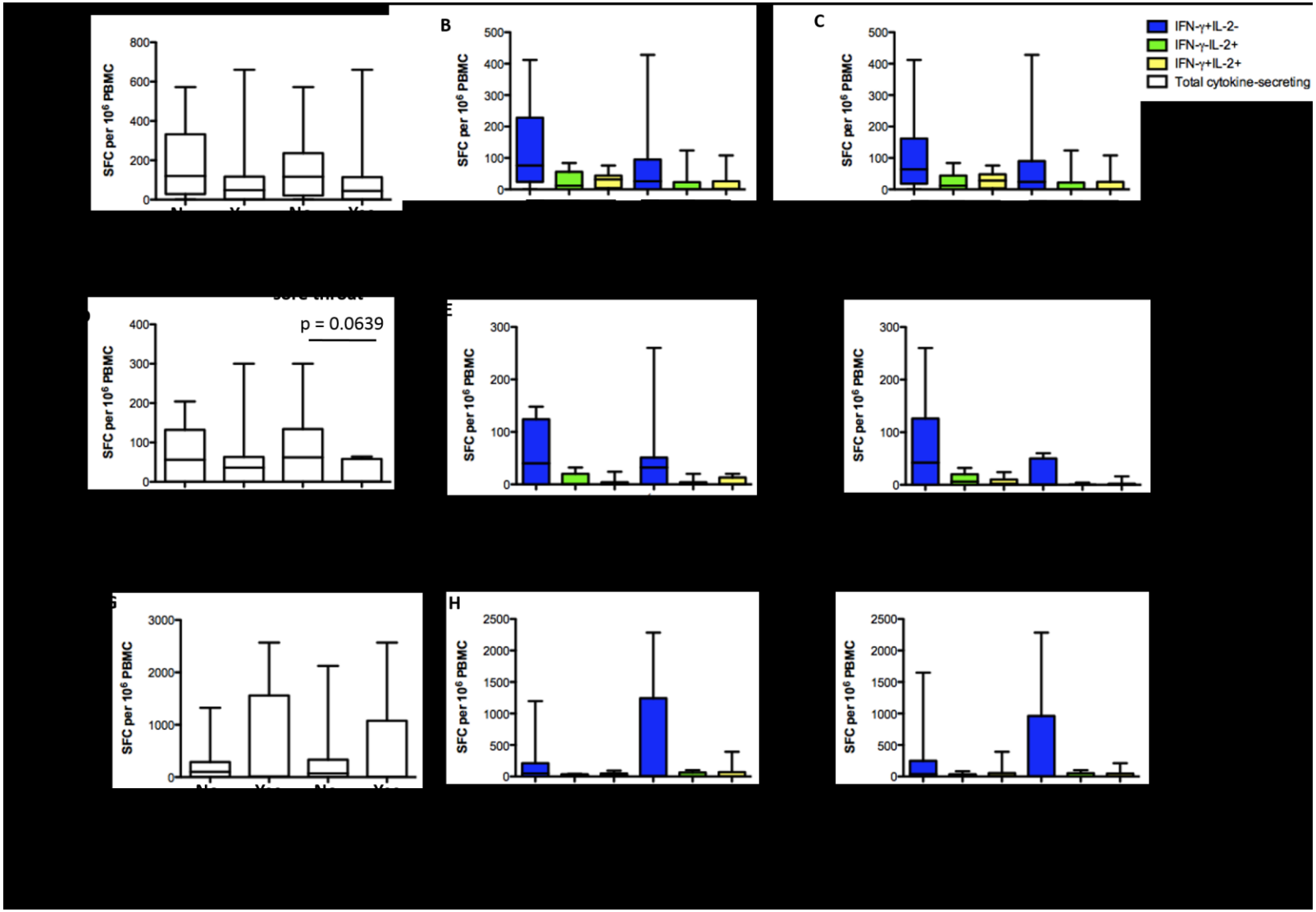
B
C
IFN-γ+IL-2-
IFN-γ-IL-2+
IFN-γ+IL-2+
Total cytokine-secreting
SFC per 10^6 PBMC
p = 0.0639
H

Figure 3.3.3 The frequencies of pre-existing cross-reactive T cells and illness severity in infected individuals.

Responses to live pH1N1 virus stimulation (A, B, C), summed responses to conserved CD8 epitopes from PB1, M1 and NP proteins (D, E, F) and responses to CMV lysate (G, H, I) of total (clear), IFN-γ+IL-2− (blue), IFN-γ− IL-2+ (green) and IFN-γ+IL-2+ dual (yellow) cytokine-secreting cells quantified by fluorescence-immunospot. The total frequency of cytokine-secreting T cells represents the summed frequencies of the three functional subsets: IFN-γ+IL-2−, IFN-γ−IL-2+ and IFN-γ+IL-2+. Cellular immune responses to live pH1N1 virus, CD8 conserved influenza epitopes and CMV lysates were determined in individuals (n = 25) developing an illness with fever (n = 13) compared to those with no fever (n = 12) and in individuals with fever and cough or sore throat (n = 15) compared to those without fever and cough or sore throat (n = 10). P values were estimated by Mann-Whitney nonparametric tests. In the box plots, the box represents the third centile (75%) and first centile (25%), with the horizontal line representing the median (50%). The whiskers represent 1.5 times the IQR. SFC, spot-forming cells.

Frequencies of pre-existing CD8 conserved epitope-specific total cytokine secreting and IFN-γ+IL-2- T cells most strongly inversely correlated with total symptom score during illness ($r = -0.508$, $p = 0.0133$ and $r = -0.437$, $p = 0.0371$, Fig. 3.3.4B and E). The weaker inverse correlations were between total symptom score and frequencies of pH1N1 virus-specific total cytokine secreting ($r = -0.387$, $p = 0.0678$, Fig. 3.3.3A), IFN-γ+IL-2- ($r = -0.367$, $p = 0.0849$, Fig. 3.3.4D) and IFN-γ+IL-2+ ($r = -0.379$, $p = 0.0747$, Fig. 3.3.4J) T cells. Conserved CD8 epitope-specific IFN-γ-IL-2+ T cells also weakly inversely correlated with total symptom score ($r = -0.392$, $p = 0.0643$, Fig. 3.3.4H). There was no correlation between the frequencies of CMV lysate-specific total cytokine secreting or any of the cytokine secreting T cell subsets and total symptom score (Fig. 3.3.4 C, F, I, L).

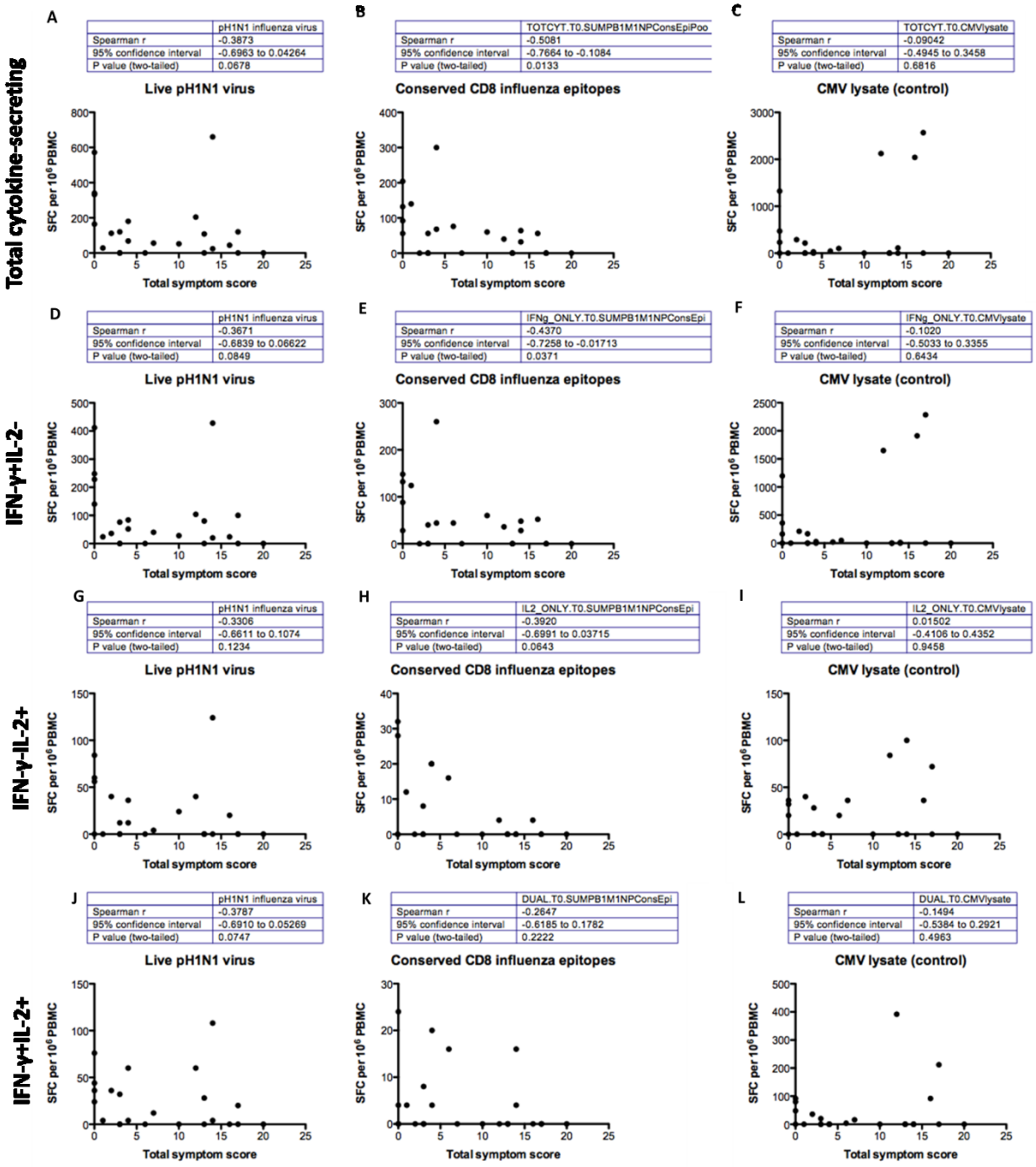

Figure 3.3.4 Inverse correlation of cross-reactive T cells and symptom score.

Correlation between symptom scores and the frequency of total (A, B, C), IFN-γ+IL-2− (D, E, F), IFN-γ-IL-2+ (G, H, I), IFN-γ+IL-2+ (J, K, L), cellular responses to live pH1N1 virus (A, D, G, J), the summed responses to conserved CD8 epitopes from PB1, M1 and NP proteins (B, E, H, K) and the responses to CMV lysate (control antigen) (C, F, I, L) quantified by fluorescence-immunospot. Symptom score was defined by totaling the scores for each of the following symptoms: fever, sore throat,

cough, headache and myalgia. r values are the Spearman rank correlation coefficients. Each circle on the plot represents an individual (n = 25).

3.3.3 Phenotype of pre-existing pH1N1 cross-reactive CD8+IFN-γ+IL-2- T cells and CD4+IFN-γ+IL-2- T cells and correlation with symptom scores

The specific phenotype of the pre-existing pH1N1-specific protection-associated T cells was determined by multiparameter flow cytometry on PBMC samples remaining from 22 of 25 infected donors. The gating strategy is shown in Fig. 3.3.5. The majority of the live pH1N1 virus-specific IFN-γ+IL-2-CD3+ response on flow cytometry in these 22 donors was from CD3+CD8+ T cells (p = 0.007, Fig. 3.3.6). Importantly, CD45RA and CCR7 expression did not change during the 18 hour *in vitro* stimulation with live pH1N1 virus (Fig. 3.3.7). Stratifying the IFN-γ+IL-2- T cell population into its constituent memory subsets using CD45RA and CCR7 showed a predominance of CD45RA+CCR7- late effector and CD45RA-CCR7- effector memory amongst both CD8+IFN-γ+IL-2- (Fig. 3.3.8A) and CD4+IFN-γ+IL-2- (Fig. 3.3.8 D) T cells in response to live pH1N1 virus. However, only the proportion of CD45RA+CCR7- late effectors of the CD8+IFN-γ+IL-2- T cells inversely correlated with total symptom score (r = -0.604, p = 0.0029, Fig. 3.3.8B). The proportion of CD45RA+CCR7- late effector subset of live pH1N1 virus-specific CD4+IFN-γ+IL-2- T cells was not associated with total symptom score (r = -0.0384, p = 0.865, Fig. 3.3.8E). Furthermore, 70% and 33% of this pre-existing protection-associated pH1N1 virus-specific CD8+IFN-γ+IL-2-CD45RA+CCR7- T cell population expressed tissue-homing marker CCR5 and degranulation marker CD107ab respectively (Fig. 3.3.8C).

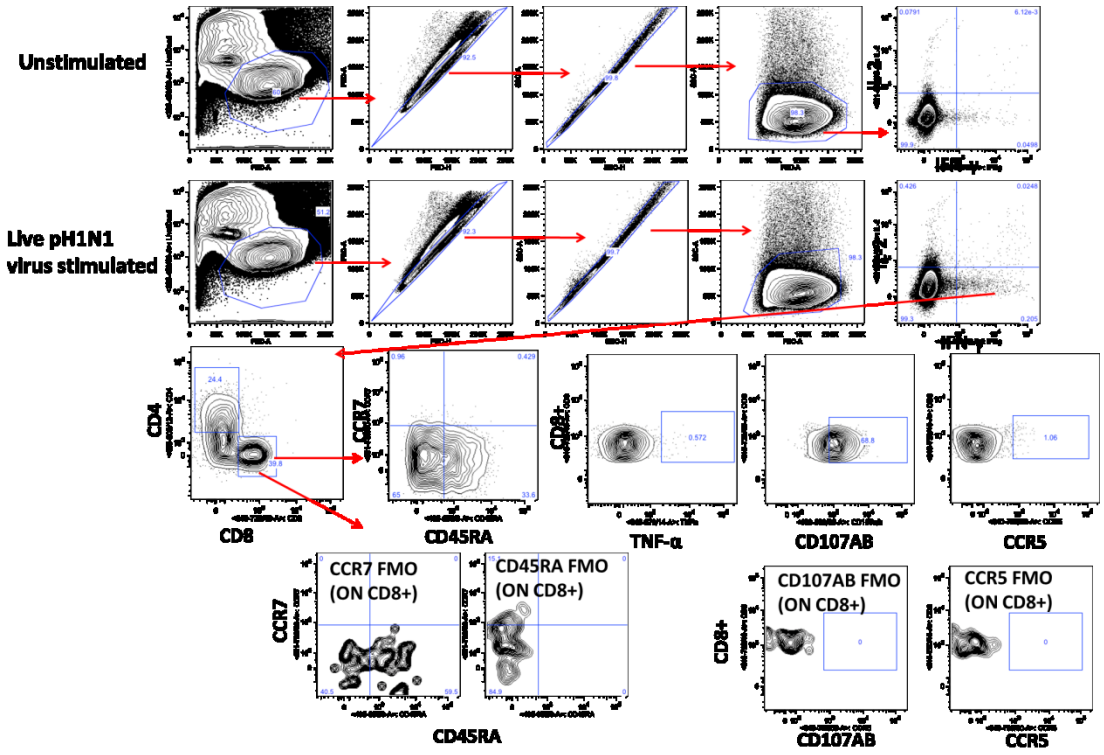

Figure 3.3.5 Gating strategy for flow cytometric analysis of CD8+IFN-γ+IL-2- cells.

Responses to live pH1N1 virus stimulation were measured by multi-parameter flow cytometry. PBMCs stimulated with live pH1N1 virus for 18 hours were stained for surface markers of memory, lung homing, degranulation and intracellular cytokines. PBMCs were gated on live, single cells, low forward and side scatter for lymphocytes, a negative dump gate for CD56, CD14 and CD19, CD3+, IFN-γ+IL-2- and CD8+CD4- gating. CD8+ cells of the CD45RA+CCR7- subset were analysed for expression of CCR5, CD107 (isotypes A and B) and TNF-α using Flowjo software. The Fluorescence Minus One (FMO) controls are shown for CCR7, CD45RA, CD107 (isotypes A and B) and CCR5 which were used to set the gates to identify positive populations.

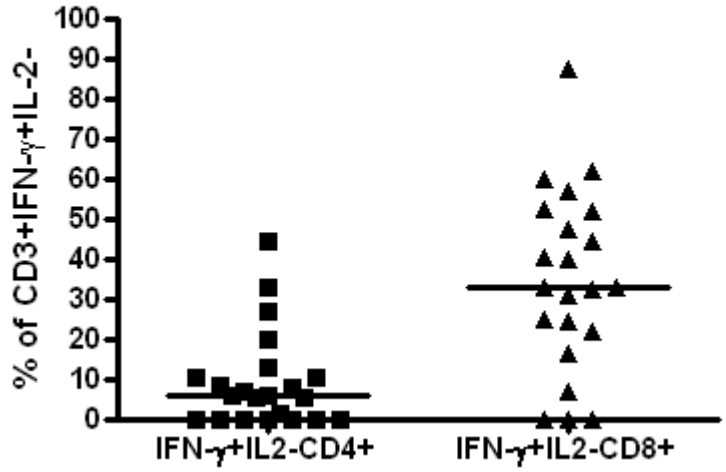

Figure 3.3.6 Percentages of pH1N1 stimulated IFN-γ+IL-2- cells that are CD3+CD4+ and CD3+CD8+.

Responses to live pH1N1 virus stimulation were measured by multi-parameter flow cytometry. PBMCs stimulated with live pH1N1 virus for 18 hours were stained and analysed as per the gating strategy in Fig. 3.3.5. Dot plots show the percentage of the gated IFN-γ+IL-2- that is CD3+CD4+ or CD3+CD8+. P value was estimated by Wilcoxon signed-rank nonparametric test (n = 22).

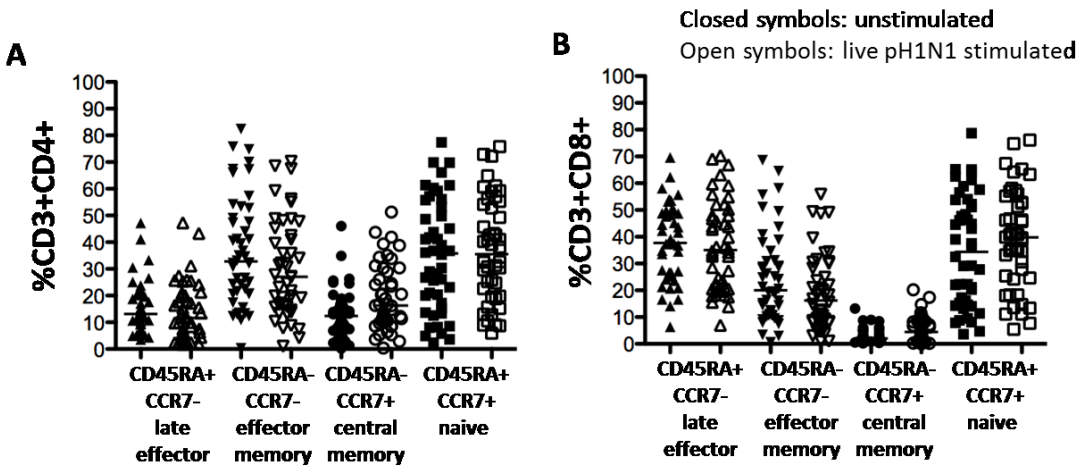

Figure 3.3.7 CD45RA and CCR7 expression is not changed by *in vitro* stimulation.

Phenotypic characterisation using multi-parameter flow cytometry of the different memory subsets of influenza virus-specific CD4+ and CD8+ T cells based on CCR7 and CD45RA surface expression following overnight stimulation of PBMCs with live pH1N1 virus (open symbols) or unstimulated controls (closed symbols) in 46 individuals (all baseline PBMC samples). Proportion of CD3+CD4+ (A) or CD3+CD8+ (B) T cells of effector memory (CD45RA-CCR7-), late effector (CD45RA+CCR7-), central memory (CD45RA-CCR7+) or naive (CD45RA+CCR7+) phenotype. Symbols represent responses for each individual with the horizontal line representing the median response. Statistical analysis by one-way ANOVA with Dunn's post-test comparisons showed no statistically significant differences in proportions of the different memory subsets between unstimulated and live virus stimulated donor responses.

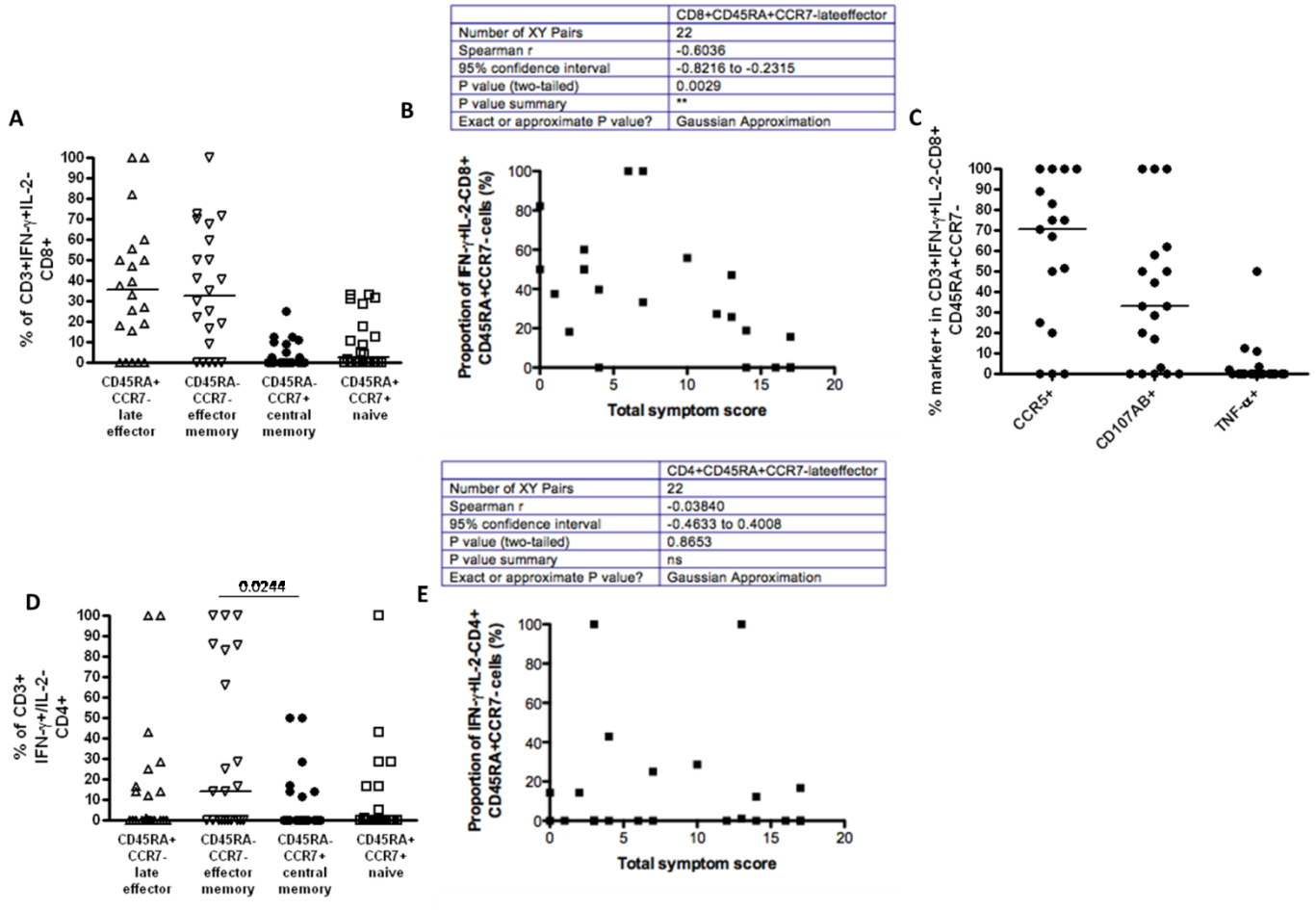

Figure 3.3.8 Inverse correlation of pre-existing pH1N1 cross-reactive late effector CD8+IFN-γ+IL-2− T cells and symptom scores.

Phenotypic characterisation was performed using multiparameter flow cytometry of the different memory subsets of influenza virus–specific CD8+IFN-γ+IL-2− cells on the basis of CCR7 and CD45RA surface expression after overnight stimulation of baseline (pre-infection) PBMCs with live pH1N1 virus in pH1N1-infected individuals (n = 22; in 3 of 25 infected individuals, samples were of insufficient quantity for flow cytometry analysis). (A) The proportions of CD8+IFN-γ+IL-2− or (D) CD4+IFN-γ+IL-2− secreting cells that were of the effector-memory (CD45RA−CCR7−), late-effector (CD45RA+CCR7−), central-memory (CD45RA−CCR7+) or naive (CD45RA+CCR7+) phenotype. (B) Correlation between the proportion of pre-existing CD3+CD8+IFN-γ+IL-2− cells of the late-effector CD45RA+CCR7− subset or (E) CD3+CD4+IFN-γ+IL-2− cells of the late-effector CD45RA+CCR7− subset and total symptom score. r values are the Spearman rank correlation coefficients. (C) In individuals with influenza-specific late-effector CD8+IFN-γ+IL-2−CD45RA+CCR7− cells (n = 17), further characterisation of these cells for expression of CD107AB, CCR5 and TNF-α was undertaken with multiparameter flow cytometry. Symbols represent the proportion of CD45RA+CCR7−CD8+IFN-γ+IL-2− cells expressing CD107AB, CCR5 and TNF-α for each individual, with the line showing the median response. Each symbol on the plot represents responses for an individual.

3.4 Phenotype of pH1N1 cross-reactive CD4+ and CD8+ T cells

In addition to the assessment of IFN-γ and IL-2 cytokine secretion (Results section 3.2), the polyfunctional profile of influenza-specific memory T cells can be comprehensively characterised in terms of other cytokines and markers important in antiviral immunity. For example: the antiviral cytokine TNF-α, the expression of CD57 as a surrogate of replicative senesence, (Akondy *et al.*, 2009). Furthermore, the expression of CCR5, a chemokine receptor responding to inflammatory signals (including the ligands CCL3, CCL4 and CCL5) resulting in cell migration and adhesion can be used to assess lung tissue homing potential (Rabin *et al.*, 1999). A multiparameter flow cytometry panel was designed and optimised to comprehensively characterise the phenotype of T cells reacting to live pH1N1 virus.

3.4.1 Study samples

In 65 of the 76 pH1N1 seronegative individuals in whom cryopreserved PBMC remained after fluorescence-immunospot responses were measured (Results section 3.2), comprehensive characterisation of PBMC responses was undertaken by flow cytometry. 61/65 and 50/65 individuals had samples of sufficient quality and quantity of PBMC to enable assessment of responses to live pH1N1 virus and CMV respectively (unstimulated negative control and PMA/I positive control responses were also assessed for each individual).

3.4.2 Comparison of influenza and CMV –specific CD4+ T cell responses

PBMC were stimulated for 18 hours with live pH1N1 virus, or CMV infected cell lysate (as a model of a latent infection). The gating strategy used to analyse the flow cytometry data is shown in Fig. 3.4.1. CD4+ T cell cytokine expression was compared between pH1N1 virus and CMV lysate -specific populations. The majority of individuals showed antigen-specific cytokine positive responses above background and the prevalence of responses were similar for pH1N1 virus-specific and CMV lysate –specific CD4+ T cells (90% and 84% of individuals respectively, Table 3.4.1). 70% (43/61), 59% (36/61) and 82% (50/61) of individuals responded to live pH1N1 virus stimulation by CD4+IFN-γ+, CD4+IL-2+ and CD4+TNF-α+ cytokine responses respectively (Table 3.4.1). Similarly 70% (35/50), 54%(27/50) and 64% (32/50) of individuals responded to CMV-lysate stimulation by CD4+IFN-γ+, CD4+IL-2+ and CD4+TNF-α+ cytokine responses respectively (Table 3.4.1). However, pH1N1-specific CD4+ cytokine responses showed a hierarchy with CD4+TNF-α+ (median = 0.05%, IQR = 0 – 0.30) response significantly higher than CD4+IFN-γ+ (median = 0.01%, IQR = 0 – 0.03) and CD4+IL-2+ (median = 0.01%, IQR = 0 - 0.02) whereas there was no hierarchy in CMV-lysate-specific CD4+ cytokine responses (Fig. 3.4.2 A and B). Furthermore, the frequency of pH1N1-specific CD4+TNF-α+ T cells was significantly higher ($p = 0.0082$) than CMV-specific CD4+TNF-α+ (median = 0.02%, IQR = 0 - 0.08) T cells respectively (Fig. 3.4.2A-B).

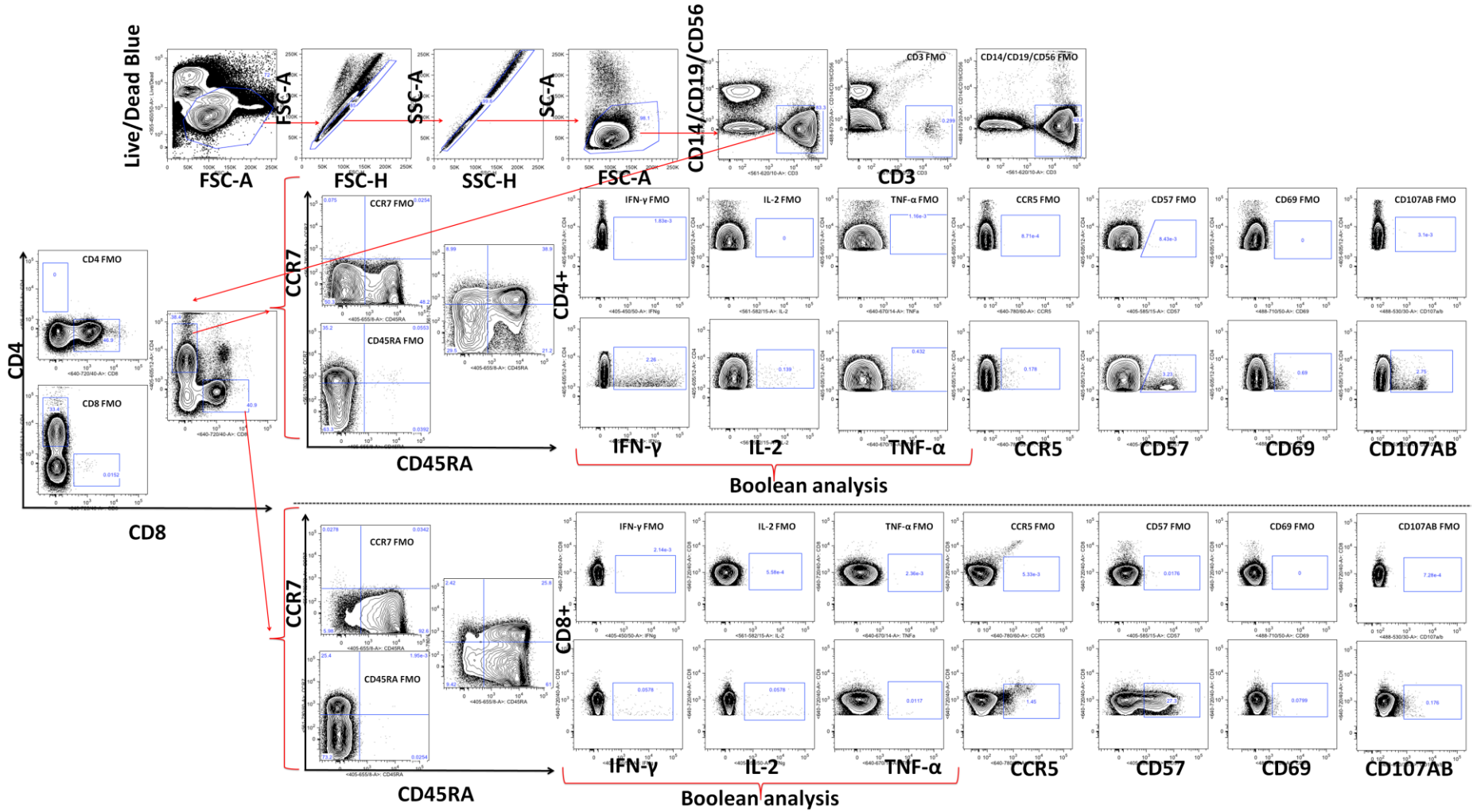
Live/Dead Blue
FSC-A
FSC-A
FSC-H
SSC-A
SSC-H
SC-A
FSC-A
CD14/CD19/CD56
CD3
CD3 FMO
CD14/CD19/CD56 FMO
CD4
CD4 FMO
CD8 FMO
CD8
CCR7
CCR7 FMO
CD45RA FMO
CD45RA
CD4+
IFN-γ FMO
IL-2 FMO
TNF-α FMO
CCR5 FMO
CD57 FMO
CD69 FMO
CD107AB FMO
IFN-γ
IL-2
TNF-α
CCR5
CD57
CD69
CD107AB
Boolean analysis
CD8+
IFN-γ FMO
IL-2 FMO
TNF-α FMO
CCR5 FMO
CD57 FMO
CD69 FMO
CD107AB FMO
IFN-γ
IL-2
TNF-α
CCR5
CD57
CD69
CD107AB
Boolean analysis

Figure 3.4.1 Gating strategy for flow cytometric analysis of CD3+CD8+ and CD3+CD4+ T cells.

Responses to live pH1N1 virus stimulation were measured by multi-parameter flow cytometry. PBMCs stimulated with live pH1N1 virus for 18 hours were stained for surface or intracellular markers. PBMCs were gated on live, single cells, low forward and side scatter for lymphocytes, a negative dump gate for CD56, CD14 and CD19 and CD3+CD4+CD8- or CD3+CD4-CD8+ T cells. CD3+CD4+CD8- or CD3+CD4-CD8+ T cells were then gated on CD45RA and CCR7 for naïve, effector and memory subsets; CD107 (isotypes A and B) for degranulation; CD69 for early activation; CCR5 for lung homing; CD57 for replicative senescence markers and intracellular cytokines (IFN-γ, IL-2, TNF-α). The Fluorescence Minus One (FMO) or unstimulated controls are shown for respective markers that were used to set the gates to identify positive populations.

	CD4+IFN-γ+	CD4+IL-2+	CD4+TNF-α+	Any cytokine response
Number of responders (% responders)				
live pH1N1 virus (total =61)	43 (70)	36 (59)	50 (82)	55 (90)
CMV lysate (total = 50)	35 (70)	27 (54)	32 (64)	42 (84)

Table 3.4.1 Prevalence of antigen-specific CD4+ T cell responses.

The numbers and proportions of pH1N1 sero-negative individuals with *ex vivo* PBMC responses to live pH1N1 virus or CMV lysate from IFN-γ, IL-2, TNF-α or any cytokine (IFN-γ+ or IL-2+ or TNF-α+) secreting CD3+CD4+CD8- T cells evaluated by flow cytometry.

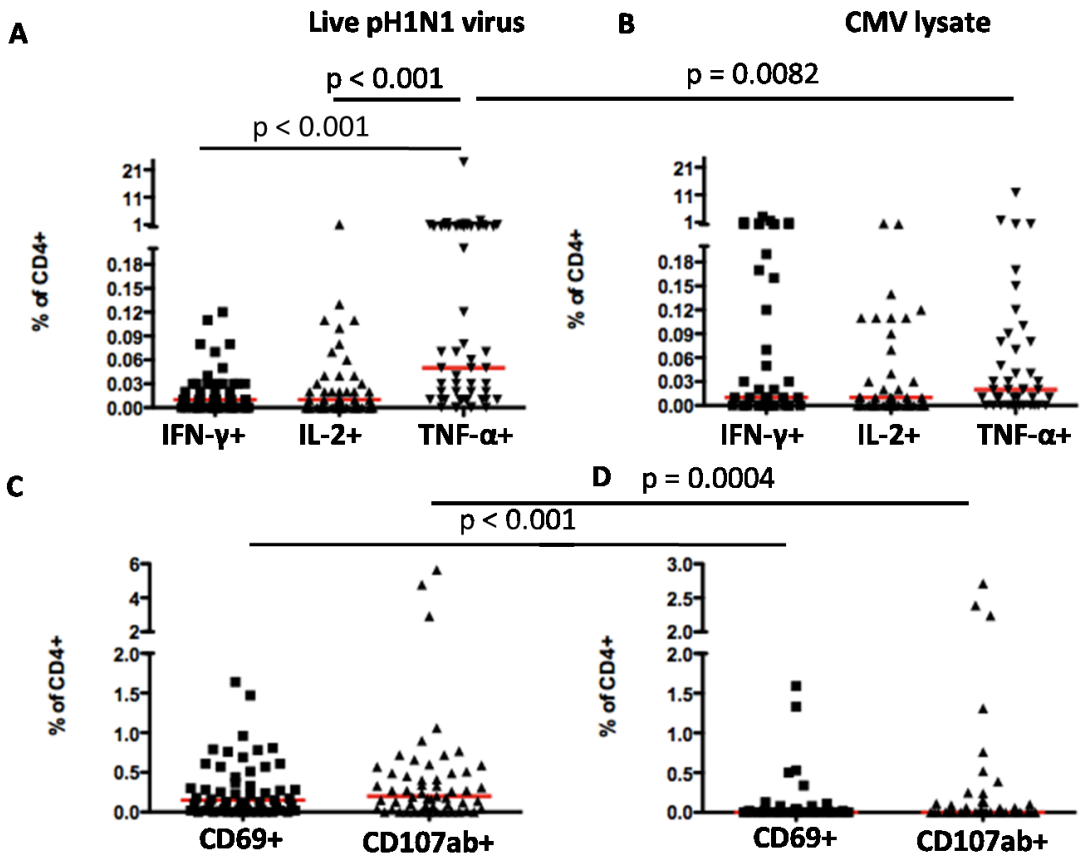

Figure 3.4.2 Comparison of pH1N1 live virus and CMV lysate -specific CD4+ T cells.

Frequency of *ex vivo* PBMC responses from CD4+IFN-γ+, CD4+IL-2+ and CD4+TNF-α+ or CD4+CD69+ and CD4+CD107ab+ T cells evaluated by flow cytometry to live pH1N1 virus (A, C) or CMV lysate (B, D) and gated as shown in Fig. 3.4.1. Each symbol represents a single individual and horizontal red lines represent the median response. Differences between subset responses were estimated by Friedman test within antigen-specific T cells or by Mann Whitney test between pH1N1 live virus and CMV lysate -specific T cells. Non-responders to antigens excluded, pH1N1 live virus: n = 55, CMV lysate: n = 42.

The seven possible cytokine expression combinations of IFN-γ, IL-2 and TNF-α and the triple negative response were analysed using boolean gating in pH1N1- specific or CMV-specific CD4+ T cells (Fig. 3.4.3). CD4+TNF-α+ single cytokine positive T cells were the highest frequency of pH1N1-specific CD4+ T cells (mean = 0.716%, SEM = 0.423), which was significantly higher than all other boolean subsets (Fig. 3.4.3A). The other detectable boolean combinations of pH1N1-specific CD4+ T cells were IL-2+ single cytokine positive (mean = 0.0226%, SEM = 0.00921) that were significantly higher ($p<0.001$) than the dual IFN-γ-IL-2+TNF-α+ (mean = 0.0116%, SEM = 0.0108) T cells, and IFN-γ+ single cytokine positive (mean = 0.0131%, SEM = 0.00263) T cells.

Although there was no hierarchy in CMV lysate-specific CD4+ cytokine responses at total cytokine level (Fig. 3.4.2B), frequencies of single IFN-γ+ (mean = 0.154%, SEM = 0.0532) CD4+ T cell subsets were significantly higher than all other boolean subsets except single TNF-α+ (mean = 0.3058%, SEM = 0.277) which was also significantly higher than IFN-γ-IL-2+TNF-α+ dual cytokine positive cells (mean = 0.00527%, SEM = 0.00448, $p < 0.01$) and triple negative (mean = 0.00714%, SEM = 0.0004, $p < 0.001$) T cells (Fig. 3.4.3B).

Consistent with the difference between the antigen-specific CD4+TNF-α+ T cells at total cytokine level, only the pH1N1-specific IFN-γ-IL-2-TNF-α+CD4+ T cell boolean subset was significantly higher ($p < 0.01$) than the

corresponding CMV-specific boolean subset (Fig. 3.4.3). Notably, low frequencies of CMV lysate-specific triple IFN-γ+IL-2+TNF-α+CD4+ T cell responses (mean = 0.0132%, SEM = 0.00822) were detectable whereas very little pH1N1-specific IFN-γ+IL-2+TNF-α+CD4+ T cell response was detected (mean = 0.00195%, SEM = 0.000565).

CD69 and CD107ab staining was used to identify antigen-specific cells expressing early activation and degranulation capacity respectively. Frequencies of pH1N1-specific CD4+CD69+ (median = 0.150%, IQR = 0 – 0.42) and CD4+CD107ab+ (median = 0.20%, IQR = 0 - 0.45) were significantly higher than CMV-specific CD4+CD69+ (median = 0%, IQR = 0 - 0.04) and CD4+CD107ab+ T cells (median = 0%, IQR = 0 - 0.13) ($p < 0.001$ and $p = 0.0004$ respectively, Fig. 3.4.2C-D).

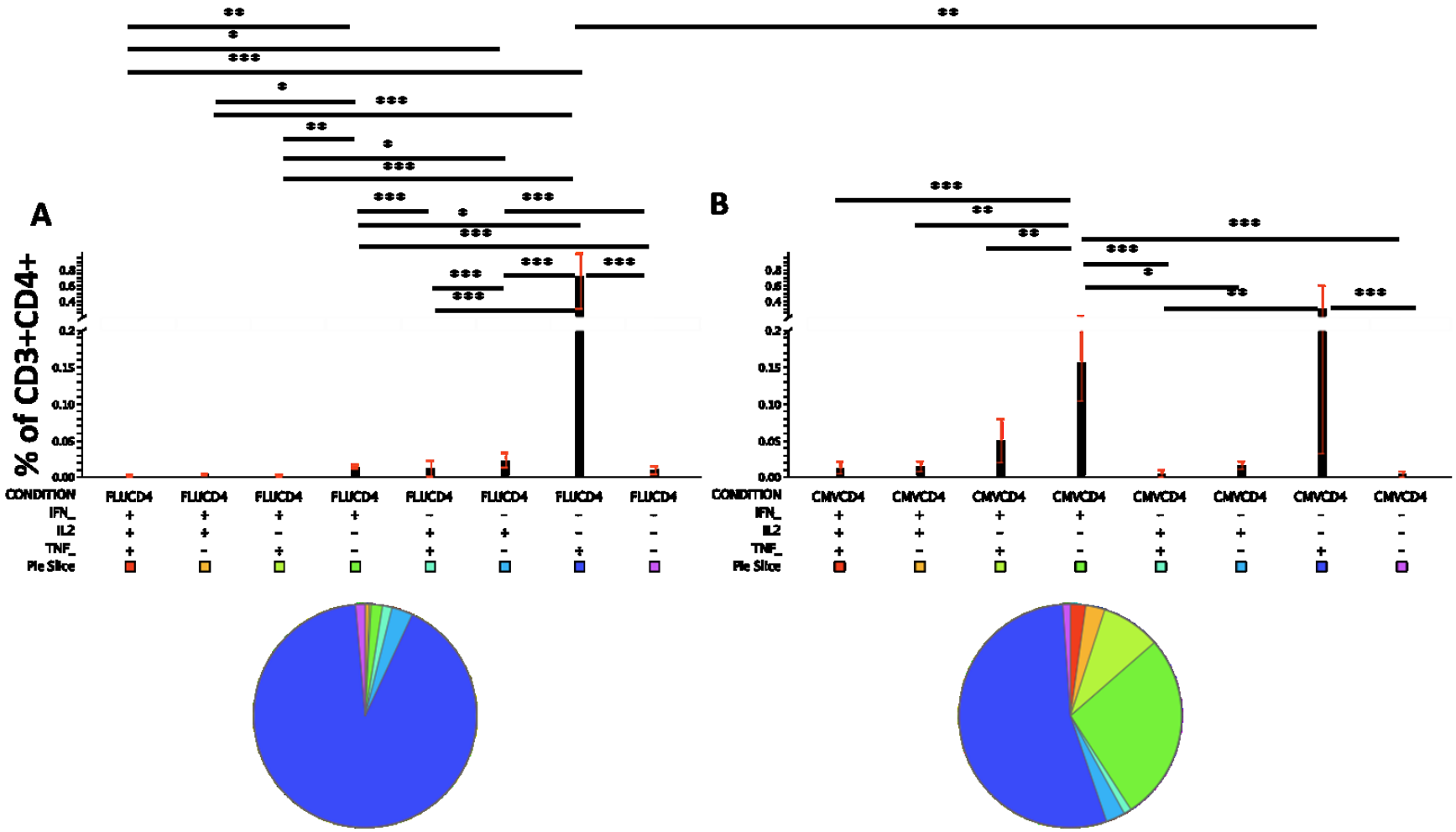

Figure 3.4.3 Cytokine profiles of pH1N1 live virus and CMV lysate -specific CD4+ T cells.

Boolean analysis using SPICE software was performed to analyse CD3+CD4+CD8- T cells for each cytokine profile of *ex vivo* PBMC responses to live pH1N1 virus (A) or CMV lysate (B) following flow cytometry staining and gating as in Fig. 3.4.1. Bars represent mean and standard error of the mean percentage positive of CD3+CD4+CD8- T cells. Differences between subset responses were estimated by Friedman test within antigen-specific T cells or by Kruskal Wallis test between pH1N1 live virus and CMV lysate -specific T cells. Pie charts represent mean proportions for each cytokine profile. Non-responders to antigens excluded, pH1N1 live virus: n = 55, CMV lysate: n = 42. * $p \leq 0.05$, ** $p \leq 0.01$, *** $p \leq 0.001$. IFN_ = IFN-γ, IL2 = IL-2, TNF_ = TNF-α.

Together these results indicate pH1N1-specific CD4+ T cells are mainly single-TNF-α+ and a lower frequency of single IFN-γ+, single IL-2+ and dual IFN-γ-IL-2+TNF-α+ cytokine positive cells. CMV-lysate specific CD4+ T cells are also mainly single-TNF-α+ and single IFN-γ+ cytokine positive cells but there was no significant difference in the frequency of these two cytokine positive subsets. The frequency of pH1N1-specific CD4+TNF-α+ T cells was significantly higher compared to CMV lysate-specific CD4+TNF-α+ T cells. Furthermore, pH1N1-specific CD4+ T cells show more degranulating (CD107ab+) and recently activated (CD69+) phenotype compared to CMV lysate-specific CD4+ T cells.

3.4.3 Memory phenotype of cytokine-expressing CD4+ T cells in influenza or CMV stimulation

To characterise the memory phenotype for each cytokine secreting CD4+ T cell population in live pH1N1 virus stimulated or CMV lysate stimulated PBMC, the expression of CD45RA and CCR7 was assessed. CD4+IFN-γ+ cells were predominantly CCR7- effector memory (CCR7-CD45RA-) or late effector (CCR7-CD45RA+) cells in both live pH1N1 virus (Fig. 3.4.4A) and CMV lysate (Fig. 3.4.4B) stimulation. Non-specific IFN-γ+ cells also showed a similar predominance of effector memory and late effector phenotype (Fig. 3.4.4C), however, all subsets were significantly different to corresponding subsets in live pH1N1 virus stimulation, hence non-specific and antigen-specific IFN-γ+ cells showed distinct memory/differentiation phenotypes.

CMV-lysate stimulated CD4+IL-2+ and CD4+TNF-α+ T cells were also predominantly CCR7- effector memory or late effector memory cells (Fig. 3.4.4E and H), however, pH1N1 stimulated CD4+IL-2+ cells had similar frequencies of naïve, Temra and Tem (Fig. 3.4.4D) and CD4+TNF-α+ T cells had similar frequencies of naïve and Temra (Fig. 3.4.4G). The most striking differences were apparent when the mean proportion of each phenotypic T cell subset was expressed in pie charts for each cytokine positive CD4+ T cell population. 45.68% of CD4+IFN-γ+ pH1N1 stimulated cells were Temra, whereas only 28.45% and 36.01% of CD4+IL-2+ and CD4+TNF-α+ pH1N1 stimulated T cells respectively were Temra. Tem predominated the CMV stimulated CD4+IFN-γ+ (55.32%), CD4+IL-2+ (46.45%) and CD4+TNF-α+ (44.25%) T cells.

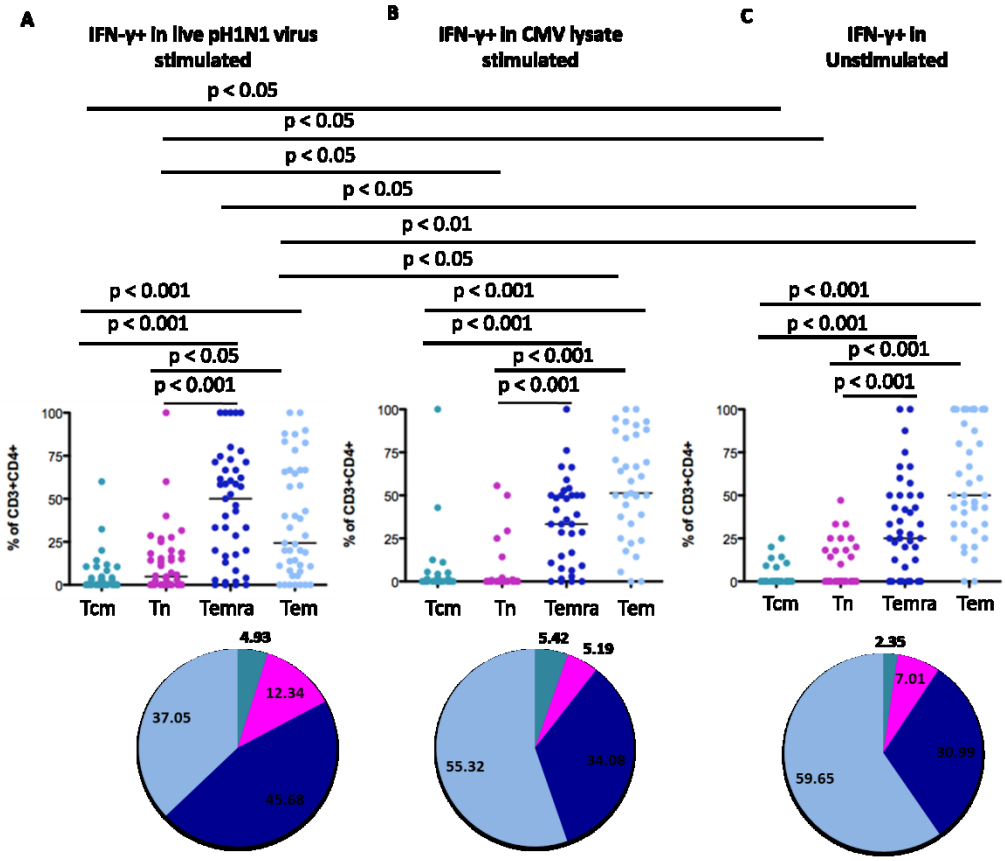

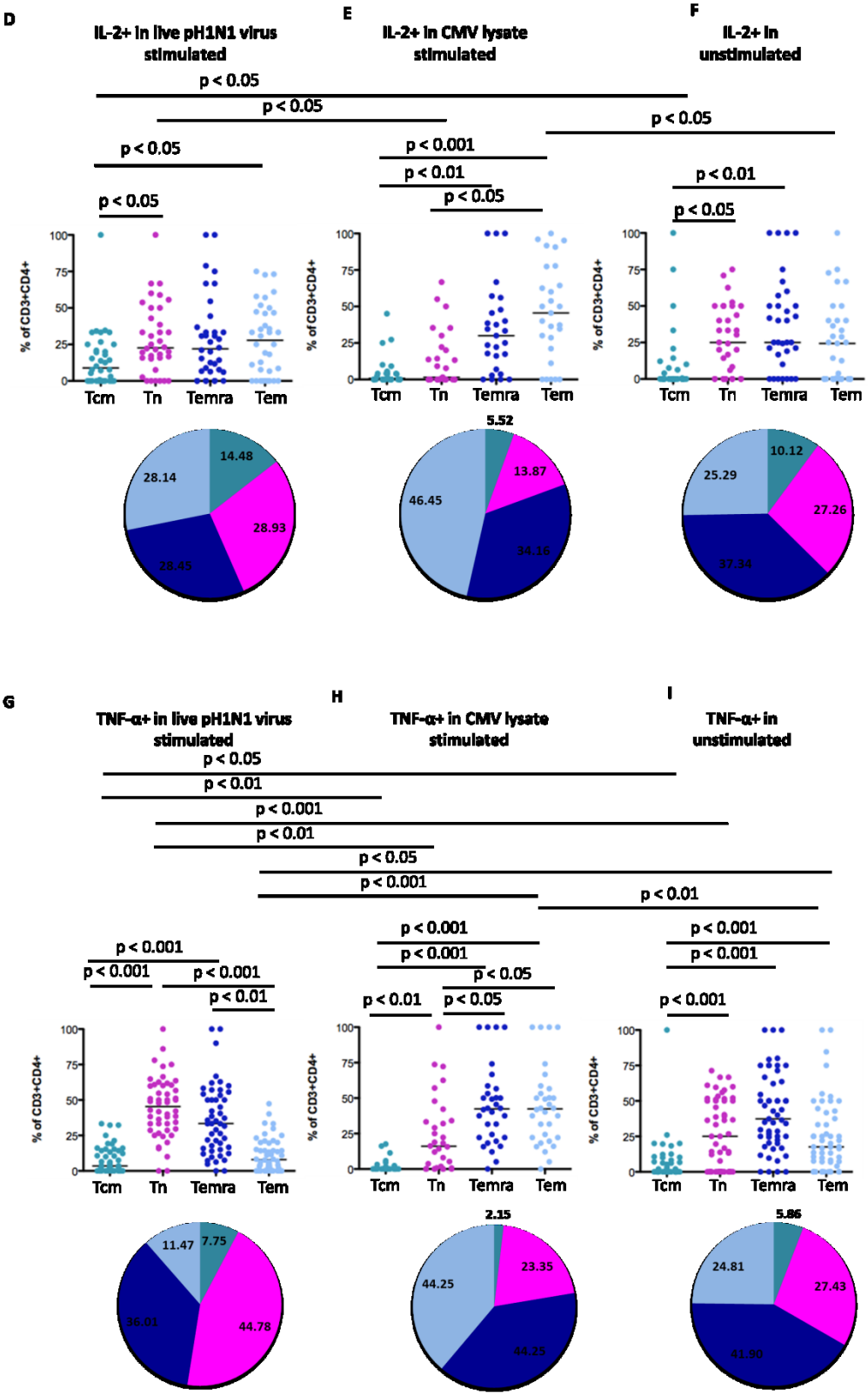

Figure 3.4.4 Effector and memory phenotype of pH1N1 live virus and CMV lysate - specific CD4+ T cells.

Phenotypic characterisation was performed using multiparameter flow cytometry of the different memory subsets of CD3+CD4+CD8-IFN-γ+ (A, B, C), CD3+CD4+CD8-IL-2+ (D, E, F) and CD3+CD4+CD8-TNF-α+ (G, H, I) T cells on the basis of CCR7 and CD45RA surface expression after 18 hour stimulation of PBMCs with live pH1N1 virus (A, D, G), CMV lysate (B, E, H) or medium only (C, F, I) stimulation. The proportion of CD3+CD4+CD8- cytokine positive T cells that were of the effector-memory (CD45RA−CCR7−), late-effector (CD45RA+CCR7−), central-memory (CD45RA−CCR7+) or naive (CD45RA+CCR7+) phenotype are shown; each symbol represents a single individual with horizontal lines at the median response. Differences between subset responses were estimated by Friedman tests within antigen-specific T cells or by Kruskal Wallis tests between live pH1N1 virus stimulation, CMV lysate stimulation and unstimulated conditions. Pie charts represent mean proportions for each cytokine profile. Non-responders to antigens excluded, n = 43, 35, 43, IFN-γ+ responses to live pH1N1 virus, CMV, or unstimulated; n = 36, 27, 33, IL-2+ responses to live pH1N1 virus, CMV, or unstimulated; n = 50, 32, 53, TNF-α+ responses to live pH1N1 virus, CMV lysate, or unstimulated.

In summary, live pH1N1 virus and CMV lysate stimulated CD4+IFN-γ+, CD4+IL-2+ and CD4+TNF-α+ T cells were heterogeneous with respect to the mean proportion of cytokine positive cells that expressed Tem and Temra phenotypes.

3.4.4 Other marker expression of cytokine-expressing CD4+ T cells in influenza or CMV stimulation

To further characterise the phenotype of antigen-specific cells, the expression of degranulation (CD107ab), activation (CD69) and tissue-homing (CCR5) markers as well as cellular senescence-associated marker (CD57) was assessed on each cytokine secreting cell population. Cytokine positive CD4+ T cells stimulated by live pH1N1 virus or CMV lysate showed a high level of inter-individual heterogeneity in expression of CD107ab, CD69, CCR5 and CD57 and the only significant difference between the two stimulations was in the proportion of CD4+IFN-γ+CD69+ T cells (median = 42.90%, IQR = 7.20% - 78.60% in pH1N1 stimulated and median = 14.30% and IQR = 0 – 29.40% in CMV lysate stimulated, p = 0.0085) (Fig. 3.4.5A-F). However, live pH1N1 virus stimulated CD4+IFN-γ+ T cells had significantly higher proportions of CD107ab+ cells (median = 20.0%, IQR = 0 - 41.37%) than CD4+TNF-α+CD107ab+ (median = 0.590%, IQR = 0 – 10.65%, $p < 0.01$) T cells. Live pH1N1 virus stimulated CD4+IFN-γ+ T cells also had significantly higher proportions of CD69+ (median = 42.9%, IQR = 7.2% - 78.6%) than CD4+IL-2+CD69+ (median = 11.4%, IQR = 0 – 40.70%, $p < 0.05$) although the proportion of CD4+IL-2+CD69+ was significantly higher than CD4+TNF-α+CD69+ (median = 5.83%, IQR = 0 – 16.27%, $p < 0.01$) T cells.

In CMV lysate stimulation, the proportion of CD4+IFN-γ+CD107ab+ T cells (median = 25.0%, IQR = 0 - 53.70%) was significantly higher ($p < 0.05$) than CD4+IL-2+CD107ab+ (median = 5.56%, IQR = 0 - 23.1%) T cells, and the

proportion of CD4+IFN-γ+CD69+ (median = 14.3%, IQR = 2.75% - 29.0%) T cells was also significantly higher than CD4+TNF-α+CD69+ (median = 3.70%, IQR = 0 – 11.0%) T cells ($p < 0.05$).

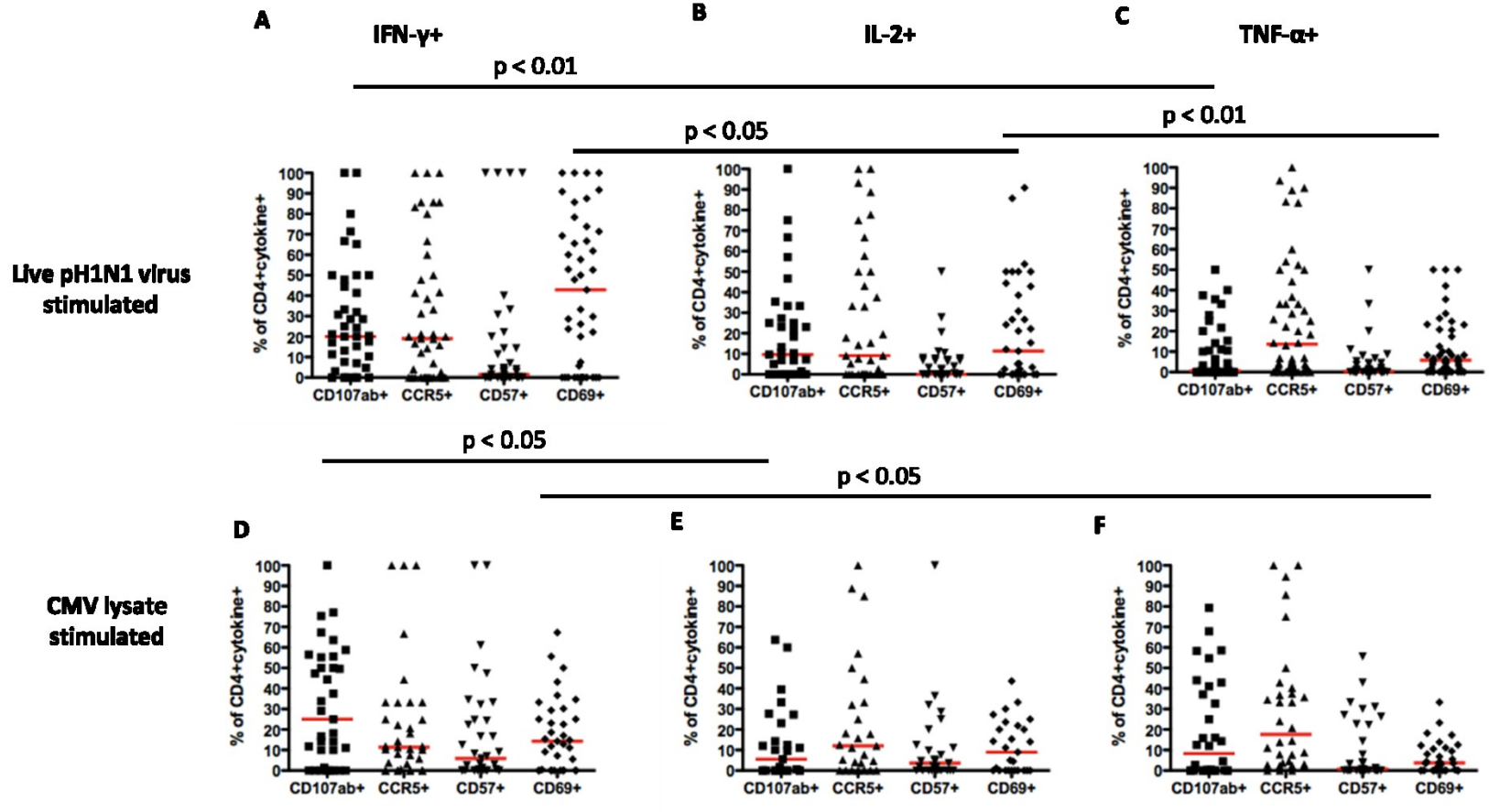

Figure 3.4.5 Phenotype of cytokine positive pH1N1 live virus and CMV lysate -specific CD4+ T cells.

Phenotypic characterisation was performed using multiparameter flow cytometry and gating as shown in Fig. 3.4.1 of CD3+CD4+CD8-IFN-γ+ (A, D), CD3+CD4+CD8-IL-2+ (B, E) and CD3+CD4+CD8-TNF-α+ (C, F) T cells after 18 hour stimulation of PBMCs with live pH1N1 virus (A, B, C) or CMV lysate (D, E, F). The proportion of CD3+CD4+CD8- cytokine positive T cells that expressed CD107 (isotypes A and B), CCR5, CD57 and CD69 are shown; each symbol represents a single individual with horizontal lines at the median response. Differences between subset responses were estimated by Kruskal Wallis test within antigen-specific T cells or by Mann Whitney test between live pH1N1 virus stimulation and CMV lysate stimulation for each phenotypic marker. Non-responders to antigens excluded, n = 43, 35, IFN-γ+ responses to live pH1N1 virus or CMV lysate; n = 36, 27, IL-2+ responses to live pH1N1 virus or CMV lysate; n = 50, 37, TNF-α+ responses to live pH1N1 virus or CMV lysate.

To summarise, the proportion of degranulation (CD107ab) and early activation (CD69) marker positive cells differ between the different cytokine positive populations in both pH1N1 stimulated and CMV-lysate stimulated CD4+ T cells. The proportion of tissue homing marker positive (CCR5) and replicative senescence marker positive (CD57) cells did not differ between different cytokine positive populations for pH1N1 stimulated or CMV-lysate stimulated CD4+ T cells.

3.4.5 Phenotype of pH1N1 cross-reactive CD8+ T cell responses

Cytokine expression, activation, degranulation, cellular senescence markers and memory phenotype of antigen-specific CD8+ T cells were also assessed. 92% (56/61) of individuals had pH1N1 virus-specific cytokine positive responses above background (Table 3.4.2). 69% (42/61), 62% (38/61) and 74% (45/61) of individuals responded to live pH1N1 virus stimulation by CD8+IFN-γ+, CD8+IL-2+ and CD8+TNF-α+ cytokine responses respectively (Table 3.4.2). Unlike pH1N1-specific CD4+ T cell responses, there was no hierarchy in pH1N1-specific responses between CD8+IFN-γ+ (median = 0.025%, IQR = 0 - 0.07%), CD8+IL-2+ (median = 0.005%, IQR = 0 – 0.02%) and CD8+TNF-α+ (median = 0.025%, IQR = 0 – 0.11%) responses (Fig. 3.4.6).

	CD8+IFN-γ+	CD8+IL-2+	CD8+TNF-α+	Any cytokine response
Number of responders (% responders)				
live pH1N1 virus (total =61)	42 (69)	38 (62)	45 (74)	56 (92)
CMV lysate (total = 50)	26 (52)	26 (52)	26 (52)	39 (78)

Table 3.4.2 Prevalence of antigen-specific CD8+ T cell responses.

The numbers and proportions of pH1N1 sero-negative individuals with *ex vivo* PBMC responses to live pH1N1 virus or CMV lysate from IFN-γ, IL-2, TNF-α or any cytokine (IFN-γ+ or IL-2+ or TNF-α+) secreting CD3+CD4-CD8+ T cells evaluated by flow cytometry.

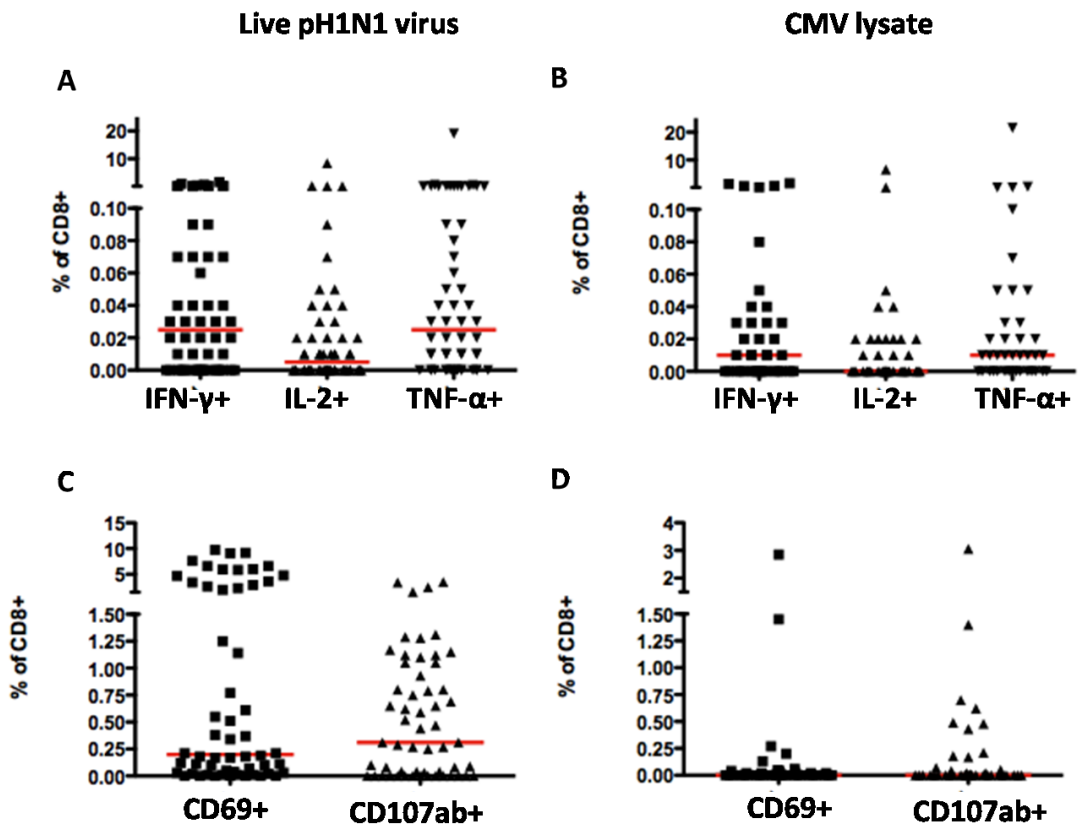

Figure 3.4.6 pH1N1 live virus and CMV lysate -specific CD8+ T cells.

Frequency of *ex vivo* PBMC responses from CD8+IFN-γ+, CD8+IL-2+ and CD8+TNF-α+ or CD8+CD69+ and CD8+CD107ab+ T cells evaluated by flow cytometry to live pH1N1 virus (A, C) or CMV lysate (B, D) and gated as shown in Fig. 3.4.1. Each symbol represents a single individual and horizontal red lines represent the median response. Differences between subset responses were estimated by Friedman test within antigen-specific T cells or by Mann Whitney test between pH1N1 live virus and CMV lysate -specific T cells. Non-responders to antigens excluded, pH1N1 live virus: n = 56, CMV lysate: n = 39.

Boolean analysis showed a predominance of TNF-α-single cytokine positive (mean = 0.326%, SEM = 0.263) and single IFN-γ+IL-2- (mean = 0.0998%, SEM = 0.035) pH1N1-specific CD8+ T cells (Fig. 3.4.7). Both these populations were significantly higher than the other triple CD8+IFN-γ+IL-2+TNF-α+ (mean = 0.001%, SEM = 0.000413), dual CD8+IFN-γ+IL-2+TNF-α- (mean = 0.00355%, SEM = 0.001), dual CD8+IFN-γ+IL-2-TNF-α+ (mean = 0.00712%, SEM = 0.00210), dual CD8+IFN-γ-IL-2+TNF-α+ (mean = 0.0769%, SEM = 0.0751), single CD8+IFN-γ-IL-2+TNF-α- (mean = 0.0897%, SEM = 0.001) cytokine positive, and triple negative CD8+IFN-γ-IL-2-TNF-α- (mean = 0.0429%, SEM = 0.0290) pH1N1-specific T cells (Fig. 3.4.7).

pH1N1-specific CD8+ T cells also expressed the early activation and degranulation markers CD8+CD69+ (median = 0.20%, IQR = 0 - 2.82%) and CD8+CD107ab+ (median = 0.31%, IQR = 0 – 3.48%) respectively (Fig. 3.4.6C). Although CMV lysate is not expected to optimally stimulate CD8+ T cells, 78% (39/50) of individuals had responses above background, with 52%, 52% and 52% of individuals responding with CD8+IFN-γ+, CD8+IL-2+ and CD8+TNF-α+ cytokine responses respectively (Table 3.4.2). The median frequency of antigen-specific cytokine positive responses were: CD8+IFN-γ+ (median = 0.01%, IQR = 0 - 0.03), CD8+IL-2+ (median = 0%, IQR = 0 - 0.02%) and CD8+TNF-α+ (median = 0.01%, IQR = 0 – 0.03%) (Fig. 3.4.6B). These were mainly single CD8+IFN-γ-IL-2-TNF-α+ (mean = 0.487%, SEM = 0.471), single CD8+IFN-γ+IL-2-TNF-α- (mean = 0.1146%, SEM = 0.0568), and an intriguing population of single CD8+IFN-γ-IL-2+TNF-α- T cells (mean =

0.0937%, SEM = 0.0858) (Fig. 3.4.7). Dual cytokine positive CD8+IFN-γ-IL-2+TNF-α+ (mean = 0.0843%, SEM = 0.0823) and CD8+IFN-γ+IL-2-TNF-α+ (mean = 0.0135%, SEM = 0.00767) were also detectable (Fig. 3.4.7B).

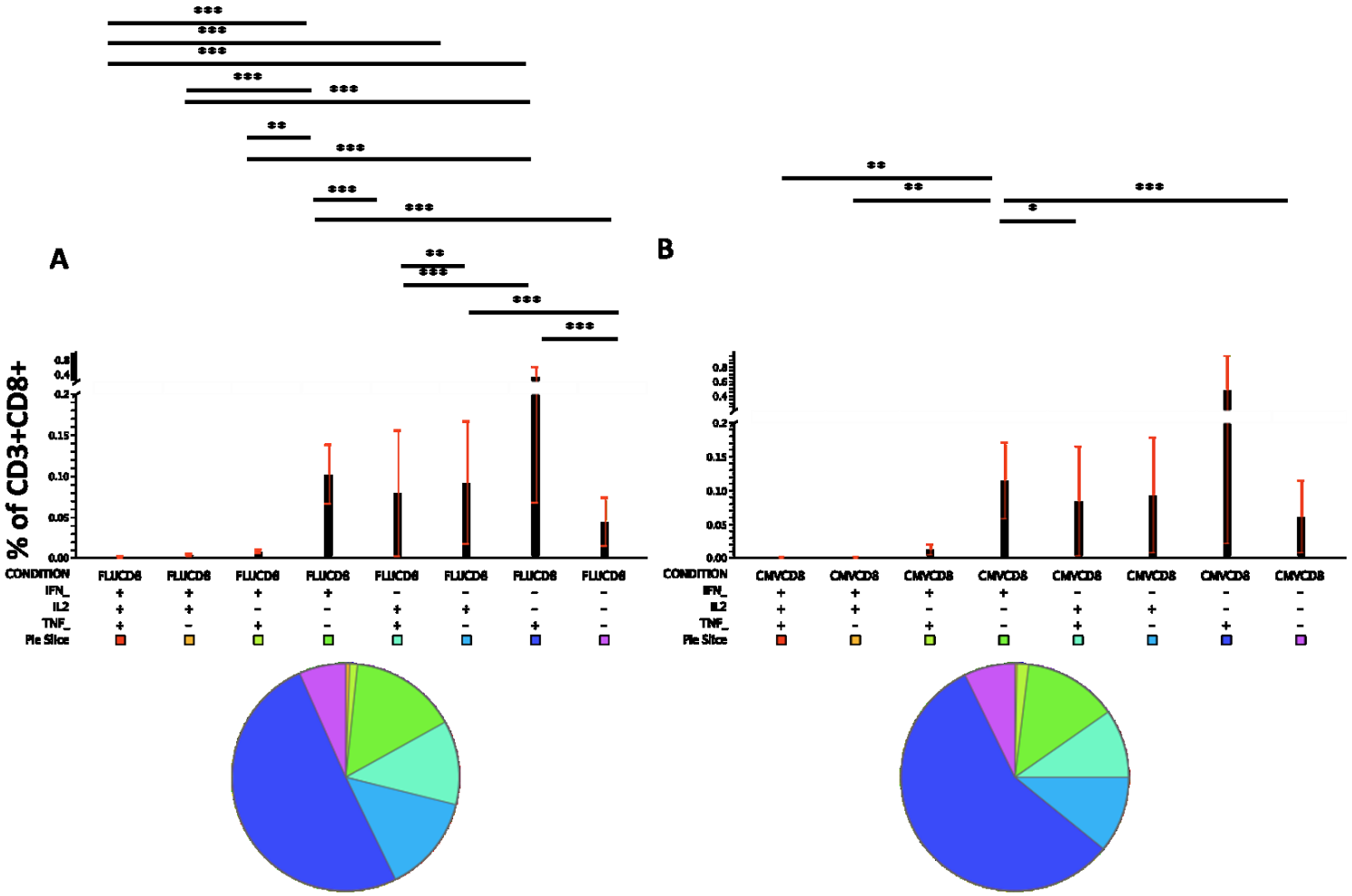

Figure 3.4.7 Cytokine profiles of pH1N1 live virus and CMV lysate -specific CD8+ T cells.

Boolean analysis using SPICE software was performed to analyse CD3+CD4-CD8+ T cells for each cytokine profile of *ex vivo* PBMC responses to live pH1N1 virus (A) or CMV lysate (B) following flow cytometry staining and gating as in Fig. 3.4.1. Bars represent mean and standard error of the mean percentage positive of CD3+CD4-CD8+ T cells. Differences between subset responses were estimated by Friedman test within antigen-specific T cells or by Kruskal Wallis test between pH1N1 live virus and CMV lysate -specific T cells. Pie charts represent mean proportions for each cytokine profile. Non-responders to antigens excluded, pH1N1 live virus: n = 56, CMV lysate: n = 39. * $p \leq 0.05$, ** $p \leq 0.01$, *** $p \leq 0.001$. IFN_ = IFN-γ, IL2 = IL-2, TNF_ = TNF-α.

Together these results indicate pH1N1-specific CD8+ T cells are mainly single-TNF-α+, single IFN-γ+ and single IL-2+ and a lower frequency of dual IFN-γ-IL-2+TNF-α+ cytokine positive cells. CMV-lysate specific CD8+ T cells are also single-TNF-α+, single IFN-γ+ and single IL-2+ cytokine positive cells.

3.4.6 Memory phenotype of cytokine secreting CD8+ T cells in influenza or CMV stimulation

Similar to the memory phenotype of CD4+IFN-γ+ cells (Fig. 3.4.4), CD8+IFN-γ+ cells were predominantly CCR7- effector memory (CCR7-CD45RA-) or late effector (CCR7-CD45RA+) T cells in both live pH1N1 virus (Fig. 3.4.8A) and CMV lysate (Fig. 3.4.8B) stimulation and this was not different from the phenotype of non-specific CD8+IFN-γ+ T cells (Fig. 3.4.8C). pH1N1 stimulated CD8+IL-2+ T cells were predominantly effector memory (Fig. 3.4.8D), however 24.7% of CD8+IL-2+ had a naïve phenotype (CCR7+CD45RA+) (Fig. 3.4.8D, pie chart). Similarly, 30.2% of CMV lysate stimulated CD8+IL-2+ T cells were of a naïve phenotype (Fig. 3.4.8E pie chart), and a similar proportion of naïve CD8+IL-2+ T cells is also represented in the non-specific CD8+IL-2+ T cell response (Fig. 3.4.8F pie chart).

In live pH1N1 virus stimulated CD8+TNF-α+ T cells, the proportion of late effector T cells was significantly higher than CD8+TNF-α+ with central memory and naïve phenotype, but not significantly different to the proportion

of CD8+TNF-α+ with an effector memory phenotype (Fig. 3.4.8G). Furthermore, the frequency of pH1N1 stimulated CD8+TNF-α+ T cells with late effector phenotype was significantly higher than non-specific CD8+TNF-α+ T cells with late effector phenotype (Fig. 3.4.8I). In CMV lysate stimulation, CD8+TNF-α+ had similar proportions of cells with naïve, late effector and effector memory phenotypes, and the only significant difference was between the proportions of CD8+TNF-α+ with central memory compared to late effector phenotype (Fig. 3.4.8H).

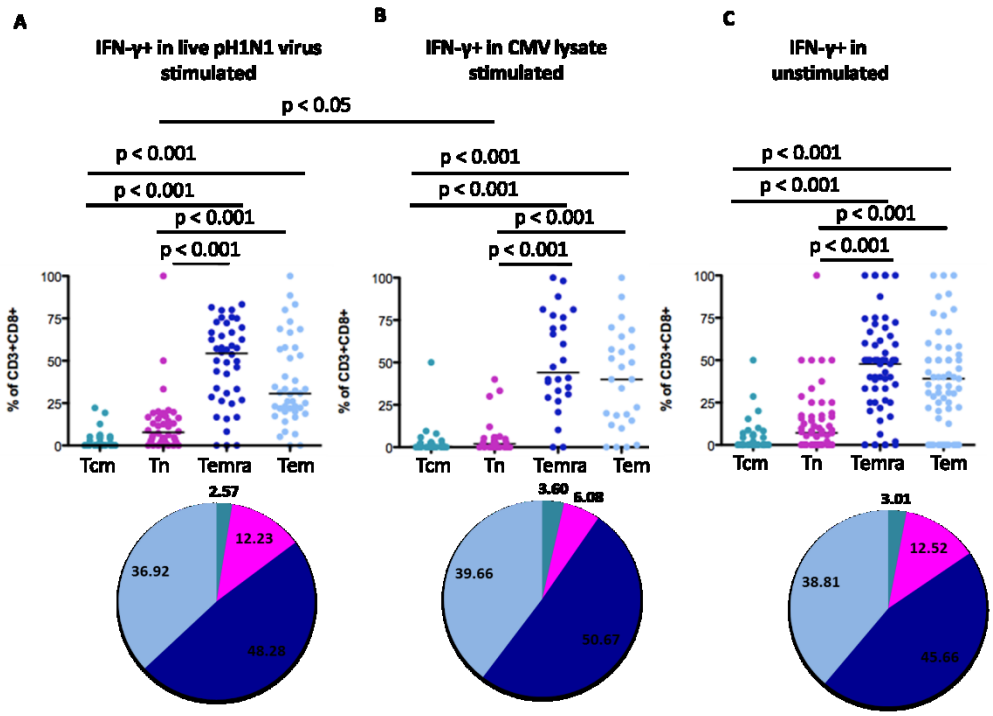

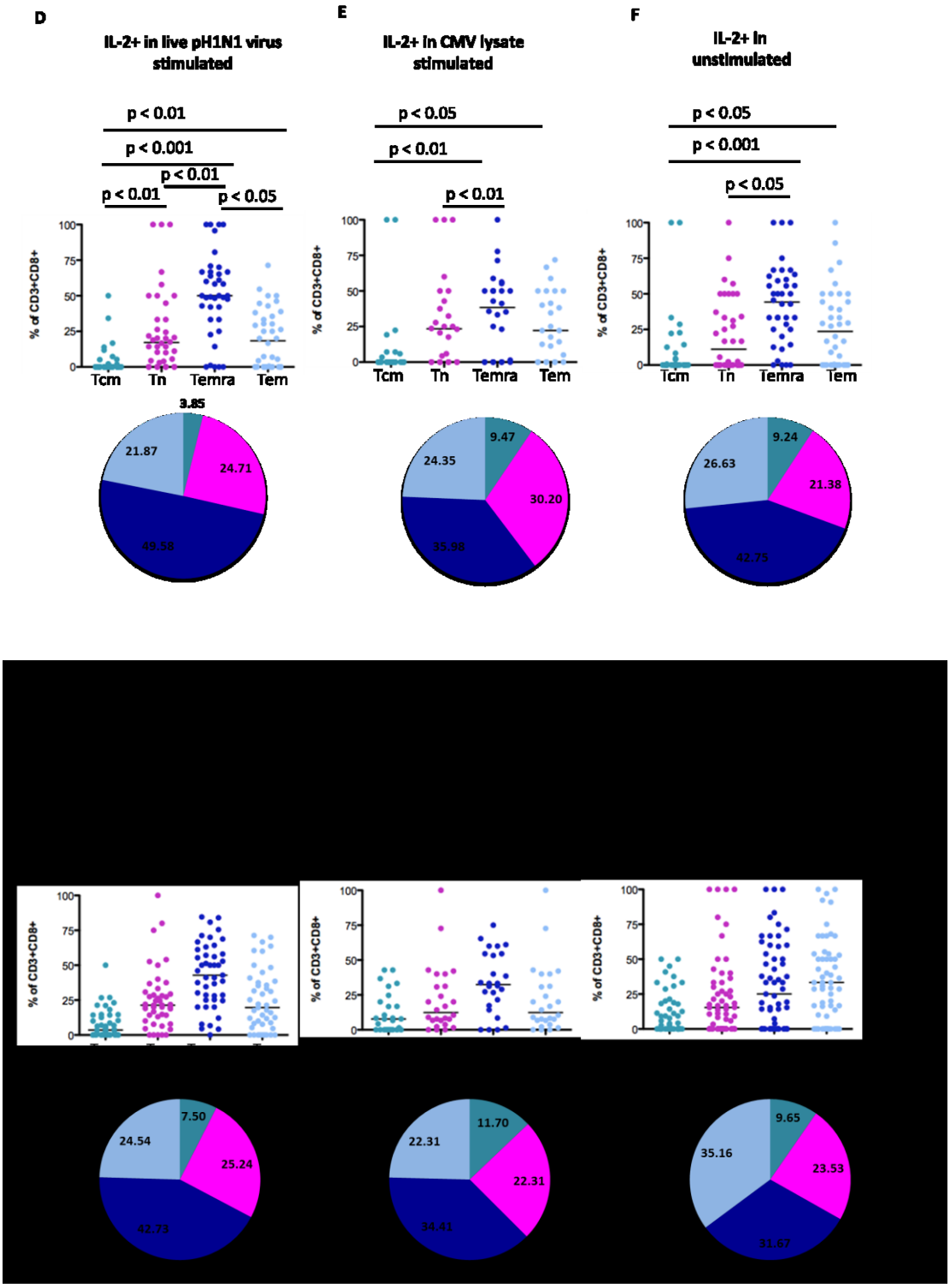

Figure 3.4.8 Effector and memory phenotype of pH1N1 live virus and CMV lysate - specific CD8+ T cells.

Phenotypic characterisation was performed using multiparameter flow cytometry of the different memory subsets of CD3+CD4-CD8+IFN-γ+ (A, B, C), CD3+CD4-CD8+IL-2+ (D, E, F) and CD3+CD4-CD8+TNF-α+ (G, H, I) T cells on the basis of

CCR7 and CD45RA surface expression after 18 hour stimulation of PBMCs with live pH1N1 virus (A, D, G), CMV lysate (B, E, H) or medium only (C, F, I) stimulation. The proportion of CD3+CD4-CD8+ cytokine positive T cells that were of the effector-memory (CD45RA−CCR7−), late-effector (CD45RA+CCR7−), central-memory (CD45RA−CCR7+) or naive (CD45RA+CCR7+) phenotype are shown; each symbol represents a single individual with horizontal lines at the median response. Differences between subset responses were estimated by Friedman test within antigen-specific T cells or by Kruskal Wallis test between live pH1N1 virus stimulation, CMV lysate stimulation and unstimulated conditions. Pie charts represent mean proportions for each cytokine profile. Non-responders to antigens excluded, n = 42, 26, 59 IFN-γ+ responses to live pH1N1, CMV, or unstimulated; n = 38, 26, 39 IL-2+ responses to live pH1N1, CMV, or unstimulated; n = 45, 26, 57 TNF-α+ responses to live pH1N1, CMV, or unstimulated.

To summarise, live pH1N1 virus stimulated CD8+IFN-γ+, CD4+IL-2+ and CD4+TNF-α+ T cells were predominantly of late effector phenotype, however, the mean proportion of CD8+ cytokine positive T cells with a naïve phenotype was lower in CD8+IFN-γ+ compared to CD8+IL-2+ and CD8+TNF-α+ positive T cells. CMV lysate stimulated CD8+IFN-γ+ T cells were also predominantly of late effector phenotype, however, CMV lysate stimulated CD8+IL-2+ and CD8+TNF-α+ T cells were more heterogeneous with respect to mean proportions of cytokine positive T cells with naïve and central memory phenotypes.

3.4.7 Other marker expression of cytokine secreting CD8+ T cells in influenza or CMV stimulation

Similar to the individual-level heterogeneity of CD4+ cytokine positive T cells (Fig. 3.4.5), CD8+ cytokine positive T cells stimulated by live pH1N1 virus or CMV lysate also showed a high level of inter-individual heterogeneity in expression of CD107ab, CD69, CCR5 and CD57 (Fig. 3.4.9). Additionally, live pH1N1 virus stimulated CD8+IFN-γ+ T cells and CD8+IL-2+ T cells differed in expression of all four of these markers. CD8+IFN-γ+ T cells contained significantly higher frequencies of CD107ab+ T cells (median 47.4%, IQR = 27.8% - 67.0%) than CD8+IL-2+ (median = 5.56%, IQR = 0 – 21.0%) or CD8+TNF-α+ (median = 8.59%, IQR = 0 – 32.40%) T cells ($p < 0.001$ and $p < 0.001$ respectively). CD8+IFN-γ+CCR5+ T cells (median = 53.7%, IQR = 33.27% – 74.14%) were also significantly higher ($p < 0.05$) than CD8+IL-2+CCR5+ T cells (median = 27.3%, IQR = 0 – 57.10%), whereas CD8+IFN-γ+CD57+ T cells were significantly lower ($p < 0.05$) than CD8+IL-2+CD57+ T cells. The proportion of CD69 expressing cells in live pH1N1 virus stimulated CD8+IFN-γ+ (median = 19.35%, IQR = 0 – 50.52%) and CD8+TNF-α+ (median = 11.8%, IQR = 0 – 49.19%) T cells was significantly higher than CD8+IL-2+ T cells expressing CD69 (median = 0.512%, IQR = 0 - 7.14%) ($p < 0.01$ and $p < 0.01$ respectively).

Proportions of CD107ab+ degraulating and early activation marker CD69+ T cells were significantly higher ($p < 0.05$ and $p< 0.05$ respectively) in CMV lysate stimulated CD8+IFN-γ+ (median = 26.4%, IQR = 6.75% - 46.05% and median = 15.6%, IQR = 1.45% - 29.75% respectively) compared to CD8+IL-2+ T cells (median = 1.15%, IQR = 0 – 24.3% and median = 0%, IQR = 0 –

10.5% respectively). CMV lysate stimulated CD8+IFN-γ+ also contained a higher proportion of CD107ab+ but a lower proportion of CCR5+ T cells (median = 5.84%, IQR = 0 - 16.55%) compared to CD8+TNF-α+ T cells (median = 1.15%, IQR = 0 - 24.3% and median = 55.15%, IQR = 32.80% - 77.50% respectively).

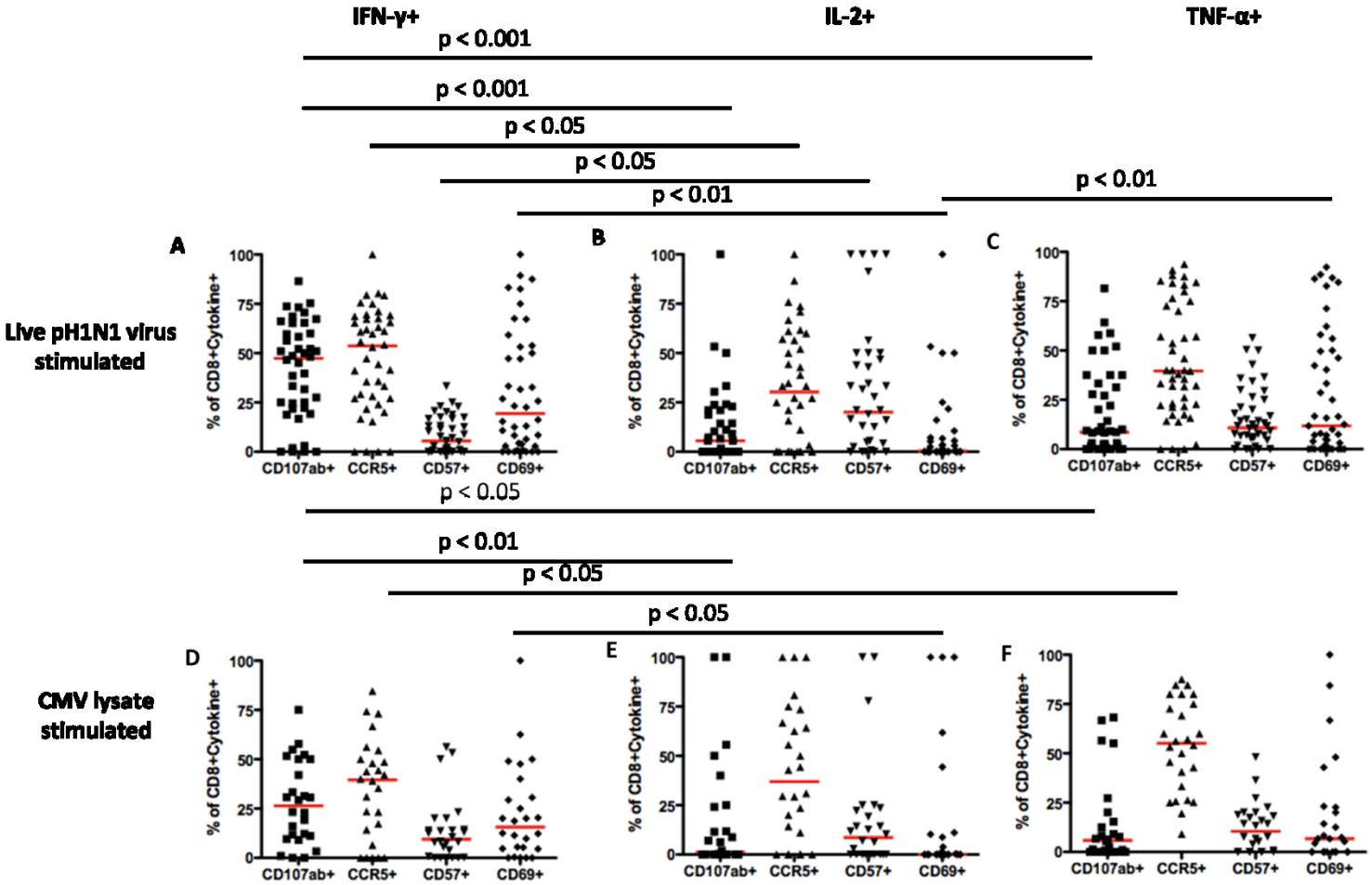
IFN-γ+
IL-2+
TNF-α+
p < 0.001
p < 0.001
p < 0.05
p < 0.05
p < 0.01
p < 0.01
A
B
C
Live pH1N1 virus stimulated
% of CD8+Cytokine+
CD107ab+
CCR5+
CD57+
CD69+
p < 0.05
p < 0.01
p < 0.05
p < 0.05
D
E
F
CMV lysate stimulated

Figure 3.4.9 Phenotype of cytokine positive pH1N1 live virus and CMV lysate -specific CD8+ T cells.

Phenotypic characterisation was performed using multiparameter flow cytometry and gating as shown in Fig. 3.4.1 of CD3+CD4-CD8+IFN-γ+ (A, D), CD3+CD4-CD8+IL-2+ (B, E) and CD3+CD4-CD8+TNF-α+ (C, F) T cells after 18 hour stimulation of PBMCs with live pH1N1 virus (A, B, C) or CMV lysate (D, E, F). The proportion of CD3+CD4-CD8+ cytokine positive T cells that expressed CD107 (isotypes A and B), CCR5, CD57 and CD69 are shown; each symbol represents a single individual with horizontal lines at the median response. Differences between subset responses were estimated by Kruskal Wallis test within antigen-specific T cells or by Mann Whitney test between live pH1N1 virus stimulation and CMV lysate stimulation for each phenotypic marker. Non-responders to antigens excluded, n = 42, 26, IFN-γ+ responses to live pH1N1 virus or CMV lysate; n = 38, 26, IL-2+ responses to live pH1N1 virus or CMV lysate; n = 45, 26, TNF-α+ responses to live pH1N1 virus or CMV lysate.

In summary, there was heterogeneity between CD8+IFN-γ+, CD8+IL-2+ and CD8+TNF-α+ T cells with respect to the proportions of cells positive for CD107ab, CD69, CCR5 and CD57 markers in both pH1N1 virus and CMV lysate stimulation.

3.5 The longitudinal development of influenza-specific memory T cells

Antigen-specific T cell responses were assessed in longitudinal PBMC samples from individuals who were naturally infected with pH1N1 or individuals who received the pH1N1 vaccine over the study period. The hypothesis was that natural influenza infection would alter the frequency of pH1N1 virus-specific T cells and would differentially induce and maintain T cell responses compared to vaccination.

3.5.1 Study samples

All available stored PBMC samples from 82 individuals with various outcomes during the study seasons 1 and 2 (Table 3.5.1) were comprehensively characterised by flow cytometry. This included 51 naturally infected individuals (26 and 25 in season 1 and season 2 respectively); 29 individuals vaccinated and seroconverted to pH1N1 vaccine (19 and 10 in season 1 and season 2 respectively); 16 individuals vaccinated but did not seroconvert to pH1N1 vaccine (8 and 8 in season 1 and season 2 respectively) and 43 individuals that were uninfected (28 and 15 in season 1 and season 2 respectively). Not all of these 82 individuals had stored PBMC from all four study time-points, but all available samples were used where possible and sample numbers are indicated in relevant figures.

Immune status and study season	T0	T1	T2	T3	Pre- (T0 or T2)	Post- (T1 or T3)
Natural infection season 1 (Total = 26)	23/24	19/19	14/15	-	34/37	35/35
Natural infection season 2 (Total = 25)	-	-	11/13	16/16		
Vaccinated and serconversion season 1 (Total = 19)	15/14	13/13	7/7		21/19	21/19
Vaccinated and serconversion season 2 (Total = 10)	-	-	6/5	8/6		
Vaccinated but no seroconversion season 1 (Total = 8)	3/3	4/4	2/2		7/7	6/7
Vaccinated but no seroconversion season 2 (Total = 8)	-	-	4/4	2/3		

Table 3.5.1 Number of individuals with infection or vaccination status and longitudinal time-points analysed by flow cytometry.

Number of individuals with analysis on CD4+/CD8+.

3.5.2 Kinetics of pH1N1-specific fluorescence-immunospot responses following natural infection

PBMC from pre- and post- infection were stimulated with live pH1N1 virus or control antigens and responses were enumerated by fluorescence-immunospot. No significant changes were detectable in frequencies of pH1N1-specific T cells from any of the three cytokine secreting subsets in either season alone (Fig. 3.5.1). However, frequencies of live pH1N1 virus-specific IFN-γ+IL-2-, IFN-γ-IL-2+ and IFN-γ+IL-2+ T cells were increased

following infection when data from individuals infected in either season was combined ($p = 0.0673$, $p = 0.0019$ and $p = 0.0395$ respectively, Fig. 3.5.1 E, K and Q). No differences were observed in the frequencies of CMV lysate-specific IFN-γ+IL-2-, IFN-γ-IL-2+ and IFN-γ+IL-2+ T cells between pre- and post-infection in either season or in the combined seasons analysis (Fig. 3.5.1 B, D, F, H, J, L, N, P, R).

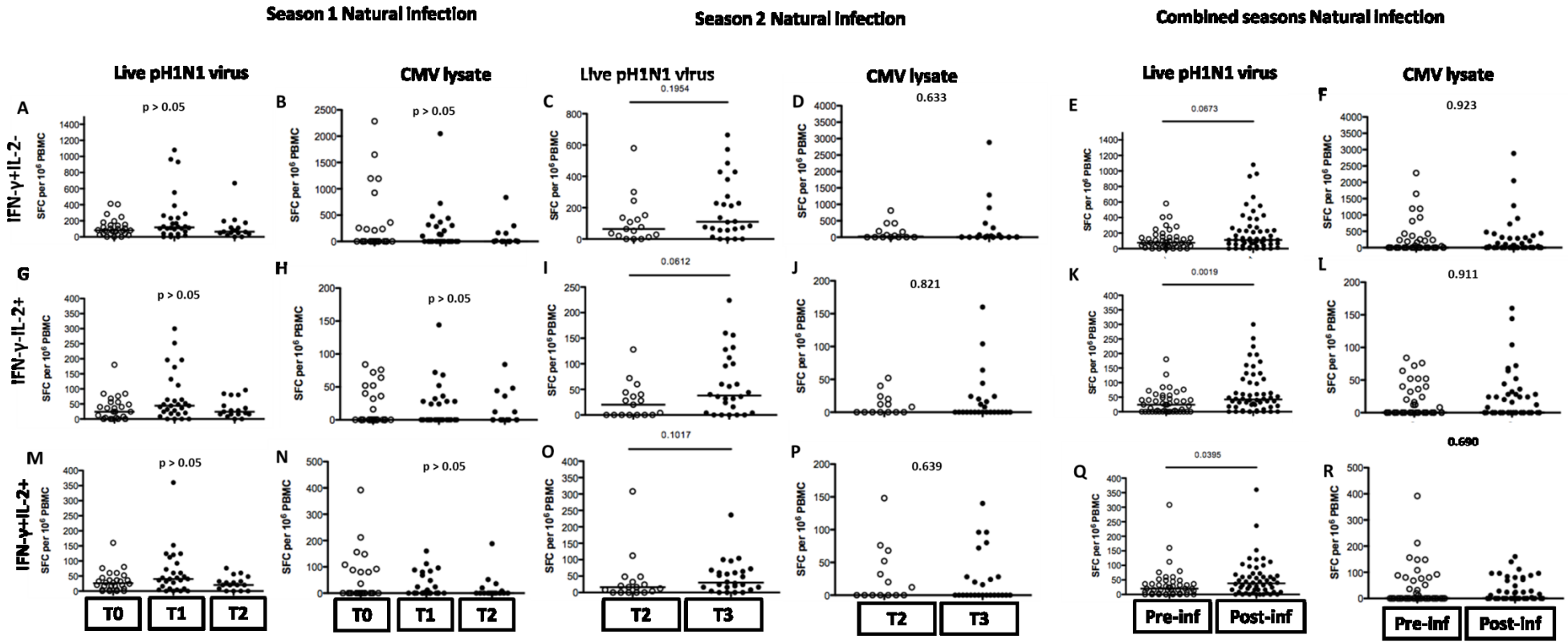

Figure 3.5.1 Kinetics of pH1N1-specific T cell responses by fluorescence-immunospot.

The magnitude of *ex vivo* PBMC responses from the IFN-γ+IL-2- (A, B, C, D, E, F), IFN-γ-IL-2+ (G, H, I, J, K, L), and IFN-γ+IL-2+ dual (M, N, O, P, Q, R) cytokine secreting subsets to live pH1N1 virus (A, C, E, G, I, K, M, O, Q) and CMV lysate (B, D, F, H, J, L, N, P, R) in individuals with incident pH1N1 infection during season 1 (A, B, G, H, M, N), season 2 (C, D, I, J, O, P) or the combined seasons data (E, F, K, L, Q, R) was determined by fluorescence-immunospot. Each symbol represents a single individual and horizontal lines represent medians. Differences between study time-points in subset responses were estimated by Kruskall-Wallis test. Non-responders to stimulation excluded, season 1: n = 28, 28, 17 to live pH1N1 virus; n = 26, 26, 16 to CMV lysate; season 2: n = 17, 26 to live pH1N1 virus; n = 14, 25 to CMV lysate; combined seasons: n = 45, 54 to live pH1N1 virus; n = 40,51 to CMV lysate. SFC, spot-forming cells; Season 1, T0: baseline (pre-infection), T1: up to 6 months post-infection, T2: up to 1.5 years post-infection. Season 2, T2: baseline (pre-infection), T3: up to 6 months post-infection. Combined seasons, Pre-inf: baseline (pre-infection), Post-inf: up to 6 months post-infection.

3.5.3 Kinetics of pH1N1 virus-specific CD4+ and CD8+ T cell responses following natural infection

To characterise the phenotype of pH1N1 infection induced T cell responses, PBMC samples remaining from infected individuals were used in multi-paratemter flow cytometry. pH1N1-specific CD4+IFN-γ+ responses were significantly increased ($p = 0.0035$) in naturally infected individuals during season 2, whilst CMV-specific CD4+IFN-γ+ responses remained unaltered ($p = 0.698$, Fig. 3.5.2B). This finding was consistent when CD4+IFN-γ+ data from individuals infected in either season were combined ($p = 0.0348$ for pH1N1 virus-specific and $p = 0.502$ for CMV lysate-specific, Fig. 3.5.2C).

Boolean analysis revealed that the pH1N1-specific CD4+IFN-γ+ response was mainly single IFN-γ+IL-2-TNF-α- (Fig. 3.4.3). The significant increase in response post-infection was also evident within this pH1N1-specific single-IFN-γ+IL-2-TNF-α- CD4+ T cell ($p = 0.0147$, Fig. 3.5.2D) but not CMV lysate-specific single- IFN-γ+IL-2-TNF-α- CD4+ T cell ($p = 0.324$, Fig. 3.5.2D) population. Interestingly, the frequencies of CD4+IL-2+ and CD4+ IFN-γ-IL-2+TNF-α- T cells were significantly lower post-infection for pH1N1-specific CD4+ T cells in season 1 ($p < 0.001$, Fig. 3.5.2E and Table 3.5.2) and in the combined seasons analysis ($p = 0.0041$ and $p = 0.0015$ Fig. 3.5.2G and H), whereas CMV-specific CD4+IL-2+ and CD4+ IFN-γ-IL-2+TNF-α- T cells in the corresponding analyses were not significantly altered ($p = 0.127$, $p = 0.109$ and $p = 0.104$, Fig. 3.5.2E, G and H). Frequencies of pH1N1-specific

CD4+TNF-α+ and CD4+ IFN-γ-IL-2-TNF-α+ T cells were not significantly altered post-infection, and this was also consistent for CMV-specific CD4+TNF-α+ and CD4+ IFN-γ-IL-2-TNF-α+ T cells (Fig. 3.5.2 I-L, Table 3.5.2).

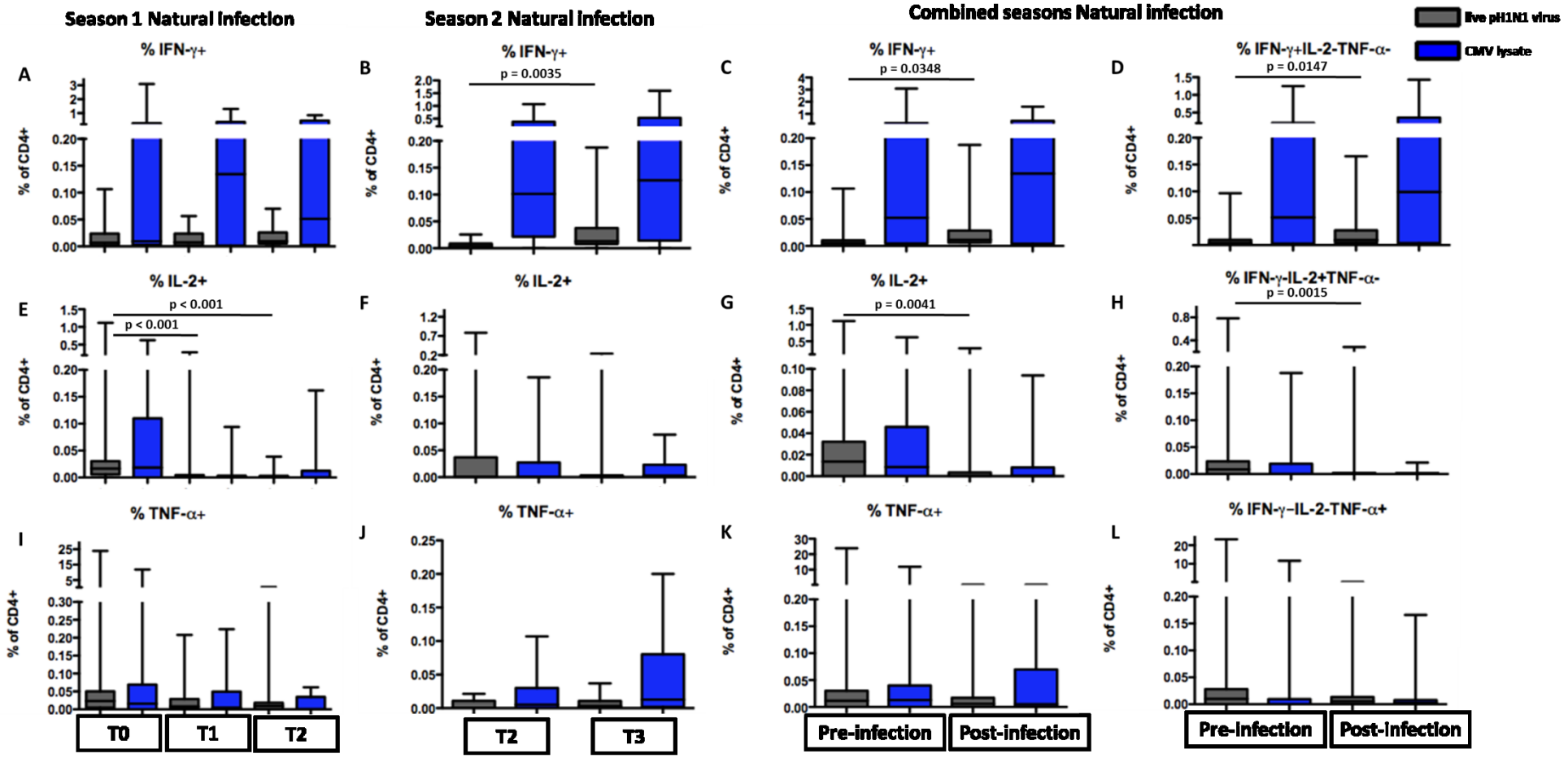
Season 1 Natural Infection
Season 2 Natural Infection
Combined seasons Natural infection
live pH1N1 virus
CMV lysate
A
% IFN-γ+
B
% IFN-γ+
p = 0.0035
C
% IFN-γ+
p = 0.0348
D
% IFN-γ+IL-2-TNF-α-
p = 0.0147
E
% IL-2+
p < 0.001
p < 0.001
F
% IL-2+
G
% IL-2+
p = 0.0041
H
% IFN-γ-IL-2+TNF-α-
p = 0.0015
I
% TNF-α+
J
% TNF-α+
K
% TNF-α+
L
% IFN-γ-IL-2-TNF-α+
% of CD4+
T0
T1
T2
T3
Pre-infection
Post-infection

Figure 3.5.2 Kinetics of pH1N1-specific CD4+ T cell responses.

The magnitude of *ex vivo* PBMC responses from the IFN-γ+ (A, B, C) and single IFN-γ+ (D), IL-2+ (E, F, G) and single IL-2+ (H), TNF-α+ (I, J, K) and single TNF-α+ (L) CD3+CD4+CD8- subsets to live pH1N1 virus and CMV lysate in individuals with incident pH1N1 infection during season 1 (A, E, I), season 2 (B, F, J) or the combined seasons data (C, D, G, H, K, L) was determined by flow cytometry and gating as shown in Fig. 3.4.1. In the box plots, the box represents the third centile (75%) and first centile (25%), with the horizontal line representing the median (50%). The whiskers represent 1.5 times the IQR. Differences between study time-points in subset responses were estimated by Kruskall-Wallis test. Non-significant p-values shown in Table 3.5.2. Non-responders to stimulation excluded, season 1: n = 23, 19, 14 to live pH1N1 virus; n = 18, 13, 9 to CMV lysate; season 2: n = 11, 16 to live pH1N1 virus; n = 13, 14 to CMV lysate; combined seasons: n = 34, 35 to live pH1N1 virus; n = 31, 27 to CMV lysate. T0: baseline (pre-infection), T1: up to 6 months post-infection, T2: up to 1.5 years post-infection. Season 2, T2: baseline (pre-infection), T3: up to 6 months post-infection. Combined seasons, Pre-inf: baseline (pre-infection), Post-inf: up to 6 months post-infection.

S1&S2 combined																		
Wilcoxon-signed rank test with all cytokine non-responders (and the pair) also excluded	**CD4+IFN-γ+**			**CD4+IL-2+**			**CD4+TNFa+**			**CD4+IFN-γ+IL-2-TNF-α-**			**CD4+IFN-γ-IL-2+TNF-α-**			**CD4+IFN-γ-IL-2-TNF-α+**		
live pH1N1 virus	0.3993	25	25	0.1443	25	25	0.781	25	25	0.3105	25	25	**0.08**	25	25	0.6677	25	25
CMV lysate	0.7022	20	20	**0.0171**	20	20	0.2066	20	20	0.7937	21	21	0.1217	21	21	0.3936	20	20
Mann Whitney test excluding individuals with a post-infection sample only and also all cytokine non-responders excluded		**n (pre-infection**	**n (post-infection)**		**n (pre-infection**	**n (post-infection)**		**n (pre-infection**	**n (post-infection)**		**n (pre-infection**	**n (post-infection)**		**n (pre-infection**	**n (post-infection)**		**n (pre-infection**	**n (post-infection)**
live pH1N1 virus	**0.0419**	34	34	**0.0077**	34	30	0.2714	34	30	**0.0556**	34	30	**0.0036**	34	30	0.2785	34	30
CMV lysate	0.751	31	21	0.1433	31	21	0.6487	31	21	0.5555	31	21	0.2191	31	21	0.4607	31	21
Mann Whitney excluding all cytokine non-responders		**n (pre-infection**	**n (post-infection)**		**n (pre-infection**	**n (post-infection)**		**n (pre-infection**	**n (post-infection)**		**n (pre-infection**	**n (post-infection)**		**n (pre-infection**	**n (post-infection)**		**n (pre-infection**	**n (post-infection)**
live pH1N1 virus	**0.0348**	34	35	**0.0041**	34	35	0.2459	34	35	**0.0147**	34	35	**0.0015**	34	35	0.167	34	35
CMV lysate	0.5023	31	27	0.1085	31	27	0.8374	31	27	0.3244	31	27	0.1039	31	27	0.2366	31	27
S1																		
1wayANOVAKruskalWallis&Dunns excluding all cytokine non-responders		**n (pre-infection**	**n (post-infection T1&T2)**		**n (pre-infection**	**n (post-infection)**		**n (pre-infection**	**n (post-infection)**		**n (pre-infection**	**n (post-infection)**		**n (pre-infection**	**n (post-infection)**		**n (pre-infection**	**n (post-infection)**
live pH1N1 virus	0.7164	23	19&14	**p<0.001T0/T1 and T1/T2**	23	19&14	0.1798	23	19&14	0.2812	23	19&14	**p<0.0001 T1/T2 and p<0.001 T2/T3**	23	19&14	0.2544	23	19&14
CMV lysate	0.9559	18	13&9	0.1266	18	13&9	0.2631	18	13&9	0.6457	18	13&9	0.2	18	13&9	0.3586	18	13&9
S2																		
Mann Whitney excluding all cytokine non-responders		**n (pre-infection**	**n (post-infection)**		**n (pre-infection**	**n (post-infection)**		**n (pre-infection**	**n (post-infection)**		**n (pre-infection**	**n (post-infection)**		**n (pre-infection**	**n (post-infection)**		**n (pre-infection**	**n (post-infection)**
live pH1N1 virus	**0.0035**	11	16	0.9773	11	16	0.6606	11	16	**0.0041**	11	16	0.9756	11	16	0.8942	11	16
CMV lysate	0.6978	13	14	1	13	14	0.3399	13	14	0.6978	13	14	0.6341	13	14	0.2265	13	14

Table 3.5.2 Significance tests between pre-infection and post-infection antigen-specific CD4+ cytokine positive T cell responses.

Similar to the changes in pH1N1-specific CD4+IFN-γ+ responses (Fig. 3.5.2), the frequencies of pH1N1-specific CD8+IFN-γ+ and CD8+IFN-γ+IL-2-TNF-α- T cells were significantly increased ($p = 0.0072$ in season 2, Fig. 3.5.3B; $p = 0.0018$ and $p = 0.0006$ in combined seasons, Fig. 3.5.3 C and D) post-infection without significant alterations in the frequencies of corresponding cytokine positive CMV-specific CD8+ T cells (Fig. 3.5.3B, C, D and Table 3.5.3). pH1N1-specific CD8+IL-2+ and a population of CD8+IFN-γ-IL-2+TNF-α- T cells were significantly lower in post-infection samples, but this was also the case for CMV-lysate specific CD8+IL-2+ and CD8+IFN-γ-IL-2+TNF-α- T cells (Fig. 3.5.3E-H, Table 3.5.3). Frequencies of pH1N1-specific or CMV-lysate-specific CD8+TNF-α+ and CD8+ IFN-γ-IL-2-TNF-α+ T cells were not significantly altered post-infection (Fig. 3.5.3 I-L, Table 3.5.3).

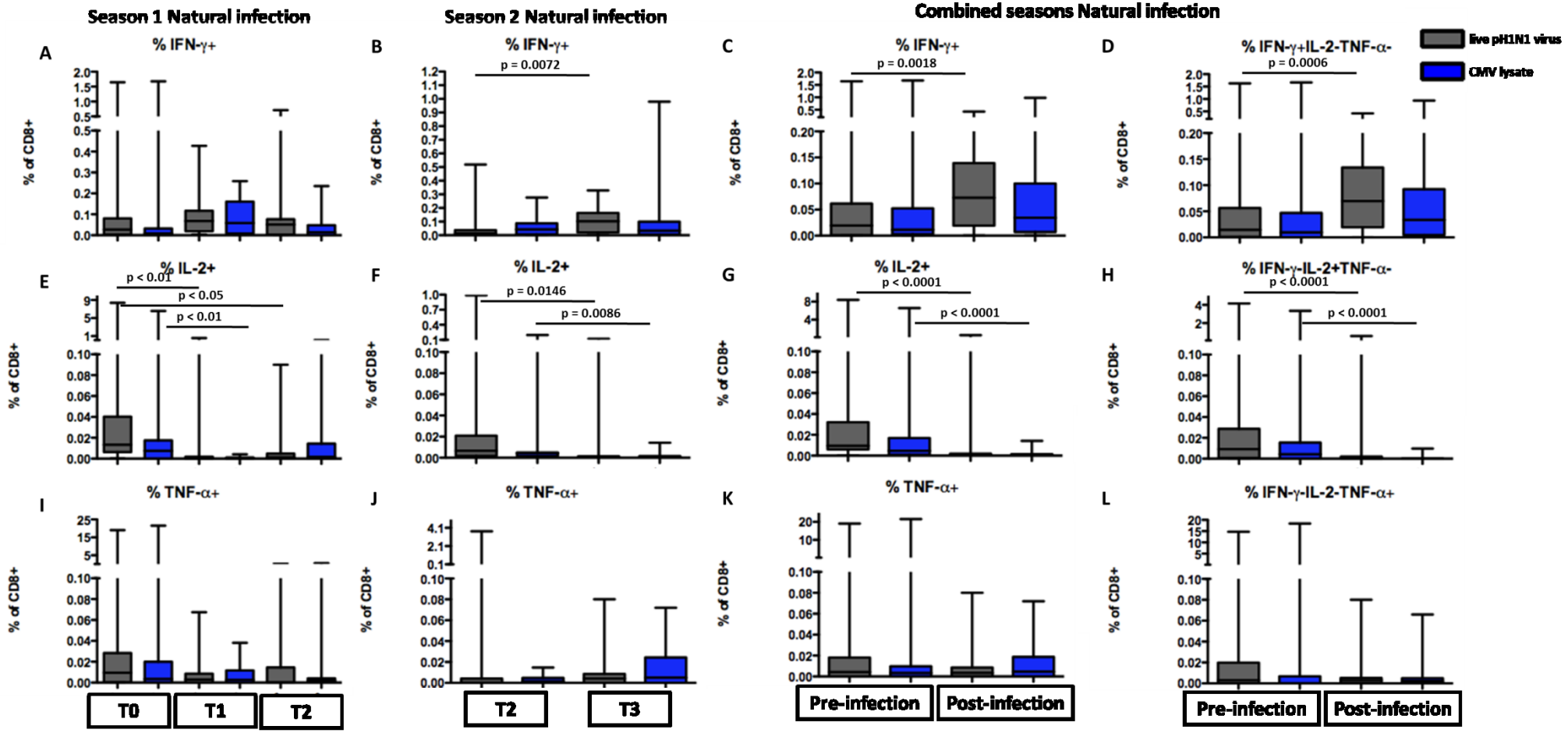

Figure 3.5.3 Kinetics of pH1N1-specific CD8+ T cell responses.

The magnitude of *ex vivo* PBMC responses from the IFN-γ+ (A, B, C) and single IFN-γ+ (D), IL-2+ (E, F, G) and single IL-2+ (H), TNF-α+ (I, J, K) and single TNF-α+ (L) CD3+CD4-CD8+ subsets to live pH1N1 virus and CMV lysate in individuals with incident pH1N1 infection during season 1 (A, E, I), season 2 (B, F, J) or the combined seasons data (C, D, G, H, K, L) was determined by flow cytometry and gating as shown in Fig. 3.4.1. In the box plots, the box represents the third centile (75%) and first centile (25%), with the horizontal line representing the median (50%). The whiskers represent 1.5 times the IQR. Differences between study time-points in subset responses were estimated by Kruskall-Wallis test. Non-significant p-values shown in Table 3.5.3. Non-responders to stimulation excluded, season 1: n = 24, 19, 15 to live pH1N1 virus; n = 18, 12, 11 to CMV lysate; season 2: n = 13, 16 to live pH1N1 virus; n = 11, 15 to CMV lysate; combined seasons: n = 37, 35 to live pH1N1 virus; n = 29, 27 to CMV lysate. T0: baseline (pre-infection), T1: up to 6 months post-infection, T2: up to 1.5 years post-infection. Season 2, T2: baseline (pre-infection), T3: up to 6 months post-infection. Combined seasons, Pre-inf: baseline (pre-infection), Post-inf: up to 6 months post-infection.

S1&S2 combined																	
Wilcoxon-signed rank test with all cytokine non-responders (and the pair) also excluded	**CD8+IFN-γ+**			**CD8+IL-2+**			**CD8+TNFa+**			**CD8+IFN-γ+IL-2-TNF-α-**			**CD8+IFN-γ-IL-2+TNF-α-**			**CD8+IFN-γ-IL-2-TNF-α+**		
live pH1N1 virus	0.0876	29	29	**0.0064**	29	29	0.1004	29	29	0.0693	29	29	**0.0288**	29	29	0.0654	29	29
CMV lysate	0.7366	16	16	**0.028**	16	16	0.6233	16	16	0.7173	16	16	**0.0068**	16	16	0.2412	16	16
Mann Whitney test excluding individuals with a post-infection sample only and also all cytokine non-responders excluded		**n (preinfection)**	**n (post-infection)**		**n (preinfection)**	**n (post-infection)**		**n (preinfection)**	**n (post-infection)**		**n (preinfection)**	**n (post-infection)**		**n (preinfection)**	**n (post-infection)**		**n (preinfection)**	**n (post-infection)**
live pH1N1 virus	**0.0104**	37	30	**< 0.0001**	37	30	0.325	37	30	**0.0039**	37	30	**0.0007**	37	30	0.6147	37	30
CMV lysate	0.1752	29	20	**0.0002**	29	20	0.5433	29	20	0.107	29	20	**< 0.0001**	29	20	0.5399	29	20
Mann Whitney excluding all cytokine non-responders		**n (preinfection)**	**n (post-infection)**		**n (preinfection)**	**n (post-infection)**		**n (preinfection)**	**n (post-infection)**		**n (preinfection)**	**n (post-infection)**		**n (preinfection)**	**n (post-infection)**		**n (preinfection)**	**n (post-infection)**
live pH1N1 virus	**0.0018**	37	35	**< 0.0001**	37	35	0.3804	37	35	**0.0006**	37	35	**< 0.0001**	37	35	0.5069	37	35
CMV lysate	0.1149	29	27	**< 0.0001**	29	27	0.4139	29	27	0.0577	29	27	**< 0.0001**	29	27	0.3675	29	27
S1																		
1wayANOVAKruskalWallis&Dunns excluding all cytokine non-responders		**n (preinfection)**	**n (post-infection)**		**n (preinfection)**	**n (post-infection)**		**n (preinfection)**	**n (post-infection)**		**n (preinfection)**	**n (post-infection)**		**n (preinfection)**	**n (post-infection)**		**n (preinfection)**	**n (post-infection)**
live pH1N1 virus	0.2453	24	19&15	**p< 0.0001(T1/T2) p<0.005 (T1/T3)**	24	19&15	0.0827	24	19&15	0.1279	24	19&15	**p< 0.0001(T1/T2)**	24	19&15	0.111	24	19&15
CMV lysate	0.1102	18	12&11	**p<0.001**	18	12&11	0.9261	18	12&11	0.0803	18	12&11	**p<0.005 (T1/T2)**	18	12&11	0.6595	18	12&11
S2																		
Mann Whitney excluding all cytokine non-responders		**n (preinfection)**	**n (post-infection)**		**n (preinfection)**	**n (post-infection)**		**n (preinfection)**	**n (post-infection)**		**n (preinfection)**	**n (post-infection)**		**n (preinfection)**	**n (post-infection)**		**n (preinfection)**	**n (post-infection)**
live pH1N1 virus	**0.0072**	13	16	**0.0146**	13	16	0.1455	13	16	**0.0101**	13	16	**0.0383**	13	16	0.3119	13	16
CMV lysate	0.9379	11	15	**0.0086**	11	15	0.1119	11	15	0.9793	11	15	**0.0011**	11	15	0.145	11	15

Table 3.5.3 Significance tests between pre-infection and post-infection antigen-specific CD8+ cytokine positive T cell responses.

In summary, natural pH1N1 infection appears to increase the frequency of CD4+ and CD8+ IFN-γ+ and IFN-γ+IL-2-TNF-α- T cells. Only pH1N1-specific CD4+IL-2+ and CD4+IFN-γ-IL-2+TNF-α- T cells were significantly lower post-infection, whereas both live pH1N1 virus and CMV lysate -specific CD8+IL-2+ and CD8+IFN-γ-IL-2+TNF-α- T cells were significantly lower post-infection.

3.5.4 Differences in pH1N1-specific CD4+ and CD8+ T cell responses between naturally infected and vaccinated individuals

Next, we hypothesised that influenza vaccination and natural infection would differentially induce and maintain T cell responses. A small number of individuals were vaccinated with pH1N1 vaccine and either seroconverted (4-fold rise in HAI titre) or did not seroconvert following vaccination. CD4+IFN-γ+ and CD4+IFN-γ+IL-2-TNF-α- T cell responses (Fig. 3.5.4) and CD8+IFN-γ+ and CD8+IFN-γ+IL-2-TNF-α- T cell responses (Fig. 3.5.5) pre- and post-vaccination were compared alongside the corresponding cytokine positive responses in naturally infected individuals.

Unlike infection, vaccination either with or without seroconversion did not alter frequencies of IFN-γ+ or single-IFN-γ+IL-2-TNF-α- CD4+ (Fig. 3.5.4) or CD8+ (Fig. 3.5.5) T cells. Furthermore, frequencies of CD4+IL-2+, CD4+IFN-γ-IL-2+TNF-α-, CD4+TNF-α+ or CD4+IFN-γ-IL-2-TNF-α+ (or CD8+IL-2+, CD8+IFN-γ-IL-2+TNF-α-, CD8+TNF-α+ or CD8+IFN-γ-IL-2-TNF-α+) T cells were also not significantly altered in vaccinated individuals between pre- and post- vaccination.

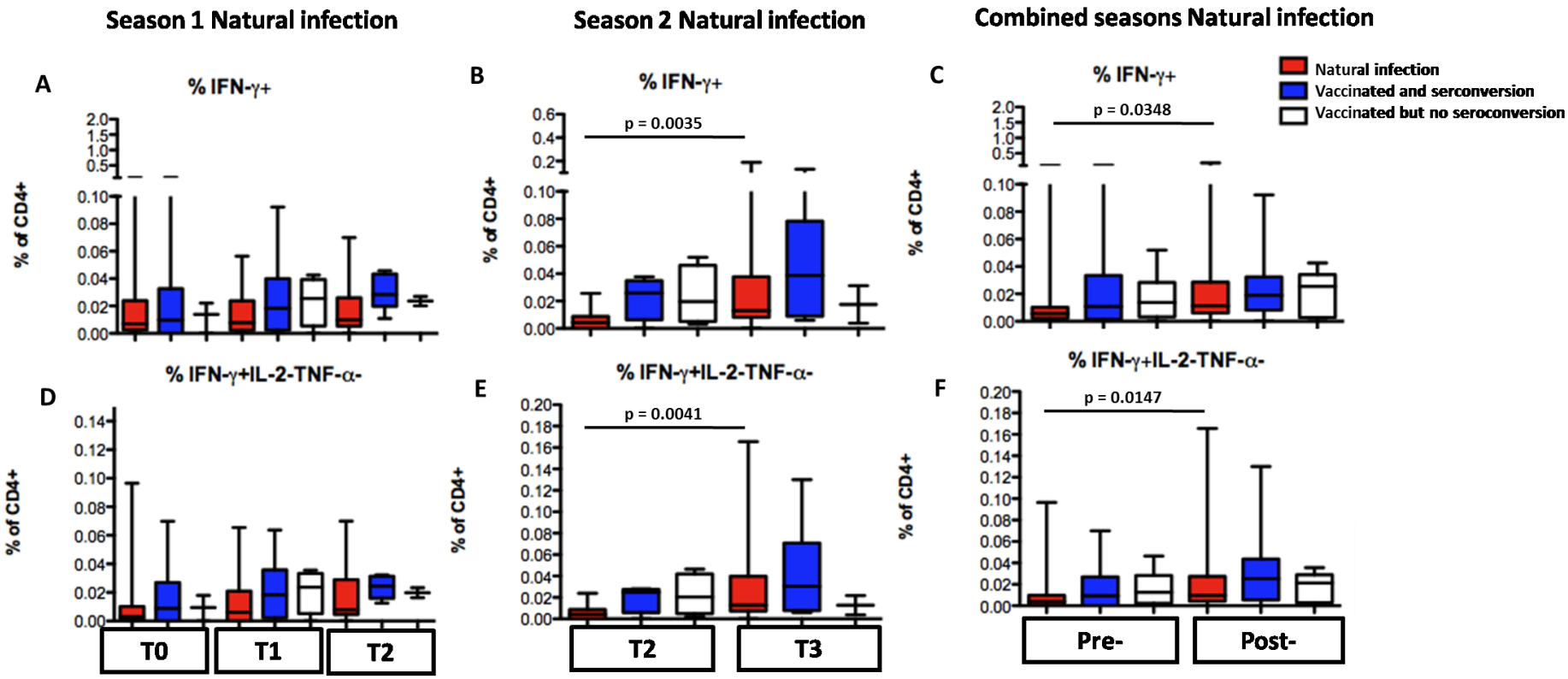

Figure 3.5.4 pH1N1-specific CD4+ T cell responses in naturally infected individuals compared to vaccinated individuals.

The magnitude of *ex vivo* PBMC responses from the IFN-γ+ (A, B, C) and single IFN-γ+ (D, E, F), CD3+CD4+CD8- subsets to live pH1N1 virus individuals with incident pH1N1 infection or were vaccinated during season 1 (A, D), season 2 (B, E) or the combined

seasons data (C, F) was determined by flow cytometry and gating as shown in Fig. 3.4.1. In the box plots, the box represents the third centile (75%) and first centile (25%), with the horizontal line representing the median (50%). The whiskers represent 1.5 times the IQR. Differences between study time-points in subset responses in season 1 were estimated by Kruskall-Wallis test and by Mann Whitney test in season 2 and combined season data. Non-responders to stimulation excluded, Season 1: n = 23, 19, 14, Natural infection; n = 15, 13, 7 Vaccinated and seroconversion; n = 3, 4, 2 Vaccinated but no seroconversion. Season 2: n = 11, 16, Natural infection; n = 6, 8 (CD4+IFN-γ+) and n = 4, 6 (CD4+IFN-γ+IL-2-TNF-α) Vaccinated and seroconversion; n = 4, 2, Vaccinated but no seroconversion; Combined seasons: n = 34, 35, Natural infection; n = 21, 21 (CD4+IFN-γ+) and n = 19, 19 (CD4+IFN-γ+IL-2-TNF-α) Vaccinated and seroconversion; n = 7, 7, Vaccinated but no seroconversion. T0: baseline (pre-infection), T1: up to 6 months post-infection, T2: up to 1.5 years post-infection. Season 2, T2: baseline (pre-infection), T3: up to 6 months post-infection. Combined seasons, Pre-inf: baseline (pre-infection), Post-inf: up to 6 months post-infection.

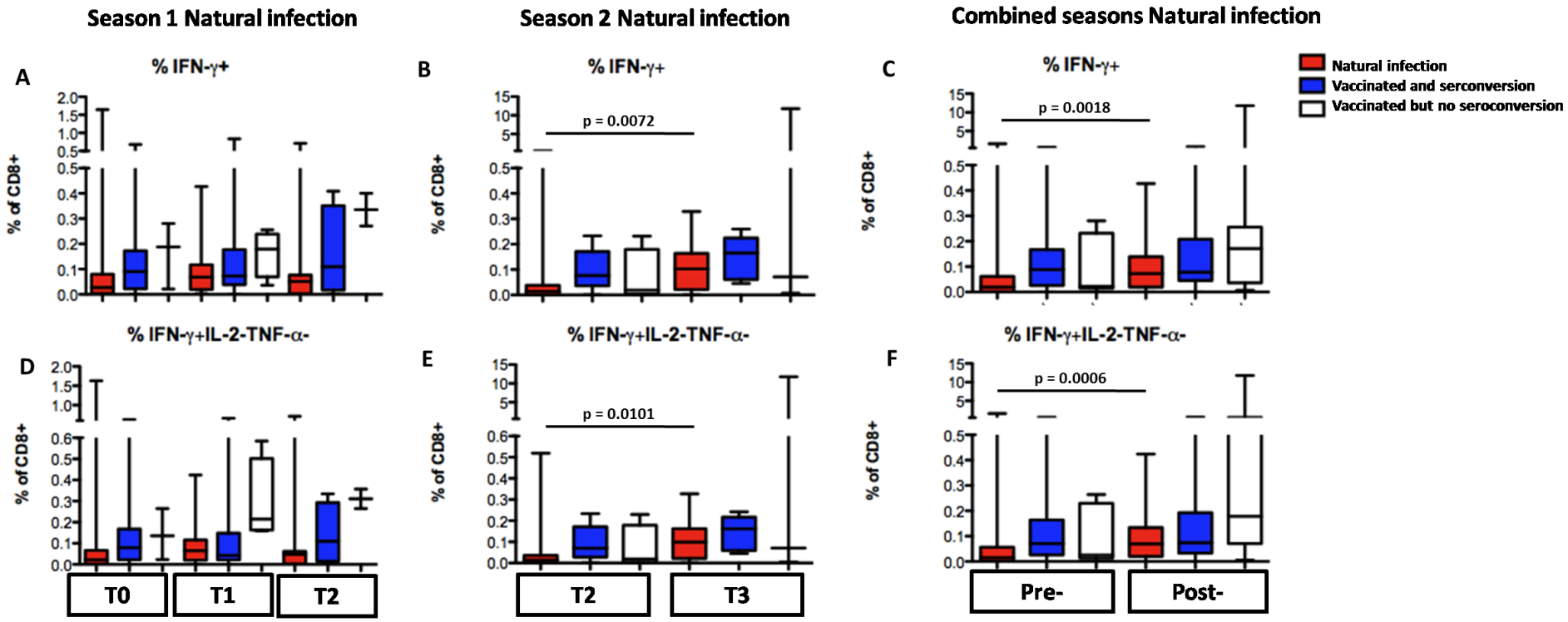

Figure 3.5.5 pH1N1-specific CD8+ T cell responses in naturally infected individuals compared to vaccinated individuals.

The magnitude of *ex vivo* PBMC responses from the IFN-γ+ (A, B, C) and single IFN-γ+ (D, E, F), CD3+CD4-CD8+ subsets to live pH1N1 virus individuals with incident pH1N1 infection or were vaccinated during season 1 (A, D), season 2 (B, E) or the combined seasons data (C, F) was

determined by flow cytometry and gating as shown in Fig. 3.4.1. In the box plots, the box represents the third centile (75%) and first centile (25%), with the horizontal line representing the median (50%). The whiskers represent 1.5 times the IQR. Differences between study time-points in subset responses in season 1 were estimated by Kruskall-Wallis test and by Mann Whitney test in season 2 and combined season data. Non-responders to stimulation excluded, Season 1: n = 24, 19, 15, Natural infection; n = 14, 13, 7 Vaccinated and seroconversion; n = 3, 4, 2 Vaccinated but no seroconversion. Season 2: n = 13, 16, Natural infection; n = 5, 6, Vaccinated and seroconversion; n = 4, 3, Vaccinated but no seroconversion; Combined seasons: n = 37, 35, Natural infection; n = 19, 19, Vaccinated and seroconversion; n = 7, 7, Vaccinated but no seroconversion. T0: baseline (pre-infection), T1: up to 6 months post-infection, T2: up to 1.5 years post-infection. Season 2, T2: baseline (pre-infection), T3: up to 6 months post-infection. Combined seasons, Pre-inf: baseline (pre-infection), Post-inf: up to 6 months post-infection.

3.5.5 Changes in CD4+ and CD8+ memory subsets in naturally infected individuals

Pre-existing pH1N1-specific CD8+IFN-γ+IL-2- T cells with a late effector phenotype (CD45RA+CCR7-) were associated with protection against symptomatic influenza infection (Fig. 3.3.7). However, the evolution of long-lasting virus-specific effector T cells following acute natural infection in humans is unknown. The proportions of naïve, central memory, late effector and effector memory T cells stratified by the expression of CD45RA and CCR7 within CD4+ cytokine positive and CD8+ cytokine positive T cells were followed in infected individuals pre- and post-infection (Fig. 3.5.6).

There was a delayed increase ($p < 0.05$, Fig. 3.5.6A) in the proportion of late effector T cells within pH1N1 stimulated CD4+IFN-γ+ at time-point 2 (up to 1.5 years following infection) in season 1. The proportion of late effector T cells within pH1N1 stimulated CD4+TNF-α+ T cells increased ($p < 0.05$, Fig. 3.5.6I) at time-point 1 (up to 6 months post-infection) and were maintained to time-point 2 in season 1. No significant changes were seen in pH1N1 stimulated CD4+ cytokine positive phenotypic subsets in season 2 (Fig. 3.5.6 B, F, J), or in CMV lysate stimulated CD4+IFN-γ+ and CD4+TNF-α+ T cells in either season (Fig. 3.5.6 C -D and Fig. 3.5.6 K -L). The proportion of effector memory cells within pH1N1 virus stimulated CD4+IL-2+ T cells was significantly reduced post-infection at time-point 1 ($p <0.05$, Fig. 3.5.6E) but returned back up to baseline levels by time-point 2 in season 1. Interestingly,

the proportion of late effector CD4+IL-2+ T cells in CMV lysate stimulation was increased at time-point 1 post-infection in season 1 ($p < 0.05$, Fig. 3.5.6G). Hence the increase in proportions of late effector T CD4+IFN-γ+ and CD4+TNF-α+ T cells were specific to pH1N1 stimulation whereas the increase in proportion of CD4+IL-2+ late effector T cells was specific to CMV-lysate stimulation. The decrease in proportion of CD4+IL-2+ effector memory T cells was specific to pH1N1 stimulation only.

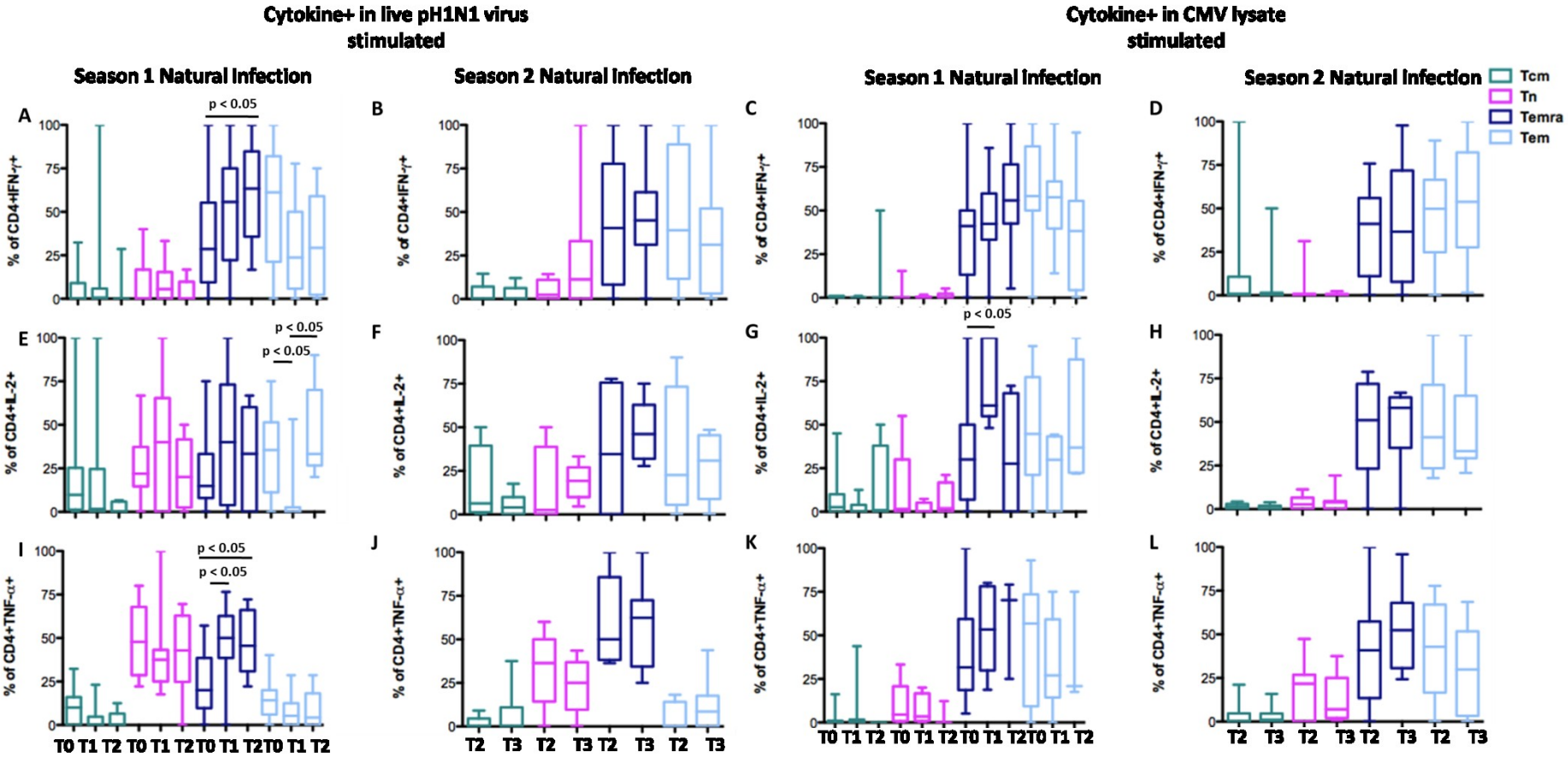

Figure 3.5.6 Longitudinal development in effector and memory subsets of pH1N1 live virus and CMV lysate -specific CD4+ T cells.

Phenotypic characterisation was performed using multiparameter flow cytometry of the different memory subsets of CD3+CD4+CD8-IFN-γ+ (A, B, C, D), CD3+CD4+CD8-IL-2+ (E, F, G, H) and CD3+CD4+CD8-TNF-α+ (I, J, K, L) T cells on the basis of CCR7 and CD45RA surface expression after 18 hour stimulation of PBMCs with live pH1N1 virus (A, B, E, F, I, J) or CMV lysate (C, D, G, H, K, L) from individuals with incident pH1N1 infection during season 1 (A, C, E, G, I, K) or season 2 (B, D, F, H, J, L). The proportion of CD3+CD4+CD8- cytokine positive T cells that were of the effector-memory (CD45RA−CCR7−), late-effector (CD45RA+CCR7−), central-memory (CD45RA−CCR7+) or naive (CD45RA+CCR7+) phenotype are shown; in the box plots, the box represents the third centile (75%) and first centile (25%), with the horizontal line representing the median (50%). The whiskers represent 1.5 times the IQR. Differences between study time-points in subset responses were estimated by Kruskal Wallis test (season 1) or by Mann Whitney test (season 2). Non-responders to stimulation excluded for each cytokine, Season 1 CD4+IFN-γ+: n = 20, 15, 12 to live pH1N1 virus and n = 15, 11, 8 to CMV lysate; Season 1 CD4+IL-2+: n = 20, 9, 5 to live pH1N1 virus and n = 11, 6, 4 to CMV lysate; Season 1 CD4+TNF-α+: n = 19, 15, 9 to live pH1N1 virus and n = 12, 9, 3 to CMV lysate; Season 2 CD4+IFN-γ+: n = 8, 15 to live pH1N1 virus and n = 12, 13 to CMV lysate; Season 2 CD4+IL-2+: n = 4, 6 to live pH1N1 virus and n = 6, 7 to CMV lysate; Season 2 CD4+TNF-α+: n = 5, 10 to live pH1N1 virus and n = 9, 11 to CMV lysate. T0: baseline (pre-infection), T1: up to 6 months post-infection, T2: up to 1.5 years post-infection. Season 2, T2: baseline (pre-infection), T3: up to 6 months post-infection.

Similar analysis based on the expression of CD45RA and CCR7 was undertaken on CD8+IFN-γ+, CD8+IL-2+ and CD8+TNF-α+ T cells in pH1N1 or CMV lysate stimulation (Fig. 3.5.7). Only pH1N1-stimulated CD8+IFN-γ+ showed a significant increase ($p < 0.05$, Fig. 3.5.7A) in the proportion of late effector T cells at time-point 2 (up to 1.5 years following infection) in season 1. CMV lysate stimulated CD8+IFN-γ+ showed a significant increase ($p < 0.05$, Fig. 3.5.7C) in the proportion of naïve T cells at time-point 2 in season 1.

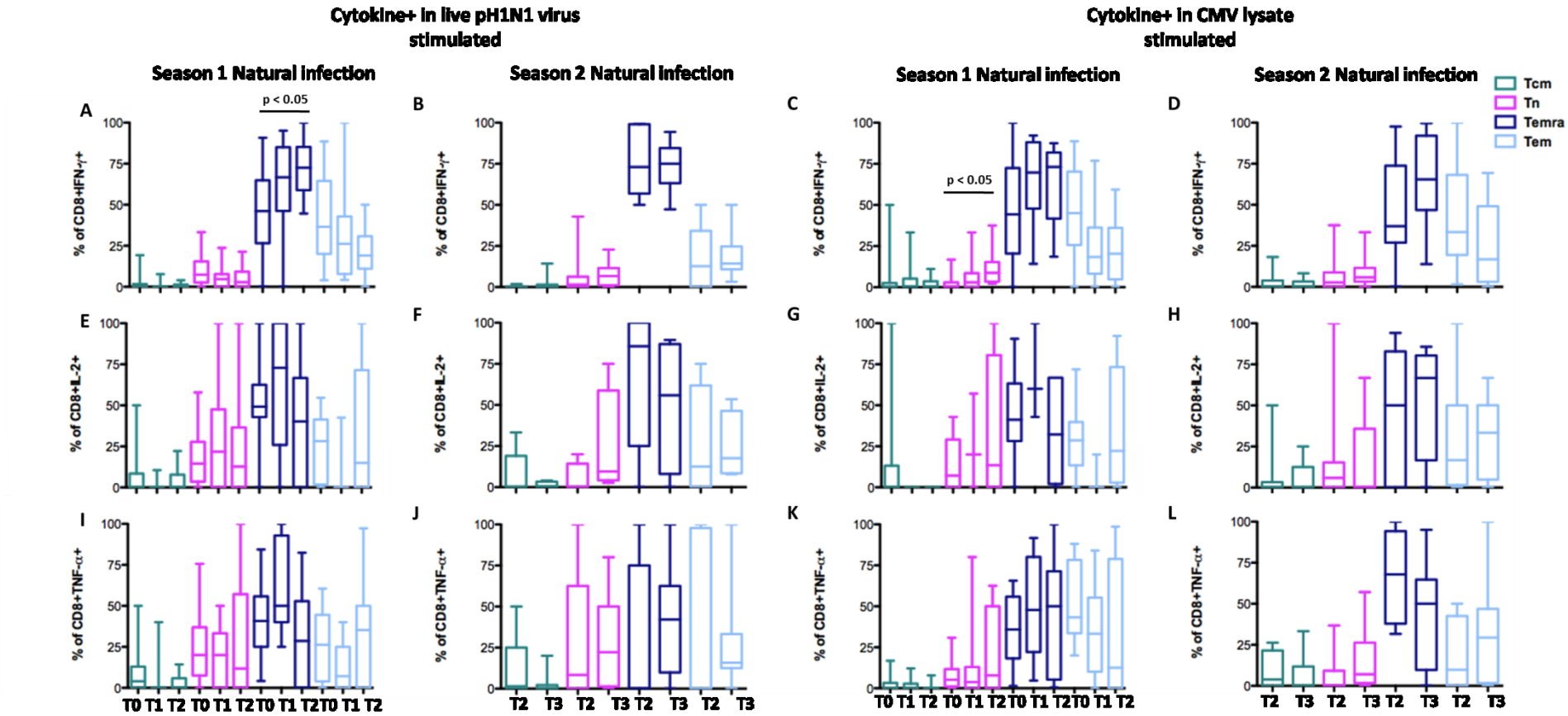

Figure 3.5.7 Longitudinal development in effector and memory subsets of pH1N1 live virus and CMV lysate -specific CD8+ T cells.

Phenotypic characterisation was performed using multiparameter flow cytometry of the different memory subsets of CD3+CD4-CD8+IFN-γ+ (A, B, C, D), CD3+CD4-CD8+IL-2+ (E, F, G, H) and CD3+CD4-CD8+TNF-α+ (I, J, K, L) T cells on the basis of CCR7 and CD45RA surface expression after 18 hour stimulation of PBMCs with live pH1N1 virus (A, B, E, F, I, J) or CMV lysate (C, D, G, H, K, L) from individuals with incident pH1N1 infection during season 1 (A, C, E, G, I, K), season 2 (B, D, F, H, J, L). The proportion of CD3+CD4-CD8+ cytokine positive T cells that were of the effector-memory (CD45RA−CCR7−), late-effector (CD45RA+CCR7−), central-memory (CD45RA−CCR7+) or naive (CD45RA+CCR7+) phenotype are shown; in the box plots, the box represents the third centile (75%) and first centile (25%), with the horizontal line representing the median (50%). The whiskers represent 1.5 times the IQR. Differences between study time-points in subset responses were estimated by Kruskal Wallis test (season 1) or by Mann Whitney test (season 2). Non-responders to stimulation excluded for each cytokine, Season 1 CD8+IFN-γ+: n = 20, 19, 12 to live pH1N1 virus and n = 12, 12, 8 to CMV lysate; Season 1 CD8+IL-2+: n = 21, 8, 10 to live pH1N1 virus and n = 13, 3, 8 to CMV lysate; Season 1 CD8+TNF-α+: n = 18, 11, 7 to live pH1N1 virus and n = 10, 8, 7 to CMV lysate; Season 2 CD8+IFN-γ+: n = 8, 15 to live pH1N1 virus and n = 10, 14 to CMV lysate; Season 2 CD8+IL-2+: n = 11, 4 to live pH1N1 virus and n = 9, 5 to CMV lysate; Season 2 CD8+TNF-α+: n = 6, 11 to live pH1N1 virus and n = 6, 11 to CMV lysate. T0: baseline (pre-infection), T1: up to 6 months post-infection, T2: up to 1.5 years post-infection. Season 2, T2: baseline (pre-infection), T3: up to 6 months post-infection.

3.5.6 Phenotype of pH1N1 virus-specific CD4+IFN-γ+ and CD8+IFN-γ+ T cells following natural infection

Since frequencies of pH1N1-specific CD4+IFN-γ+ and CD8+IFN-γ+ responses were increased following infection (Fig. 3.5.2 and Fig. 3.5.3), the expression of degranulation (CD107ab), early activation (CD69), tissue-homing (CCR5) and cellular senescence-associated (CD57) markers by these CD4+IFN-γ+ and CD8+IFN-γ+ T cells was assessed in infected individuals. Infection did not alter the proportion of pH1N1-specific CD4+IFN-γ+ (Fig. 3.5.8A-F) or CD8+IFN-γ+ (Fig. 3.5.9A-F) T cells expressing CCR5, CD57 or CD107ab compared to pre-infection. However, the proportion of pH1N1-specific and CMV lysate-specific CD4+IFN-γ+ and CD8+IFN-γ+ T cells expressing CD69 was significantly increased post-infection compared to pre-infection (Fig. 3.5.8G-H and Fig. 3.5.9G). Of note, non-specific CD8+IFN-γ+CD69+ T cells in unstimulated condition were also significantly increased in season 1.

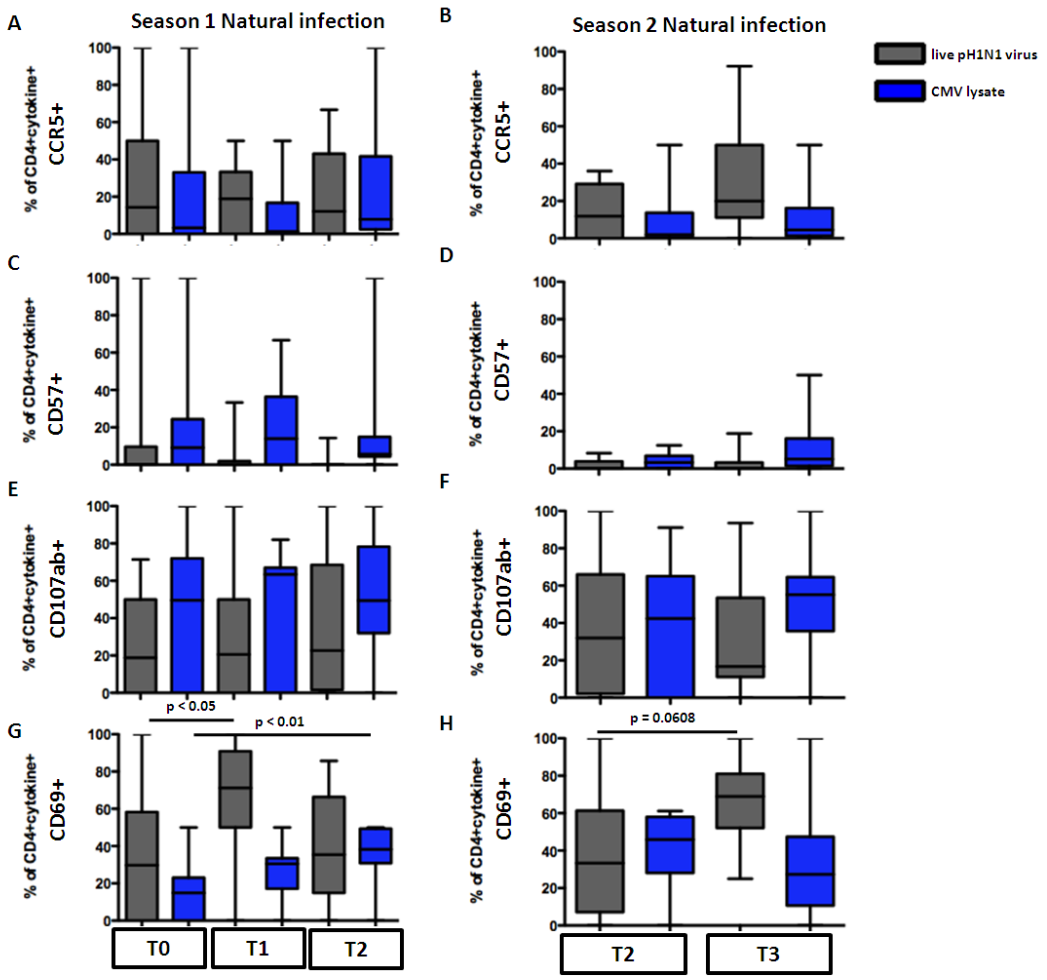

Figure 3.5.8 Longitudinal changes in pH1N1 live virus and CMV lysate -specific CD4+IFN-γ+ T cells.

Phenotypic characterisation was performed using multiparameter flow cytometry and gating as shown in Fig. 3.4.1 of CD3+CD4+CD8-IFN-γ+ T cells after 18 hour stimulation of PBMCs with live pH1N1 virus or CMV lysate in individuals with incident pH1N1 infection during season 1 (A, C, E, G) or season 2 (B, D, F, H). The proportion of CD3+CD4+CD8- cytokine positive T cells that expressed CCR5 (A, B), CD57 (C, D), CD107 (isotypes A and B) (E, F), and CD69 (G, H) are shown. In the box plots, the box represents the third centile (75%) and first centile (25%), with the horizontal line representing the median (50%). The whiskers represent 1.5 times the IQR. Differences between study time-points in each phenotypic marker were estimated by Kruskal Wallis test (season 1) or by Mann Whitney test between (season 2). Non-responders to stimulation excluded, Season 1: n = 20, 15, 12 to live

pH1N1 virus and n = 15, 11, 8 to CMV lysate; Season 2: n = 8, 15 to live pH1N1 virus and n = 12, 13 to CMV lysate. T0: baseline (pre-infection), T1: up to 6 months post-infection, T2: up to 1.5 years post-infection. Season 2, T2: baseline (pre-infection), T3: up to 6 months post-infection.

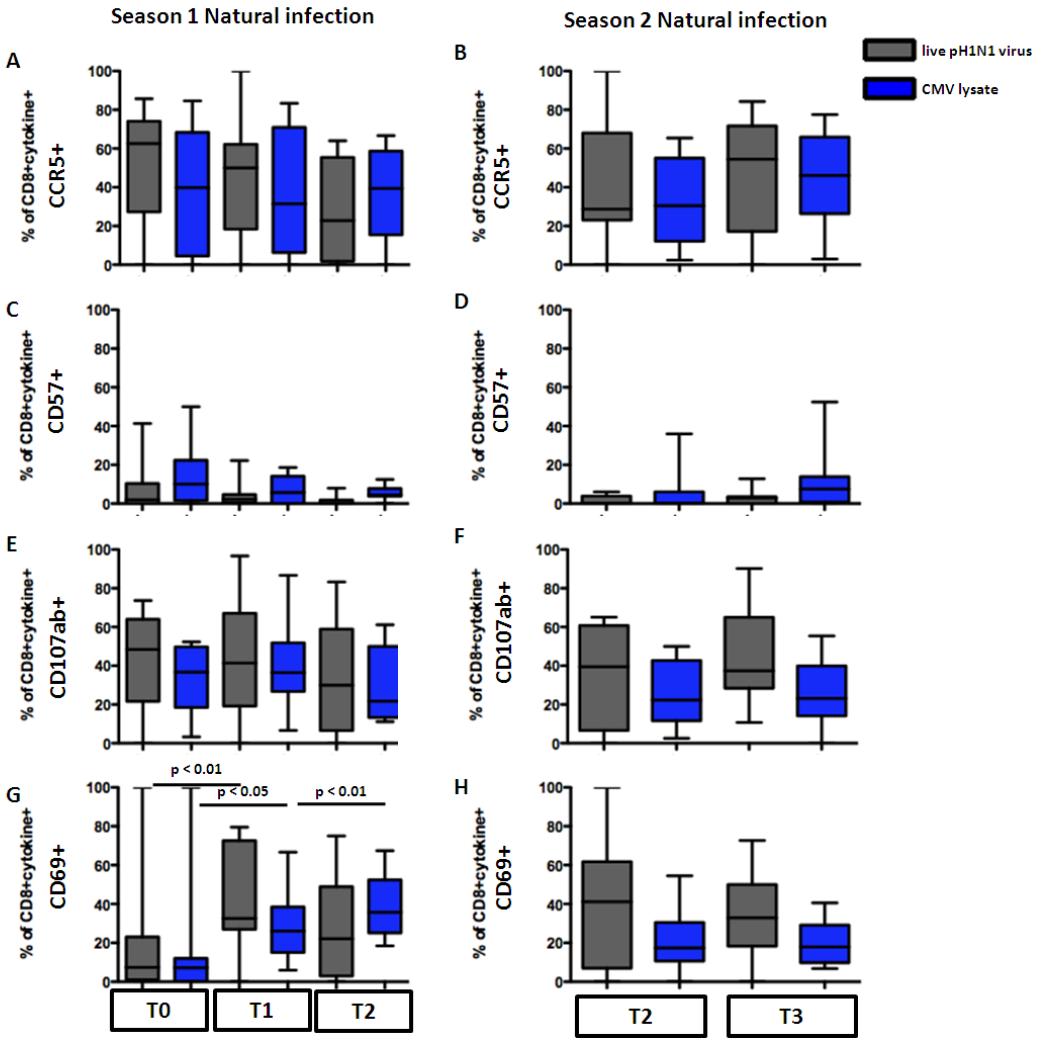

Figure 3.5.9 Longitudinal changes in pH1N1 live virus and CMV lysate -specific CD8+IFN-γ+ T cells.

Phenotypic characterisation was performed using multiparameter flow cytometry and gating as shown in Fig. 3.4.1 of CD3+CD4-CD8+IFN-γ+ T cells after 18 hour

stimulation of PBMCs with live pH1N1 virus or CMV lysate in individuals with incident pH1N1 infection during season 1 (A, C, E, G) or season 2 (B, D, F, H). The proportion of CD3+CD4-CD8+ cytokine positive T cells that expressed CCR5 (A, B), CD57 (C, D), CD107 (isotypes A and B) (E, F), and CD69 (G, H) are shown. In the box plots, the box represents the third centile (75%) and first centile (25%), with the horizontal line representing the median (50%). The whiskers represent 1.5 times the IQR. Differences between study time-points in each phenotypic marker were estimated by Kruskal Wallis test (season 1) or by Mann Whitney test between (season 2). Non-responders to stimulation excluded, Season 1: n = 20, 19, 12 to live pH1N1 virus and n = 12, 12, 8 to CMV lysate; Season 2: n = 8, 15 to live pH1N1 virus and n = 10, 14 to CMV lysate. T0: baseline (pre-infection), T1: up to 6 months post-infection, T2: up to 1.5 years post-infection. Season 2, T2: baseline (pre-infection), T3: up to 6 months post-infection.

3.5.7 Baseline predictors of post-infection pH1N1 virus-specific T cell responses

Frequencies of pH1N1 virus-specific IFN-γ+IL-2-, IFN-γ-IL-2+ and IFN-γ+IL-2+ T cell responses in fluorescence-immunospot (Fig. 3.5.1D, I and N) and pH1N1-specific CD4+ and CD8+ IFN-γ+ and IFN-γ+IL-2-TNF-α- T cells (Fig. 3.5.2 and Fig. 3.5.3) were increased post-infection compared to pre-infection. Next, correlations between pre-infection and post-infection responses were determined. The hypothesis was that pre-existing pH1N1 cross-reactive T cell responses would predict the increase in frequency of pH1N1-specific T cells post-infection.

The increase in frequencies of pH1N1 virus-specific IFN-γ+IL-2- and IFN-γ-IL-2+ responses post-infection compared to pre-infection was not significantly correlated with pre-infection frequencies of any of the three functional subsets enumerated by fluorescence-immunospot (Fig. 3.5.10). However, the increase in frequency of pH1N1 virus-specific dual IFN-γ+IL-2+ response post-infection was positively correlated (r = 0.438, p = 0.0175) with pre-existing pH1N1-specific IFN-γ+IL-2- responses (Fig. 3.5.10G).

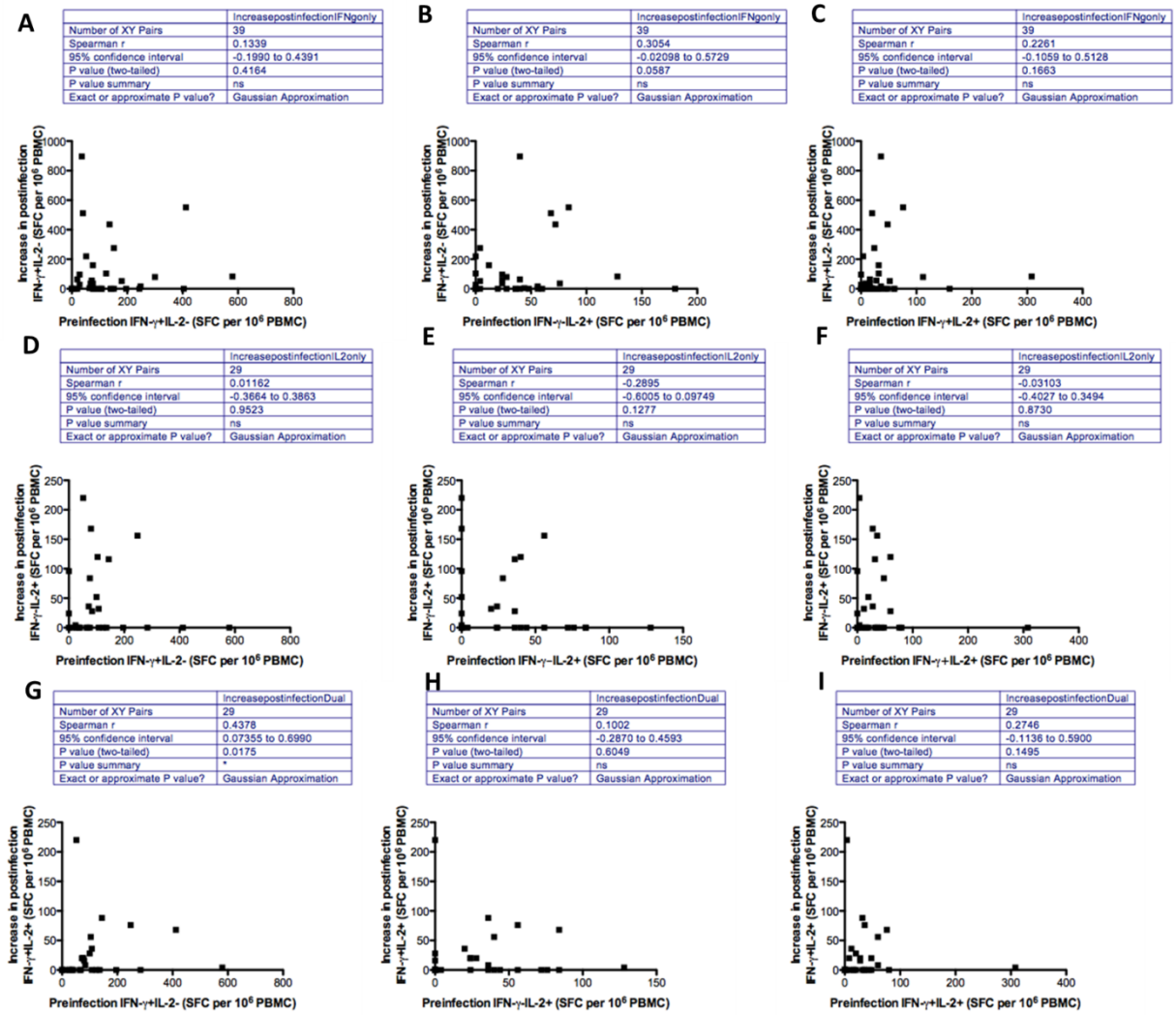

Figure 3.5.10 Correlation between baseline and post-infection pH1N1 virus-specific responses by fluorescence-immunospot.

Correlation between the increase in frequency between pre-infection and post-infection time-points in the IFN-γ+IL-2− (A, B, C), IFN-γ-IL-2+ (D, E, F), IFN-γ+IL-2+ (G, H, I) cellular responses to live pH1N1 virus quantified by fluorescence-immunospot and the pre-infection IFN-γ+IL-2− (A, D, G), IFN-γ-IL-2+ (B, E, H), IFN-γ+IL-2+ (C, F, I) cellular responses to live pH1N1 virus in individuals with incident pH1N1 infection during the study (seasons 1 and 2 combined). r values are the Spearman rank correlation coefficients. Each symbol on the plot represents an individual (n = 29 pairs). SFC, spot-forming cells.

Conversely, frequencies of pH1N1-specific pre-infection CD4+IFN-γ+ and CD4+TNF-α+ T cells were inversely associated (r = -0.693, p = 0.0001 and r = -0.506, p = 0.0099) with the increase in post-infection pH1N1-specific CD4+IFN-γ+ response (Fig. 3.5.11 B and C). Furthermore, the increase in post-infection pH1N1-specific CD4+IFN-γ+IL-2-TNF-α- T cells was also inversely correlated with pre-infection pH1N1-specific CD4+IFN-γ+IL-2-TNF-α- T cells (r = -0.479, p = 0.0134, Fig. 3.5.9E). Pre-infection pH1N1-specific CD4+IL-2+ or CD4+IFN-γ-IL-2+TNF-α- T cell responses were not significantly correlated with the increase in post-infection pH1N1-specific CD4+IFN-γ+ or CD4+IFN-γ+IL-2-TNF-α- T cell response respectively (r = -0.326, p = 0.111 and r = -0.118, p = 0.565, Fig. 3.5.11 A and D). In pH1N1-specific CD8+IFN-γ+ and CD8+IFN-γ+IL-2-TNF-α- T cells, only the frequencies of pre-infection pH1N1-specific CD8+IFN-γ+ and CD8+IFN-γ+IL-2-TNF-α- T cells respectively were inversely correlated with post-infection responses (r = -0.541, p = 0.0025 and r = -0.569, p = 0.0013, Fig. 3.5.12 B and E).

A

	Post-Pre(IFNg+)
Spearman r	-0.3268
95% confidence interval	-0.6467 to 0.09082
P value (two-tailed)	0.1108

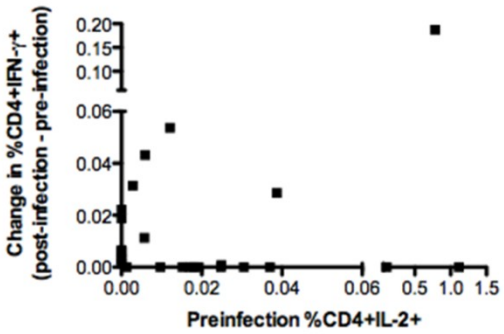

B

	Post-Pre(IFNg+)
Spearman r	-0.6937
95% confidence interval	-0.8579 to -0.4008
P value (two-tailed)	0.0001

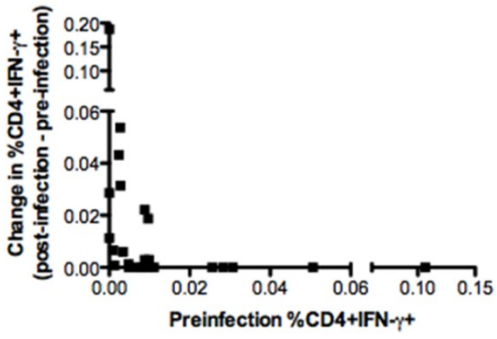

C

	Post-Pre(IFNg+)
Spearman r	-0.5056
95% confidence interval	-0.7561 to -0.1258
P value (two-tailed)	0.0099

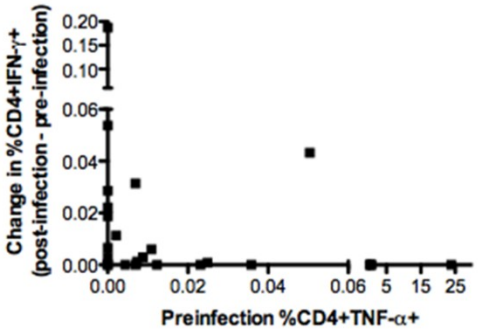

D

	Post-Pre(IFNg+IL2-TNFa-)
Spearman r	-0.1183
95% confidence interval	-0.4928 to 0.2932
P value (two-tailed)	0.5650

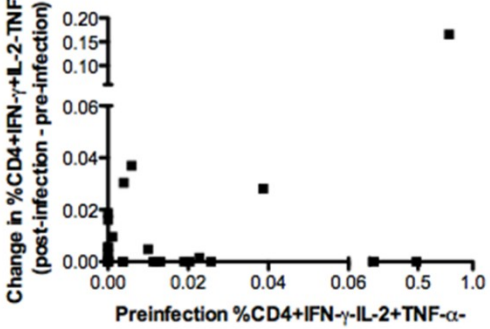

E

	Post-Pre(IFNg+IL2-TNFa-)
Spearman r	-0.4785
95% confidence interval	-0.7361 to -0.09983
P value (two-tailed)	0.0134

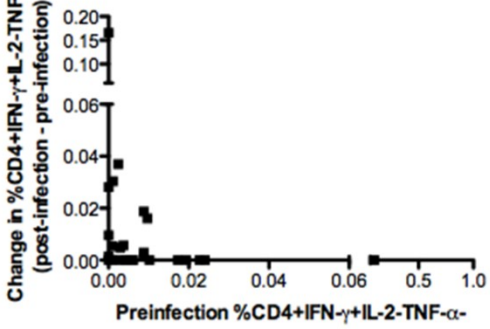

F

	Post-Pre(IFNg+IL2-TNFa-)
Spearman r	-0.3529
95% confidence interval	-0.6582 to 0.05209
P value (two-tailed)	0.0770

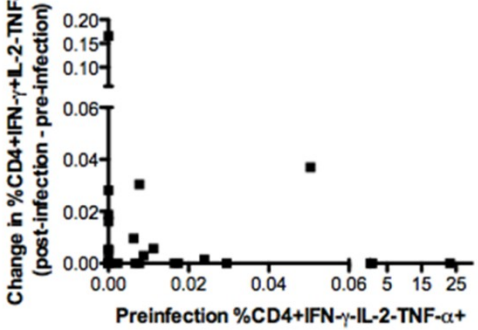

Figure 3.5.11 Correlation between baseline and post-infection pH1N1 virus-specific CD4+ T cell responses.

Correlation between the increase in frequency between pre-infection and post-infection time-points in the CD3+CD4+CD8-IFN-γ+ (A, B, C) and CD3+CD4+CD8-IFN-γ+ IL-2-TNF-α- (D, E, F) T cells to live pH1N1 virus and the pre-infection CD3+CD4+CD8-IL-2+ (A), CD3+CD4+CD8-IFN-γ+ (B), CD3+CD4+CD8-TNF-α+(C), CD3+CD4+CD8-IFN-γ-IL-2+TNF-α- (D), CD3+CD4+CD8-IFN-γ+IL-2-TNF-α- (E), CD3+CD4+CD8-IFN-γ-IL-2-TNF-α+ (F) T cell responses to live pH1N1 virus in individuals with incident pH1N1 infection during the study (seasons 1 and 2 combined). r values are the Spearman rank correlation coefficients. Each symbol on the plot represents an individual, non-responders to stimulation excluded (n = 25 pairs).

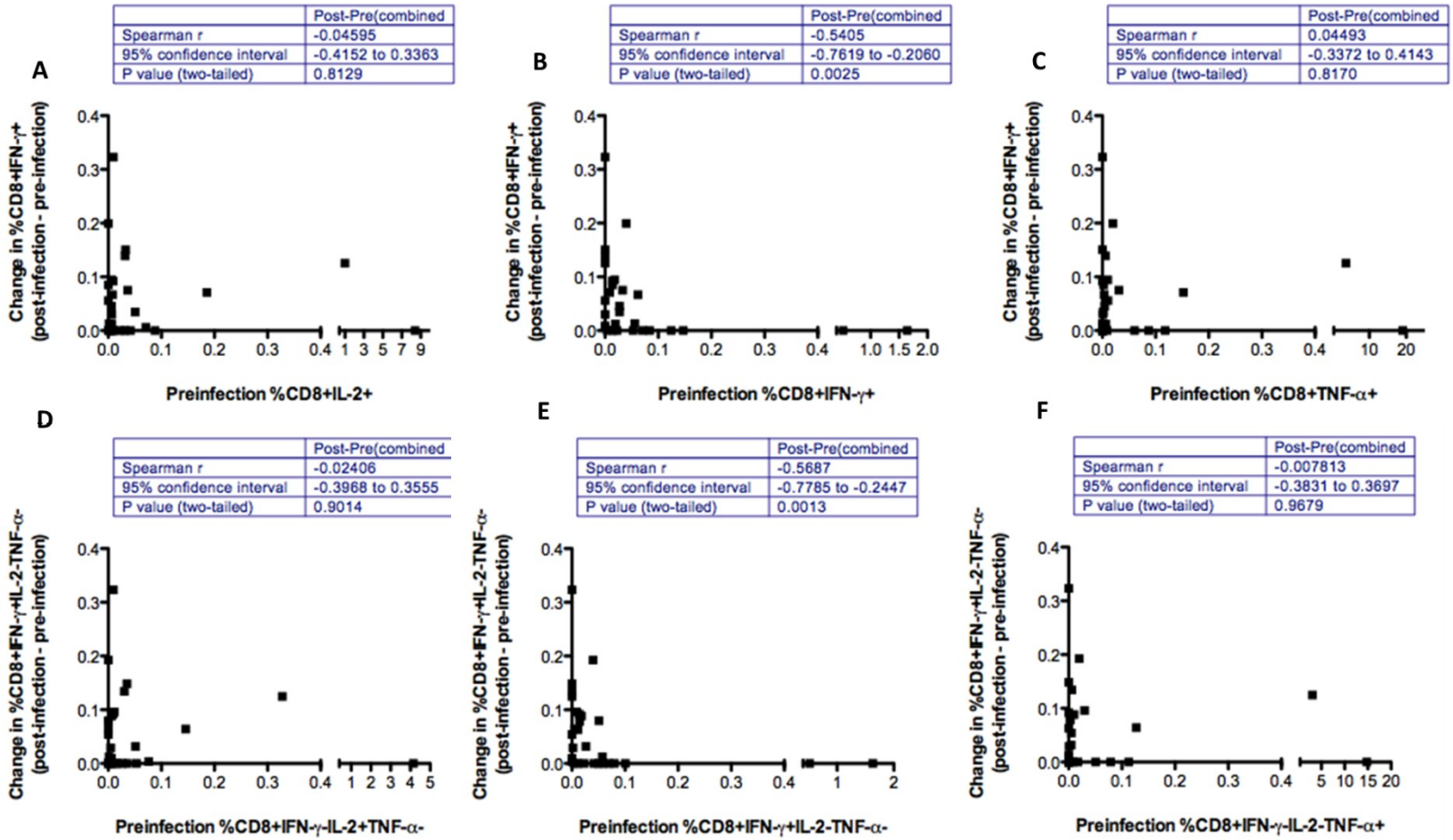

Figure 3.5.12 Correlation between baseline and post-infection pH1N1 virus-specific CD8+ T cell responses.

Correlation between the increase in frequency between pre-infection and post-infection time-points in the CD3+CD4-CD8+IFN-γ+ (A, B, C) and CD3+CD4-CD8+IFN-γ+ IL-2-TNF-α- (D, E, F) T cells to live pH1N1 virus and the pre-infection CD3+CD4-CD8+IL-2+ (A), CD3+CD4-CD8+IFN-γ+ (B), CD3+CD4-CD8+TNF-α+(C), CD3+CD4-CD8+IFN-γ-IL-2+TNF-α- (D), CD3+CD4-CD8+IFN-γ+IL-2-TNF-α- (E), CD3+CD4-CD8+IFN-γ-IL-2-TNF-α+ (F) T cell responses to live pH1N1 virus in individuals with incident pH1N1 infection during the study (seasons 1 and 2 combined). r values are the Spearman rank correlation coefficients. Each circle on the plot represents an individual, non-responders to stimulation excluded (n = 29 pairs).

4 DISCUSSION

The role of T cell-mediated HSI against natural influenza infection in humans has not been demonstrated prior to our study. This is partly due to requirement for a setting where a novel influenza virus enters a population naïve to this novel strain, a scenario that only occurs during influenza pandemics. Such a setting allows testing of the role of T cells in protecting against symptomatic influenza illness in the absence of strain-specific antibodies. We therefore exploited the 2009 H1N1 pandemic to test the association of pH1N1 cross-reactive T cells with natural influenza infection outcomes, and to characterise the longitudinal development of pH1N1-specific responses in infected individuals.

4.1 A sensitive and reproducible fluorescence-immunospot assay

Functional T-cell subsets are critical determinants of protection and pathogenesis in infectious diseases. Multiple-cytokine-secreting T cells have been associated with protective immunity to viral (Betts *et al.*, 2006), bacterial (Wilkinson & Wilkinson, 2010) and parasitic infections (Darrah *et al.*, 2007); hence measurement of a single cytokine may not be sufficient for detection of a clinically effective pathogen-specific immune response (Slota *et al.*, 2011). Therefore, the accurate quantitative enumeration of functional T cell subsets is central to immunology. The findings presented in **Results section 3.1** demonstrate fluorescence-immunospot as a sensitive and reproducible assay for multiple-cytokine profiling of *ex vivo* T cell

responses in the context of human clinical studies. The assay has low background facilitating high signal-to-noise output to detect low frequency antigen-specific responses; intra-assay and inter-assay CVs of less than 14% and 24% respectively, and stability of response across a range of input T cell number. Notably, IL-2 responses in fluorescence-immunospot were more sensitive to the effects of cryopreservation and anti-CD28 co-stimulation compared to IFN-γ responses.

In longitudinal studies conducted over long periods of time using human samples, reproducibility and sample expenditure of an immunological assay are important considerations. We have demonstrated intra- and inter- assay CV values of fluorescence-immunospot that are low and similar to dual-colour IFN-γ/IL-2 ELISpot (Boulet *et al.*, 2007) and IFN-γ single-colour ELISpot (Mwau *et al.*, 2002) reported in other studies. The inclusion of a number of different antigens to stimulate both CD4 T cell (PPD, CMV- lysate and EBV- lysate) and CD8 T cell (influenza M1 peptide pool) subsets demonstrates that fluorescence-immunospot can measure responses from both CD4 and CD8 T cells. Reproducibility is essential for clinical trials measuring responses to infection and vaccination. Hence low CVs will enable the confident use of fluorescence-immunospot for monitoring multiple-cytokine-secreting functional T cell responses in human cohort studies.

In comparison to the optimal input T cell number reported for dual colour ELISpot in a 96-well plate format (Boulet *et al.*, 2007), our results suggest that using 200, 000 cells per well is sufficient to detect antigen-specific responses *ex vivo* in

fluorescence-immunospot (**Results section 3.1**). Unlike in the dual colour ELISpot (Boulet *et al.*, 2007), we did not detect a linear increase in any cytokine responses with increasing cell input, or an upper limit of detection using a range of 1 – 4 x 10^5 cells per well in fluorescence-immunospot (**Results section 3.1**). This may be due to the lower ambiguity of detection in fluorescence-immunospot compared to dual colour ELISpot. Hence in cases where sample availability is extremely limited, fluorescence-immunospot could still be employed to reliably quantify antigen-specific responses using inputs of 1 – 2 x 10^5 cells per well. Importantly, fluorescence-immunospot enables measurement of two cytokine-secreting populations simultaneously, but uses only half the number of cells than would be required if measuring each cytokine alone in single colour ELISpot. Low sample expenditure is a significant factor in human studies with limited cell availability and fluorescence-immunospot demonstrates this advantage.

There are some aspects of IFN-γ/IL-2 fluorescence-immunospot assay that have been highlighted during this comprehensive assessment of the basic parameters concerning the execution and performance of this assay. Casey *et al.* demonstrated that negative control well responses are significantly higher in fluorescence-immunospot compared to single-colour ELISpot (attributed to co-stimulatory anti-CD28 in fluorescence-immunospot) (Casey *et al.*, 2010). We incorporate the largest data set to date reporting low background responses in fluorescence-immunospot from PBMC of healthy individuals (**Results section 3.1**). We also demonstrate higher background IL-2 responses than IFN-γ responses. Hence the signal-to-noise

ratio in fluorescence-immunospot may be lower than in single-colour ELISpot, especially for IL-2 responses (**Results section 3.1**). However, this factor may be outweighed by the significant advantage of fluorescence-immunospot in lower sample expenditure to gain information on three cytokine-secreting profiles simultaneously.

The use of cryopreserved samples in clinical trials and longitudinal studies greatly enhances immune monitoring capabilities of an assay. We found significant strong correlations between fresh and frozen-thawed PBMC for total IFN-γ+ and IFN-γ+IL-2+ dual responses in fluorescence-immunospot using PBMC cryopreserved for 2 weeks (**Results section 3.1**). This is consistent with previously published literature on the effects of cryopreservation on single-colour IFN-γ and IL-2 antigen-specific ELISpot responses (Kreher *et al.*, 2003). However, total IL-2+ responses from fresh and frozen-thawed PBMC were only moderately correlated (**Results section 3.1**). Increased apoptosis of antigen-specific CD4+ T cells compared to CD8+ T cells following long-term cryopreservation (> 300 days) has been reported (Owen *et al.*, 2007), hence the same mechanism could have accounted for lower antigen-specific CD4+ T cell-derived IL-2 in frozen-thawed PBMC responses in our observations. This implies that consistent use of either fresh or frozen-thawed samples in fluorescence-immunospot is required to ensure comparability of responses throughout a study.

One other caveat is the effect of anti-CD28 to compensate for antibody sequestration in IFN-γ/IL-2 fluorescence-immunospot. Interestingly, the anti-CD28 compensation for antibody capture does not enhance cytokine responses for all antigens equally. The frequencies of CMV-lysate or M1 peptide pool-specific responses were not significantly enhanced with anti-CD28, and this was independent of the concentration of anti-CD28 used (**Results section 3.1**). In cases such as EBV-lysate-specific responses, antibody capture effect is significant and using anti-CD28 enables detection of a higher frequency of responses overall and especially for IL-2 responses (**Results section 3.1**). A previous study using anti-CD28 in IFN-γ ELISpot proposed that the T cell activation threshold may be reduced by the costimulatory signal, thus a higher frequency of cytokine-secreting memory T cells can be detected even at saturating antigen concentrations (Ott *et al.*, 2004). We demonstrate that IL-2 in EBV lysate stimulation is mainly secreted by CD4+ T cells, whereas IL-2 in M1 peptide pool or CMV lysate stimulated PBMC is from both CD4+ and CD8+ T cells (**Results section 3.1**). Hence the difference in responses to anti-CD28 between EBV-lysate compared to M1 peptide pool may be due to the enhanced effect of co-stimulation on CD4 T cell derived IL-2 secretion. This suggests that the use of anti-CD28 (and the concentration used) in IFN-γ/IL-2 fluorescence-immunospot could be considered on an individual antigen basis. However, for consistency and comparability between stimulation conditions, we used the manufacturer's recommended concentration of 0.5 μg/mL anti-CD28 co-stimulation in all subsequent experimental results presented (**Results sections 3.2 – 3.3**).

IFN-γ and IL-2 fluorescence-immunospot has been exemplified (**Results section 3.1**), but other commercially available kits (© Mabtech AB) include detection of IL-5, IL-13 and IL-17A in addition to IFN-γ. Future studies could assess similar basic parameters in fluorescence-immunospot available with other cytokine combinations. Our data in conjunction with previous work conducted in our laboratory (Casey *et al.*, 2010) demonstrate fluorescence-immunospot as an assay with sensitivity and reproducibility similar to single-colour ELISpot. Hence IFN-γ and IL-2 fluorescence-immunospot has been used to characterise low frequency pH1N1-specific T cells in PBMC stored cryopreserved from individuals at pre- and post- influenza infection time-points. Pre-stimulation of cryopreserved-thawed PBMC with 0.5 μg/mL anti-CD28 prior to plating (2 – 2.5 x 10^5 PBMC per well) in fluorescence-immunospot was kept consistent throughout experiments. This was to minimise the variability in effects of cryopreservation and anti-CD28 co-stimulation on IL-2 fluorescence-immunospot responses.

4.2 Phenotype of pH1N1 cross-reactive cellular responses in pH1N1 naïve individuals

In a cohort of 76 pH1N1-naive healthy young adults, there were a high proportion of individuals with circulating cross-reactive T cells to at least one of the three immunodominant pH1N1 core proteins (PB1, M1 and NP) (58% of individuals); to live pH1N1 virus (75% of individuals) and to pH1N1 inactivated vaccine (63% of individuals) (**Results section 3.2**). This is consistent with other studies (Tu *et al.*, 2010, Ge *et al.*, 2010, Richards *et al.*, 2010, Gras *et al.*, 2010, Scheible *et al.*, 2011)

identifying cross-reactive CD4+ and CD8+ T cells pre-existing in naïve individuals that recognise and respond to novel pH1N1 virus *ex vivo*.

The difference in prevalence response to the peptide pools and live virus or inactivated vaccines in our results may be due to differences in antigen processing and presentation (Germain, 1986). The 15-mer synthetic peptides used (**Results section 3.2**) would be expected to predominantly stimulate MHC class I-restricted CD8+ T cell responses within PBMC, whereas natural processing and presentation of epitopes from live pH1N1 virus and inactivated vaccine strain virus by APC could stimulate CD4+ and CD8+ T cells within PBMC.

A prevalence of 58 - 75% response to antigens reported in Results section 3.2 is lower than the prevalence of 80 - 90% to the same antigens (core antigen peptide pool and live virus or inactivated vaccines) that we report in a different subset of individuals (n = 33) from the same study cohort (Sridhar *et al.*, 2012). While both populations were seronegative for pH1N1-specific antibodies by HAI assay and the same fluorescence-immunospot protocol was used, there are some differences that may have contributed to the discrepancy in prevalence of pre-existing response to core proteins between the two study populations. Firstly, the sample sizes were n = 76 in this thesis (**Results section 3.2**) and n = 33 in Sridhar *et al*. Secondly, different thresholds for cut-offs in IFN-γ/IL-2 fluorescence-immunospot were used to define responders in the two studies. At the time of publishing our first paper, thresholds for cut-offs equating to 2 standard deviations of the mean value of the background

response wells in 62 independent PBMC samples were used (Sridhar *et al.*, 2012). By completion of experimental work for this thesis, thresholds for cut-offs equating to 2 standard deviations of the mean value of the background fluorescence-immunospot response wells in 323 independent PBMC samples were generated (**Results section 3.1**). The thresholds from this significantly larger sample size were used consistently in all subsequent IFN-γ/IL-2 fluorescence-immunospot analysis and results presented in this thesis (**Results section 3.2 – 3.3**).

IAVs sH1N1 and sH3N2 have been circulating in the human population prior to the emergence of the novel pH1N1 (WHO, 2014a). Hence it would be expected that individuals previously exposed to these influenza strains pre-pandemic would exhibit T cell responses, and that these T cells cross-react with conserved antigens from the novel pH1N1. Indeed, there is 98%, 94% and 90% amino acid sequence similarity respectively in PB1 (Berthoud *et al.*, 2011), M1 and NP of pH1N1 compared to pre-pandemic circulating sH1N1 and 97%, 92% and 90% amino acid sequence similarity compared to pre-pandemic circulating sH3N2 (NCBI BLAST sequence analysis http://www.ncbi.nlm.nih.gov). Therefore, a high proportion of individuals naïve to pH1N1 would be expected to have T cells induced by prior exposure through infection with sH1N1 and sH3N2 that could cross-react with the novel pH1N1 (live virus). Since all the inactivated vaccines used contain core proteins from A/Puerto Rico/8/1934 (**Introduction section 1.1.6**), it would be expected that similar proportions of individuals would have T cells responding to the pH1N1, sH1N1 and sH3N2 inactivated vaccine viruses (**Results section 3.2**).

In a landmark paper by Sallusto *et al*. IFN-γ and IL-2 cytokine-secretion profiles of T cells were used to differentiate effector and memory T cells with distinct homing marker CCR7 expression (Sallusto *et al.*, 1999). Furthermore, Pantaleo and Harari have proposed a paradigm for different viral infection models based on antigen load and exposure reflected by distinct T cell cytokine signatures (Pantaleo & Harari, 2006). According to this paradigm, conditions of acute antigen exposure or uncontrolled chronic persistent infections such as HIV-1 are associated with a predominantly IFN-γ-secreting T cell signature; acute exposure with cleared antigens such as tetanus toxoid or influenza are associated with a predominantly IL-2-secreting T cell signature, and controlled persistent infections such as latent CMV or latent EBV are associated with single-IL-2, single IFN-γ and IL-2/IFN-γ polyfunctional cytokine-secreting T cells (Harari *et al.*, 2004, Harari *et al.*, 2005, Harari *et al.*, 2004).

Based on this model of influenza as an acute and cleared infection (Pantaleo & Harari, 2006), and that circulation of seasonal IAV in the UK had ceased by the end of February 2009 (WHO, 2014a), we hypothesised that there would be a predominantly IL-2-secreting signature of T cells cross-reactive with pH1N1 in individuals. Contrary to this hypothesis, there was a predominance in the frequency of IFN-γ+IL-2- T cells specific to pH1N1 measured by fluorescence-immunospot (**Results section 3.2**); a signature that has been associated with acute antigen exposure or uncontrolled chronic persistent infections (Pantaleo & Harari, 2006).

Interestingly, this predominance of single IFN-γ+ response to live pH1N1 virus was not observed by flow cytometry and boolean analysis in CD4+ or CD8+ T cell populations (**Results section 3.4**). Although *ex vivo* PBMC stimulation conditions were similar between the two assays (18 hours stimulation at 37°C, 5% CO_2), the observed difference could be due to inherent differences in the optimised protocols used in each assay to measure responses to live pH1N1 virus. This includes different MOI (1 in fluorescence-immunospot, 5 in flow cytometry); use of 0.5 μg/mL anti-CD28 co-stimulation in fluorescence-immunospot but no co-stimulation used in flow cytometry, and the detection of secreted cytokines in fluorescence-immunospot compared to staining of intra-cellular cytokines in flow cytometry. Thus comparability of the two assays is limited.

Nevertheless, the predominance of IFN-γ+IL-2- T cells to pH1N1 (core antigens, live virus and inactivated vaccine) and sH1N1 inactivated vaccine (and predominance of IFN-γ+IL-2- and IFN-γ+IL-2+ to sH3N2 inactivated vaccine) (**Results section 3.2**) appears real and not an artefact of the fluorescence-immunospot experimental system. Regardless of the mode of antigen stimulation, the dominance of IFN-γ+IL-2- pH1N1 cross-reactive or sH1N1-specific T cells was evident whether PBMC were stimulated with live virus to mimic natural processing of antigens, or inactivated virus strains to stimulate processing of recombinant antigens for the preferential recognition by CD4+ T cells. This finding is also consistent with the only other report assessing the polyfunctionality of pH1N1 cross-reactive CD8+ T cells showing predominance of single IFN-γ+ pH1N1-specific CD8+ T cells and little

polyfunctionality based on IFN-γ, IL-2 and TNF-α ICS (Scheible *et al.*, 2011). Furthermore, the possibility that fluorescence-immunospot biased our results by preferentially enumerating IFN-γ rather than IL-2 is unlikely given that a predominance of IFN-γ+IL-2+ dual-cytokine secreting T cells to *Mycobacterium tuberculosis* antigens was revealed using this assay in our laboratory (Casey *et al.*, 2010).

IFN-γ is secreted by antigen-specific T cells in PBMC upon recognition of antigen (Morris *et al.*, 1982) and T cell derived IFN-γ is important in the antiviral response to influenza with rapid activation (Lalvani *et al.*, 1997). Furthermore, in some animal models, IFN-γ has been demonstrated to mediate influenza viral clearance and protection against pathology (Seo *et al.*, 2002, Bot *et al.*, 1998, Karupiah *et al.*, 1998), although there are also conflicting reports (Nguyen *et al.*, 2000). In an IFN-γ knock out mouse model of influenza, IFN-γ was dispensible for cytotoxicity (mediated by *ex-vivo* CD4+ T cells in the lungs), but necessary for complete protection of challenged mice from weight loss (IFN-γ-/- mice showed ~70% survival following lethal influenza challenge which was significantly lower compared to wild type mice) (Brown *et al.*, 2012). Also, the majority of literature reports on T cell-mediated HSI in animal models and human studies have measured CD4+ or CD8+ T cell IFN-γ production as an effector mechanism (**Introduction Table 1.4.1**).

In contrast to influenza-specific CD8+ T cells, there are a small number of reports on the characterisation of influenza-specific CD4+ T cells, and of these the majority are described in mouse models with very few human studies. Lee *et al*. characterised M1-specific CD4+ T cell clones from human PBMC that were cross-reactive between H5N1 and sH3N2, demonstrating expression of IFN-γ, IL-2 and TNF-α by these cells upon peptide stimulation or recognition of target cells infected with recombinant vaccinia virus vectors expressing M1 of H5N1 (Lee *et al.*, 2008). Tetramer-guided epitope mapping and antigen-specific HLA-II tetramers were used to demonstrate H5N1 cross-reactive CD4+ T cells secreting IFN-γ, TNF-α, IL-5, and IL-13 (in culture supernatants) with a CD45RA- memory phenotype in PBMC from healthy Caucasian individuals naïve to H5N1 (Roti *et al.*, 2008). Interestingly, another study found that influenza viral lysate -specific CD4+ T cells were positive for IFN-γ, IL-2 and TNF-α (by ICS) but did not express CD107ab (Kannanganat *et al.*, 2007). Consistent with this, we found pH1N1-specific CD4+ T cells positive for IFN-γ, IL-2 and TNF-α and low frequencies of CD107ab+ cells within CD4+ cytokine+ T cells (**Results section 3.4**). The differences between pH1N1-specific CD4+ and CD8+ T cell responses, such as a hierarchy in the CD4+ T cell cytokine response but not in the CD8+ T cell cytokine response to pH1N1 (**Results section 3.4**) may reflect differences in development of memory of the two different subsets (Seder & Ahmed, 2003).

We noted differences in the cytokine expression profiles between pH1N1 virus cross-reactive and CMV lysate-specific CD4+ T cells. Particularly with respect to a hierarchy of response and a predominant single TNF-α+ response among cytokine

positive pH1N1 virus cross-reactive CD4+ T cells, but a lack of hierarchy and more dual (IFN-γ+TNF-α+) in the CMV-specific CD4+ T cell response (**Results section 3.4**). This is somewhat consistent with the paradigm proposed by Pantaleo and Harari in which distinct T cell cytokine signatures reflect different viral infection models based on antigen load and exposure (Harari *et al.*, 2004, Harari *et al.*, 2005, Harari *et al.*, 2004). However, we also observe a predominance of single TNF-α+ cells within live pH1N1 virus cross-reactive CD4+ T cells (**Results section 3.4**). A recent study characterising human CD4+ T cells to peptide pools from pH1N1 (A/California/04/09) demonstrated a higher proportion of IFN-γ-IL-2+TNF-α+ CD4+ T cells (termed non-polarized, primed precursor T cells (Thpp)) against non-conserved peptides compared to peptide pools containing conserved peptides that induced more IFN-γ+TNF-α+ CD4+ T cells (Weaver *et al.*, 2013). Hence it may be that our results reflect Thpp-like CD4+ T cells (with or without IL-2) against non-conserved antigens in live pH1N1. An alternative explanation is our detection and characterisation of different antigen-specific subpopulations within a heterogeneous CD4+ T cell population when using whole live virus compared to CMV viral lysate.

Our phenotypic characterisation of cytokine-secreting influenza cross-reactive CD8+ T cells by flow cytometry showed that they are predominantly comprised of CD45RA+CCR7- Temra and CD45RA-CCR7- Tem (**Results section 3.4**), consistent with some reports (Tu *et al.*, 2010, Greenbaum *et al.*, 2009) but in contrast to others reporting a predominance of Tcm cells (Lee *et al.*, 2008). Existing literature report circulating, low frequency (< 1% of total CD8+ T cells) influenza-

peptide (M1 immunodominant HLA-A2 restricted) -specific CD8+ of Tem, Temra or Tcm (defined by CD45RA/CCR7 expression) phenotype that are detectable in human PBMC (Zimmerli *et al.*, 2005, Hoji & Rinaldo, 2005, Almanzar *et al.*, 2007, Touvrey *et al.*, 2009). Cytokine-positive influenza viral lysate -specific (Kannanganat *et al.*, 2007) or HA-peptide tetramer-specific (Lucas *et al.*, 2004) CD4+ T cells were predominantly Tcm cells. In contrast to this, we found that live pH1N1 virus cross-reactive CD4+ cytokine positive T cells were predominantly Tem and Temra (**Results section 3.4**). This difference may be due to detection and characterisation of different antigen-specific subpopulations within a heterogeneous CD4+ T cell population when using influenza viral lysate, peptide-tetramer complexes or whole live virus.

M1 epitope-specific tetramer positive CD8+ T cells in influenza asymptomatic or non-acutely infected individuals were a heterogenous population of cells containing both immature (CD27+ CD28+ CD62L+ HLA-DR-) primed memory T cells (CD45RA-), and cells expressing moderate levels of the terminal differentiation marker CD94, granzyme A/B, perforin, and CCR5 and CXCR3 associated with a more mature, effector memory phenotype (Hoji & Rinaldo, 2005, Almanzar *et al.*, 2007) and express the degranulation marker CD107 indicating cytotoxic potential (Makedonas *et al.*, 2010). Consistently, our analysis revealed that about half of pH1N1-cross-reactive CD8+ cytokine+ T cells (specifically CD8+IFN-γ+ T cells) were positive for CD107ab (**Results section 3.4**). A lower proportion (medians of 5 – 25%) of pH1N1-cross-reactive CD4+ cytokine+ T cells were also positive for CD107ab (**Results**

section 3.4), consistent with other recent reports (Wilkinson *et al.*, 2012) and suggesting a direct antiviral effect from cytotoxic CD4+ T cells that have been reported in chronic viral infections (Appay *et al.*, 2002).

CD57 was used as a marker of replicative senescence, as used by Akondy *et al*. characterising Yellow-Fever virus vaccine-induced CD8+ T cell responses, importantly showing that CD45RA+CCR7- Temra cells proliferated to antigen stimulation, and lacked CD57 expression, hence CD45RA+CCR7- Temra cells may not necessarily be terminally differentiated (Akondy *et al.*, 2009). Notably, low proportions (medians < 20%) of pH1N1-cross-reactive cytokine positive CD4+ and CD8+ T cells were CD57 positive (**Results section 3.4**), indicating low replicative senescence. This could hint at a mechanism of maintenance of these pH1N1 cross-reactive T cells *in vivo*.

In mouse models, the chemokine receptor CCR5 has been shown to be important in directing CD8+ T cells to the lungs of mice infected with Sendai virus (Kohlmeier *et al.*, 2008). Mice deficient in CCR5 also showed increased mortality following influenza infection (Dawson *et al.*, 2000, Fadel *et al.*, 2008). Furthermore, an increased allele frequency for the CCR5Δ32 polymorphism was observed among individuals with confirmed severe pH1N1 infection who suffered respiratory failure and required admission to intensive care (Keynan *et al.*, 2010). Hence, we assessed the expression of CCR5 on pH1N1-specific T cells as a marker of tissue homing to

sites of inflammation, and found high inter-individual heterogeneity but a median of up to 50% of pH1N1 cross-reactive, cytokine-secreting CD4+ and CD8+ T cells were positive for CCR5 (**Results section 3.4**), indicating homing potential to inflammation in lungs upon influenza infection.

CD69, an early activation marker that is up-regulated on activated T cells following antigenic stimulation (Marzio *et al.*, 1999) was expressed by our cytokine-positive antigen-specific cells. It is interesting that CD69 expression did not correlate completely with antigen-specific cytokine positive CD4+ or CD8+ T cells. Among CD4+ and CD8+ cytokine positive T cells, IFN-γ+ cells showed highest proportions of CD69 expressing cells compared to IL-2+ or TNF-α+ T cells; up to half of live pH1N1 virus cross-reactive CD4+IFN-γ+ T cells, and up to 20% median proportions of live pH1N1 virus cross-reactive CD8+IFN-γ+ T cells were positive for CD69 (**Results section 3.4**). The lack of complete correlation between early activation marker CD69-positive and cytokine-positive cells may be due to staining and detection of cell surface CD69 expression compared to intracellular cytokine accumulation.

We selected a flow cytometric data analysis strategy to gate on markers including CD69 within the functionally defined, antigen stimulated cytokine positive CD4+ or CD8+ T cells. Our approach is different to some other published flow cytometry analysis strategies (Karanikas *et al.*, 2000) that gate on bulk CD4+ or CD8+ T cells that are activated (CD69+) followed by gating on cytokine positive cells. Our gating

strategy was selected to enable consistency in analysis of antigen-specific data, since CMV lysate-specific CD69 expression on bulk CD4+ or CD8+ T cells was not consistently detectable in our cohort (**Results section 3.4**). The reason for this is unknown, but due to limited sample availability, we did not perform serological tests to detect anti-CMV antibodies for identification of CMV seropositivity in this cohort of healthy individuals. Hence CMV seronegativity accounting for low CMV lysate-specific activation (CD69+) measured by flow cytometry cannot be ruled out. However, this seems unlikely given that CMV lysate-specific cytokine positive T cells in the same cohort were detectable both by fluorescence-immunospot (**Results section 3.2**) and flow cytometry (**Results section 3.4**), and a previous study found concordant results between CMV seropositivity and CMV-specific CD4+IFN-γ+ T cells in a large cohort of individuals (Sester *et al.*, 2003). Furthermore, it is estimated that approximately 50 – 60 % of adults in the UK are CMV seropositive (Potter et al., 2012, Ling *et al.*, 2003).

The circulating pH1N1 cross-reactive T cells we detected in healthy pH1N1 naïve individuals display the potential to traffic to the lungs during the inflammatory response following influenza infection (CCR5+), display an activated, antigen-experienced phenotype (Tem and Temra) with low replicative senescence (CD57), undergo rapid degranulation (CD107ab+) and secrete cytokines (IFN-γ+, IL-2+, TNF-α+) upon encounter with pH1N1-infected host cells. These attributes suggest a pre-existing, circulating population of CD4+ and CD8+ T cells with a role in local viral

containment or clearance and limiting the severity of symptoms following influenza infection.

4.3 Cellular correlate of protection against symptomatic influenza

During an influenza pandemic in which susceptible individuals lack protective neutralising antibodies, the most favourable outcome of infection is symptom-free, or a reduced severity of illness. The 2009 H1N1 pandemic presented the opportunity to prospectively identify a cellular immune correlate of protection against illness caused by natural influenza infection with an antigenic shift variant reassortant virus, in a population seronegative to pH1N1 by HAI assay.

Using the optimised fluorescence-immunospot assay (**Results section 3.1**), a predominance of IFN-γ+IL-2- pH1N1 cross-reactive T cells were detectable in PBMC from healthy, pH1N1 naïve individuals (**Results section 3.2**). Further flow cytometry analyses revealed a phenotype consistent with mediating some level of protection upon influenza infection (**Results section 3.4**). In mouse models, T cell-mediated HSI does not prevent infection and thereby does not provide sterilising immunity (Yap & Ada, 1978). Consistent with this, pre-existing T cells were not associated with risk of subsequent pH1N1 infection in our cohort (**Results section 3.3**). However, a higher frequency of pre-existing pH1N1 CD8 conserved epitope -specific T cells were associated with decreased risk of fever, fewer ILI symptoms and reduced illness severity score in pH1N1 infected individuals (**Results section 3.3**). High rates

of infection, associated with low prevalence of pH1N1 cross-reactive antibodies, but low case-fatality in < 45 year old adults during the 2009 H1N1 pandemic was suggestive of protective HSI against severe disease in this age group (Hardelid *et al.*, 2010). Our findings of the high prevalence of pH1N1 cross-reactive T cells in healthy adults (**Results section 3.2**), within which the CD8+IFN-γ+IL-2-CD45RA+CCR7- late effector T cells were correlated with protection against community-acquired pH1N1 influenza illness (**Results section 3.3**), leads to the postulation that T cell-mediated HSI may have in part accounted for the mild clinical illness observed in young adults during the 2009 pandemic. It is possible that the epidemiological observations of the 2009 H1N1 pandemic may have been due to a less pathogenic pandemic influenza strain (Arias *et al.*, 2009), lower co-morbidities and/or host genetic factors (Keynan *et al.*, 2013). However, evidence of pre-existing T cells limiting illness severity from a recent human experimental influenza challenge study (Wilkinson *et al.*, 2012) is consistent with the notion of T cell-mediated HSI, and we have further demonstrated this during a natural influenza pandemic (**Results section 3.3**).

It is worth pointing out that the data presented in Results section 3.3 has been published (Sridhar *et al.*, 2013), but the analysis of IFN-γ/IL-2 fluorescence-immunospot responses are different as explained previously for Results section 3.2 (see Discussion section 4.2). Despite the use of thresholds for cut-offs in the re-analysed data for Results section 3.3 compared to the published report (Sridhar *et al.*, 2013), the quantitative CD8+ T cell correlate of protection against symptom score

was statistically consistent. Similarly, control CMV antigen responses in the re-analysed data were not associated with illness severity.

Our data is consistent with challenge studies in many animal models (**Introduction Table 1.4.1**) including mice, but also ferrets and nonhuman primates that more closely model human influenza infection physiologically and immunologically. However our data contradicts Wilkinson *et al*. on the subset of T cells associated with diminution of clinical symptoms in humans. Wilkinson *et al*. reported homosubtypic (against seasonal circulating sH1N1 and sH3N2) IFN-γ+ CD4+ but not CD8+ T cells inversely associated with illness severity in the experimental challenge model using direct nasal inoculation of a high-dose, less virulent, serially passaged laboratory adapted live virus strain (Wilkinson *et al.*, 2012). We demonstrate an association of heterosubtypic CD8+IFN-γ+IL-2-CD45RA+CCR7- but not CD4+ T cells in a community exposure setting of naturally acquired infection with mild to moderate illness during a pandemic (**Results section 3.3**). Hence the protective correlate differs in the two markedly different settings – one of natural infection following human-to-human transmission, and the other of high-dose artificial challenge experiment. This inherent difference in infection setting may be one of the reasons for the difference in the subset of T cells associated with asymptomatic infection identified by the two studies. We believe that our ability to exploit a setting of natural infection has significant advantage over an artificial high-dose challenge experiment in identifying a T cell correlate of protection relevant to natural infection.

Experiments in a mouse model of respiratory viral infection (parainfluenza virus) have demonstrated the importance of circulating effector memory (CD62L-low) CD8+ T cells in recall responses in the lung following secondary infection (Roberts & Woodland, 2004). Protection against and control of other intracellular pathogens have been associated with effector memory T cells (Hansen *et al.*, 2009, Puissant-Lubrano *et al.*, 2010). Importantly, in a mouse model of lethal pulmonary influenza infection, adoptively transferred influenza-specific IFN-γ producing CD8+ effector T cell clones promoted lung viral clearance and survival, whereas equal numbers of their naïve counterparts could not protect against disease (Cerwenka *et al.*, 1999). While there exist contrasting reports on the protective capacity of Tcm versus effector and Tem subsets in different pathogen infection mouse models (Wherry *et al.*, 2003, Roberts & Woodland, 2004, Bachmann *et al.*, 2005, Olson *et al.*, 2013), there have been no reports of the protective capacity of Temra in infectious diseases. To our knowledge, we are the first to report a CD8+ Temra subset correlating with protection against symptomatic influenza infection in humans (**Results section 3.3**).

The late effector CD8+IFN-γ+IL-2- Temra cell correlate of protection against symptomatic influenza that we have identified might in part mitigate the clinical severity of anticipated pandemics such as the highly pathogenic H5N1 influenza (Gambotto *et al.*, 2008), since a large proportion of healthy, H5N1 naïve individuals have detectable T cell responses to H5N1 core proteins (Lee *et al.*, 2008, Roti *et al.*, 2008, Jameson *et al.*, 1999, Kreijtz *et al.*, 2008). However, the difference in virulence

of pandemic strains may also circumvent T cell-mediated protection. The protection-associated T cells could also provide protection against re-exposure to annually circulating seasonal influenza strains. Influenza cross-reactive T cells are more likely to recognise influenza drift variants that are estimated to arise every 2 – 3 years (Smith *et al.*, 2004). Humoral immunity is evaded by such heterologous drifted strains; hence T cell-mediated immunity could limit illness severity and symptoms caused by seasonal influenza.

4.4 Durability of influenza-specific memory T cells in natural infection

We identify durable protection-associated pH1N1-specific CD8+IFN-γ+ late effector Temra cells in naturally infected individuals longitudinally followed for up to 1.5 years post-infection (**Results section 3.5, Fig. 3.5.7A**). Importantly, this durability was detected in the absence of re-infection in our cohort, implying true maintenance of late effector cells. This finding is unexpected given the existing literature on the longevity of this subset of T cells in other infection models. Hantavirus-specific CD8+tetramer+Temra were detectable *ex vivo* up to 13 years post-infection, but this was documented from 3 individuals and in an endemic area where re-infection was a possibility (Manigold *et al.*, 2010). A study on CMV-specific CD4+ T cells showed stable maintenance over 1.2 – 2.3 years documented from only 8 individuals, and in a subset of these individuals, the CMV-specific CD4+ T cells were shown to have a Temra phenotype (Sester *et al.*, 2002). Similarly, EBV-specific CD8+ T cells with Temra phenotype were maintained to at least 1 yr after infectious mononucleosis across 12 individuals (Dunne *et al.*, 2002).

Taken together, these studies give plausibility to the maintenance of Temra in the case of chronic or latent infection (CMV and EBV) or re-exposure to an acute infection in an endemic setting (Hantavirus). It is important to note that in these reports (Manigold *et al.*, 2010, Sester *et al.*, 2002, Dunne *et al.*, 2002) there are no pre-infection time-points for comparison and the apparent durability is demonstrated in cross-sectional times across different individuals. Hence the careful study of the kinetics of the response from pre-infection through longitudinal follow-up is unique to our study. Although re-exposure to pH1N1 in a community setting cannot be chategorically ruled out, none of the infected individuals had evidence of re-infection by paired serology during the influenza seasons in the study period. Hence our finding of the maintenance of pH1N1-specific CD8+ Temra following pH1N1 infection (**Results section 3.5**) is notable.

Pre-existing, durable protective T cells may partly explain evidence of HSI and the durability of protection against symptomatic influenza during influenza pandemics inferred from epidemiological studies (Slepushkin, 1959, Epstein, 2006, Sonoguchi *et al.*, 1985, Cowling *et al.*, 2010). In the Cleveland family study, adults infected with seasonal H1N1 in the period 1950 – 1957 were less likely to be symptomatically infected 4 – 6 years later with H2N2 in the 1957 pandemic (OR: 0.294, 95% CI: 0.01 – 3.07), although the non-significant effect was attributed to a small sample size (n = 18) (Epstein, 2006). During the same pandemic, another study showed that Russian factory workers reporting symptomatic ILI during seasonal H1N1 in the spring of

1957 were less likely to be symptomatic 2 – 3 months later in the summer 1957 H2N2 pandemic (OR: 0.418, 95% CI: 0.304 – 0.575) (Slepushkin, 1959). This protection to H2N2 was maintained (albeit at a reduced level compared to the spring outbreak) by 6 – 7 months later in the autumn of 1957 (OR: 0.625, 95% CI: 0.530 – 0.737) (Slepushkin, 1959). In another study, Japanese schoolchildren infected with H3N2 were less likely to be infected days to weeks (from 23 days – 18 weeks) later with H1N1 re-emergence in 1977 – 1978, with differences in risk between high school children (OR: 0.059, 95% CI: 0.019 – 0.131) and primary school children (OR: 0.154, 95% CI: 0.076 – 0.309) attributed to increasing prior exposure to seasonal influenza strains with age (Sonoguchi *et al.*, 1985). Finally, during the recent 2009 H1N1 pandemic, children infected with seasonal influenza 6 – 11 months prior were less likely to have laboratory-confirmed pH1N1 in the following season (OR: 0.35, 95% CI: 0.14-0.87) (Cowling *et al.*, 2010).

It is interesting that there is an increase in OR for symptomatic infection during a pandemic with increasing time since exposure or infection with a pre-pandemic seasonal influenza strain (compare ORs in Sonoguchi *et al*., 1985 to Slepushkin *et al*., 1959, Cowling *et al*., 2010 and Epstein, 2006). There are obvious limitations in the direct comparison across these studies including differences in age groups, different geographical locations and ethnicities and differences in viral pandemic strains. Nevertheless the data is suggestive of increasing risk of symptomatic infection with time since previous documented infection as has been noted by others (Couch & Kasel, 1983, Mathews *et al.*, 2010), implying that components of HSI to

influenza can wane over the time-scales reported across these studies. Our data shows that the frequency of protection-associated CD8+ T cells to influenza are maintained from 6 months to up to 1.5 years post-infection in pH1N1 naturally infected individuals (**Results section 3.5**). In 21 of these individuals, the exact date of infection could be ascertained and this showed that there was a median of 96 days (range 55 – 155 days) between infection and the first time-point measure post-infection. The second and third time-points post-infection were medians of 316.5 days and 483.5 days post-infection respectively, ascertained from 8 individuals. If we postulate that the decline in strength of protection over time observed in the previous epidemiological studies is due to a decline in influenza-specific CD8+ T cells mediating symptomatic protection, then the highest protection (lowest risk of symptomatic infection) is evident early post-infection (range of 23 - 126 days in Sonoguchi *et al*., 1985). Protection declines later post-infection (by 2 – 3 months in Slepushkin *et al*., 1959) and is followed by maintenance (at 6 – 7 months in Slepushkin *et al*., 1959, 4 – 6 years in Epstein, 2006 and 6 – 11 months in Cowling *et al*., 2010). Hence our data on the kinetics of the influenza-specific T cell response post natural influenza infection is consistent with the later maintenance in the strength of protection over the time-scales observed in epidemiological studies of HSI.

Other studies in humans have reported induction of influenza-specific CD8+ T cells post-infection (Hillaire *et al.*, 2011b, McMichael *et al.*, 1983a), although to date there has been only 1 report of durability of pH1N1-specific CD4+ and CD8+ T cell

responses in a single naturally infected individual followed longitudinally (Wagar *et al.*, 2011). These studies have suggested an overall decline in influenza-specific T cell responses over the time periods of 2 – 43 days (Hillaire *et al.*, 2011b) or up to 700 days (Wagar *et al.*, 2011) post symptom onset. The decline in HLA -restricted CTL responses to influenza during the 6-year study period in McMichael *et al*. was attributed to a reduced influenza activity in the study region time period (McMichael *et al.*, 1983a). Our data (**Results section 3.5**) is the first to show durability of a protection-associated CD8+ T cell subset in a larger cohort of up to 45 naturally infected individuals longitudinally followed from pre-infection for up to 1.5 years.

Importantly, we did not detect significant alterations in any other cytokine-secreting CD4+ or CD8+ T cell subsets, except a decrease in frequency of total IL-2+ and single IL-2+ antigen-specific CD4+ and CD8+ T cells post pH1N1 infection (**Results section 3.5**). While this was unexpected, the effect was apparent for both pH1N1-specific and CMV lysate-specific T cells. To our knowledge, this decrease in antigen-specific T cell IL-2 responses was not due to technical aspects of the flow cytometry assay since longitudinal samples from individuals were processed in batch and the same flow cytometer settings were used across all experiments to minimise intra-assay variability in longitudinal results on an individual basis. Furthermore, we did not use co-stimulation in our stimulation protocol although it is frequently used in flow cytometry and ICS for increasing sensitivity of the assay to detect low frequency *ex vivo* responses (Lamoreaux *et al.*, 2006). In fluorescence-immunospot we did detect a weaker correlation of antigen-specific total IL-2+ PBMC responses in

cryopreserved-thawed PBMC compared to fresh PBMC which was not the same in the case of antigen-specific total IFN-γ+ PBMC responses (**Results section 3.1**). Therefore the decrease in frequency of total IL-2+ and single IL-2+ antigen-specific CD4+ and CD8+ T cells detected by flow cytometry from cryopreserved-thawed PBMC (**Results section 3.5**) may reflect the selective negative effect of cryopreservation (independent of time of cryopreservation) on IL-2 responses.

Since pH1N1-specific CD4+IFN-γ+ and CD8+IFN-γ+ T cell responses were significantly increased post natural pH1N1 infection (**Results section 3.5**), we explored the relationship between the increase in total- or single- IFN-γ+ CD4+ and CD8+ T cell responses post-infection with pre-infection frequencies. We found inverse correlations between post-infection rise in IFN-γ+ and pre-infection IFN-γ+ in both CD4+ and CD8+ T cells specific to pH1N1 (**Results section 3.5**). The post-infection rise in CD4+IFN-γ+ T cells was also inversely correlated with pre-infection CD4+ TNF-α+ T cells. Consistently, inverse correlations of pre-vaccination CD4+IFN-γ+ and CD8+IFN-γ+ T cells with post-vaccination CD4+IFN-γ+ and CD8+IFN-γ+ respectively been reported following influenza vaccination with TIV and LAIV (He *et al.*, 2006, Co *et al.*, 2008, He *et al.*, 2008, Chirkova *et al.*, 2011). Together, these data suggest that frequencies of influenza-specific CD4+ and CD8+ T cells existing prior to infection or vaccination affects the ability of infection or vaccination to significantly increase responses post- infection or vaccination respectively. This inverse relationship may be as a result of pre-exposure influenza-

specific T cells rapidly eliminating influenza-containing APCs, thereby limiting T cell expansion post-exposure (Co *et al.*, 2008).

4.5 Implications of our findings for influenza vaccination

In a small subset of individuals from our cohort that were vaccinated with the pH1N1 vaccine during the study period, vaccination with or without seroconversion did not significantly alter the frequency of pH1N1-specific CD4+ or CD8+ cytokine-secreting T cells (**Results section 3.5**). Notably, seasonal influenza vaccination received > 6 months prior did not affect the frequency or cytokine-secreting profile of pre-existing pH1N1 cross-reactive T cells (**Results section 3.2** and Sridhar *et al*., 2012). Previous studies report increases in the frequency of core antigen epitope-specific CD8+ T cells detectable 1 month after seasonal influenza vaccination in humans (Tu *et al.*, 2010, Terajima *et al.*, 2008). However, reports in animal models suggest that inactivated seasonal influenza vaccination may hamper the development of HSI (Bodewes *et al.*, 2011b, Bodewes *et al.*, 2010). This effect is also reported in children aged 2 – 9 years old where influenza-specific CD8+ T cell responses were detectable in unvaccinated children, but the age-dependent increase in influenza-specific CD8+ T cells was not detected in children vaccinated every year with seasonal influenza vaccines from age 4 onwards (Bodewes *et al.*, 2011c).

In conjunction with the existing literature, our data (**Results sections 3.2 and 3.5**) suggest that influenza infection is able to maintain influenza cross-reactive T cell

responses, in contrast to vaccination with inactivated seasonal influenza. Additionally, the durable maintenance of a protection-associated CD8+ T cell subset in naturally infected individuals suggests that successful T cell-based influenza vaccines may need to boost and maintain responses similar to natural infection to afford protection against illness severity with influenza. However, a larger sample size would be required to confirm this difference between infection and vaccination maintaining frequencies of pH1N1-specific T cells.

The strongest association with limiting illness severity was with summed T cell responses to conserved CD8 T cell epitopes from core proteins PB1, M1 and NP (**Results section 3.3**). Hence in the absence of detectable cross-reactive neutralising antibodies, CD8+ HLA class I- restricted T cells specific for epitopes conserved across IAV subtypes may confer broad protection against illness severity following infection with IAVs. Our findings provide an immunological surrogate of protection (that is durable CD8+IFN-γ+IL-2- T cell responses), and target antigen epitopes (based on the 91 highly conserved CD8 T cell epitopes from PB1, M1 and NP) for the development and evaluation of broadly protective universal influenza vaccines conferring protection against illness caused by viruses evading humoral immunity. Furthermore, the frequency of CD8+IFN-γ+IL-2- T cells could be used as a biomarker for risk stratification of individuals most likely to become symptomatic in the event of pandemics, and thus would inform vaccination strategies to prioritise populations most at-risk of increased illness severity with influenza.

4.6 Study limitations

Our longitudinal cohort study conducted during a rapidly evolving pandemic in real time has limitations inherent to such research settings. Research ethics approval was obtained after the first wave of pH1N1 in the UK (April – August 2009) had occurred hence recruitment of individuals was commenced prior to the second wave (September – November 2009), and individuals were followed through the second (September 2009 - April 2010) and third waves of the pandemic (August 2010 – April 2011). Serum and PBMC isolated from whole blood collected at each study time-point were bio-banked, hence cryopreserved PBMC were used in all immunological assays. While at least 30 x 10^6 PBMC were stored for each individual, variable loss of viable cell quantity through cryopreservation and thawing limited the number of assays that could be used to characterise immunological responses. Further epitope mapping of T cell responses identified to conserved peptides from core antigens PB1, M1, NP could not be performed due to this limitation of sample availability.

We excluded individuals reporting multiple ILI episodes (analysis in Results section 3.3); hence the use of stringent criteria to reliably identify distinct clinical outcomes in the community-based study setting reduced the sample size for individuals with incident influenza infection. Furthermore, not all individuals recruited remained to follow-up time-points 1, 2 and 3, therefore further diminishing sample sizes available for longitudinal analysis. The community-based nature of the study resulted in a cohort in which the majority of infected individuals had mild to moderate illness, representing only part of the full clinical spectrum of influenza disease severity.

Hence the use of our identified CD8+IFN-γ+IL-2- late effector T cells as a surrogate of protection in clinical trials of new universal influenza vaccines will need to be in combination with robust clinical endpoints including protection from severe illness.

Although the findings in this healthy adult cohort of staff and students at Imperial College London may be generalisable to other healthy adult populations with similar demography, the results cannot be directly extrapolated to individuals at high risk of severe illness caused by pandemic H1N1. Hence future studies could assess the protection-associated T cell subset in other populations including young children, pregnant women, the elderly and HIV-1 infected patients and other immunocompromised individuals. The protective correlate against severe illness and fatal disease may be different in high-risk individuals, although some level of protective effect of T cells might be expected in such cases.

Our study was designed to specifically address the role of CD8+ T cells in HSI using conserved CD8 T cell epitopes stimulating CD8+ T cell responses by fluorescence-immunospot. Longer peptides optimal for processing and presentation of CD4 epitopes were not used; hence we cannot exclude the possibility of correlation of CD4+ T cells with illness severity. HAI and microneutralisation assays were used to select individuals lacking cross-reactive neutralising antibodies to the HA1 head region and HA2 stem regions of pH1N1 virus HA respectively, thereby excluding the contribution of these demonstrated in other studies to limit disease (Wrammert *et al.*,

2011). Antibodies directed to other viral proteins including NA (Couch *et al.*, 1974) and M2 ectodomain (Grandea *et al.*, 2010) have been shown to have a protective effect. An age-dependent increasing prevalence of non-neutralising serum antibodies inducing antibody-dependent cellular cytotoxicity toward pH1N1 virus has also been reported (Jegaskanda *et al.*, 2013a), with protective HSI demonstrated in macaques (Jegaskanda *et al.*, 2013b). These antibodies are not detected by the standard assays used in our study, and it is conceivable that such antibodies in conjunction with cellular immunity may have a role in limiting illness severity following influenza infection. Similarly, mucosal responses in human experimental challenge (Hayden *et al.*, 1998), or systemic innate immune responses in human infection (Everitt *et al.*, 2012) studies, that have been shown to protect against severe disease were not measured in our study.

4.7 Future work

Future work could address some of the limitations outlined above, but the challenge in studying HSI to natural influenza infection in humans is the requirement for occurrence of a influenza pandemic in which a novel antigenically shifted virus is introduced. Fluorescence-immunospot was selected due to the high sensitivity of this assay to detect low frequency, cytokine-secreting antigen-specific responses that would be expected for pH1N1 cross-reactive T cells in healthy individuals naïve to pH1N1. To minimise the effect of inter-assay variation, cryopreserved PBMC samples from different study time-points available for each individual were processed in batch in both fluorescence-immunospot and flow cytometry. Inter-assay

CV determined for fluorescenece-immunospot was low (**Results section 3.1**), hence future cohort studies of a similar design could consider processing of PBMC in real time to optimise sample availability and minimise the effects of cryopreservation on assay results (**Results section 3.1**).

The size of our recruited cohort was based on a power calculation to detect differences between symptomatic and asymptomatic infected individuals to address the role of pre-existing cross-reactive CD8+ T cells (**Material and methods section 2.2**). Hence we were only able to assess the effect of influenza vaccination due to incidental vaccination in a small subset of our cohort. Future longitudinal studies following individuals post-vaccination and comparing cross-reactive T cell responses pre- and post- vaccination would enable comprehensive assessment of the effect of vaccination on heterosubtypic immune mediators. More immediate future work planned in our laboratory involves determining whether the vaccination programme with LAIV which is being rolled out nationally, starting in autumn 2014 in the UK, can induce HSI against new influenza strains, and if so, whether and to what extent our identified T cell correlate mediates this immunity.

Our study cohort captured mild to moderate illness in a community-acquired infection setting among young adults only. An increasing cumulative life-time exposure to influenza is expected with increasing age, hence it will be interesting to test the hypothesis that the frequency of heterosubtypic T cells increases with age in a study population including young children, young adult and older adult age groups. It will

also be important to test whether the protective T cell correlate against mild to moderate illness is also associated with protection against severe illness. We have demonstrated a cellular correlate of protection against symptomatic influenza illness in the accessible peripheral blood compartment. However, the primary mediator of protection against influenza illness severity may be local rather than systemic, and could be a different cell population, as suggested by murine work (Wu *et al.*, 2014). Furthermore, another study has reported high frequencies of circulating NP- and M1-specific CD4+IFN-γ+ T cells in pH1N1 infected hospitalised patients within 48 hours of symptom onset correlating with severe disease outcomes (Zhao *et al.*, 2012). Hence it will be important to assess the temporal and anatomical relationship between our identified cellular correlate of protection to that observed at the sites of infection in the respiratory tract (URT and/or LRT); the relationship and relative contributions of systemic versus local cellular mediators of protection, and how these develop longitudinally following antigen exposure in humans.

4.8 Summary

In conclusion, using an optimised fluorescence-immunospot assay (**Results section 3.1**), our data identify cross-reactive T cells pre-existing in naïve individuals that recognise and respond to novel pH1N1 virus *ex vivo* (**Results section 3.2** and Sridhar *et al*., 2012). Through detailed phenotypic characterisation (**Results section 3.4**), we demonstrate that pre-existing CD8+IFN-γ+IL-2- Temra (CD45RA+CCR7-) cells limit disease severity following incident pH1N1 infection in the absence of protective strain-specific antibodies (**Results section 3.3** and Sridhar *et al*., 2013).

Furthermore, we show that this protection-associated T cell subset is durably maintained in the absence of re-infection up to 1.5 years post infection, and that pre-exposure frequencies of pH1N1-specific T cells may impact the post-infection pH1N1-specific T cell frequencies (**Results section 3.5**). These findings may have important implications in the development and evaluation of new influenza vaccines.

5 REFERENCES

Abelin, A., Colegate, T., Gardner, S., Hehme, N. & Palache, A. (2011) Lessons from pandemic influenza A(H1N1): the research-based vaccine industry's perspective. *Vaccine* **29(6)** 1135-1138.

Akondy, R.S., Monson, N.D., Miller, J.D., Edupuganti, S., Teuwen, D., Wu, H., Quyyumi, F., Garg, S., Altman, J.D., Del Rio, C., Keyserling, H.L., Ploss, A., Rice, C.M., Orenstein, W.A., Mulligan, M.J. & Ahmed, R. (2009) The Yellow Fever Virus Vaccine Induces a Broad and Polyfunctional Human Memory CD8+ T Cell Response. *The Journal of Immunology* **183(12)** 7919-7930.

Almanzar, G., Herndler-Brandstetter, D., Chaparro, S.V., Jenewein, B., Keller, M. & Grubeck-Loebenstein, B. (2007) Immunodominant peptides from conserved influenza proteins--a tool for more efficient vaccination in the elderly? *Wiener Medizinische Wochenschrift (1946)* **157(5-6)** 116-121.

Appay, V., Zaunders, J.J., Papagno, L., Sutton, J., Jaramillo, A., Waters, A., Easterbrook, P., Grey, P., Smith, D., McMichael, A.J., Cooper, D.A., Rowland-Jones, S.L. & Kelleher, A.D. (2002) Characterization of CD4(+) CTLs ex vivo. *Journal of Immunology (Baltimore, Md.: 1950)* **168(11)** 5954-5958.

Arias, C.F., Escalera-Zamudio, M., Soto-Del Rio Mde, L., Cobian-Guemes, A.G., Isa, P. & Lopez, S. (2009) Molecular anatomy of 2009 influenza virus A (H1N1). *Archives of Medical Research* **40(8)** 643-654.

Askonas, B.A., Taylor, P.M. & Esquivel, F. (1988) Cytotoxic T cells in influenza infection. *Annals of the New York Academy of Sciences* **532** 230-237.

Atsmon, J., Kate-Ilovitz, E., Shaikevich, D., Singer, Y., Volokhov, I., Haim, K.Y. & Ben-Yedidia, T. (2012) Safety and immunogenicity of multimeric-001--a novel universal influenza vaccine. *Journal of Clinical Immunology* **32(3)** 595-603.

Avetisyan, G., Ragnavolgyi, E., Toth, G.T., Hassan, M. & Ljungman, P. (2005) Cell-mediated immune responses to influenza vaccination in healthy volunteers and allogeneic stem cell transplant recipients. *Bone Marrow Transplantation* **36(5)** 411-415.

Bachmann, M.F., Wolint, P., Schwarz, K., Jager, P. & Oxenius, A. (2005) Functional properties and lineage relationship of CD8+ T cell subsets identified by expression of IL-7 receptor alpha and CD62L. *Journal of Immunology (Baltimore, Md.: 1950)* **175(7)** 4686-4696.

Behrens, G. & Stoll, M. (2006) Pathogenesis and Immunology. In: Kamps, B. S., Hoffmann, C. & Preiser, W. (eds.) *Influenza Report.* 1st edition. Flying publisher, pp. 92-105.

Benton, K.A., Misplon, J.A., Lo, C.Y., Brutkiewicz, R.R., Prasad, S.A. & Epstein, S.L. (2001) Heterosubtypic immunity to influenza A virus in mice lacking IgA, all Ig, NKT cells, or gamma delta T cells. *Journal of Immunology (Baltimore, Md.: 1950)* **166(12)** 7437-7445.

Berthoud, T.K., Hamill, M., Lillie, P.J., Hwenda, L., Collins, K.A., Ewer, K.J., Milicic, A., Poyntz, H.C., Lambe, T., Fletcher, H.A., Hill, A.V. & Gilbert, S.C. (2011) Potent CD8+ T-cell immunogenicity in humans of a novel heterosubtypic influenza A vaccine, MVA-NP+M1. *Clinical Infectious Diseases : An Official Publication of the Infectious Diseases Society of America* **52(1)** 1-7.

Betts, M.R., Nason, M.C., West, S.M., De Rosa, S., Migueles, S.A., Abraham, J., Lederman, M.M., Benito, J.M., Goepfert, P.A., Connors, M., Roederer, M. & Koup, R.A. (2006) HIV nonprogressors preferentially maintain highly functional HIV-specific CD8+ T cells. *Blood* **107** 4781-9.

Betts, R.J., Prabhu, N., Ho, A.W., Lew, F.C., Hutchinson, P.E., Rotzschke, O., Macary, P.A. & Kemeny, D.M. (2012) Influenza A virus infection results in a robust, antigen-responsive, and widely disseminated Foxp3+ regulatory T cell response. *Journal of Virology* **86(5)** 2817-2825.

Black, S., Nicolay, U., Vesikari, T., Knuf, M., Del Giudice, G., Della Cioppa, G., Tsai, T., Clemens, R. & Rappuoli, R. (2011) Hemagglutination inhibition antibody titers as a correlate of protection for inactivated influenza vaccines in children. *The Pediatric Infectious Disease Journal* **30(12)** 1081-1085.

Bodewes, R., de Mutsert, G., van der Klis, F.R., Ventresca, M., Wilks, S., Smith, D.J., Koopmans, M., Fouchier, R.A., Osterhaus, A.D. & Rimmelzwaan, G.F. (2011a) Prevalence of antibodies against seasonal influenza A and B viruses in children in Netherlands. *Clinical and Vaccine Immunology : CVI* **18(3)** 469-476.

Bodewes, R., Kreijtz, J.H., Geelhoed-Mieras, M.M., van Amerongen, G., Verburgh, R.J., van Trierum, S.E., Kuiken, T., Fouchier, R.A., Osterhaus, A.D. & Rimmelzwaan, G.F. (2011b) Vaccination against seasonal influenza A/H3N2 virus reduces the induction of heterosubtypic immunity against influenza A/H5N1 virus infection in ferrets. *Journal of Virology* **85(6)** 2695-2702.

Bodewes, R., Fraaij, P.L.A., Geelhoed-Mieras, M.M., van Baalen, C.A., Tiddens, H.A.W.M., van Rossum, A.M.C., van der Klis, F.R., Fouchier, R.A.M., Osterhaus, A.D.M.E. & Rimmelzwaan, G.F. (2011c) Annual vaccination against influenza hampers development of virus-specific CD8+ T cell immunity in children. *The Journal of Virology* **85(22)** 11995-2000.

Bodewes, R., Kreijtz, J.H.C.M., Hillaire, M., Geelhoed-Mieras, M.M., Fouchier, R.A.M., Osterhaus, A.D.M.E. & Rimmelzwaan, G.F. (2010) Vaccination with whole inactivated virus vaccine affects the induction of heterosubtypic immunity against influenza A/H5N1 and immunodominance of virus specific CD8+ T cell responses in mice. *Journal of General Virology* **91(Pt7)** 1743-1753.

Bommakanti, G., Citron, M.P., Hepler, R.W., Callahan, C., Heidecker, G.J., Najar, T.A., Lu, X., Joyce, J.G., Shiver, J.W., Casimiro, D.R., ter Meulen, J., Liang, X. & Varadarajan, R. (2010) Design of an HA2-based Escherichia coli expressed influenza immunogen that protects mice from pathogenic challenge. *Proceedings of the National Academy of Sciences of the United States of America* **107(31)** 13701-13706.

Bot, A., Bot, S. & Bona, C.A. (1998) Protective role of gamma interferon during the recall response to influenza virus. *Journal of Virology* **72(8)** 6637-6645.

Boulet, S., Ndongala, M.L., Peretz, Y., Boisvert, M.P., Boulassel, M.R., Tremblay, C., Routy, J.P., Sekaly, R.P. & Bernard, N.F. (2007) A dual color ELISPOT method for the simultaneous detection of IL-2 and IFN-gamma HIV-specific immune responses. *J Immunol Methods* **320** 18-29.

Brincks, E.L., Katewa, A., Kucaba, T.A., Griffith, T.S. & Legge, K.L. (2008) CD8 T cells utilize TRAIL to control influenza virus infection. *Journal of Immunology (Baltimore, Md.: 1950)* **181(7)** 4918-4925.

Brincks, E.L., Roberts, A.D., Cookenham, T., Sell, S., Kohlmeier, J.E., Blackman, M.A. & Woodland, D.L. (2013) Antigen-specific memory regulatory CD4+Foxp3+ T cells control memory responses to influenza virus infection. *Journal of Immunology (Baltimore, Md.: 1950)* **190(7)** 3438-3446.

Brokstad, K.A., Cox, R.J., Eriksson, J.C., Olofsson, J., Jonsson, R. & Davidsson, A. (2001) High prevalence of influenza specific antibody secreting cells in nasal mucosa. *Scandinavian Journal of Immunology* **54(1-2)** 243-247.

Brown, D.M., Lee, S., Garcia-Hernandez Mde, L. & Swain, S.L. (2012) Multifunctional CD4 cells expressing gamma interferon and perforin mediate protection against lethal influenza virus infection. *Journal of Virology* **86(12)** 6792-6803.

Carding, S.R., Allan, W., Kyes, S., Hayday, A., Bottomly, K. & Doherty, P.C. (1990) Late dominance of the inflammatory process in murine influenza by gamma/delta + T cells. *The Journal of Experimental Medicine* **172(4)** 1225-1231.

Carrat, F., Vergu, E., Ferguson, N.M., Lemaitre, M., Cauchemez, S., Leach, S. & Valleron, A.J. (2008) Time lines of infection and disease in human influenza: a review of volunteer challenge studies. *American Journal of Epidemiology* **167(7)** 775-785.

Casey, R., Blumenkrantz, D., Millington, K., Montamat-Sicotte, D., Kon, O.M., Wickremasinghe, M., Bremang, S., Magtoto, M., Sridhar, S., Connell, D. & Lalvani, A. (2010) Enumeration of functional T-cell subsets by fluorescence-immunospot defines signatures of pathogen burden in tuberculosis. *PloS One* **5(12)** e15619.

Cate, T.R., Couch, R.B., Kasel, J.A. & Six, H.R. (1977) Clinical trials of monovalent influenza A/New Jersey/76 virus vaccines in adults: reactogenicity, antibody response, and antibody persistence. *The Journal of Infectious Diseases* **136 Suppl** S450-5.

Cerwenka, A., Morgan, T.M. & Dutton, R.W. (1999) Naive, Effector, and Memory CD8 T Cells in Protection Against Pulmonary Influenza Virus Infection: Homing Properties Rather Than Initial Frequencies Are Crucial. *The Journal of Immunology* **163(10)** 5535-5543.

Champagne, P., Ogg, G.S., King, A.S., Knabenhans, C., Ellefsen, K., Nobile, M., Appay, V., Rizzardi, G.P., Fleury, S., Lipp, M., Forster, R., Rowland-Jones, S., Sekaly, R.P., McMichael, A.J. & Pantaleo, G. (2001) Skewed maturation of memory HIV-specific CD8 T lymphocytes. *Nature* **410(6824)** 106-111.

Chauvat, A., Benhamouda, N., Gey, A., Lemoine, F.M., Paulie, S., Carrat, F., Gougeon, M.L., Rozenberg, F., Krivine, A., Baillou, C., Lehmann, P., Quintin-Colonna, F., Launay, O. & Tartour, E. (2013) Clinical validation of IFNgamma/IL-10 and IFNgamma/IL-2 FluoroSpot assays for the detection of Tr1 T cells and influenza vaccine monitoring in humans. *Human Vaccines & Immunotherapeutics* **10(1)**.

Chirkova, T.V., Naykhin, A.N., Petukhova, G.D., Korenkov, D.A., Donina, S.A., Mironov, A.N. & Rudenko, L.G. (2011) Memory T-cell immune response in healthy young adults vaccinated with live attenuated influenza A (H5N2) vaccine. *Clinical and Vaccine Immunology : CVI* **18(10)** 1710-1718.

Christensen, J.P., Doherty, P.C., Branum, K.C. & Riberdy, J.M. (2000) Profound protection against respiratory challenge with a lethal H7N7 influenza A virus by increasing the magnitude of CD8(+) T-cell memory. *Journal of Virology* **74(24)** 11690-11696.

Clements, M.L., Betts, R.F., Tierney, E.L. & Murphy, B.R. (1986) Serum and nasal wash antibodies associated with resistance to experimental challenge with influenza A wild-type virus. *Journal of Clinical Microbiology* **24(1)** 157-160.

ClinicalTrials.gov. (2014) *A Phase I Study of Candidate Influenza Vaccines MVA-NP+M1 and ChAdOx1 NP+M1.* [Online] Available from: http://clinicaltrials.gov/ct2/show/NCT01818362 [Accessed 27 May 2014].

Co, M.D., Orphin, L., Cruz, J., Pazoles, P., Green, K.M., Potts, J., Leporati, A.M., Babon, J.A., Evans, J.E., Ennis, F.A. & Terajima, M. (2009) In vitro evidence that commercial influenza vaccines are not similar in their ability to activate human T cell responses. *Vaccine* **27(2)** 319-327.

Co, M.D.T., Orphin, L., Cruz, J., Pazoles, P., Rothman, A.L., Ennis, F.A. & Terajima, M. (2008) Discordance between antibody and T cell responses in recipients of trivalent inactivated influenza vaccine. *Vaccine* **26(16)** 1990-1998.

Cohen, M., Zhang, X.Q., Senaati, H.P., Chen, H.W., Varki, N.M., Schooley, R.T. & Gagneux, P. (2013) Influenza A penetrates host mucus by cleaving sialic acids with neuraminidase. *Virology Journal* **10** 321-422X-10-321.

Corti, D., Suguitan, A.L.,Jr, Pinna, D., Silacci, C., Fernandez-Rodriguez, B.M., Vanzetta, F., Santos, C., Luke, C.J., Torres-Velez, F.J., Temperton, N.J., Weiss, R.A., Sallusto, F., Subbarao, K. & Lanzavecchia, A. (2010) Heterosubtypic neutralising antibodies are produced by individuals immunized with a seasonal influenza vaccine. *The Journal of Clinical Investigation* **120(5)** 1663-1673.

Couch, R.B., Atmar, R.L., Franco, L.M., Quarles, J.M., Wells, J., Arden, N., Nino, D. & Belmont, J.W. (2013) Antibody correlates and predictors of immunity to naturally occurring influenza in humans and the importance of antibody to the neuraminidase. *The Journal of Infectious Diseases* **207(6)** 974-981.

Couch, R.B. & Kasel, J.A. (1983) Immunity to influenza in man. *Annual Review of Microbiology* **37** 529-549.

Couch, R.B., Kasel, J.A., Gerin, J.L., Schulman, J.L. & Kilbourne, E.D. (1974) Induction of partial immunity to influenza by a neuraminidase-specific vaccine. *The Journal of Infectious Diseases* **129(4)** 411-420.

Cowling, B.J., Ng, S., Ma, E.S., Cheng, C.K., Wai, W., Fang, V.J., Chan, K.H., Ip, D.K., Chiu, S.S., Peiris, J.S. & Leung, G.M. (2010) Protective efficacy of seasonal influenza vaccination against seasonal and pandemic influenza virus infection during 2009 in Hong Kong. *Clinical Infectious Diseases : An Official Publication of the Infectious Diseases Society of America* **51(12)** 1370-1379.

Cox, R.J., Brokstad, K.A. & Ogra, P. (2004) Influenza virus: immunity and vaccination strategies. Comparison of the immune response to inactivated and live, attenuated influenza vaccines. *Scandinavian Journal of Immunology* **59(1)** 1-15.

Darrah, P.A., Patel, D.T., De Luca, P.M., Lindsay, R.W., Davey, D.F., Flynn, B.J., Hoff, S.T., Andersen, P., Reed, S.G., Morris, S.L., Roederer, M. & Seder, R.A. (2007) Multifunctional TH1 cells define a correlate of vaccine-mediated protection against Leishmania major. *Nature Medicine* **13(7)** 843-850.

Dawood, F.S., Iuliano, A.D., Reed, C., Meltzer, M.I., Shay, D.K., Cheng, P.Y., Bandaranayake, D., Breiman, R.F., Brooks, W.A., Buchy, P., Feikin, D.R., Fowler, K.B., Gordon, A., Hien, N.T., Horby, P., Huang, Q.S., Katz, M.A., Krishnan, A., Lal, R., Montgomery, J.M., Molbak, K., Pebody, R., Presanis, A.M., Razuri, H., Steens, A., Tinoco, Y.O., Wallinga, J., Yu, H., Vong, S., Bresee, J. & Widdowson, M.A. (2012) Estimated global mortality associated with the first 12 months of 2009 pandemic influenza A H1N1 virus circulation: a modelling study. *The Lancet Infectious Diseases* **12(9)** 687-695.

Dawson, T.C., Beck, M.A., Kuziel, W.A., Henderson, F. & Maeda, N. (2000) Contrasting effects of CCR5 and CCR2 deficiency in the pulmonary inflammatory response to influenza A virus. *The American Journal of Pathology* **156(6)** 1951-1959.

De Filette, M., Fiers, W., Martens, W., Birkett, A., Ramne, A., Lowenadler, B., Lycke, N., Jou, W.M. & Saelens, X. (2006) Improved design and intranasal delivery of an M2e-based human influenza A vaccine. *Vaccine* **24(44-46)** 6597-6601.

Department of Heath, UK. (2009) *Immunisation against infectious diseases - The Green Book. Chapter 23a. Pandemic influenza A(H1N1)v 2009 (swine flu) - 21 October 2009.* [Online] Available from: http://webarchive.nationalarchives.gov.uk/20091022095029/http://www.dh.gov.uk/prod_consum_dh/groups/dh_digitalassets/@dh/@en/documents/digitalasset/dh_107408.pdf [Accessed 23 April 2014].

Dunne, P.J., Faint, J.M., Gudgeon, N.H., Fletcher, J.M., Plunkett, F.J., Soares, M.V., Hislop, A.D., Annels, N.E., Rickinson, A.B., Salmon, M. & Akbar, A.N. (2002) Epstein-Barr virus-specific CD8(+) T cells that re-express CD45RA are apoptosis-resistant memory cells that retain replicative potential. *Blood* **100(3**) 933-940.

Eggink, D., Goff, P.H. & Palese, P. (2014) Guiding the immune response against influenza virus hemagglutinin toward the conserved stalk domain by hyperglycosylation of the globular head domain. *Journal of Virology* **88(1**) 699-704.

Ellebedy, A.H. & Webby, R.J. (2009) Influenza vaccines. *Vaccine* **27(Supplement 4**) D65-D68.

Ellis, J., Iturriza, M., Allan, R., Bermingham, A., Brown, K., Gray, J. & Brown, D. (2009) Evaluation of four real-time PCR assays for detection of influenza A(H1N1)v viruses. *Euro Surveillance* **14(22**) 19230.

Ennis, F.A., Rook, A.H., Qi, Y.H., Schild, G.C., Riley, D., Pratt, R. & Potter, C.W. (1981) HLA restricted virus-specific cytotoxic T-lymphocyte responses to live and inactivated influenza vaccines. *Lancet* **2(8252**) 887-891.

Epstein, S.L. (2006) Prior H1N1 influenza infection and susceptibility of Cleveland Family Study participants during the H2N2 pandemic of 1957: an experiment of nature. *The Journal of Infectious Diseases* **193(1**) 49-53.

Epstein, S.L., Lo, C.Y., Misplon, J.A., Lawson, C.M., Hendrickson, B.A., Max, E.E. & Subbarao, K. (1997) Mechanisms of heterosubtypic immunity to lethal influenza A virus infection in fully immunocompetent, T cell-depleted, beta2-microglobulin-

deficient, and J chain-deficient mice. *Journal of Immunology (Baltimore, Md.: 1950)* **158(3**) 1222-1230.

Everitt, A.R., Clare, S., Pertel, T., John, S.P., Wash, R.S., Smith, S.E., Chin, C.R., Feeley, E.M., Sims, J.S., Adams, D.J., Wise, H.M., Kane, L., Goulding, D., Digard, P., Anttila, V., Baillie, J.K., Walsh, T.S., Hume, D.A., Palotie, A., Xue, Y., Colonna, V., Tyler-Smith, C., Dunning, J., Gordon, S.B., GenISIS Investigators, MOSAIC Investigators, Smyth, R.L., Openshaw, P.J., Dougan, G., Brass, A.L. & Kellam, P. (2012) IFITM3 restricts the morbidity and mortality associated with influenza. *Nature* **484(7395**) 519-523.

Fadel, S.A., Bromley, S.K., Medoff, B.D. & Luster, A.D. (2008) CXCR3-deficiency protects influenza-infected CCR5-deficient mice from mortality. *European Journal of Immunology* **38(12**) 3376-3387.

Fereidouni, S.R., Starick, E., Beer, M., Wilking, H., Kalthoff, D., Grund, C., Hauslaigner, R., Breithaupt, A., Lange, E. & Harder, T.C. (2009) Highly pathogenic avian influenza virus infection of mallards with homo- and heterosubtypic immunity induced by low pathogenic avian influenza viruses. *PloS One* **4(8**) e6706.

Flynn, K.J., Riberdy, J.M., Christensen, J.P., Altman, J.D. & Doherty, P.C. (1999) In vivo proliferation of naive and memory influenza-specific CD8(+) T cells. *Proceedings of the National Academy of Sciences of the United States of America* **96(15**) 8597-8602.

Fonteneau, J.F., Gilliet, M., Larsson, M., Dasilva, I., Munz, C., Liu, Y.J. & Bhardwaj, N. (2003) Activation of influenza virus-specific CD4+ and CD8+ T cells: a new role for plasmacytoid dendritic cells in adaptive immunity. *Blood* **101(9**) 3520-3526.

Forrest, B.D., Pride, M.W., Dunning, A.J., Capeding, M.R.Z., Chotpitayasunondh, T., Tam, J.S., Rappaport, R., Eldridge, J.H. & Gruber, W.C. (2008) Correlation of Cellular Immune Responses with Protection against Culture-Confirmed Influenza Virus in Young Children. *Clinical and Vaccine Immunology* **15(7**) 1042-1053.

Gambotto, A., Barratt-Boyes, S.M., de Jong, M.D., Neumann, G. & Kawaoka, Y. (2008) Human infection with highly pathogenic H5N1 influenza virus. *Lancet* **371(9622**) 1464-1475.

Garten, R.J., Davis, C.T., Russell, C.A., Shu, B., Lindstrom, S., Balish, A., Sessions, W.M., Xu, X., Skepner, E., Deyde, V., Okomo-Adhiambo, M., Gubareva, L., Barnes, J., Smith, C.B., Emery, S.L., Hillman, M.J., Rivailler, P., Smagala, J., de Graaf, M., Burke, D.F., Fouchier, R.A., Pappas, C., Alpuche-Aranda, C.M., Lopez-Gatell, H., Olivera, H., Lopez, I., Myers, C.A., Faix, D., Blair, P.J., Yu, C., Keene, K.M., Dotson, P.D.,Jr, Boxrud, D., Sambol, A.R., Abid, S.H., St George, K., Bannerman, T., Moore, A.L., Stringer, D.J., Blevins, P., Demmler-Harrison, G.J., Ginsberg, M., Kriner, P., Waterman, S., Smole, S., Guevara, H.F., Belongia, E.A., Clark, P.A., Beatrice, S.T., Donis, R., Katz, J., Finelli, L., Bridges, C.B., Shaw, M., Jernigan, D.B., Uyeki, T.M., Smith, D.J., Klimov, A.I. & Cox, N.J. (2009) Antigenic and genetic characteristics of swine-origin 2009 A(H1N1) influenza viruses circulating in humans. *Science (New York, N.Y.)* **325(5937**) 197-201.

Gatherer, D. (2009) The 2009 H1N1 influenza outbreak in its historical context. *Journal of Clinical Virology : The Official Publication of the Pan American Society for Clinical Virology* **45(3**) 174-178.

Gazagne, A., Claret, E., Wijdenes, J., Yssel, H., Bousquet, F., Levy, E., Vielh, P., Scotte, F., Goupil, T.L., Fridman, W.H. & Tartour, E. (2003) A Fluorospot assay to detect single T lymphocytes simultaneously producing multiple cytokines. *Journal of Immunological Methods* **283(1-2**) 91-98.

Ge, X., Tan, V., Bollyky, P.L., Standifer, N.E., James, E.A. & Kwok, W.W. (2010) Assessment of Seasonal Influenza A Virus-Specific CD4 T-Cell Responses to 2009 Pandemic H1N1 Swine-Origin Influenza A Virus. *The Journal of Virology* **84(7**) 3312-3319.

Gerhard, W. (2001) The role of the antibody response in influenza virus infection. *Current Topics in Microbiology and Immunology* **26**0 171-190.

Germain, R.N. (1986) Immunology. The ins and outs of antigen processing and presentation. *Nature* **322(6081**) 687-689.

GeurtsvanKessel, C.H. & Lambrecht, B.N. (2008) Division of labor between dendritic cell subsets of the lung. *Mucosal Immunology* **1(6**) 442-450.

GeurtsvanKessel, C.H., Willart, M.A., van Rijt, L.S., Muskens, F., Kool, M., Baas, C., Thielemans, K., Bennett, C., Clausen, B.E., Hoogsteden, H.C., Osterhaus, A.D., Rimmelzwaan, G.F. & Lambrecht, B.N. (2008) Clearance of influenza virus from the lung depends on migratory langerin+CD11b- but not plasmacytoid dendritic cells. *The Journal of Experimental Medicine* **205(7**) 1621-1634.

Gioia, C., Castilletti, C., Tempestilli, M., Piacentini, P., Bordi, L., Chiappini, R., Agrati, C., Squarcione, S., Ippolito, G., Puro, V., Capobianchi, M.R. & Poccia, F. (2008) Cross-subtype immunity against avian influenza in persons recently vaccinated for influenza. *Emerging Infectious Diseases* **14(1)** 121-128.

Gorse, G.J. & Belshe, R.B. (1990) Enhancement of anti-influenza A virus cytotoxicity following influenza A virus vaccination in older, chronically ill adults. *Journal of Clinical Microbiology* **28(11)** 2539-2550.

Gotch, F., McMichael, A., Smith, G. & Moss, B. (1987) Identification of viral molecules recognized by influenza-specific human cytotoxic T lymphocytes. *The Journal of Experimental Medicine* **165(2)** 408-416.

Grandea, A.G.,3rd, Olsen, O.A., Cox, T.C., Renshaw, M., Hammond, P.W., Chan-Hui, P.Y., Mitcham, J.L., Cieplak, W., Stewart, S.M., Grantham, M.L., Pekosz, A., Kiso, M., Shinya, K., Hatta, M., Kawaoka, Y. & Moyle, M. (2010) Human antibodies reveal a protective epitope that is highly conserved among human and nonhuman influenza A viruses. *Proceedings of the National Academy of Sciences of the United States of America* **107(28)** 12658-12663.

Gras, S., Kedzierski, L., Valkenburg, S.A., Laurie, K., Liu, Y.C., Denholm, J.T., Richards, M.J., Rimmelzwaan, G.F., Kelso, A., Doherty, P.C., Turner, S.J., Rossjohn, J. & Kedzierska, K. (2010) Cross-reactive CD8+ T-cell immunity between

the pandemic H1N1-2009 and H1N1-1918 influenza A viruses. *Proceedings of the National Academy of Sciences of the United States of America* **107(28)** 12599-12604.

Grebe, K.M., Yewdell, J.W. & Bennink, J.R. (2008) Heterosubtypic immunity to influenza A virus: where do we stand? *Microbes and Infection* **10(9)** 1024-1029.

Greenbaum, J.A., Kotturi, M.F., Kim, Y., Oseroff, C., Vaughan, K., Salimi, N., Vita, R., Ponomarenko, J., Scheuermann, R.H., Sette, A. & Peters, B. (2009) Pre-existing immunity against swine-origin H1N1 influenza viruses in the general human population. *Proceedings of the National Academy of Sciences of the United States of America* **106(48)** 20365-20370.

Guo, H., Santiago, F., Lambert, K., Takimoto, T. & Topham, D.J. (2011) T cell-mediated protection against lethal 2009 pandemic H1N1 influenza virus infection in a mouse model. *Journal of Virology* **85(1)** 448-455.

Guthrie, T., Hobbs, C.G., Davenport, V., Horton, R.E., Heyderman, R.S. & Williams, N.A. (2004) Parenteral influenza vaccination influences mucosal and systemic T cell-mediated immunity in healthy adults. *The Journal of Infectious Diseases* **190(11)** 1927-1935.

Hamada, H., Garcia-Hernandez Mde, L., Reome, J.B., Misra, S.K., Strutt, T.M., McKinstry, K.K., Cooper, A.M., Swain, S.L. & Dutton, R.W. (2009) Tc17, a unique subset of CD8 T cells that can protect against lethal influenza challenge. *Journal of Immunology (Baltimore, Md.: 1950)* **182(6)** 3469-3481.

Hamann, D., Baars, P.A., Rep, M.H., Hooibrink, B., Kerkhof-Garde, S.R., Klein, M.R. & van Lier, R.A. (1997) Phenotypic and functional separation of memory and effector human CD8+ T cells. *The Journal of Experimental Medicine* **186(9)** 1407-1418.

Hansen, S.G., Vieville, C., Whizin, N., Coyne-Johnson, L., Siess, D.C., Drummond, D.D., Legasse, A.W., Axthelm, M.K., Oswald, K., Trubey, C.M., Piatak, M.,Jr, Lifson, J.D., Nelson, J.A., Jarvis, M.A. & Picker, L.J. (2009) Effector memory T cell

responses are associated with protection of rhesus monkeys from mucosal simian immunodeficiency virus challenge. *Nature Medicine* **15(3)** 293-299.

Harari, A., Vallelian, F., Meylan, P.R. & Pantaleo, G. (2005) Functional heterogeneity of memory CD4 T cell responses in different conditions of antigen exposure and persistence. *Journal of Immunology (Baltimore, Md.: 1950)* **174(2)** 1037-1045.

Harari, A., Vallelian, F. & Pantaleo, G. (2004) Phenotypic heterogeneity of antigen-specific CD4 T cells under different conditions of antigen persistence and antigen load. *European Journal of Immunology* **34(12)** 3525-3533.

Harari, A., Dutoit, V., Cellerai, C., Bart, P., Du Pasquier, R.A. & Pantaleo, G. (2006) Functional signatures of protective antiviral T-cell immunity in human virus infections. *Immunological Reviews* **211(1)** 236-254.

Harari, A., Petitpierre, S., Vallelian, F. & Pantaleo, G. (2004) Skewed representation of functionally distinct populations of virus-specific CD4 T cells in HIV-1–infected subjects with progressive disease: changes after antiretroviral therapy. *Blood* **103(3)** 966-972.

Hardelid, P., Andrews, N.J., Hoschler, K., Stanford, E., Baguelin, M., Waight, P.A., Zambon, M. & Miller, E. (2010) Assessment of baseline age-specific antibody prevalence and incidence of infection to novel influenza A/H1N1 2009. *Health Technology Assessment (Winchester, England)* **14(55)** 115-192.

Hartshorn, K., Reid, K., White, M., Jensenius, J., Morris, S., Tauber, A. & Crouch, E. (1996) Neutrophil deactivation by influenza A viruses: mechanisms of protection after viral opsonization with collectins and hemagglutination-inhibiting antibodies. *Blood* **87(8)** 3450-3461.

Hayden, F.G., Fritz, R., Lobo, M.C., Alvord, W., Strober, W. & Straus, S.E. (1998) Local and systemic cytokine responses during experimental human influenza A virus infection. Relation to symptom formation and host defense. *The Journal of Clinical Investigation* **101(3)** 643-649.

He, X.S., Draghi, M., Mahmood, K., Holmes, T.H., Kemble, G.W., Dekker, C.L., Arvin, A.M., Parham, P. & Greenberg, H.B. (2004) T cell-dependent production of IFN-gamma by NK cells in response to influenza A virus. *The Journal of Clinical Investigation* **114(12)** 1812-1819.

He, X.S., Holmes, T.H., Sasaki, S., Jaimes, M.C., Kemble, G.W., Dekker, C.L., Arvin, A.M. & Greenberg, H.B. (2008) Baseline levels of influenza-specific CD4 memory T-cells affect T-cell responses to influenza vaccines. *PloS One* **3(7)** e2574.

He, X.S., Holmes, T.H., Zhang, C., Mahmood, K., Kemble, G.W., Lewis, D.B., Dekker, C.L., Greenberg, H.B. & Arvin, A.M. (2006) Cellular immune responses in children and adults receiving inactivated or live attenuated influenza vaccines. *Journal of Virology* **80(23)** 11756-11766.

He, X., Holmes, T., Mahmood, K., Kemble, G., Dekker, C., Arvin, A. & Greenberg, H. (2008) Phenotypic Changes in Influenza-Specific CD8+ T Cells after Immunization of Children and Adults with Influenza Vaccines. *The Journal of Infectious Diseases* **197(6)** 803-811.

Heinen, P.P., de Boer-Luijtze, E.A. & Bianchi, A.T. (2001) Respiratory and systemic humoral and cellular immune responses of pigs to a heterosubtypic influenza A virus infection. *The Journal of General Virology* **82(Pt 11)** 2697-2707.

Hers, J.F. (1966) Disturbances of the ciliated epithelium due to influenza virus. *The American Review of Respiratory Disease* **93(3)** Suppl:162-77.

Hillaire, M.L., van Trierum, S.E., Kreijtz, J.H., Bodewes, R., Geelhoed-Mieras, M.M., Nieuwkoop, N.J., Fouchier, R.A., Kuiken, T., Osterhaus, A.D. & Rimmelzwaan, G.F. (2011a) Cross-protective immunity against influenza pH1N1 2009 viruses induced by seasonal influenza A (H3N2) virus is mediated by virus-specific T-cells. *The Journal of General Virology* **92(Pt 10)** 2339-2349.

Hillaire, M.L.B., van Trierum, S.E., Bodewes, R., van Baalen, C.A., van Binnendijk, R.S., Koopmans, M.P., Fouchier, R.A.M., Osterhaus, A.D.M.E. & Rimmelzwaan, G.F. (2011b) Characterization of the human CD8+ T cell response following infection

with 2009 pandemic influenza H1N1 virus. *The Journal of Virology* **85(22)** 12057-12061.

Ho, A.W., Prabhu, N., Betts, R.J., Ge, M.Q., Dai, X., Hutchinson, P.E., Lew, F.C., Wong, K.L., Hanson, B.J., Macary, P.A. & Kemeny, D.M. (2011) Lung CD103+ dendritic cells efficiently transport influenza virus to the lymph node and load viral antigen onto MHC class I for presentation to CD8 T cells. *Journal of Immunology (Baltimore, Md.: 1950)* **187(11)** 6011-6021.

Ho, L., Denney, L., Luhn, K., Teoh, D., Clelland, C. & McMichael, A. (2008) Activation of invariant NKT cells enhances the innate immune response and improves the disease course in influenza?A virus infection. *European Journal of Immunology* **38(7)** 1913-1922.

Hobson, D., Curry, R.L., Beare, A.S. & Ward-Gardner, A. (1972) The role of serum haemagglutination-inhibiting antibody in protection against challenge infection with influenza A2 and B viruses. *The Journal of Hygiene* **70(4)** 767-777.

Hoft, D.F., Babusis, E., Worku, S., Spencer, C.T., Lottenbach, K., Truscott, S.M., Abate, G., Sakala, I.G., Edwards, K.M., Creech, C.B., Gerber, M.A., Bernstein, D.I., Newman, F., Graham, I., Anderson, E.L. & Belshe, R.B. (2011) Live and inactivated influenza vaccines induce similar humoral responses, but only live vaccines induce diverse T-cell responses in young children. *The Journal of Infectious Diseases* **204(6)** 845-853.

Hogan, R.J., Usherwood, E.J., Zhong, W., Roberts, A.A., Dutton, R.W., Harmsen, A.G. & Woodland, D.L. (2001) Activated antigen-specific CD8+ T cells persist in the lungs following recovery from respiratory virus infections. *Journal of Immunology (Baltimore, Md.: 1950)* **166(3)** 1813-1822.

Hoji, A. & Rinaldo, C.R.,Jr (2005) Human CD8+ T cells specific for influenza A virus M1 display broad expression of maturation-associated phenotypic markers and chemokine receptors. *Immunology* **115(2)** 239-245.

Hsu, A.C., Parsons, K., Barr, I., Lowther, S., Middleton, D., Hansbro, P.M. & Wark, P.A. (2012) Critical role of constitutive type I interferon response in bronchial epithelial cell to influenza infection. *PloS One* **7(3)** e32947.

Hwang, I., Scott, J.M., Kakarla, T., Duriancik, D.M., Choi, S., Cho, C., Lee, T., Park, H., French, A.R., Beli, E., Gardner, E. & Kim, S. (2012) Activation mechanisms of natural killer cells during influenza virus infection. *PloS One* **7(12)** e51858.

Jameson, J., Cruz, J., Terajima, M. & Ennis, F.A. (1999) Human CD8+ and CD4+ T lymphocyte memory to influenza A viruses of swine and avian species. *Journal of Immunology (Baltimore, Md.: 1950)* **162(12)** 7578-7583.

Jameson, J.M., Cruz, J., Costanzo, A., Terajima, M. & Ennis, F.A. (2010) A role for the mevalonate pathway in the induction of subtype cross-reactive immunity to influenza A virus by human gammadelta T lymphocytes. *Cellular Immunology* **264(1)** 71-77.

Jegaskanda, S., Laurie, K.L., Amarasena, T.H., Winnall, W.R., Kramski, M., De Rose, R., Barr, I.G., Brooks, A.G., Reading, P.C. & Kent, S.J. (2013a) Age-associated cross-reactive antibody-dependent cellular cytotoxicity toward 2009 pandemic influenza A virus subtype H1N1. *The Journal of Infectious Diseases* **208(7)** 1051-1061.

Jegaskanda, S., Weinfurter, J.T., Friedrich, T.C. & Kent, S.J. (2013b) Antibody-dependent cellular cytotoxicity is associated with control of pandemic H1N1 influenza virus infection of macaques. *Journal of Virology* **87(10)** 5512-5522.

Jelley-Gibbs, D.M., Brown, D.M., Dibble, J.P., Haynes, L., Eaton, S.M. & Swain, S.L. (2005) Unexpected prolonged presentation of influenza antigens promotes CD4 T cell memory generation. *The Journal of Experimental Medicine* **202(5)** 697-706.

Jin, H. & Chen, Z. (2014) Production of live attenuated influenza vaccines against seasonal and potential pandemic influenza viruses. *Current Opinion in Virology* **6C** 34-39.

Johns, M.C., Eick, A.A., Blazes, D.L., Lee, S.E., Perdue, C.L., Lipnick, R., Vest, K.G., Russell, K.L., DeFraites, R.F. & Sanchez, J.L. (2010) Seasonal influenza vaccine and protection against pandemic (H1N1) 2009-associated illness among US military personnel. *PloS One* **5(5)** e10722.

Kaech, S.M. (2014) Celebrating diversity in memory T cells. *Journal of Immunology (Baltimore, Md.: 1950)* **192(3)** 837-839.

Kannanganat, S., Ibegbu, C., Chennareddi, L., Robinson, H.L. & Amara, R.R. (2007) Multiple-cytokine-producing antiviral CD4 T cells are functionally superior to single-cytokine-producing cells. *Journal of Virology* **81(16)** 8468-8476.

Kapoor, S. & Dhama, K. (2014) Prevention and Control of Influenza Viruses. In: *Insight into Influenza Viruses of Animals and Humans.* 1st edition. Cham, Springer International Publishing AG, pp. 187-188.

Karanikas, V., Lodding, J., Maino, V.C. & McKenzie, I.F. (2000) Flow cytometric measurement of intracellular cytokines detects immune responses in MUC1 immunotherapy. *Clinical Cancer Research : An Official Journal of the American Association for Cancer Research* **6(3)** 829-837.

Karupiah, G., Chen, J.H., Mahalingam, S., Nathan, C.F. & MacMicking, J.D. (1998) Rapid interferon gamma-dependent clearance of influenza A virus and protection from consolidating pneumonitis in nitric oxide synthase 2-deficient mice. *The Journal of Experimental Medicine* **188(8)** 1541-1546.

Katz, J., Hancock, K., Veguilla, V., Zhong, W., Lu, X.H., Sun, H., Butler, E., Dong, L., Liu, F., Li, Z.N., DeVos, J., Gargiullo, P. & Cox, N. (2009) Serum Cross-Reactive Antibody Response to a Novel Influenza A (H1N1) Virus After Vaccination with Seasonal Influenza Vaccine. *Morbidity and Mortality Weekly Report* **58(19)** 521-524.

Kelly, H., Peck, H.A., Laurie, K.L., Wu, P., Nishiura, H. & Cowling, B.J. (2011) The age-specific cumulative incidence of infection with pandemic influenza H1N1 2009 was similar in various countries prior to vaccination. *PloS One* **6(8)** e21828.

Keynan, Y., Juno, J., Meyers, A., Ball, T.B., Kumar, A., Rubinstein, E. & Fowke, K.R. (2010) Chemokine receptor 5Δ32 allele in patients with severe pandemic (H1N1) 2009. *Emerging Infectious Diseases* **16(10)** 1621-1622.

Keynan, Y., Malik, S. & Fowke, K.R. (2013) The role of polymorphisms in host immune genes in determining the severity of respiratory illness caused by pandemic H1N1 influenza. *Public Health Genomics* **16(1-2)** 9-16.

Klebanoff, C.A., Gattinoni, L., Torabi-Parizi, P., Kerstann, K., Cardones, A.R., Finkelstein, S.E., Palmer, D.C., Antony, P.A., Hwang, S.T., Rosenberg, S.A., Waldmann, T.A. & Restifo, N.P. (2005) Central memory self/tumor-reactive CD8+ T cells confer superior antitumor immunity compared with effector memory T cells. *Proceedings of the National Academy of Sciences of the United States of America* **102(27)** 9571-9576.

Knipe, D. M., Howley, P. M., Griffin, D. E., Lamb, R. A., Martin, M. A., Roizman, B. & Straus, S. E. (2006) Specific Virus Families. In: *Fields Virology.* 5th edition. United States, Lippincott Williams & Wilkins, pp. 1693-1739.

Kohlmeier, J.E., Miller, S.C., Smith, J., Lu, B., Gerard, C., Cookenham, T., Roberts, A.D. & Woodland, D.L. (2008) The chemokine receptor CCR5 plays a key role in the early memory CD8+ T cell response to respiratory virus infections. *Immunity* **29(1)** 101-113.

Kok, W.L., Denney, L., Benam, K., Cole, S., Clelland, C., McMichael, A.J. & Ho, L.P. (2012) Pivotal Advance: Invariant NKT cells reduce accumulation of inflammatory monocytes in the lungs and decrease immune-pathology during severe influenza A virus infection. *Journal of Leukocyte Biology* **91(3)** 357-368.

Krammer, F., Pica, N., Hai, R., Margine, I. & Palese, P. (2013) Chimeric hemagglutinin influenza virus vaccine constructs elicit broadly protective stalk-specific antibodies. *Journal of Virology* **87(12)** 6542-6550.

Kreher, C.R., Dittrich, M.T., Guerkov, R., Boehm, B.O. & Tary-Lehmann, M. (2003) CD4+ and CD8+ cells in cryopreserved human PBMC maintain full functionality in cytokine ELISPOT assays. *Journal of Immunological Methods* **278(1-2)** 79-93.

Kreijtz, J.H., Bodewes, R., van Amerongen, G., Kuiken, T., Fouchier, R.A., Osterhaus, A.D. & Rimmelzwaan, G.F. (2007) Primary influenza A virus infection induces cross-protective immunity against a lethal infection with a heterosubtypic virus strain in mice. *Vaccine* **25(4)** 612-620.

Kreijtz, J.H., Bodewes, R., van den Brand, J.M., de Mutsert, G., Baas, C., van Amerongen, G., Fouchier, R.A., Osterhaus, A.D. & Rimmelzwaan, G.F. (2009) Infection of mice with a human influenza A/H3N2 virus induces protective immunity against lethal infection with influenza A/H5N1 virus. *Vaccine* **27(36)** 4983-4989.

Kreijtz, J.H., de Mutsert, G., van Baalen, C.A., Fouchier, R.A., Osterhaus, A.D. & Rimmelzwaan, G.F. (2008) Cross-recognition of avian H5N1 influenza virus by human cytotoxic T-lymphocyte populations directed to human influenza A virus. *Journal of Virology* **82(11)** 5161-5166.

Kreijtz, J.H., Fouchier, R.A. & Rimmelzwaan, G.F. (2011) Immune responses to influenza virus infection. *Virus Research* **162(1-2)** 19-30.

Kuiken, T., Riteau, B., Fouchier, R.A. & Rimmelzwaan, G.F. (2012) Pathogenesis of influenza virus infections: the good, the bad and the ugly. *Current Opinion in Virology* **2(3)** 276-286.

La Gruta, N.L., Turner, S.J. & Doherty, P.C. (2004) Hierarchies in Cytokine Expression Profiles for Acute and Resolving Influenza Virus-Specific CD8+ T Cell Responses: Correlation of Cytokine Profile and TCR Avidity. *The Journal of Immunology* **172(9)** 5553-5560.

Lalvani, A., Brookes, R., Hambleton, S., Britton, W.J., Hill, A.V. & McMichael, A.J. (1997) Rapid effector function in CD8+ memory T cells. *The Journal of Experimental Medicine* **186(6)** 859-865.

Lambert, L.C. & Fauci, A.S. (2010) Influenza Vaccines for the Future. *New England Journal of Medicine* **363(21)** 2036-2044.

Lamere, M.W., Lam, H.T., Moquin, A., Haynes, L., Lund, F.E., Randall, T.D. & Kaminski, D.A. (2011) Contributions of Antinucleoprotein IgG to Heterosubtypic Immunity against Influenza Virus. *Journal of Immunology (Baltimore, Md.: 1950)* **186(7)** 4331-4339.

Lamoreaux, L., Roederer, M. & Koup, R. (2006) Intracellular cytokine optimization and standard operating procedure. *Nature Protocols* **1(3)** 1507-1516.

Lanthier, P.A., Huston, G.E., Moquin, A., Eaton, S.M., Szaba, F.M., Kummer, L.W., Tighe, M.P., Kohlmeier, J.E., Blair, P.J., Broderick, M., Smiley, S.T. & Haynes, L. (2011) Live attenuated influenza vaccine (LAIV) impacts innate and adaptive immune responses. *Vaccine* **29(44)** 7849-7856.

Laursen, N.S. & Wilson, I.A. (2013) Broadly neutralising antibodies against influenza viruses. *Antiviral Research* **98(3)** 476-483.

Lee, L.Y., Ha do, L.A., Simmons, C., de Jong, M.D., Chau, N.V., Schumacher, R., Peng, Y.C., McMichael, A.J., Farrar, J.J., Smith, G.L., Townsend, A.R., Askonas, B.A., Rowland-Jones, S. & Dong, T. (2008) Memory T cells established by seasonal human influenza A infection cross-react with avian influenza A (H5N1) in healthy individuals. *The Journal of Clinical Investigation* **118(10)** 3478-3490.

Lee, Y.T., Kim, K.H., Ko, E.J., Lee, Y.N., Kim, M.C., Kwon, Y.M., Tang, Y., Cho, M.K., Lee, Y.J. & Kang, S.M. (2014) New vaccines against influenza virus. *Clinical and Experimental Vaccine Research* **3(1)** 12-28.

Li, C.K., Rappuoli, R. & Xu, X.N. (2013) Correlates of protection against influenza infection in humans--on the path to a universal vaccine? *Current Opinion in Immunology* **25(4)** 470-476.

Li, X., Miao, H., Henn, A., Topham, D.J., Wu, H., Zand, M.S. & Mosmann, T.R. (2012) Ki-67 expression reveals strong, transient influenza specific CD4 T cell responses after adult vaccination. *Vaccine* **30(31)** 4581-4584.

Liang, S., Mozdzanowska, K., Palladino, G. & Gerhard, W. (1994) Heterosubtypic immunity to influenza type A virus in mice. Effector mechanisms and their longevity. *Journal of Immunology (Baltimore, Md.: 1950)* **152(4)** 1653-1661.

Lillie, P.J., Berthoud, T.K., Powell, T.J., Lambe, T., Mullarkey, C., Spencer, A.J., Hamill, M., Peng, Y., Blais, M.E., Duncan, C.J., Sheehy, S.H., Havelock, T., Faust, S.N., Williams, R.L., Gilbert, A., Oxford, J., Dong, T., Hill, A.V. & Gilbert, S.C. (2012) Preliminary assessment of the efficacy of a T-cell-based influenza vaccine, MVA-NP+M1, in humans. *Clinical Infectious Diseases : An Official Publication of the Infectious Diseases Society of America* **55(1)** 19-25.

Limberis, M.P., Adam, V.S., Wong, G., Gren, J., Kobasa, D., Ross, T.M., Kobinger, G.P., Tretiakova, A. & Wilson, J.M. (2013) Intranasal antibody gene transfer in mice and ferrets elicits broad protection against pandemic influenza. *Science Translational Medicine* **5(187)** 187ra72.

Ling, P.D., Lednicky, J.A., Keitel, W.A., Poston, D.G., White, Z.S., Peng, R., Liu, Z., Mehta, S.K., Pierson, D.L., Rooney, C.M., Vilchez, R.A., Smith, E.O. & Butel, J.S. (2003) The dynamics of herpesvirus and polyomavirus reactivation and shedding in healthy adults: a 14-month longitudinal study. *The Journal of Infectious Diseases* **187(10)** 1571-1580.

Liu, W., Ma, M.J., Tang, F., He, C., Zhang, X.A., Jiang, L.F., Xin, D.S., Hu, C.Y., Looman, C. & Cao, W.C. (2012) Host immune response to A(H1N1)pdm09 vaccination and infection: a one-year prospective study on six cohorts of subjects. *Vaccine* **30(32)** 4785-4789.

Lucas, M., Day, C.L., Wyer, J.R., Cunliffe, S.L., Loughry, A., McMichael, A.J. & Klenerman, P. (2004) Ex vivo phenotype and frequency of influenza virus-specific CD4 memory T cells. *Journal of Virology* **78(13)** 7284-7287.

Lukacher, A.E., Braciale, V.L. & Braciale, T.J. (1984) In vivo effector function of influenza virus-specific cytotoxic T lymphocyte clones is highly specific. *The Journal of Experimental Medicine* **160(3)** 814-826.

Maecker, H.T., Rinfret, A., D'Souza, P., Darden, J., Roig, E., Landry, C., Hayes, P., Birungi, J., Anzala, O., Garcia, M., Harari, A., Frank, I., Baydo, R., Baker, M., Holbrook, J., Ottinger, J., Lamoreaux, L., Epling, C.L., Sinclair, E., Suni, M.A., Punt, K., Calarota, S., El-Bahi, S., Alter, G., Maila, H., Kuta, E., Cox, J., Gray, C., Altfeld, M., Nougarede, N., Boyer, J., Tussey, L., Tobery, T., Bredt, B., Roederer, M., Koup, R., Maino, V.C., Weinhold, K., Pantaleo, G., Gilmour, J., Horton, H. & Sekaly, R.P. (2005) Standardization of cytokine flow cytometry assays. *BMC Immunology* **6** 13.

Mahnke, Y.D., Brodie, T.M., Sallusto, F., Roederer, M. & Lugli, E. (2013) The who's who of T-cell differentiation: Human memory T-cell subsets. *European Journal of Immunology* **43(11)** 2797-2809.

Makedonas, G., Hutnick, N., Haney, D., Amick, A.C., Gardner, J., Cosma, G., Hersperger, A.R., Dolfi, D., Wherry, E.J., Ferrari, G. & Betts, M.R. (2010) Perforin and IL-2 upregulation define qualitative differences among highly functional virus-specific human CD8 T cells. *PLoS Pathogens* **6(3)** e1000798.

Manigold, T., Mori, A., Graumann, R., Llop, E., Simon, V., Ferres, M., Valdivieso, F., Castillo, C., Hjelle, B. & Vial, P. (2010) Highly differentiated, resting gn-specific memory CD8+ T cells persist years after infection by andes hantavirus. *PLoS Pathogens* **6(2)** e1000779.

Marzio, R., Mauel, J. & Betz-Corradin, S. (1999) CD69 and regulation of the immune function. *Immunopharmacology and Immunotoxicology* **21(3)** 565-582.

Masopust, D. & Picker, L.J. (2012) Hidden memories: frontline memory T cells and early pathogen interception. *Journal of Immunology (Baltimore, Md.: 1950)* **188(12)** 5811-5817.

Masopust, D., Vezys, V., Marzo, A.L. & Lefrancois, L. (2001) Preferential localization of effector memory cells in nonlymphoid tissue. *Science (New York, N.Y.)* **291(5512)** 2413-2417.

Mathews, J.D., McBryde, E.S., McVernon, J., Pallaghy, P.K. & McCaw, J.M. (2010) Prior immunity helps to explain wave-like behaviour of pandemic influenza in 1918-9. *BMC Infectious Diseases* **10** 128-2334-10-128.

Matrosovich, M.N., Matrosovich, T.Y., Gray, T., Roberts, N.A. & Klenk, H.D. (2004) Human and avian influenza viruses target different cell types in cultures of human airway epithelium. *Proceedings of the National Academy of Sciences of the United States of America* **101(13)** 4620-4624.

Mbawuike, I.N., Pacheco, S., Acuna, C.L., Switzer, K.C., Zhang, Y. & Harriman, G.R. (1999) Mucosal immunity to influenza without IgA: an IgA knockout mouse model. *Journal of Immunology (Baltimore, Md.: 1950)* **162(5)** 2530-2537.

McElhaney, J.E. (2008) Influenza vaccination in the elderly: seeking new correlates of protection and improved vaccines. *Aging Health* **4(6)** 603-613.

McElhaney, J.E., Xie, D., Hager, W.D., Barry, M.B., Wang, Y., Kleppinger, A., Ewen, C., Kane, K.P. & Bleackley, R.C. (2006) T Cell Responses Are Better Correlates of Vaccine Protection in the Elderly. *The Journal of Immunology* **176(10)** 6333-6339.

McGill, J., Heusel, J.W. & Legge, K.L. (2009) Innate immune control and regulation of influenza virus infections. *Journal of Leukocyte Biology* **86(4)** 803-812.

McGill, J., Van Rooijen, N. & Legge, K.L. (2008) Protective influenza-specific CD8 T cell responses require interactions with dendritic cells in the lungs. *The Journal of Experimental Medicine* **205(7)** 1635-1646.

McMichael, A.J., Gotch, F., Cullen, P., Askonas, B. & Webster, R.G. (1981) The human cytotoxic T cell response to influenza A vaccination. *Clinical and Experimental Immunology* **43(2)** 276-284.

McMichael, A.J., Gotch, F.M., Dongworth, D.W., Clark, A. & Potter, C.W. (1983a) Declining T-cell immunity to influenza, 1977-82. *Lancet* **2(8353)** 762-764.

McMichael, A.J., Gotch, F.M., Noble, G.R. & Beare, P.A. (1983b) Cytotoxic T-cell immunity to influenza. *The New England Journal of Medicine* **309(1)** 13-17.

McMichael, A.J., Michie, C.A., Gotch, F.M., Smith, G.L. & Moss, B. (1986) Recognition of influenza A virus nucleoprotein by human cytotoxic T lymphocytes. *The Journal of General Virology* **67(Pt 4)** 719-726.

Miller, E., Hoschler, K., Hardelid, P., Stanford, E., Andrews, N. & Zambon, M. (2010) Incidence of 2009 pandemic influenza A H1N1 infection in England: a cross-sectional serological study. *Lancet* **375(9720)** 1100-1108.

Monticelli, L.A., Sonnenberg, G.F., Abt, M.C., Alenghat, T., Ziegler, C.G., Doering, T.A., Angelosanto, J.M., Laidlaw, B.J., Yang, C.Y., Sathaliyawala, T., Kubota, M., Turner, D., Diamond, J.M., Goldrath, A.W., Farber, D.L., Collman, R.G., Wherry, E.J. & Artis, D. (2011) Innate lymphoid cells promote lung-tissue homeostasis after infection with influenza virus. *Nature Immunology* **12(11)** 1045-1054.

Monto, A.S., Gravenstein, S., Elliott, M., Colopy, M. & Schweinle, J. (2000) Clinical signs and symptoms predicting influenza infection. *Archives of Internal Medicine* **160(21)** 3243-3247.

Monto, A.S., Koopman, J.S. & Longini, I.M.,Jr (1985) Tecumseh study of illness. XIII. Influenza infection and disease, 1976-1981. *American Journal of Epidemiology* **121(6)** 811-822.

Morris, A.G., Lin, Y.L. & Askonas, B.A. (1982) Immune interferon release when a cloned cytotoxic T-cell line meets its correct influenza-infected target cell. *Nature* **295(5845)** 150-152.

Murasko, D.M., Bernstein, E.D., Gardner, E.M., Gross, P., Munk, G., Dran, S. & Abrutyn, E. (2002) Role of humoral and cell-mediated immunity in protection from influenza disease after immunization of healthy elderly. *Experimental Gerontology* **37(2-3)** 427-439.

Murphy, B.R., Nelson, D.L., Wright, P.F., Tierney, E.L., Phelan, M.A. & Chanock, R.M. (1982) Secretory and systemic immunological response in children infected with live attenuated influenza A virus vaccines. *Infection and Immunity* **36(3)** 1102-1108.

Mwau, M., McMichael, A.J. & Hanke, T. (2002) Design and validation of an enzyme-linked immunospot assay for use in clinical trials of candidate HIV vaccines. *AIDS Research and Human Retroviruses* **18(9)** 611-618.

Ng, D.H., Skehel, J.J., Kassiotis, G. & Langhorne, J. (2014) Recovery of an antiviral antibody response following attrition caused by unrelated infection. *PLoS Pathogens* **10(1)** e1003843.

Ng, W.C., Tate, M.D., Brooks, A.G. & Reading, P.C. (2012) Soluble host defense lectins in innate immunity to influenza virus. *Journal of Biomedicine & Biotechnology* **2012** 732191.

Nguyen, H.H., Moldoveanu, Z., Novak, M.J., van Ginkel, F.W., Ban, E., Kiyono, H., McGhee, J.R. & Mestecky, J. (1999) Heterosubtypic immunity to lethal influenza A virus infection is associated with virus-specific CD8(+) cytotoxic T lymphocyte responses induced in mucosa-associated tissues. *Virology* **254(1)** 50-60.

Nguyen, H.H., van Ginkel, F.W., Vu, H.L., McGhee, J.R. & Mestecky, J. (2001) Heterosubtypic immunity to influenza A virus infection requires B cells but not CD8+ cytotoxic T lymphocytes. *The Journal of Infectious Diseases* **183(3)** 368-376.

Nguyen, H.H., van Ginkel, F.W., Vu, H.L., Novak, M.J., McGhee, J.R. & Mestecky, J. (2000) Gamma interferon is not required for mucosal cytotoxic T-lymphocyte responses or heterosubtypic immunity to influenza A virus infection in mice. *Journal of Virology* **74(12)** 5495-5501.

Nichol, K. & Treanor, J. (2006) Vaccines for Seasonal and Pandemic Influenza. *The Journal of Infectious Diseases* **194** S111-S118.

Nicholls, J.M. (2013) The battle between influenza and the innate immune response in the human respiratory tract. *Infection & Chemotherapy* **45(1)** 11-21.

Novel Swine-Origin Influenza A (H1N1) Virus Investigation Team, (2009) Emergence of a Novel Swine-Origin Influenza A (H1N1) Virus in Humans. *The New England Journal of Medicine* **360(25)** 2605-2615.

Ohrmalm, L., Smedman, C., Wong, M., Broliden, K., Tolfvenstam, T. & Norbeck, O. (2013) Decreased functional T lymphocyte-mediated cytokine responses in patients with chemotherapy-induced neutropenia. *Journal of Internal Medicine* **274(4)** 363-370.

Olson, J.A., McDonald-Hyman, C., Jameson, S.C. & Hamilton, S.E. (2013) Effector-like CD8(+) T cells in the memory population mediate potent protective immunity. *Immunity* **38(6)** 1250-1260.

O'Neill, E., Krauss, S.L., Riberdy, J.M., Webster, R.G. & Woodland, D.L. (2000) Heterologous protection against lethal A/HongKong/156/97 (H5N1) influenza virus infection in C57BL/6 mice. *The Journal of General Virology* **81(Pt 11)** 2689-2696.

Oshansky, C.M., Gartland, A.J., Wong, S.S., Jeevan, T., Wang, D., Roddam, P.L., Caniza, M.A., Hertz, T., Devincenzo, J.P., Webby, R.J. & Thomas, P.G. (2014) Mucosal immune responses predict clinical outcomes during influenza infection independently of age and viral load. *American Journal of Respiratory and Critical Care Medicine* **189(4)** 449-462.

Osterholm, M.T., Kelley, N.S., Sommer, A. & Belongia, E.A. (2012) Efficacy and effectiveness of influenza vaccines: a systematic review and meta-analysis. *The Lancet Infectious Diseases* **12(1)** 36-44.

Ott, P.A., Berner, B.R., Herzog, B.A., Guerkov, R., Yonkers, N.L., Durinovic-Bello, I., Tary-Lehmann, M., Lehmann, P.V. & Anthony, D.D. (2004) CD28 costimulation enhances the sensitivity of the ELISPOT assay for detection of antigen-specific memory effector CD4 and CD8 cell populations in human diseases. *Journal of Immunological Methods* **285(2)** 223-235.

Owen, R.E., Sinclair, E., Emu, B., Heitman, J.W., Hirschkorn, D.F., Epling, C.L., Tan, Q.X., Custer, B., Harris, J.M., Jacobson, M.A., McCune, J.M., Martin, J.N., Hecht, F.M., Deeks, S.G. & Norris, P.J. (2007) Loss of T cell responses following long-term cryopreservation. *Journal of Immunological Methods* **326(1–2)** 93-115.

Paget, C., Ivanov, S., Fontaine, J., Blanc, F., Pichavant, M., Renneson, J., Bialecki, E., Pothlichet, J., Vendeville, C., Barba-Spaeth, G., Huerre, M.R., Faveeuw, C., Si-Tahar, M. & Trottein, F. (2011) Potential role of invariant NKT cells in the control of pulmonary inflammation and CD8+ T cell response during acute influenza A virus H3N2 pneumonia. *Journal of Immunology (Baltimore, Md.: 1950)* **186(10)** 5590-5602.

Pantaleo, G. & Harari, A. (2006) Functional signatures in antiviral T-cell immunity for monitoring virus-associated diseases. *Nature Reviews.Immunology* **6(5)** 417-423.

Pathirana, R.D., Bredholt, G., Akselsen, P.E., Pedersen, G.K. & Cox, R.J. (2012) A(H1N1)pdm09 vaccination of health care workers: improved immune responses in low responders following revaccination. *The Journal of Infectious Diseases* **206(11)** 1660-1669.

Pica, N., Hai, R., Krammer, F., Wang, T.T., Maamary, J., Eggink, D., Tan, G.S., Krause, J.C., Moran, T., Stein, C.R., Banach, D., Wrammert, J., Belshe, R.B., Garcia-Sastre, A. & Palese, P. (2012) Hemagglutinin stalk antibodies elicited by the 2009 pandemic influenza virus as a mechanism for the extinction of seasonal H1N1 viruses. *Proceedings of the National Academy of Sciences of the United States of America* **109(7)** 2573-2578.

Potter, M., MacMahon, E., Dark, J., Cornish, J., Bedford-Russell, A., Gupta, G., MacLennan, S., Pawson, R. & and Parker, A. (2012) *Report of the cytomegalovirus steering group.* [Online] Available from: https://www.gov.uk/government/uploads/system/uploads/attachment_data/file/215126/dh_132966.pdf [Accessed 23 April 2014].

Potter, C.W. & Oxford, J.S. (1979) Determinants of immunity to influenza infection in man. *British Medical Bulletin* **35(1)** 69-75.

Powell, T.J., Peng, Y., Berthoud, T.K., Blais, M.E., Lillie, P.J., Hill, A.V., Rowland-Jones, S.L., McMichael, A.J., Gilbert, S.C. & Dong, T. (2013) Examination of influenza specific T cell responses after influenza virus challenge in individuals vaccinated with MVA-NP+M1 vaccine. *PloS One* **8(5)** e62778.

Powell, T.J., Silk, J.D., Sharps, J., Fodor, E. & Townsend, A.R. (2012) Pseudotyped influenza A virus as a vaccine for the induction of heterotypic immunity. *Journal of Virology* **86(24)** 13397-13406.

Powell, T.J., Strutt, T., Reome, J., Hollenbaugh, J.A., Roberts, A.D., Woodland, D.L., Swain, S.L. & Dutton, R.W. (2007) Priming with cold-adapted influenza A does not prevent infection but elicits long-lived protection against supralethal challenge with heterosubtypic virus. *Journal of Immunology (Baltimore, Md.: 1950)* **178(2)** 1030-1038.

Powers, D.C., McElhaney, J.E., Florendo, O.A.,Jr, Manning, M.C., Upshaw, C.M., Bentley, D.W. & Wilkinson, B.E. (1997) Humoral and cellular immune responses following vaccination with purified recombinant hemagglutinin from influenza A (H3N2) virus. *The Journal of Infectious Diseases* **175(2)** 342-351.

Public Health England. (2012) *Influenza vaccine composition.* [Online] Available from: http://www.hpa.org.uk/web/HPAweb&HPAwebStandard/HPAweb_C/1195733812968 [Accessed 23 April 2014].

Puissant-Lubrano, B., Bossi, P., Gay, F., Crance, J.M., Bonduelle, O., Garin, D., Bricaire, F., Autran, B. & Combadiere, B. (2010) Control of vaccinia virus skin lesions by long-term-maintained IFN-gamma+TNF-alpha+ effector/memory CD4+ lymphocytes in humans. *The Journal of Clinical Investigation* **120(5**) 1636-1644.

Quast, S., Zhang, W., Shive, C., Kovalovski, D., Ott, P.A., Herzog, B.A., Boehm, B.O., Tary-Lehmann, M., Karulin, A.Y. & Lehmann, P.V. (2005) IL-2 absorption affects IFN-gamma and IL-5, but not IL-4 producing memory T cells in double color cytokine ELISPOT assays. *Cellular Immunology* **237(1**) 28-36.

Rabin, R.L., Park, M.K., Liao, F., Swofford, R., Stephany, D. & Farber, J.M. (1999) Chemokine receptor responses on T cells are achieved through regulation of both receptor expression and signaling. *Journal of Immunology (Baltimore, Md.: 1950)* **162(7**) 3840-3850.

Racaniello, V. (2009) *Viruses and the respiratory tract.* [Online] Available from: http://www.virology.ws/2009/05/21/viruses-and-the-respiratory-tract/ [Accessed 30 May 2014].

Ray, S.J., Franki, S.N., Pierce, R.H., Dimitrova, S., Koteliansky, V., Sprague, A.G., Doherty, P.C., de Fougerolles, A.R. & Topham, D.J. (2004) The collagen binding alpha1beta1 integrin VLA-1 regulates CD8 T cell-mediated immune protection against heterologous influenza infection. *Immunity* **20(2**) 167-179.

Reinhardt, R.L., Khoruts, A., Merica, R., Zell, T. & Jenkins, M.K. (2001) Visualizing the generation of memory CD4 T cells in the whole body. *Nature* **410(6824**) 101-105.

Richards, K.A., Topham, D., Chaves, F.A. & Sant, A.J. (2010) Cutting edge: CD4 T cells generated from encounter with seasonal influenza viruses and vaccines have broad protein specificity and can directly recognize naturally generated epitopes derived from the live pandemic H1N1 virus. *Journal of Immunology (Baltimore, Md.: 1950)* **185(9**) 4998-5002.

Roberts, A.D. & Woodland, D.L. (2004) Cutting edge: effector memory CD8+ T cells play a prominent role in recall responses to secondary viral infection in the lung. *Journal of Immunology (Baltimore, Md.: 1950)* **172(11**) 6533-6537.

Rogers, G.N. & Paulson, J.C. (1983) Receptor determinants of human and animal influenza virus isolates: differences in receptor specificity of the H3 hemagglutinin based on species of origin. *Virology* **127(2**) 361-373.

Roman, F., Clement, F., Dewe, W., Walravens, K., Maes, C., Willekens, J., De Boever, F., Hanon, E. & Leroux-Roels, G. (2011) Effect on cellular and humoral immune responses of the AS03 adjuvant system in an A/H1N1/2009 influenza virus vaccine administered to adults during two randomized controlled trials. *Clinical and Vaccine Immunology : CVI* **18(5**) 835-843.

Rose, M.A., Zielen, S. & Baumann, U. (2012) Mucosal immunity and nasal influenza vaccination. *Expert Review of Vaccines* **11(5**) 595-607.

Roti, M., Yang, J., Berger, D., Huston, L., James, E.A. & Kwok, W.W. (2008) Healthy Human Subjects Have CD4+ T Cells Directed against H5N1 Influenza Virus. *The Journal of Immunology* **180(3**) 1758-1768.

Sallusto, F., Lenig, D., Forster, R., Lipp, M. & Lanzavecchia, A. (1999) Two subsets of memory T lymphocytes with distinct homing potentials and effector functions. *Nature* **401(6754**) 708-712.

Scheible, K., Zhang, G., Baer, J., Azadniv, M., Lambert, K., Pryhuber, G., Treanor, J.J. & Topham, D.J. (2011) CD8+ T cell immunity to 2009 pandemic and seasonal H1N1 influenza viruses. *Vaccine* **29(11**) 2159-2168.

Schenkel, J.M., Fraser, K.A., Vezys, V. & Masopust, D. (2013) Sensing and alarm function of resident memory CD8(+) T cells. *Nature Immunology* **14(5**) 509-513.

Schmidt, T., Dirks, J., Enders, M., Gartner, B.C., Uhlmann-Schiffler, H., Sester, U. & Sester, M. (2012) CD4+ T-cell immunity after pandemic influenza vaccination cross-reacts with seasonal antigens and functionally differs from active influenza infection. *European Journal of Immunology* **42(7**) 1755-1766.

Schulman, J.L. & Kilbourne, E.D. (1965) Induction of Partial Specific Heterotypic Immunity in Mice by a Single Infection with Influenza a Virus. *Journal of Bacteriology* **8**9 170-174.

Sealy, R., Surman, S., Hurwitz, J.L. & Coleclough, C. (2003) Antibody response to influenza infection of mice: different patterns for glycoprotein and nucleocapsid antigens. *Immunology* **108(4**) 431-439.

Seder, R.A. & Ahmed, R. (2003) Similarities and differences in CD4+ and CD8+ effector and memory T cell generation. *Nature Immunology* **4(9**) 835-842.

Seder, R.A., Darrah, P.A. & Roederer, M. (2008) T-cell quality in memory and protection: implications for vaccine design. *Nat Rev Immunol* 8 247-58.

Seo, S.H., Peiris, M. & Webster, R.G. (2002) Protective cross-reactive cellular immunity to lethal A/Goose/Guangdong/1/96-like H5N1 influenza virus is correlated

with the proportion of pulmonary CD8(+) T cells expressing gamma interferon. *Journal of Virology* **76(10**) 4886-4890.

Seo, S.H. & Webster, R.G. (2001) Cross-reactive, cell-mediated immunity and protection of chickens from lethal H5N1 influenza virus infection in Hong Kong poultry markets. *Journal of Virology* **75(6**) 2516-2525.

Sester, M., Gartner, B.C., Sester, U., Girndt, M., Mueller-Lantzsch, N. & Kohler, H. (2003) Is the cytomegalovirus serologic status always accurate? A comparative analysis of humoral and cellular immunity. *Transplantation* **76(8**) 1229-1230.

Sester, M., Sester, U., Gartner, B., Kubuschok, B., Girndt, M., Meyerhans, A. & Kohler, H. (2002) Sustained high frequencies of specific CD4 T cells restricted to a single persistent virus. *Journal of Virology* **76(8**) 3748-3755.

Shahid, Z., Kleppinger, A., Gentleman, B., Falsey, A.R. & McElhaney, J.E. (2010) Clinical and immunologic predictors of influenza illness among vaccinated older adults. *Vaccine* **28(38**) 6145-6151.

Skoner, D.P., Gentile, D.A., Patel, A. & Doyle, W.J. (1999) Evidence for cytokine mediation of disease expression in adults experimentally infected with influenza A virus. *The Journal of Infectious Diseases* **180(1**) 10-14.

Slepushkin, A.N. (1959) The effect of a previous attack of A1 influenza on susceptibility to A2 virus during the 1957 outbreak. *Bulletin of the World Health Organisation* **20(2-3**) 297-301.

Slota, M., Lim, J.B., Dang, Y. & Disis, M.L. (2011) ELISpot for measuring human immune responses to vaccines. *Expert Review of Vaccines* **10(3**) 299-306.

Smith, D.J., Lapedes, A.S., de Jong, J.C., Bestebroer, T.M., Rimmelzwaan, G.F., Osterhaus, A.D. & Fouchier, R.A. (2004) Mapping the antigenic and genetic evolution of influenza virus. *Science (New York, N.Y.)* **305(5682**) 371-376.

Sonoguchi, T., Naito, H., Hara, M., Takeuchi, Y. & Fukumi, H. (1985) Cross-subtype protection in humans during sequential, overlapping, and/or concurrent epidemics

caused by H3N2 and H1N1 influenza viruses. *The Journal of Infectious Diseases* **151(1**) 81-88.

Spensieri, F., Borgogni, E., Zedda, L., Bardelli, M., Buricchi, F., Volpini, G., Fragapane, E., Tavarini, S., Finco, O., Rappuoli, R., Del Giudice, G., Galli, G. & Castellino, F. (2013) Human circulating influenza-CD4+ ICOS1+IL-21+ T cells expand after vaccination, exert helper function, and predict antibody responses. *Proceedings of the National Academy of Sciences of the United States of America* **110(35**) 14330-14335.

Sridhar, S., Begom, S., Bermingham, A., Hoschler, K., Adamson, W., Carman, W., Bean, T., Barclay, W., Deeks, J.J. & Lalvani, A. (2013) Cellular immune correlates of protection against symptomatic pandemic influenza. *Nature Medicine* **19(10)** 1305-1312.

Sridhar, S., Begom, S., Bermingham, A., Ziegler, T., Roberts, K.L., Barclay, W.S., Openshaw, P. & Lalvani, A. (2012) Predominance of heterosubtypic IFN-gamma-only-secreting effector memory T cells in pandemic H1N1 naive adults. *European Journal of Immunology* **42(11)** 2913-2924.

Steel, J., Staeheli, P., Mubareka, S., Garcia-Sastre, A., Palese, P. & Lowen, A.C. (2010) Transmission of pandemic H1N1 influenza virus and impact of prior exposure to seasonal strains or interferon treatment. *Journal of Virology* **84(1)** 21-26.

Straight, T.M., Ottolini, M.G., Prince, G.A. & Eichelberger, M.C. (2006) Evidence of a cross-protective immune response to influenza A in the cotton rat model. *Vaccine* **24(37-39)** 6264-6271.

Sui, J., Sheehan, J., Hwang, W.C., Bankston, L.A., Burchett, S.K., Huang, C.Y., Liddington, R.C., Beigel, J.H. & Marasco, W.A. (2011) Wide prevalence of heterosubtypic broadly neutralising human anti-influenza a antibodies. *Clinical Infectious Diseases : An Official Publication of the Infectious Diseases Society of America* **52(8)** 1003-1009.

Sun, J., Madan, R., Karp, C.L. & Braciale, T.J. (2009) Effector T cells control lung inflammation during acute influenza virus infection by producing IL-10. *Nature Medicine* **15(3)** 277-284.

Sung, S.S., Fu, S.M., Rose, C.E.,Jr, Gaskin, F., Ju, S.T. & Beaty, S.R. (2006) A major lung CD103 (alphaE)-beta7 integrin-positive epithelial dendritic cell population expressing Langerin and tight junction proteins. *Journal of Immunology (Baltimore, Md.: 1950)* **176(4)** 2161-2172.

Tamura, S. & Kurata, T. (2004) Defense mechanisms against influenza virus infection in the respiratory tract mucosa. *Japanese Journal of Infectious Diseases* **57(6)** 236-247.

Tate, M.D., Ioannidis, L.J., Croker, B., Brown, L.E., Brooks, A.G. & Reading, P.C. (2011) The role of neutrophils during mild and severe influenza virus infections of mice. *PloS One* **6(3)** e17618.

Taylor, P.M. & Askonas, B.A. (1986) Influenza nucleoprotein-specific cytotoxic T-cell clones are protective in vivo. *Immunology* **58(3)** 417-420.

Terajima, M., Cruz, J., Leporati, A.M., Orphin, L., Babon, J.A., Co, M.D., Pazoles, P., Jameson, J. & Ennis, F.A. (2008) Influenza A virus matrix protein 1-specific human CD8+ T-cell response induced in trivalent inactivated vaccine recipients. *Journal of Virology* **82(18)** 9283-9287.

Thompson, M. G., Shay, D. K., Zhou, H., Bridges, C. B., Cheng, P. Y., Burns, E., Bresee, J. S. & Cox, N. J. (2010) *Estimates of Deaths Associated with Seasonal Influenza - United States, 1976 - 2007.* [Online] Available from: http://www.cdc.gov/mmwr/preview/mmwrhtml/mm5933a1.htm [Accessed 17.03.2014].

Throsby, M., van den Brink, E., Jongeneelen, M., Poon, L.L., Alard, P., Cornelissen, L., Bakker, A., Cox, F., van Deventer, E., Guan, Y., Cinatl, J., ter Meulen, J., Lasters, I., Carsetti, R., Peiris, M., de Kruif, J. & Goudsmit, J. (2008) Heterosubtypic

neutralising monoclonal antibodies cross-protective against H5N1 and H1N1 recovered from human IgM+ memory B cells. *PloS One* **3(12**) e3942.

Topham, D.J., Tripp, R.A. & Doherty, P.C. (1997) CD8+ T cells clear influenza virus by perforin or Fas-dependent processes. *Journal of Immunology (Baltimore, Md.: 1950)* **159(11**) 5197-5200.

Touvrey, C., Derré, L., Devevre, E., Corthesy, P., Romero, P., Rufer, N. & Speiser, D.E. (2009) Dominant Human CD8 T Cell Clonotypes Persist Simultaneously as Memory and Effector Cells in Memory Phase. *The Journal of Immunology* **182(11**) 6718-6726.

Townsend, A.R. & Skehel, J.J. (1984) The influenza A virus nucleoprotein gene controls the induction of both subtype specific and cross-reactive cytotoxic T cells. *The Journal of Experimental Medicine* **160(2**) 552-563.

Tricco, A.C., Chit, A., Soobiah, C., Hallett, D., Meier, G., Chen, M.H., Tashkandi, M., Bauch, C.T. & Loeb, M. (2013) Comparing influenza vaccine efficacy against mismatched and matched strains: a systematic review and meta-analysis. *BMC Medicine* **1**1 153-7015-11-153.

Trifonov, V., Khiabanian, H. & Rabadan, R. (2009) Geographic dependence, surveillance, and origins of the 2009 influenza A (H1N1) virus. *The New England Journal of Medicine* **361(2**) 115-119.

Tu, W., Mao, H., Zheng, J., Liu, Y., Chiu, S.S., Qin, G., Chan, P.L., Lam, K.T., Guan, J., Zhang, L., Guan, Y., Yuen, K.Y., Peiris, J.S. & Lau, Y.L. (2010) Cytotoxic T lymphocytes established by seasonal human influenza cross-react against 2009 pandemic H1N1 influenza virus. *Journal of Virology* **84(13**) 6527-6535.

Turley, C.B., Rupp, R.E., Johnson, C., Taylor, D.N., Wolfson, J., Tussey, L., Kavita, U., Stanberry, L. & Shaw, A. (2011) Safety and immunogenicity of a recombinant M2e-flagellin influenza vaccine (STF2.4xM2e) in healthy adults. *Vaccine* **29(32**) 5145-5152.

Valkenburg, S.A., Rutigliano, J.A., Ellebedy, A.H., Doherty, P.C., Thomas, P.G. & Kedzierska, K. (2011) Immunity to seasonal and pandemic influenza A viruses. *Microbes and Infection / Institut Pasteur* **13(5**) 489-501.

Van Reeth, K. (2000) Cytokines in the pathogenesis of influenza. *Veterinary Microbiology* **74(1-2**) 109-116.

van Riel, D., den Bakker, M.A., Leijten, L.M., Chutinimitkul, S., Munster, V.J., de Wit, E., Rimmelzwaan, G.F., Fouchier, R.A., Osterhaus, A.D. & Kuiken, T. (2010) Seasonal and pandemic human influenza viruses attach better to human upper respiratory tract epithelium than avian influenza viruses. *The American Journal of Pathology* **176(4**) 1614-1618.

van Riel, D., Munster, V.J., de Wit, E., Rimmelzwaan, G.F., Fouchier, R.A., Osterhaus, A.D. & Kuiken, T. (2007) Human and avian influenza viruses target different cells in the lower respiratory tract of humans and other mammals. *The American Journal of Pathology* **171(4**) 1215-1223.

Vogt, A., Mahe, B., Costagliola, D., Bonduelle, O., Hadam, S., Schaefer, G., Schaefer, H., Katlama, C., Sterry, W., Autran, B., Blume-Peytavi, U. & Combadiere, B. (2008) Transcutaneous anti-influenza vaccination promotes both CD4 and CD8 T cell immune responses in humans. *Journal of Immunology (Baltimore, Md.: 1950)* **180(3**) 1482-1489.

Wagar, L.E., Rosella, L., Crowcroft, N., Lowcock, B., Drohomyrecky, P.C., Foisy, J., Gubbay, J., Rebbapragada, A., Winter, A.L., Achonu, C., Ward, B.J. & Watts, T.H. (2011) Humoral and cell-mediated immunity to pandemic H1N1 influenza in a Canadian cohort one year post-pandemic: implications for vaccination. *PloS One* **6(11**) e28063.

Wang, T.T., Tan, G.S., Hai, R., Pica, N., Ngai, L., Ekiert, D.C., Wilson, I.A., Garcia-Sastre, A., Moran, T.M. & Palese, P. (2010) Vaccination with a synthetic peptide from the influenza virus hemagglutinin provides protection against distinct viral subtypes. *Proceedings of the National Academy of Sciences of the United States of America* **107(44**) 18979-18984.

Weaver, J.M., Yang, H., Roumanes, D., Lee, F.E., Wu, H., Treanor, J.J. & Mosmann, T.R. (2013) Increase in IFNgamma(-)IL-2(+) cells in recent human CD4 T cell responses to 2009 pandemic H1N1 influenza. *PloS One* **8(3)** e57275.

Weinfurter, J.T., Brunner, K., Capuano, S.V.,3rd, Li, C., Broman, K.W., Kawaoka, Y. & Friedrich, T.C. (2011) Cross-reactive T cells are involved in rapid clearance of 2009 pandemic H1N1 influenza virus in nonhuman primates. *PLoS Pathogens* **7(11)** e1002381.

Wells, M.A., Ennis, F.A. & Albrecht, P. (1981) Recovery from a viral respiratory infection. II. Passive transfer of immune spleen cells to mice with influenza pneumonia. *Journal of Immunology (Baltimore, Md.: 1950)* **126(3)** 1042-1046.

Wherry, E.J., Teichgraber, V., Becker, T.C., Masopust, D., Kaech, S.M., Antia, R., von Andrian, U.H. & Ahmed, R. (2003) Lineage relationship and protective immunity of memory CD8 T cell subsets. *Nature Immunology* **4(3)** 225-234.

WHO. (2010) *Director-General's opening statement at virtual press conference.* [Online] Available from: http://web.archive.org/web/20110526060208/http://www.who.int/mediacentre/news/statements/2010/h1n1_vpc_20100810/en/index.html [Accessed 23 April 2014].

WHO. (2014a) *FluNet Influenza Laboratory Surveillance Information in United Kingdom of Great Britain and Northern Ireland by the Global Influenza Surveillance and Response System.* [Online] Available from: http://www.who.int/influenza/gisrs_laboratory/flunet/en/ [Accessed 23 April 2014].

WHO. (2014b) *Influenza fact sheet No. 211.* [Online] Available from: http://www.who.int/mediacentre/factsheets/fs211/en/ [Accessed 17.03.14].

WHO. (2013) *Recommended composition of influenza virus vaccines for use in 2013 - 14 northern hemisphere influenza seasons.* [Online] Available from: http://www.who.int/influenza/vaccines/virus/recommendations/2013_14_north/en/ [Accessed 23 April 2014].

Wilkinson, K.A. & Wilkinson, R.J. (2010) Polyfunctional T cells in human tuberculosis. *European Journal of Immunology* **40(8**) 2139-2142.

Wilkinson, T.M., Li, C.K., Chui, C.S., Huang, A.K., Perkins, M., Liebner, J.C., Lambkin-Williams, R., Gilbert, A., Oxford, J., Nicholas, B., Staples, K.J., Dong, T., Douek, D.C., McMichael, A.J. & Xu, X.N. (2012) Preexisting influenza-specific CD4+ T cells correlate with disease protection against influenza challenge in humans. *Nature Medicine* **18(2**) 274-280.

Wraith, D.C., Vessey, A.E. & Askonas, B.A. (1987) Purified influenza virus nucleoprotein protects mice from lethal infection. *The Journal of General Virology* **68 (Pt 2)(Pt 2**) 433-440.

Wrammert, J., Koutsonanos, D., Li, G.M., Edupuganti, S., Sui, J., Morrissey, M., McCausland, M., Skountzou, I., Hornig, M., Lipkin, W.I., Mehta, A., Razavi, B., Del Rio, C., Zheng, N.Y., Lee, J.H., Huang, M., Ali, Z., Kaur, K., Andrews, S., Amara, R.R., Wang, Y., Das, S.R., O'Donnell, C.D., Yewdell, J.W., Subbarao, K., Marasco, W.A., Mulligan, M.J., Compans, R., Ahmed, R. & Wilson, P.C. (2011) Broadly cross-reactive antibodies dominate the human B cell response against 2009 pandemic H1N1 influenza virus infection. *The Journal of Experimental Medicine* **208(1**) 181-193.

Wu, T., Hu, Y., Lee, Y.T., Bouchard, K.R., Benechet, A., Khanna, K. & Cauley, L.S. (2014) Lung-resident memory CD8 T cells (TRM) are indispensable for optimal cross-protection against pulmonary virus infection. *Journal of Leukocyte Biology* **95(2)** 215-224.

Yap, K.L. & Ada, G.L. (1978) The recovery of mice from influenza A virus infection: adoptive transfer of immunity with influenza virus-specific cytotoxic T lymphocytes recognizing a common virion antigen. *Scandinavian Journal of Immunology* **8(5)** 413-420.

Yap, K.L., Ada, G.L. & McKenzie, I.F. (1978) Transfer of specific cytotoxic T lymphocytes protects mice inoculated with influenza virus. *Nature* **273(5659)** 238-239.

Yetter, R.A., Barber, W.H. & Small, P.A.,Jr (1980) Heterotypic immunity to influenza in ferrets. *Infection and Immunity* **29(2)** 650-653.

Yewdell, J.W., Bennink, J.R., Smith, G.L. & Moss, B. (1985) Influenza A virus nucleoprotein is a major target antigen for cross-reactive anti-influenza A virus cytotoxic T lymphocytes. *Proceedings of the National Academy of Sciences of the United States of America* **82(6)** 1785-1789.

Yin, J.K., Chow, M.Y., Khandaker, G., King, C., Richmond, P., Heron, L. & Booy, R. (2012) Impacts on influenza A(H1N1)pdm09 infection from cross-protection of seasonal trivalent influenza vaccines and A(H1N1)pdm09 vaccines: systematic review and meta-analyses. *Vaccine* **30(21)** 3209-3222.

Yu, W.C., Chan, R.W., Wang, J., Travanty, E.A., Nicholls, J.M., Peiris, J.S., Mason, R.J. & Chan, M.C. (2011) Viral replication and innate host responses in primary human alveolar epithelial cells and alveolar macrophages infected with influenza H5N1 and H1N1 viruses. *Journal of Virology* **85(14)** 6844-6855.

Yu, X., Tsibane, T., McGraw, P.A., House, F.S., Keefer, C.J., Hicar, M.D., Tumpey, T.M., Pappas, C., Perrone, L.A., Martinez, O., Stevens, J., Wilson, I.A., Aguilar, P.V., Altschuler, E.L., Basler, C.F. & Crowe, J.E.,Jr (2008) Neutralizing antibodies derived from the B cells of 1918 influenza pandemic survivors. *Nature* **455(7212)** 532-536.

Zambon, M.C. (2001) The pathogenesis of influenza in humans. *Reviews in Medical Virology* **11(4)** 227-241.

Zebedee, S.L. & Lamb, R.A. (1988) Influenza A virus M2 protein: monoclonal antibody restriction of virus growth and detection of M2 in virions. *Journal of Virology* **62(8)** 2762-2772.

Zhang, H., Wang, L., Compans, R.W. & Wang, B.Z. (2014) Universal influenza vaccines, a dream to be realized soon. *Viruses* **6(5)** 1974-1991.

Zhao, Y., Zhang, Y.H., Denney, L., Young, D., Powell, T.J., Peng, Y.C., Li, N., Yan, H.P., Wang, D.Y., Shu, Y.L., Kendrick, Y., McMichael, A.J., Ho, L.P. & Dong, T. (2012) High levels of virus-specific CD4+ T cells predict severe pandemic influenza

A virus infection. *American Journal of Respiratory and Critical Care Medicine* **186(12)** 1292-1297.

Zimmerli, S.C., Harari, A., Cellerai, C., Vallelian, F., Bart, P. & Pantaleo, G. (2005) HIV-1-specific IFN-γ/IL-2-secreting CD8 T cells support CD4-independent proliferation of HIV-1-specific CD8 T cells. *Proceedings of the National Academy of Sciences of the United States of America* **102(20)** 7239-7244.

Zweerink, H.J., Askonas, B.A., Millican, D., Courtneidge, S.A. & Skehel, J.J. (1977a) Cytotoxic T cells to type A influenza virus; viral hemagglutinin induces A-strain specificity while infected cells confer cross-reactive cytotoxicity. *European Journal of Immunology* **7(9)** 630-635.

Zweerink, H.J., Courtneidge, S.A., Skehel, J.J., Crumpton, M.J. & Askonas, B.A. (1977b) Cytotoxic T cells kill influenza virus infected cells but do not distinguish between serologically distinct type A viruses. *Nature* **267(5609)** 354-356.

6 APPENDIX

Table 6.1 Expected conserved HLA-I CD8 9-mer epitopes of influenza A virus proteins Polymerase Basic Protein 1 (PB1), Matrix 1 (M1) and Nucleoprotein (NP) and predicted HLA restriction.

Protein	Peptide ID	Amino Acid position and Sequence	HLA restriction
PB1	PB1/1	4-NPTLLFLKV-12	HLA-A2
PB1	PB1/2	16-NAISTTFPY-24	HLA-A2
PB1	PB1/3	22-FPYTGDPPY-30	ND
PB1	PB1/4	30-YSHGTGTGY-38	HLA-A1, A26, A30, A29
PB1	PB1/5	77-NEPSGYAQT-85	HLA-A1
PB1	PB1/6	81-GYAQTDCVL-89	ND
PB1	PB1/7	83-AQTDCVLEA-91	ND
PB1	PB1/8	123-TQGRQTYDW-131	ND
PB1	PB1/9	127-QTYDWTLNR-135	ND
PB1	PB1/10	221-ALTLNTMTK-229	ND
PB1	PB1/11	228-TKDAERGKL-236	ND
PB1	PB1/12	230-DAERGKLKR-238	ND
PB1	PB1/13	233-RGKLKRRAI-241	ND
PB1	PB1/14	235-KLKRRAIAT-243	HLA-B27
PB1	PB1/15	238-RRAIATPGM-246	HLA-B27
PB1	PB1/16	240-AIATPGMQI-248	HLA-B27
PB1	PB1/17	243-TPGMQIRGF-251	ND
PB1	PB1/18	271-LPVGGNEKK-279	ND
PB1	PB1/19	274-GGNEKKAKL-282	ND
PB1	PB1/20	275-GNEKKAKLA-283	ND
PB1	PB1/21	277-EKKAKLANV-285	ND
PB1	PB1/22	280-AKLANVVRK-288	ND
PB1	PB1/23	281-KLANVVRKM-289	ND
PB1	PB1/24	340-APIMFSNKM-348	ND
PB1	PB1/25	342-IMFSNKMAR-350	ND
PB1	PB1/26	343-MFSNKMARL-351	ND
PB1	PB1/27	347-KMARLGKGY-355	HLA-B62
PB1	PB1/28	349-ARLGKGYMF-357	HLA-B27
PB1	PB1/29	403-LSPGMMMGM-411	HLA-A2
PB1	PB1/30	404-SPGMMMGMF-412	HLA-A2
PB1	PB1/31	407-MMMGMFNML-415	HLA-A2
PB1	PB1/32	410-GMFNMLSTV-418	HLA-A2
PB1	PB1/33	411-MFNMLSTVL-419	HLA-A2
PB1	PB1/34	413-NMLSTVLGV-421	HLA-A2
PB1	PB1/35	439-DGLQSSDDF-447	ND
PB1	PB1/36	441-LQSSDDFAL-449	ND
PB1	PB1/37	443-SSDDFALIV-451	ND
PB1	PB1/38	475-INMSKKKSY-483	HLA-A3, A11, A31, A68
PB1	PB1/39	487-TGTFEFTSF-495	HLA-A03, A11, A31, A68
PB1	PB1/40	489-TFEFTSFFY-497	HLA-A1
PB1	PB1/41	491-EFTSFFYRY-499	
PB1	PB1/42	497-YRYGFVANF-505	HLA-A24
PB1	PB1/43	501-FVANFSMEL-509	HLA-A2
PB1	PB1/44	504-NFSMELPSF-512	HLA-A2
PB1	PB1/45	598-LYNIRNLHI-606	ND
PB1	PB1/46	658-DAVATTHSW-666	ND
PB1	PB1/47	669-KRNRSILNT-677	ND
PB1	PB1/48	697-EKFFPSSSY-705	ND
PB1	PB1/49	698-KFFPSSSYR-706	ND
PB1	PB1/50	699-FFPSSSYRR-707	ND
PB1	PB1/51	716-EAMVSRARI-724	ND
M1	M1/1	29-EDVFAGKNT-37	HLA-A3
M1	M1/2	31-VFAGKNTDL-39	HLA-A2
M1	M1/3	37-TDLEALMEW-45	ND
M1	M1/4	49-RPILSPLTK-57	HLA-A3
M1	M1/5	51-ILSPLTKGI-59	HLA-A2
M1	M1/6	56-TKGILGFVF-64	HLA-A2
M1	M1/7	58-GILGFVFTL-66	HLA-A2
M1	M1/8	60-LGFVFTLTV-68	HLA-A2
M1	M1/9	66-LTVPSERGL-74	HLA-A2
M1	M1/10	68-VPSERGLQR-76	HLA-A2
M1	M1/11	71-ERGLQRRRF-79	HLA-A2
M1	M1/12	75-QRRRFVQNA-83	HLA-A2
M1	M1/13	76-RRRFVQNAL-84	HLA-A2
M1	M1/14	122-GALASCMGL-130	HLA-B35
M1	M1/15	123-ALASCMGLI-131	HLA-B35
M1	M1/16	124-LASCMGLIY-132	HLA-B35
M1	M1/17	126-SCMGLIYNR-134	HLA-A3, A11, A31,

			A33, A68, B27, B35
M1	M1/18	177-NRMVLASTT-185	HLA-A3, A11
M1	M1/19	179-MVLASTTAK-187	HLA-A3, A11
M1	M1/20	180-VLASTTAKA-188	HLA-A3, A11
M1	M1/21	181-LASTTAKAM-189	HLA-A3, A11
NP	NP/1	88-DPKKTGGPI-96	HLA-A68
NP	NP/2	89-PKKTGGPIY-97	HLA-A68
NP	NP/3	147-TYQRTRALV-155	HLA-B15
NP	NP/4	149-QRTRALVRT-157	HLA-A68
NP	NP/5	158-GMDPRMCSL-166	HLA-2
NP	NP/6	164-CSLMQGSTL-172	HLA-B15
NP	NP/7	166-LMQGSTLPR-174	HLA-B15
NP	NP/8	218-AYERMCNIL-226	HLA-B18
NP	NP/9	225-ILKGKFQTA-233	HLA-B8
NP	NP/10	226-LKGKFQTAA-234	HLA-B15
NP	NP/11	245-SRNPGNAEI-253	HLA-B15
NP	NP/12	250-NAEIEDLIF-258	HLA-B40
NP	NP/13	256-LIFLARSAL-264	HLA-A2
NP	NP/14	257-IFLARSALI-265	HLA-A2
NP	NP/15	258-FLARSALIL-266	HLA-A3
NP	NP/16	296-YSLVGIDPF-304	HLA-B15
NP	NP/17	462-GVFELSDEK-470	HLA-B15
NP	NP/18	463-VFELSDEKA-471	HLA-B15
NP	NP/19	464-FELSDEKAT-472	HLA-B15

Table 6.2 15-mer overlapping peptides from M1 antigen of influenza A/California/07/09

Protein	Peptide id	Peptide sequence
M1	M1 1	MSLLTEVETYVLSII
M1	M1 2	EVETYVLSIIPSGPL
M1	M1 3	VLSIIPSGPLKAEIA
M1	M1 4	PSGPLKAEIAQRLES
M1	M1 5	KAEIAQRLESVFAGK
M1	M1 6	QRLESVFAGKNTDLE
M1	M1 7	VFAGKNTDLEALMEW
M1	M1 8	NTDLEALMEWLKTRP
M1	M1 9	ALMEWLKTRPILSPL
M1	M1 10	LKTRPILSPLTKGIL
M1	M1 11	ILSPLTKGILGFVFT
M1	M1 12	TKGILGFVFTLTVPS
M1	M1 13	GFVFTLTVPSERGLQ
M1	M1 14	LTVPSERGLQRRRFV
M1	M1 15	ERGLQRRRFVQNALN
M1	M1 16	RRRFVQNALNGNGDP
M1	M1 17	QNALNGNGDPNNMDR
M1	M1 18	GNGDPNNMDRAVKLY
M1	M1 19	NNMDRAVKLYKKLKR
M1	M1 20	AVKLYKKLKREITFH
M1	M1 21	KKLKREITFHGAKEV
M1	M1 22	EITFHGAKEVSLSYS
M1	M1 23	GAKEVSLSYSTGALA
M1	M1 24	SLSYSTGALASCMGL
M1	M1 25	TGALASCMGLIYNRM
M1	M1 26	SCMGLIYNRMGTVTT
M1	M1 27	IYNRMGTVTTEAAFG
M1	M1 28	GTVTTEAAFGLVCAT
M1	M1 29	EAAFGLVCATCEQIA
M1	M1 30	LVCATCEQIADSQHR
M1	M1 31	CEQIADSQHRSHRQM
M1	M1 32	DSQHRSHRQMATTTN
M1	M1 33	SHRQMATTTNPLIRH
M1	M1 34	ATTTNPLIRHENRMV
M1	M1 35	PLIRHENRMVLASTT
M1	M1 36	ENRMVLASTTAKAME
M1	M1 37	LASTTAKAMEQMAGS
M1	M1 38	AKAMEQMAGSSEQAA
M1	M1 39	QMAGSSEQAAEAMEV
M1	M1 40	SEQAAEAMEVANQTR
M1	M1 41	EAMEVANQTRQMVHA
M1	M1 42	ANQTRQMVHAMRTIG
M1	M1 43	QMVHAMRTIGTHPSS
M1	M1 44	MRTIGTHPSSSAGLK
M1	M1 45	THPSSSAGLKDDLLE
M1	M1 46	SAGLKDDLLENLQAY
M1	M1 47	DDLLENLQAYQKRMG
M1	M1 48	NLQAYQKRMGVQMQR
M1	M1 49	QKRMGVQMQRFK

Table 6.3 15-mer overlapping peptides from NP antigen of influenza A/California/07/09

Protein	Peptide id	Peptide sequence
NP	NP 1	MASQGTKRSYEQMET
NP	NP 2	TKRSYEQMETGGERQ
NP	NP 3	EQMETGGERQDATEI
NP	NP 4	GGERQDATEIRASVG
NP	NP 5	DATEIRASVGRMIGG
NP	NP 6	RASVGRMIGGIGRFY
NP	NP 7	RMIGGIGRFYIQMCT
NP	NP 8	IGRFYIQMCTELKLS
NP	NP 9	IQMCTELKLSDYDGR
NP	NP 10	ELKLSDYDGRLIQNS
NP	NP 11	DYDGRLIQNSITIER
NP	NP 12	LIQNSITIERMVLSA
NP	NP 13	ITIERMVLSAFDERR
NP	NP 14	MVLSAFDERRNKYLE
NP	NP 15	FDERRNKYLEEHPSA
NP	NP 16	NKYLEEHPSAGKDPK
NP	NP 17	EHPSAGKDPKKTGGP
NP	NP 18	GKDPKKTGGPIYRRV
NP	NP 19	KTGGPIYRRVDGKWM
NP	NP 20	IYRRVDGKWMRELIL
NP	NP 21	DGKWMRELILYDKEE
NP	NP 22	RELILYDKEEIRRVW
NP	NP 23	YDKEEIRRVWRQANN
NP	NP 24	IRRVWRQANNGEDAT
NP	NP 25	RQANNGEDATAGLTH
NP	NP 26	GEDATAGLTHIMIWH
NP	NP 27	AGLTHIMIWHSNLND
NP	NP 28	IMIWHSNLNDATYQR
NP	NP 29	SNLNDATYQRTRALV
NP	NP 30	ATYQRTRALVRTGMD
NP	NP 31	TRALVRTGMDPRMCS
NP	NP 32	RTGMDPRMCSLMQGS
NP	NP 33	PRMCSLMQGSTLPRR
NP	NP 34	LMQGSTLPRRSGAAG
NP	NP 35	TLPRRSGAAGAAVKG
NP	NP 36	SGAAGAAVKGVGTIA
NP	NP 37	AAVKGVGTIAMELIR
NP	NP 38	VGTIAMELIRMIKRG
NP	NP 39	MELIRMIKRGINDRN
NP	NP 40	MIKRGINDRNFWRGE
NP	NP 41	INDRNFWRGENGRRT
NP	NP 42	FWRGENGRRTRVAYE
NP	NP 43	NGRRTRVAYERMCNI
NP	NP 44	RVAYERMCNILKGKF
NP	NP 45	RMCNILKGKFQTAAQ
NP	NP 46	LKGKFQTAAQRAMMD
NP	NP 47	QTAAQRAMMDQVRES
NP	NP 48	RAMMDQVRESRNPGN
NP	NP 49	QVRESRNPGNAEIED
NP	NP 50	RNPGNAEIEDLIFLA
NP	NP 51	AEIEDLIFLARSALI
NP	NP 52	LIFLARSALILRGSV
NP	NP 53	RSALILRGSVAHKSC
NP	NP 54	LRGSVAHKSCLPACV
NP	NP 55	AHKSCLPACVYGLAV
NP	NP 56	LPACVYGLAVASGHD
NP	NP 57	YGLAVASGHDFEREG
NP	NP 58	ASGHDFEREGYSLVG
NP	NP 59	FEREGYSLVGIDPFK
NP	NP 60	YSLVGIDPFKLLQNS
NP	NP 61	IDPFKLLQNSQVVSL
NP	NP 62	LLQNSQVVSLMRPNE
NP	NP 63	QVVSLMRPNENPAHK
NP	NP 64	MRPNENPAHKSQLVW
NP	NP 65	NPAHKSQLVWMACHS
NP	NP 66	SQLVWMACHSAAFED

NP	**NP 67**	**MACHSAAFEDLRVSS**
NP	**NP 68**	**AAFEDLRVSSFIRGK**
NP	**NP 69**	**LRVSSFIRGKKVIPR**
NP	**NP 70**	**FIRGKKVIPRGKLST**
NP	**NP 71**	**KVIPRGKLSTRGVQI**
NP	**NP 72**	**GKLSTRGVQIASNEN**
NP	**NP 73**	**RGVQIASNENVETMD**
NP	**NP 74**	**ASNENVETMDSNTLE**
NP	**NP 75**	**VETMDSNTLELRSRY**
NP	**NP 76**	**SNTLELRSRYWAIRT**
NP	**NP 77**	**LRSRYWAIRTRSGGN**
NP	**NP 78**	**WAIRTRSGGNTNQQK**
NP	**NP 79**	**RSGGNTNQQKASAGQ**
NP	**NP 80**	**TNQQKASAGQISVQP**
NP	**NP 81**	**ASAGQISVQPTFSVQ**
NP	**NP 82**	**ISVQPTFSVQRNLPF**
NP	**NP 83**	**TFSVQRNLPFERATV**
NP	**NP 84**	**RNLPFERATVMAAFS**
NP	**NP 85**	**ERATVMAAFSGNNEG**
NP	**NP 86**	**MAAFSGNNEGRTSDM**
NP	**NP 87**	**GNNEGRTSDMRTEVI**
NP	**NP 88**	**RTSDMRTEVIRMMES**
NP	**NP 89**	**RTEVIRMMESAKPED**
NP	**NP 90**	**RMMESAKPEDLSFQG**
NP	**NP 91**	**AKPEDLSFQGRGVFE**
NP	**NP 92**	**LSFQGRGVFELSDEK**
NP	**NP 93**	**RGVFELSDEKATNPI**
NP	**NP 94**	**LSDEKATNPIVPSFD**
NP	**NP 95**	**ATNPIVPSFDMSNEG**
NP	**NP 96**	**VPSFDMSNEGSYFFG**
NP	**NP 97**	**MSNEGSYFFGDNAEE**
NP	**NP 98**	**SYFFGDNAEEYDS**

Table 6.4 15-mer overlapping peptides from PB1 antigen of influenza A/California/07/09

Protein	Peptide id	Peptide sequence
PB1	PB1 1	MDVNPTLLFLKIPAQ
PB2	PB1 2	TLLFLKIPAQNAIST
PB3	PB1 3	KIPAQNAISTTFPYT
PB4	PB1 4	NAISTTFPYTGDPPY
PB5	PB1 5	TFPYTGDPPYSHGTG
PB6	PB1 6	GDPPYSHGTGTGYTM
PB7	PB1 7	SHGTGTGYTMDTVNR
PB8	PB1 8	TGYTMDTVNRTHQYS
PB9	PB1 9	DTVNRTHQYSEKGKW
PB10	PB1 10	THQYSEKGKWTTNTE
PB11	PB1 11	EKGKWTTNTETGAPQ
PB12	PB1 12	TTNTETGAPQLNPID
PB13	PB1 13	TGAPQLNPIDGPLPE
PB14	PB1 14	LNPIDGPLPEDNEPS
PB15	PB1 15	GPLPEDNEPSGYAQT
PB16	PB1 16	DNEPSGYAQTDCVLE
PB17	PB1 17	GYAQTDCVLEAMAFL
PB18	PB1 18	DCVLEAMAFLEESHP
PB19	PB1 19	AMAFLEESHPGIFEN
PB20	PB1 20	EESHPGIFENSCLET
PB21	PB1 21	GIFENSCLETMEVVQ
PB22	PB1 22	SCLETMEVVQQTRVD
PB23	PB1 23	MEVVQQTRVDKLTQG
PB24	PB1 24	QTRVDKLTQGRQTYD
PB25	PB1 25	KLTQGRQTYDWTLNR
PB26	PB1 26	RQTYDWTLNRNQPAA
PB27	PB1 27	WTLNRNQPAATALAN
PB28	PB1 28	NQPAATALANTIEVF
PB29	PB1 29	TALANTIEVFRSNGL
PB30	PB1 30	TIEVFRSNGLTANES
PB31	PB1 31	RSNGLTANESGRLID
PB32	PB1 32	TANESGRLIDFLKDV
PB33	PB1 33	GRLIDFLKDVMESMN
PB34	PB1 34	FLKDVMESMNKEEIE
PB35	PB1 35	MESMNKEEIEITTHF
PB36	PB1 36	KEEIEITTHFQRKRR
PB37	PB1 37	ITTHFQRKRRVRDNM
PB38	PB1 38	QRKRRVRDNMTKKMV
PB39	PB1 39	VRDNMTKKMVTQRTI
PB40	PB1 40	TKKMVTQRTIGKKKQ
PB41	PB1 41	TQRTIGKKKQRLNKR
PB42	PB1 42	GKKKQRLNKRGYLIR
PB43	PB1 43	RLNKRGYLIRALTLN
PB44	PB1 44	GYLIRALTLNTMTKD
PB45	PB1 45	ALTLNTMTKDAERGK
PB46	PB1 46	TMTKDAERGKLKRRA
PB47	PB1 47	AERGKLKRRAIATPG
PB48	PB1 48	LKRRAIATPGMQIRG
PB49	PB1 49	IATPGMQIRGFVYFV
PB50	PB1 50	MQIRGFVYFVETLAR
PB51	PB1 51	FVYFVETLARSICEK
PB52	PB1 52	ETLARSICEKLEQSG
PB53	PB1 53	SICEKLEQSGLPVGG
PB54	PB1 54	LEQSGLPVGGNEKKA
PB55	PB1 55	LPVGGNEKKAKLANV
PB56	PB1 56	NEKKAKLANVVRKMM
PB57	PB1 57	KLANVVRKMMTNSQD
PB58	PB1 58	VRKMMTNSQDTEISF
PB59	PB1 59	TNSQDTEISFTITGD
PB60	PB1 60	TEISFTITGDNTKWN
PB61	PB1 61	TITGDNTKWNENQNP
PB62	PB1 62	NTKWNENQNPRMFLA
PB63	PB1 63	ENQNPRMFLAMITYI
PB64	PB1 64	RMFLAMITYITRNQP
PB65	PB1 65	MITYITRNQPEWFRN
PB66	PB1 66	TRNQPEWFRNILSMA

PB67	PB1 67	EWFRNILSMAPIMFS
PB68	PB1 68	ILSMAPIMFSNKMAR
PB69	PB1 69	PIMFSNKMARLGKGY
PB70	PB1 70	NKMARLGKGYMFESK
PB71	PB1 71	LGKGYMFESKRMKIR
PB72	PB1 72	MFESKRMKIRTQIPA
PB73	PB1 73	RMKIRTQIPAEMLAS
PB74	PB1 74	TQIPAEMLASIDLKY
PB75	PB1 75	EMLASIDLKYFNEST
PB76	PB1 76	IDLKYFNESTKKKIE
PB77	PB1 77	FNESTKKKIEKIRPL
PB78	PB1 78	KKKIEKIRPLLIDGT
PB79	PB1 79	KIRPLLIDGTASLSP
PB80	PB1 80	LIDGTASLSPGMMMG
PB81	PB1 81	ASLSPGMMMGMFNML
PB82	PB1 82	GMMMGMFNMLSTVLG
PB83	PB1 83	MFNMLSTVLGVSILN
PB84	PB1 84	STVLGVSILNLGQKK
PB85	PB1 85	VSILNLGQKKYTKTI
PB86	PB1 86	LGQKKYTKTIYWWDG
PB87	PB1 87	YTKTIYWWDGLQSSD
PB88	PB1 88	YWWDGLQSSDDFALI
PB89	PB1 89	LQSSDDFALIVNAPN
PB90	PB1 90	DFALIVNAPNHEGIQ
PB91	PB1 91	VNAPNHEGIQAGVDR
PB92	PB1 92	HEGIQAGVDRFYRTC
PB93	PB1 93	AGVDRFYRTCKLVGI
PB94	PB1 94	FYRTCKLVGINMSKK
PB95	PB1 95	KLVGINMSKKKSYIN
PB96	PB1 96	NMSKKKSYINKTGTF
PB97	PB1 97	KSYINKTGTFEFTSF
PB98	PB1 98	KTGTFEFTSFFYRYG
PB99	PB1 99	EFTSFFYRYGFVANF
PB100	PB1 100	FYRYGFVANFSMELP
PB101	PB1 101	FVANFSMELPSFGVS

PB102	PB1 102	SMELPSFGVSGVNES
PB103	PB1 103	SFGVSGVNESADMSI
PB104	PB1 104	GVNESADMSIGVTVI
PB105	PB1 105	ADMSIGVTVIKNNMI
PB106	PB1 106	GVTVIKNNMINNDLG
PB107	PB1 107	KNNMINNDLGPATAQ
PB108	PB1 108	NNDLGPATAQMALQL
PB109	PB1 109	PATAQMALQLFIKDY
PB110	PB1 110	MALQLFIKDYRYTYR
PB111	PB1 111	FIKDYRYTYRCHRGD
PB112	PB1 112	RYTYRCHRGDTQIQT
PB113	PB1 113	CHRGDTQIQTRRSFE
PB114	PB1 114	QIQTRRSFELKKLW
PB115	PB1 115	RRSFELKKLWDQTQS
PB116	PB1 116	LKKLWDQTQSKVGLL
PB117	PB1 117	DQTQSKVGLLVSDGG
PB118	PB1 118	KVGLLVSDGGPNLYN
PB119	PB1 119	VSDGGPNLYNIRNLH
PB120	PB1 120	PNLYNIRNLHIPEVC
PB121	PB1 121	IRNLHIPEVCLKWEL
PB122	PB1 122	IPEVCLKWELMDDDY
PB123	PB1 123	LKWELMDDDYRGRLC
PB124	PB1 124	MDDDYRGRLCNPLNP
PB125	PB1 125	RGRLCNPLNPFVSHK
PB126	PB1 126	NPLNPFVSHKEIDSV
PB127	PB1 127	FVSHKEIDSVNNAVV
PB128	PB1 128	EIDSVNNAVVMPAHG
PB129	PB1 129	NNAVVMPAHGPAKSM
PB130	PB1 130	MPAHGPAKSMEYDAV
PB131	PB1 131	PAKSMEYDAVATTHS
PB132	PB1 132	EYDAVATTHSWIPKR
PB133	PB1 133	ATTHSWIPKRNRSIL
PB134	PB1 134	WIPKRNRSILNTSQR
PB135	PB1 135	NRSILNTSQRGILED
PB136	PB1 136	NTSQRGILEDEQMYQ

PB137	**PB1 137**	**GILEDEQMYQKCCNL**
PB138	**PB1 138**	**EQMYQKCCNLFEKFF**
PB139	**PB1 139**	**KCCNLFEKFFPSSSY**
PB140	**PB1 140**	**FEKFFPSSSYRRPVG**
PB141	**PB1 141**	**PSSSYRRPVGISSMV**
PB142	**PB1 142**	**RRPVGISSMVEAMVS**
PB143	**PB1 143**	**ISSMVEAMVSRARID**
PB144	**PB1 144**	**EAMVSRARIDARVDF**
PB145	**PB1 145**	**RARIDARVDFESGRI**
PB146	**PB1 146**	**ARVDFESGRIKKEEF**
PB147	**PB1 147**	**ESGRIKKEEFSEIMK**
PB148	**PB1 148**	**KKEEFSEIMKICSTI**
PB149	**PB1 149**	**SEIMKICSTIEELRR**
PB150	**PB1 150**	**ICSTIEELRRQK**

Table 6.5 Camera and count settings for fluorescence-immunospot optimisation work.	Fluorescence-immunospot Optical filter 1 (Cy3)	Fluorescence-immunospot Optical filter 2 (FITC)
CAMERA SETTINGS		
Brightness	36	36
Hue	51	51
Saturation	291	321
Sharpness	1	1
Gamma	0	0
White Balance -R	103	83
White Balance -B	53	53
Gain	32	96
Exposure/Shutter	1100	2409
COUNT SETTINGS		
Algorithm	v.3.2.x	v.3.2.x
Intensity Minimum	5	15
Gradient Minimum	2	1
Size Minimum	50	50
Emphasis	Tiny	Tiny

Table 6.6 Camera and count settings for fluorescence-immunospot on Immunoflu samples.	Fluorescence-immunospot Optical filter 1 (Cy3)	Fluorescence-immunospot Optical filter 2 (FITC)
CAMERA SETTINGS		
Brightness	0	0
Hue	40	40
Saturation	214	256
Sharpness	0	0
Gamma	0	0
White Balance -R	85	84
White Balance -B	51	44
Gain	32	96
Exposure/Shutter	1783	2795
COUNT SETTINGS		
Algorithm	v.3.2.x	v.3.2.x
Intensity Minimum	5	22
Gradient Minimum	2	1
Size Minimum	50	50
Emphasis	Tiny	Tiny

Figure 6.1 Titrating antibody-fluorochrome conjugates for multi-parameter flow cytometry panel. Numbers next to plots are dilution factors (by volume) of antibody-fluorochrome conjugates (A – M).

A

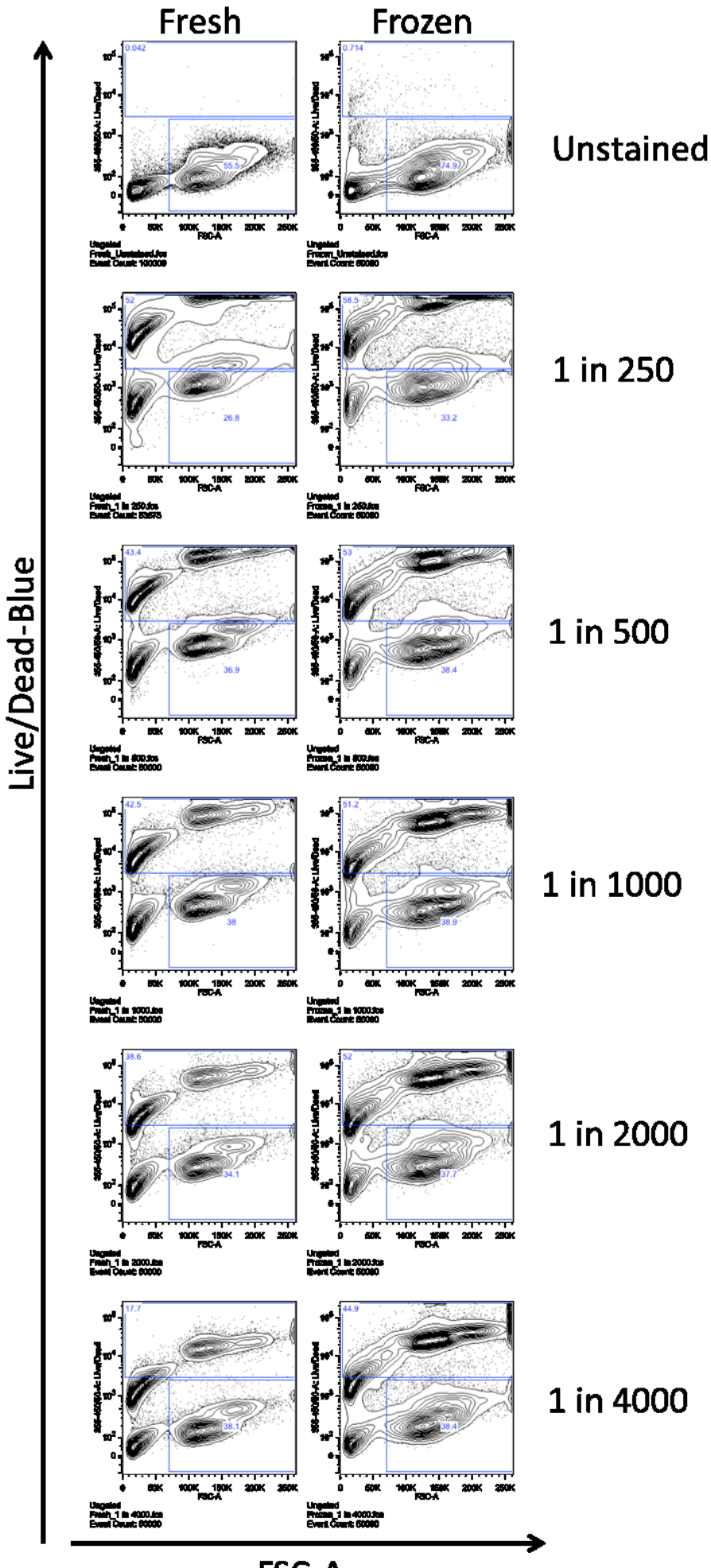
Fresh
Frozen
Unstained
1 in 250
1 in 500
1 in 1000
1 in 2000
1 in 4000
Live/Dead-Blue
FSC-A

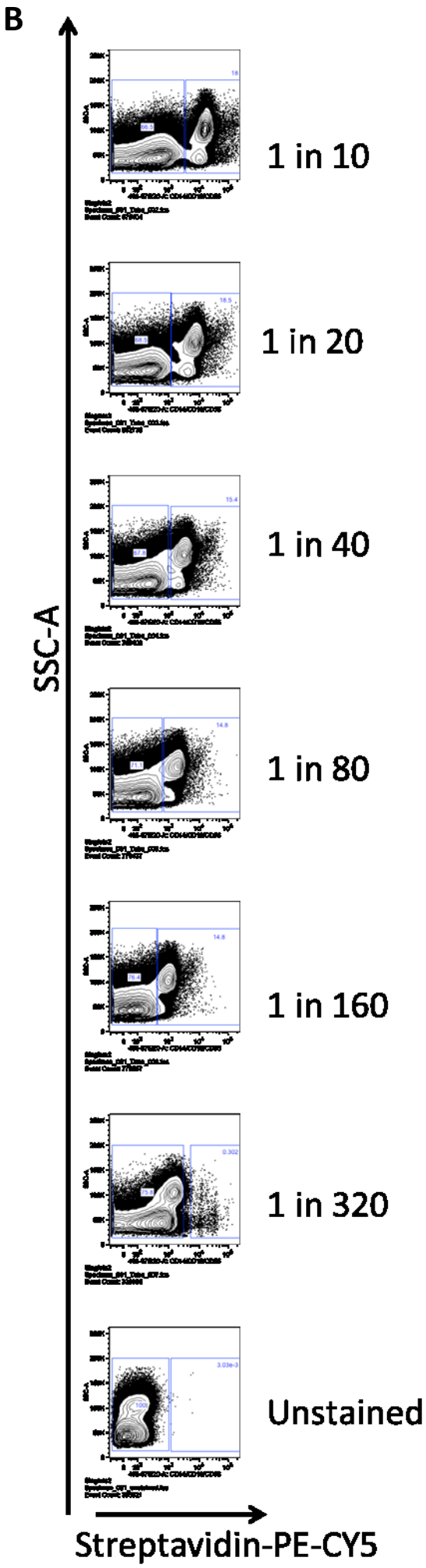
B
SSC-A
1 in 10
1 in 20
1 in 40
1 in 80
1 in 160
1 in 320
Unstained
Streptavidin-PE-CY5

C

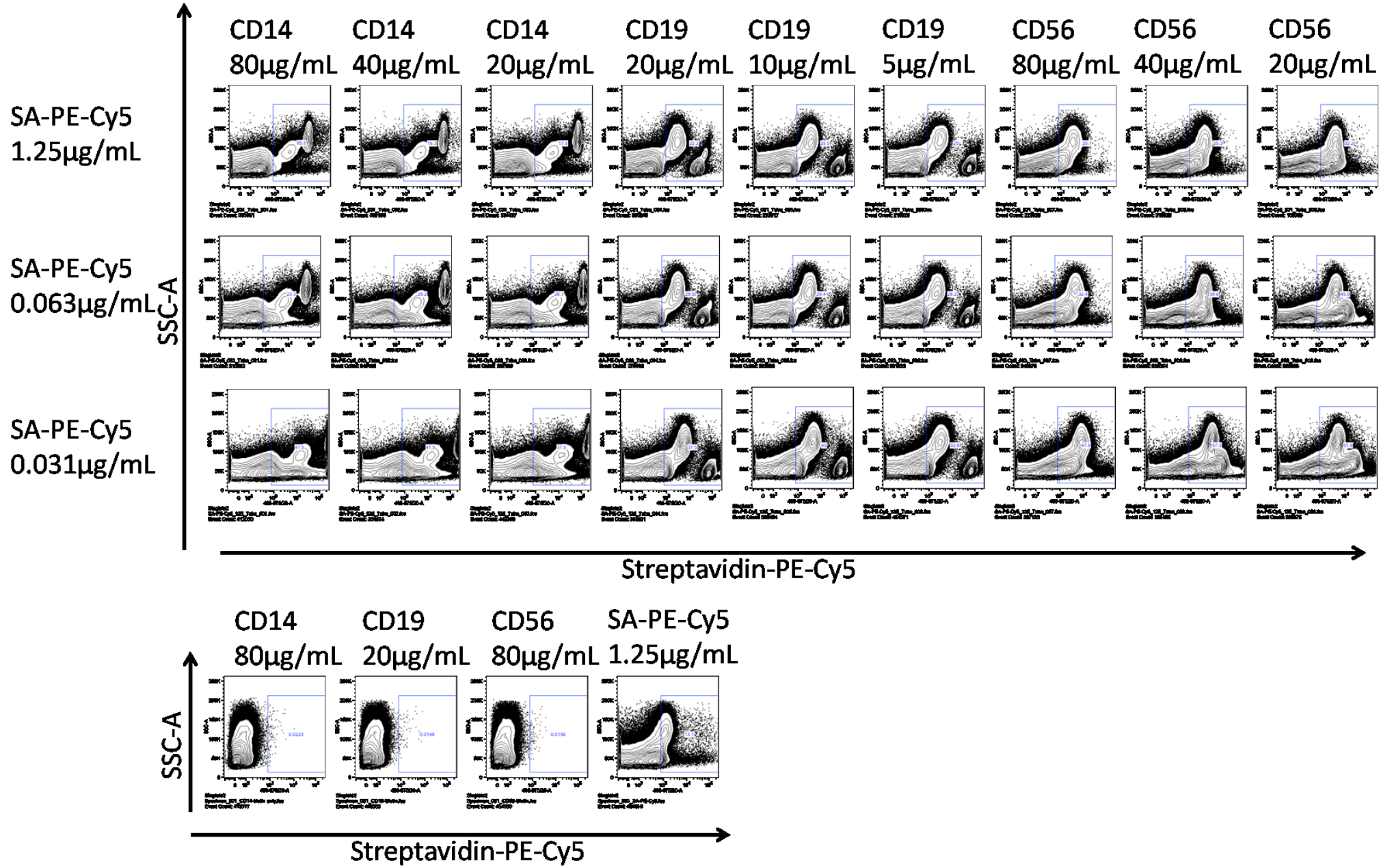
CD14 80µg/mL
CD14 40µg/mL
CD14 20µg/mL
CD19 20µg/mL
CD19 10µg/mL
CD19 5µg/mL
CD56 80µg/mL
CD56 40µg/mL
CD56 20µg/mL
SA-PE-Cy5 1.25µg/mL
SA-PE-Cy5 0.063µg/mL
SA-PE-Cy5 0.031µg/mL
SSC-A
Streptavidin-PE-Cy5
CD14 80µg/mL
CD19 20µg/mL
CD56 80µg/mL
SA-PE-Cy5 1.25µg/mL
SSC-A
Streptavidin-PE-Cy5

D

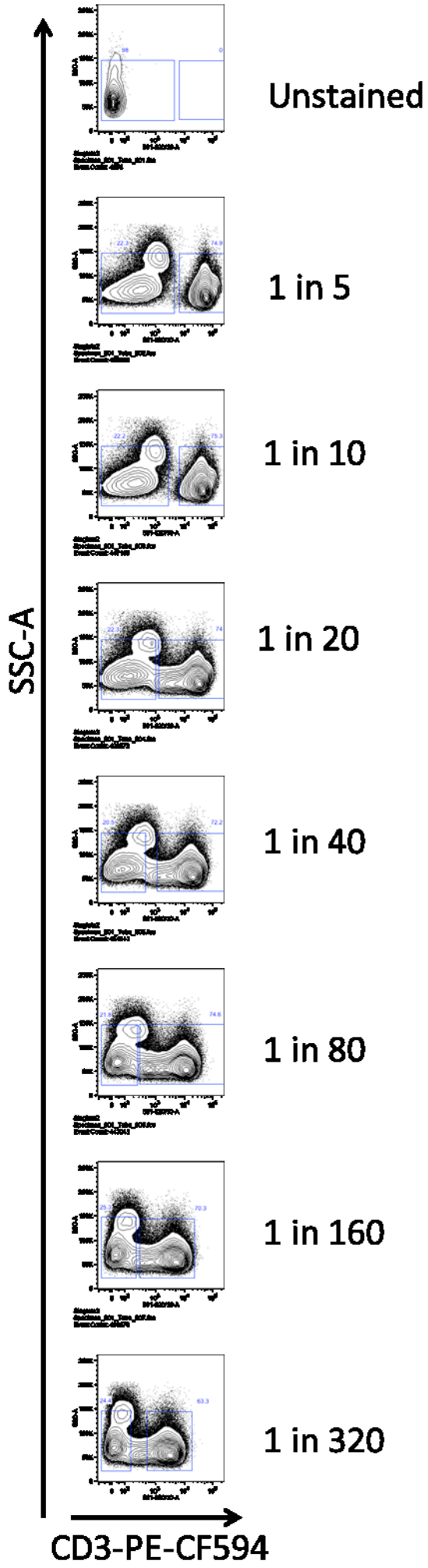
Unstained
1 in 5
1 in 10
1 in 20
1 in 40
1 in 80
1 in 160
1 in 320
SSC-A
CD3-PE-CF594

E

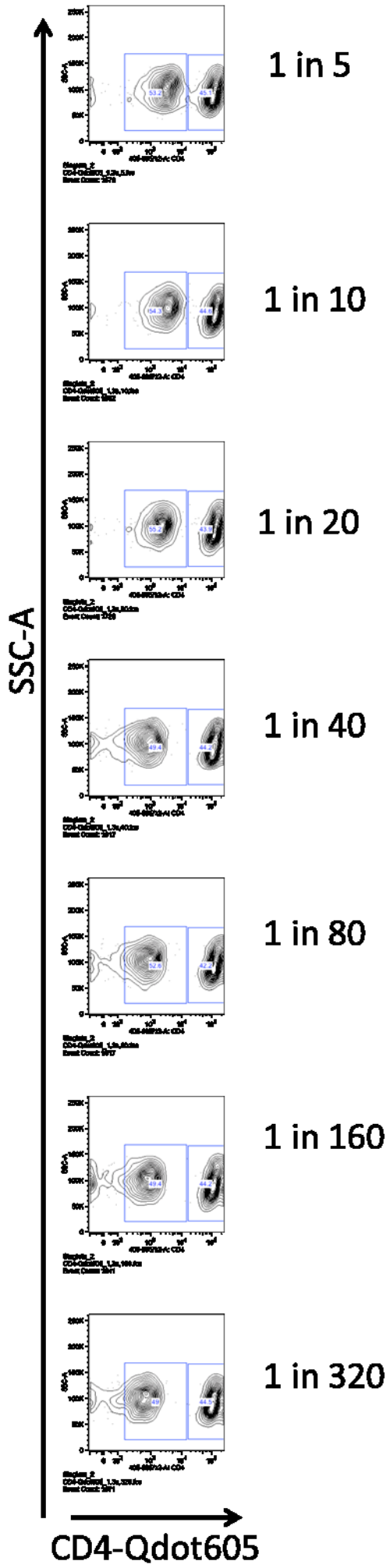
1 in 5
1 in 10
1 in 20
1 in 40
1 in 80
1 in 160
1 in 320
SSC-A
CD4-Qdot605

F

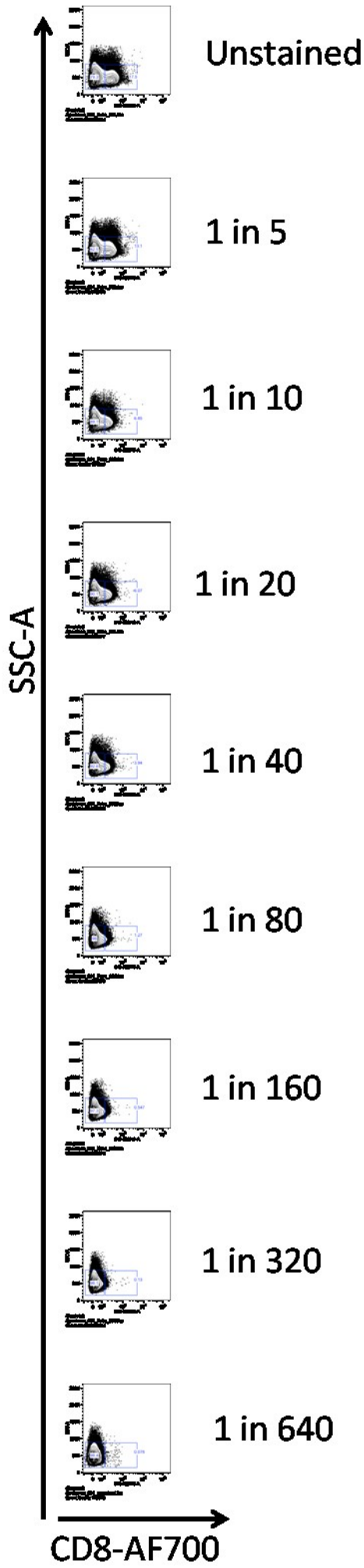
Unstained
1 in 5
1 in 10
1 in 20
1 in 40
1 in 80
1 in 160
1 in 320
1 in 640
SSC-A
CD8-AF700

G

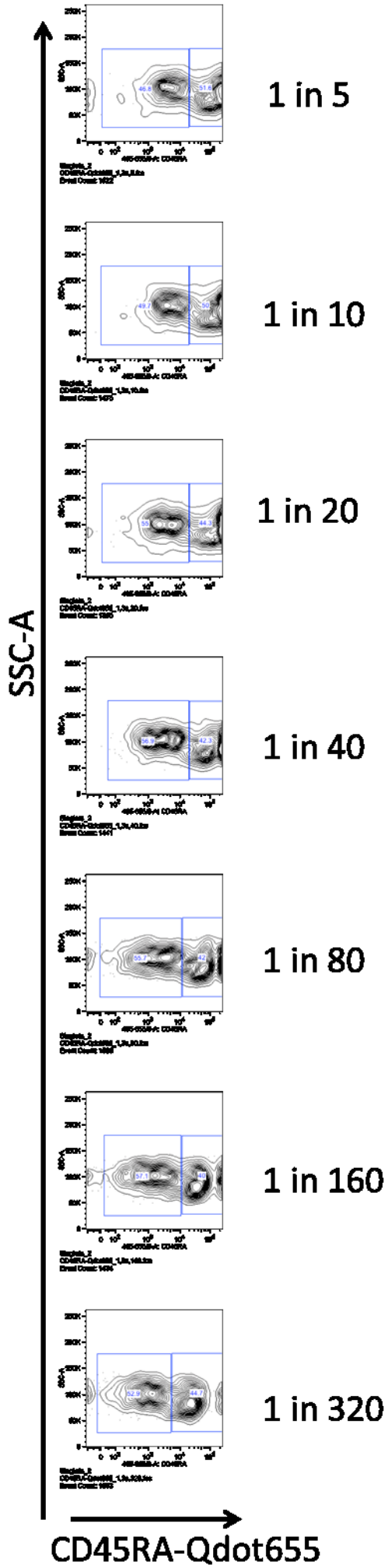
1 in 5
1 in 10
1 in 20
1 in 40
1 in 80
1 in 160
1 in 320
SSC-A
CD45RA-Qdot655

H

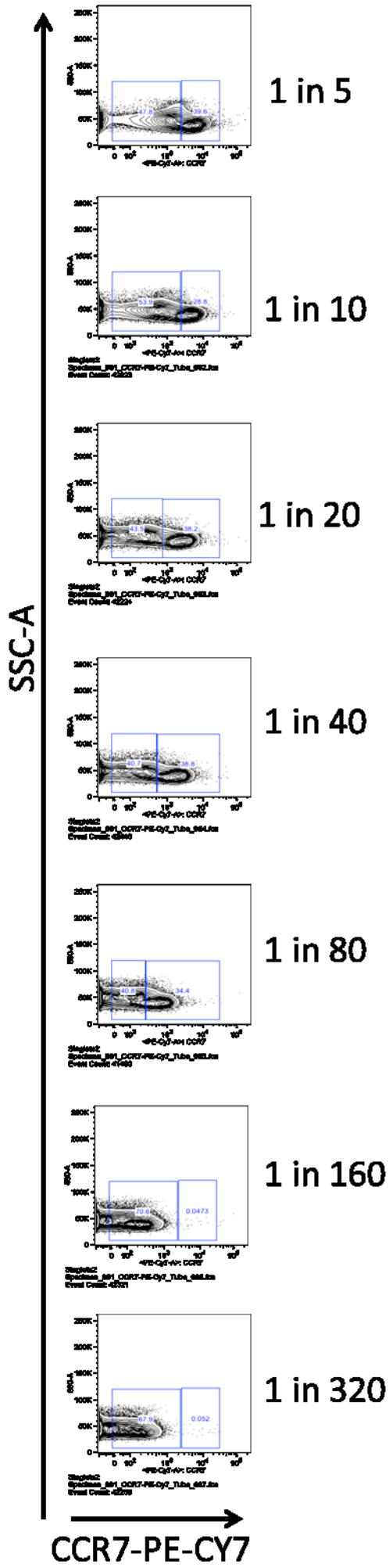

I

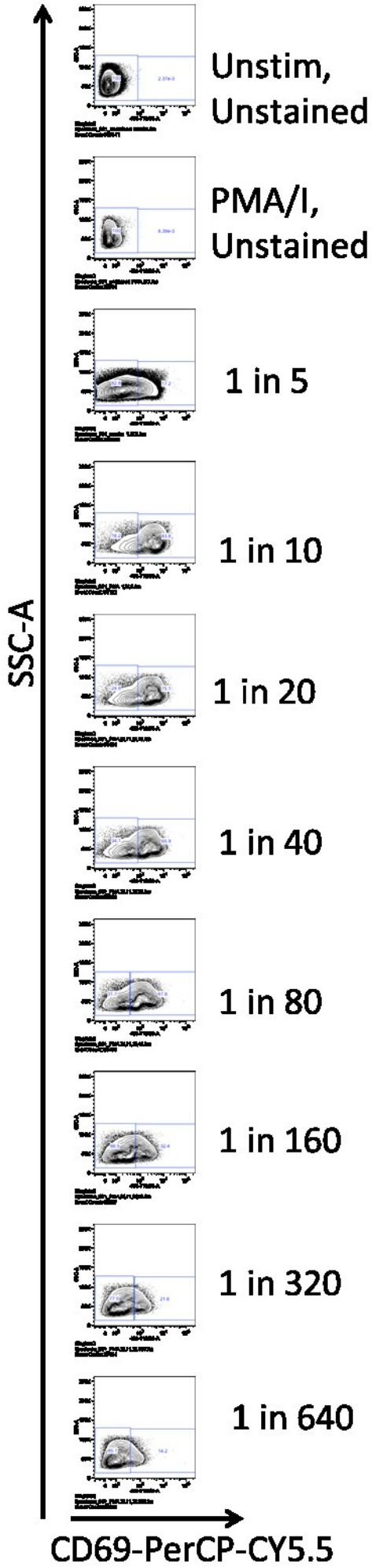
Unstim,
Unstained
PMA/I,
Unstained
1 in 5
1 in 10
1 in 20
1 in 40
1 in 80
1 in 160
1 in 320
1 in 640
SSC-A
CD69-PerCP-CY5.5

J

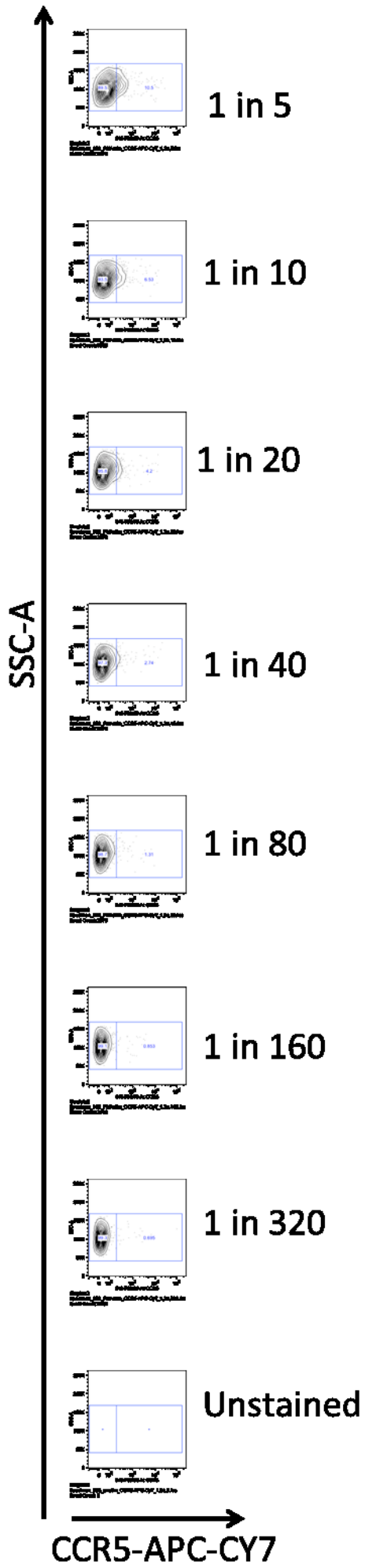
1 in 5
1 in 10
1 in 20
1 in 40
1 in 80
1 in 160
1 in 320
Unstained
SSC-A
CCR5-APC-CY7

K

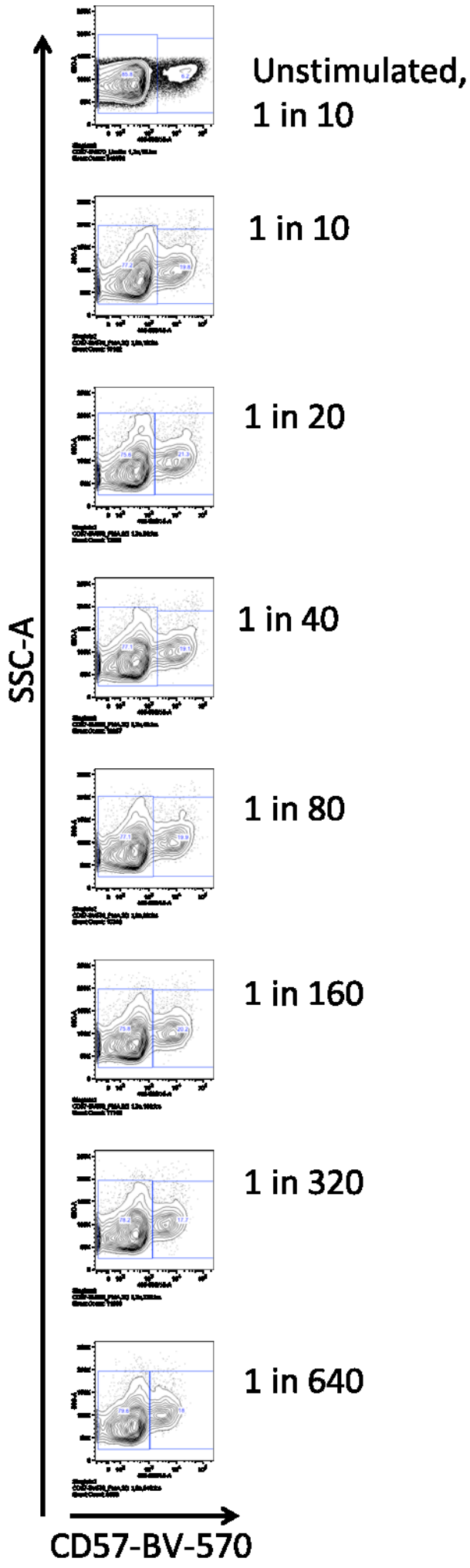
Unstimulated, 1 in 10
1 in 10
1 in 20
1 in 40
1 in 80
1 in 160
1 in 320
1 in 640
SSC-A
CD57-BV-570

L

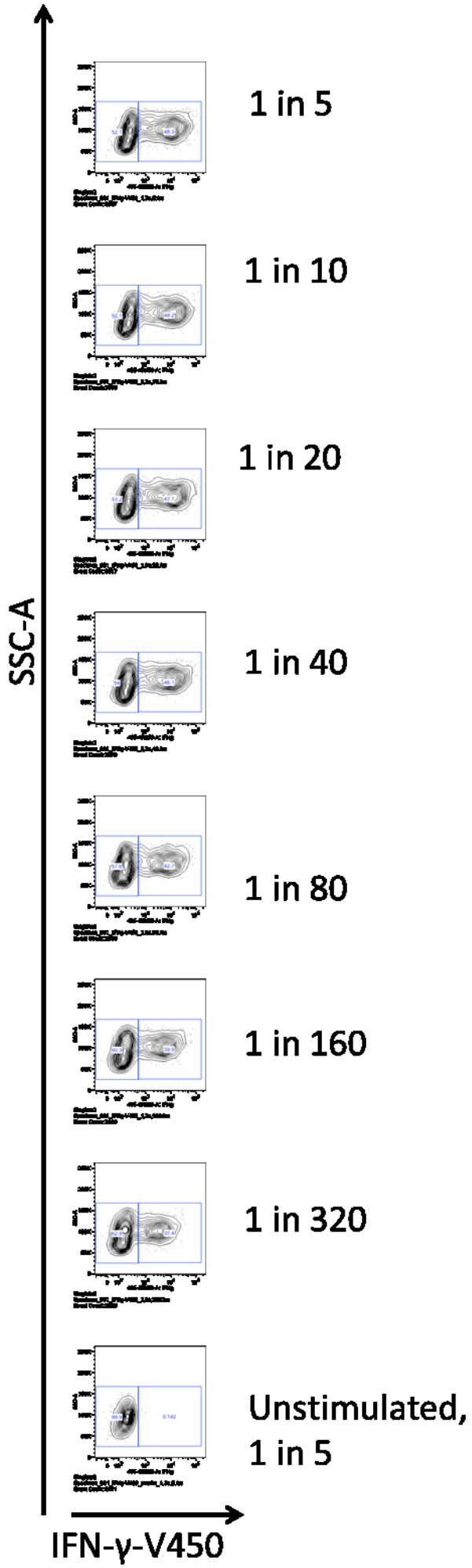
1 in 5
1 in 10
1 in 20
1 in 40
1 in 80
1 in 160
1 in 320
Unstimulated,
1 in 5
SSC-A
IFN-γ-V450

M

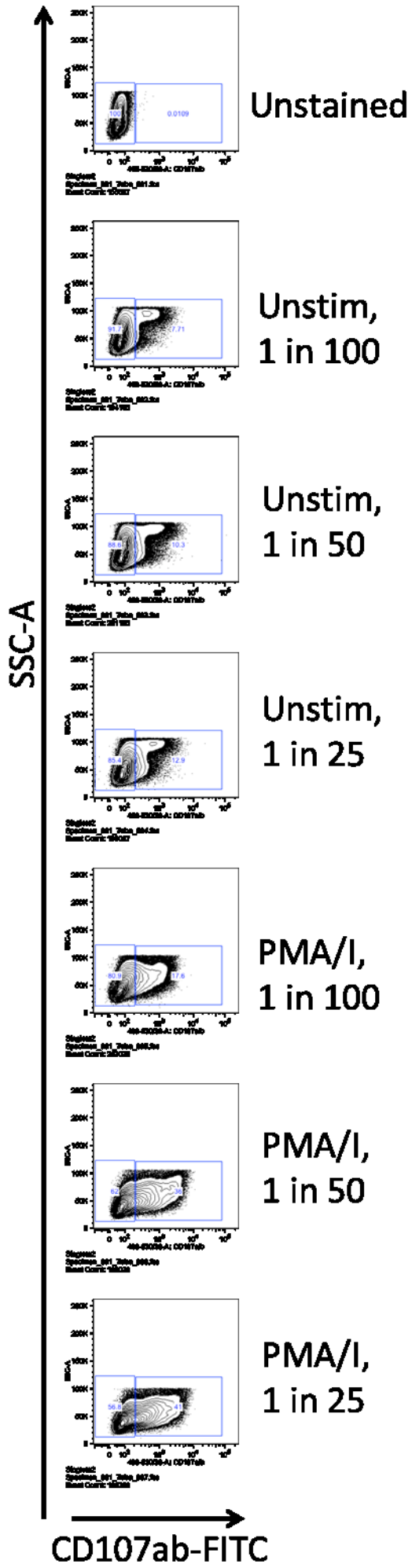
SSC-A
CD107ab-FITC
Unstained
Unstim,
1 in 100
Unstim,
1 in 50
Unstim,
1 in 25
PMA/I,
1 in 100
PMA/I,
1 in 50
PMA/I,
1 in 25

Table 6.7 Live/Dead Blue on fresh and frozen PBMC							
Staining antibody dilution (by volume)	Live/Dead Blue-positive (% of total)	Live/Dead Blue-positive (Geom. Mean)	Live/Dead Blue-positive (SD)	Live/Dead Blue-negative (% of total)	Live/Dead Blue-negative (Geom. Mean)	Live/Dead Blue-negative (SD)	STAIN INDEX
Fresh_Unstained.fcs	0.04	6477.00	25185.00	55.50	140.00	168.00	37.72
Fresh_1 in 250.fcs	52.00	40257.00	103000.00	26.80	1284.00	399.00	97.68
Fresh_1 in 500.fcs	43.40	38197.00	83925.00	36.90	860.00	517.00	72.22
Fresh_1 in 1000.fcs	42.50	21401.00	57392.00	38.00	594.00	448.00	46.44
Fresh_1 in 2000.fcs	38.60	11455.00	34161.00	34.10	360.00	311.00	35.68
Fresh_1 in 4000.fcs	17.70	14809.00	16800.00	38.10	186.00	188.00	77.78
Frozen_Unstained.fcs	0.71	10495.00	40128.00	74.90	151.00	189.00	54.73
Frozen_1 in 250.fcs	58.50	78214.00	104000.00	33.20	1090.00	464.00	166.22
Frozen_1 in 500.fcs	53.00	60407.00	79130.00	38.40	723.00	488.00	122.30
Frozen_1 in 1000.fcs	51.20	37688.00	58212.00	38.90	491.00	402.00	92.53
Frozen_1 in 2000.fcs	52.00	36494.00	54860.00	37.70	402.00	388.00	93.02
Frozen_1 in 4000.fcs	44.90	25982.00	36938.00	38.40	286.00	294.00	87.40

Table 6.8 Streptavidin-PE-CY5

Staining antibody dilution (by volume)	CD14/CD19/CD56-SA-PE-CY5-positive (% of PBMC singlets)	CD14/CD19/CD56-SA-PE-CY5-positive (Geom. Mean)	CD14/CD19/CD56-SA-PE-CY5-positive (SD)	CD14/CD19/CD56-SA-PE-CY5-negative (% of PBMC singlets)	CD14/CD19/CD56-SA-PE-CY5-negative (Geom. Mean)	CD14/CD19/CD56-SA-PE-CY5-negative (SD)	STAIN INDEX
1 in 10	18.00	14120.00	14934.00	66.50	235.00	454.00	30.58
1 in 20	18.50	5496.00	5977.00	68.50	123.00	215.00	24.99
1 in 40	15.40	2750.00	2532.00	67.80	116.00	197.00	13.37
1 in 80	14.80	1498.00	1566.00	71.10	81.60	144.00	9.84
1 in 160	14.80	857.00	695.00	76.40	54.30	107.00	7.50
1 in 320	0.30	16491.00	18637.00	75.80	329.00	535.00	30.21

Table 6.9 CD3-PE-CF594							
Staining antibody dilution (by volume)	**CD3-PE-CF594-positive (% of PBMC singlets)**	**CD3-PE-CF594-positive (Geom. Mean)**	**CD3-PE-CF594-positive (SD)**	**CD3-PE-CF594-negative (% of PBMC singlets)**	**CD3-PE-CF594-negative (Geom. Mean)**	**CD3-PE-CF594-negative (SD)**	**STAIN INDEX**
Unstained	**0**	**0**	**0**	**98**	**8.1**	**29.2**	**-0.28**
1 in 5	**74.9**	**56352**	**24566**	**22.3**	**319**	**630**	**88.94**
1 in 10	**75.3**	**40981**	**20604**	**22.2**	**237**	**453**	**89.94**
1 in 20	**74**	**20278**	**17577**	**22.3**	**160**	**254**	**79.20**
1 in 40	**72.2**	**13918**	**10729**	**20.5**	**101**	**124**	**111.43**
1 in 80	**74.6**	**5174**	**6844**	**21.8**	**68.9**	**78.7**	**64.87**
1 in 160	**70.3**	**3106**	**3161**	**25.3**	**57.6**	**69.9**	**43.61**
1 in 320	**63.3**	**2471**	**1796**	**24.4**	**33.1**	**51.2**	**47.62**

Table 6.10 CD4-QDOT605							
Staining antibody dilution (by volume)	**CD4-QDOT605-positive (% of PBMC singlets)**	**CD4-QDOT605-positive (Geom. Mean)**	**CD4-QDOT605-positive (SD)**	**CD4-QDOT605-negative (% of PBMC singlets)**	**CD4-QDOT605-negative (Geom. Mean)**	**CD4-QDOT605-negative (SD)**	**STAIN INDEX**
1 in 5	**45.10**	**112000.00**	**41274.00**	**53.20**	**2749.00**	**1965.00**	**55.60**
1 in 10	**44.60**	**130000.00**	**43494.00**	**54.30**	**2881.00**	**1877.00**	**67.72**
1 in 20	**43.90**	**130000.00**	**43784.00**	**55.20**	**1935.00**	**1281.00**	**99.97**
1 in 40	**44.20**	**124000.00**	**47635.00**	**49.40**	**777.00**	**821.00**	**150.09**
1 in 80	**42.20**	**130000.00**	**47571.00**	**52.60**	**747.00**	**615.00**	**210.17**
1 in 160	**44.20**	**126000.00**	**53919.00**	**49.40**	**736.00**	**616.00**	**203.35**
1 in 320	**44.50**	**119000.00**	**53586.00**	**49.00**	**605.00**	**439.00**	**269.69**

Table 6.11 CD8-AF700							
Staining antibody dilution (by volume)	CD8-AF700-positive (% of PBMC singlets)	CD8-AF700-positive (Geom. Mean)	CD8-AF700-positive (SD)	CD8-AF700-negative (% of PBMC singlets)	CD8-AF700-negative (Geom. Mean)	CD8-AF700-negative (SD)	STAIN INDEX
1 in 5	17.50	286.00	147.00	79.30	12.30	30.80	8.89
1 in 10	13.10	241.00	120.00	82.50	13.00	31.80	7.17
1 in 20	6.85	211.00	87.50	89.10	13.50	32.60	6.06
1 in 40	6.07	205.00	73.30	90.10	13.00	32.40	5.93
1 in 80	3.94	195.00	77.60	92.60	13.40	32.40	5.60
1 in 160	1.27	183.00	90.70	96.00	12.30	30.10	5.67
1 in 320	0.55	178.00	142.00	97.30	11.40	28.60	5.83
1 in 640	0.13	184.00	182.00	98.10	9.10	25.20	6.94
Unstained	0.08	303.00	183.00	98.40	3.45	28.40	10.55

Table 6.12 CD45RA-QDOT655							
Staining antibody dilution (by volume)	**CD45RA-QDOT655-positive (% of PBMC singlets)**	**CD45RA-QDOT655-positive (Geom. Mean)**	**CD45RA-QDOT655-positive (SD)**	**CD45RA-QDOT655-negative (% of PBMC singlets)**	**CD45RA-QDOT655-negative (Geom. Mean)**	**CD45RA-QDOT655-negative (SD)**	**STAIN INDEX**
1 in 5	**51.60**	**112000.00**	**80001.00**	**46.80**	**4416.00**	**5020.00**	**21.43**
1 in 10	**50.00**	**110000.00**	**82754.00**	**49.70**	**4687.00**	**4790.00**	**21.99**
1 in 20	**44.30**	**108000.00**	**84784.00**	**55.00**	**3486.00**	**4853.00**	**21.54**
1 in 40	**42.30**	**91476.00**	**80157.00**	**56.90**	**2544.00**	**4751.00**	**18.72**
1 in 80	**42.00**	**59432.00**	**76428.00**	**55.70**	**1487.00**	**2868.00**	**20.20**
1 in 160	**40.00**	**45119.00**	**70422.00**	**57.10**	**1309.00**	**2567.00**	**17.07**
1 in 320	**44.70**	**21954.00**	**49290.00**	**52.90**	**785.00**	**1188.00**	**17.82**

Table 6.13 CCR7-PE-CY7							
Staining antibody dilution (by volume)	**CCR7-PE-CY7-positive (% of PBMC singlets)**	**CCR7-PE-CY7-positive (Geom. Mean)**	**CCR7-PE-CY7-positive (SD)**	**CCR7-PE-CY7-negative (% of PBMC singlets)**	**CCR7-PE-CY7-negative (Geom. Mean)**	**CCR7-PE-CY7-negative (SD)**	**STAIN INDEX**
1 in 5	**39.6**	**5315**	**3000**	**47.8**	**752**	**620**	**7.36**
1 in 10	**28.8**	**4557**	**2333**	**53.9**	**440**	**584**	**7.05**
1 in 20	**38.2**	**2235**	**1667**	**43.5**	**170**	**188**	**10.98**
1 in 40	**38.8**	**1558**	**1306**	**40.7**	**143**	**140**	**10.11**
1 in 80	**34.4**	**592**	**612**	**40.8**	**88**	**77.7**	**6.49**
1 in 160	**0.05**	**5930**	**4332**	**70.6**	**130**	**189**	**30.69**
1 in 320	**0.05**	**8508**	**8669**	**67.9**	**109**	**147**	**57.14**

Table 6.14 CD69-PERCP-CY5.5							
Staining antibody dilution (by volume)	**CD69-PERCP-CY5.5-positive (% of PBMC singlets)**	**CD69-PERCP-CY5.5-positive (Geom. Mean)**	**CD69-PERCP-CY5.5-positive (SD)**	**CD69-PERCP-CY5.5-negative (% of PBMC singlets)**	**CD69-PERCP-CY5.5-negative (Geom. Mean)**	**CD69-PERCP-CY5.5-negative (SD)**	**STAIN INDEX**
Unstained (Unstimulated)	**0.00**	**931.00**	**72.70**	**100.00**	**26.70**	**40.00**	**22.61**
Unstained (PMA/I)	**0.01**	**988.00**	**70.20**	**100.00**	**35.30**	**42.80**	**22.26**
1 in 5	**17.20**	**1588.00**	**1645.00**	**82.80**	**148.00**	**200.00**	**7.20**
1 in 10	**83.80**	**3437.00**	**2886.00**	**16.20**	**296.00**	**232.00**	**13.54**
1 in 20	**75.10**	**2824.00**	**2468.00**	**24.90**	**282.00**	**220.00**	**11.55**
1 in 40	**65.90**	**2267.00**	**2161.00**	**34.10**	**249.00**	**218.00**	**9.26**
1 in 80	**67.60**	**1229.00**	**1559.00**	**31.70**	**140.00**	**104.00**	**10.47**
1 in 160	**32.40**	**1335.00**	**989.00**	**66.50**	**193.00**	**166.00**	**6.88**
1 in 320	**21.60**	**1029.00**	**614.00**	**77.50**	**154.00**	**136.00**	**6.43**
1 in 640	**14.20**	**641.00**	**1187.00**	**85.10**	**109.00**	**91.80**	**5.80**

Table 6.15 CCR5-APC-CY7							
Staining antibody dilution (by volume)	**CCR5-APC-CY7-positive (% of PBMC singlets)**	**CCR5-APC-CY7-positive (Geom. Mean)**	**CCR5-APC-CY7-positive (SD)**	**CCR5-APC-CY7-negative (% of PBMC singlets)**	**CCR5-APC-CY7-negative (Geom. Mean)**	**CCR5-APC-CY7-negative (SD)**	**STAIN INDEX**
1 in 5	**10.50**	**433.00**	**3166.00**	**89.50**	**65.80**	**53.90**	**6.81**
1 in 10	**6.53**	**420.00**	**2089.00**	**93.50**	**47.80**	**47.80**	**7.79**
1 in 20	**4.20**	**427.00**	**2510.00**	**95.80**	**41.60**	**46.80**	**8.24**
1 in 40	**2.74**	**521.00**	**3693.00**	**97.30**	**31.70**	**41.90**	**11.68**
1 in 80	**1.31**	**623.00**	**1801.00**	**98.70**	**20.60**	**34.30**	**17.56**
1 in 160	**0.85**	**807.00**	**1144.00**	**99.10**	**14.10**	**28.60**	**27.72**
1 in 320	**0.70**	**1035.00**	**22260.00**	**99.30**	**11.60**	**25.60**	**39.98**

Table 6.16 CD57-BV570							
Staining antibody dilution (by volume)	**CD57-BV570-positive (% of PBMC singlets)**	**CD57-BV570-positive (Geom. Mean)**	**CD57-BV570-positive (SD)**	**CD57-BV570-negative (% of PBMC singlets)**	**CD57-BV570-negative (Geom. Mean)**	**CD57-BV570-negative (SD)**	**STAIN INDEX**
1: CD57-BV570_Unstim 1,3a,10.fcs	**6.20**	**13198.00**	**22647.00**	**85.80**	**173.00**	**228.00**	**75.79**
1 in 10	**19.80**	**8831.00**	**24000.00**	**77.20**	**332.00**	**335.00**	**26.37**
1 in 20	**21.30**	**8853.00**	**20656.00**	**75.60**	**258.00**	**271.00**	**34.02**
1 in 40	**19.10**	**9525.00**	**15583.00**	**77.10**	**251.00**	**320.00**	**37.64**
1 in 80	**19.90**	**7296.00**	**16277.00**	**77.10**	**222.00**	**242.00**	**32.52**
1 in 160	**20.20**	**6510.00**	**9835.00**	**75.80**	**217.00**	**233.00**	**29.65**
1 in 320	**17.70**	**4738.00**	**5318.00**	**78.20**	**216.00**	**235.00**	**21.57**
1 in 640	**18.00**	**3276.00**	**3348.00**	**79.60**	**209.00**	**202.00**	**15.29**

Table 6.17 IFN-γ-V450							
Staining antibody dilution (by volume)	**IFN-γ-V450-positive (% of PBMC singlets)**	**IFN-γ-V450-positive (Geom. Mean)**	**IFN-γ-V450-positive (SD)**	**IFN-γ-V450-negative (% of PBMC singlets)**	**IFN-γ-V450-negative (Geom. Mean)**	**IFN-γ-V450-negative (SD)**	**STAIN INDEX**
1 in 5	**48.30**	**6112.00**	**14887.00**	**52.10**	**237.00**	**96.90**	**60.63**
1 in 10	**48.20**	**6797.00**	**15782.00**	**52.10**	**234.00**	**92.50**	**70.95**
1 in 20	**47.10**	**7006.00**	**18940.00**	**53.20**	**219.00**	**90.90**	**74.66**
1 in 40	**46.10**	**6213.00**	**15516.00**	**54.00**	**197.00**	**91.20**	**65.96**
1 in 80	**42.70**	**5153.00**	**12040.00**	**57.60**	**170.00**	**94.30**	**52.84**
1 in 160	**39.90**	**4066.00**	**8966.00**	**60.30**	**162.00**	**92.60**	**42.16**
1 in 320	**37.40**	**2862.00**	**4933.00**	**62.90**	**155.00**	**98.80**	**27.40**
Unstimulated (1 in 5)	**0.14**	**836.00**	**186.00**	**99.90**	**175.00**	**71.70**	**9.22**

Table 6.18 CD107ab-FITC							
Staining antibody dilution (by volume)	**CD107AB-FITC-positive (% of PBMC singlets)**	**CD107AB-FITC-positive (Geom. Mean)**	**CD107AB-FITC-positive (SD)**	**CD107AB-FITC-negative (% of PBMC singlets)**	**CD107AB-FITC-negative (Geom. Mean)**	**CD107AB-FITC-negative (SD)**	**STAIN INDEX**
UNSTAINED	**0.01**	**318.00**	**99.60**	**100.00**	**49.20**	**24.10**	**11.15**
UNSTIM 1 in 100	**7.71**	**472.00**	**450.00**	**91.70**	**73.60**	**34.80**	**11.45**
UNSTIM 1 in 50	**10.30**	**476.00**	**776.00**	**88.60**	**85.30**	**37.70**	**10.36**
UNSTIM 1 in 25	**12.90**	**439.00**	**594.00**	**85.40**	**93.90**	**40.10**	**8.61**
PMA/I 1 in 100	**17.60**	**487.00**	**525.00**	**80.90**	**80.40**	**42.60**	**9.54**
PMA/I 1 in 50	**36.00**	**631.00**	**1119.00**	**62.00**	**91.90**	**42.70**	**12.63**
PMA/I 1 in 25	**41.00**	**608.00**	**1037.00**	**56.80**	**98.40**	**42.60**	**11.96**